The Role of Latent TGFβ Binding Protein 4 in Elastic Fibre Assembly and Disruption in Autosomal Recessive Cutis Laxa 1C

A thesis submitted to the University of Manchester for the degree of Doctor of Philosophy (PhD) in the Faculty of Biology, Medicine and Health

2020

Yasmene F. Alanazi

Division of Cell Matrix Biology & Regenerative Medicine

School of Biological Sciences

Table of content

Word count: 47831

List of Figures

Chapter 1: Introduction

Chapter 3: Autosomal recessive Cutis Laxa 1C Mutations Disrupt the Structure and Interactions of Latent TGFβ binding protein 4 (LTBP4)

Chapter 4: Structural and Functional Consequences of a Point mutation in the N-terminal region of LTBP4 in Autosomal Recessive Cutis Laxa type 1C

Chapter 5: Functional similarities and interaction between Latent TGFβ binding protein 4 and Latent TGFβ binding protein 1

Chapter 6: General Discussion

Appendix 2: Supplementary Data and Methods

List of Tables

Chapter 1: Introduction

Chapter 3: Autosomal recessive Cutis Laxa 1C Mutations Disrupt the Structure and Interactions of Latent TGFβ binding protein 4 (LTBP4)

Chapter 4: Structural and Functional Consequences of a Point mutation in the N-terminal region of LTBP4 in Autosomal Recessive Cutis Laxa type 1C

Abstract

LTBP4 belongs to a family of large secreted TGFβ binding glycoproteins that are structurally related to fibrillin-1. LTBP4 mutations are linked to an ARCL1C that is characterised by generalised cutis laxa and severely disrupted elastic fibres in several visceral organs including the lung. LTBP4 assists in regulating TGFβ1 biology by mediating its folding and secretion and extracellular matrix bioavailability by targeting latent TGFβ and mediating its sequestration via interaction with fibrillin-1. LTBP4 is also essential for promoting elastic fibre assembly via interaction with fibulin-4 and -5. Although LTBP4 plays a vital role in elastogenesis, the molecular mechanism by which it regulates elastic fibre assembly is poorly understood, and its structure is not defined yet.

To understand the role of LTBP4 in elastogenesis and how ARCL1C-causing mutations impact on LTBP4 leading to defective elastic fibre assembly, it was essential to determine the structure of LTBP4. Using recombinant wildtype LTBP4 constructs and ARCL1C mutants, LTBP4 hydrodynamics and nanostructure have been determined using complementary biophysical methods and compared to analyze any differences. Findings presented in this thesis demonstrate novel structural information on the wildtype LTBP4 and define conformational changes induced by ARCL1C. The monomeric LTBP4 C-terminal region was found to adopt an elongated and flexible conformation. In a comparison of the mutant, C1286S, to the wildtype, minimal conformational change has been induced. While the C1186R mutation caused a more considerable conformational change and resulted in a conformational transition. The monomeric LTBP4 N-terminal region was found to adopt an elongated and inflexible conformation while the C244G mutant resulted in a more compact protein.

Previous studies have demonstrated that LTBP4 promotes elastogenesis by interacting with fibulin-4 and fibulin-5 via its N-terminal region and by interacting with fibrillin-1 via its C-terminal region. Matrix deposition of LTBP4 is dependent on fibrillin-1 deposition. While matrix deposition of fibulin-5 is dependent on the proper deposition of LTBP4, moreover, it has been demonstrated that fibronectin and heparin/heparan sulphate (HS) mediate LTBP4 matrix deposition via its N-terminal region. Using binding studies, how ARCL1C mutations may impact on LTBP4 molecular interactions with these proteins, that are involved in LTBP4 deposition and elastogenesis, has been investigated. Data presented here demonstrate that ARCL1C mutants could bind to these matrix partners but with slightly altered affinity depending on the position of the substituted highly conserved cysteine. Findings shown here also identify tropoelastin and LTBP1 as novel matrix partners, suggesting new roles for LTBP4.

Previous work by our group demonstrated that LTBP1 can self-assemble and that transglutaminase 2 (TG2) stabilises its assembly and cross-linking to fibrillin-1. Using binding studies and TG2 cross-linking assays, LTBP4 self-assembly and cross-linking with fibrillin-1 was investigated. Data here demonstrate that LTBP4 does not self-interact or cross-link nor cross-link to fibrillin-1 via TG2. Moreover, data here show a novel non-covalent interaction with small latent complex (SLC) and that interaction of LTBP1 with fibrillin-1 is not altered by the formation of the large latent complex (LLC).

Collectively, data presented in this thesis contribute to understanding the role of LTBP4 in elastogenesis and highlight the importance of the highly conserved cysteines in LTBP4 structure and function.

Declaration

I declare that no portion of the work referred to in this thesis has been submitted in support of an application for another degree or qualification of this or any other university or other institute of learning.

Yasmene Falah Alanazi

15th March 2020

Copyright Statement

i. The author of this thesis (including any appendices and/or schedules to this thesis) owns certain copyright or related rights in it (the "Copyright") and s/he has given The University of Manchester certain rights to use such Copyright, including for administrative purposes.

ii. Copies of this thesis, either in full or in extracts and whether in hard or electronic copy, may be made only in accordance with the Copyright, Designs and Patents Act 1988 (as amended) and regulations issued under it or, where appropriate, in accordance with licensing agreements which the University has from time to time. This page must form part of any such copies made.

iii. The ownership of certain Copyright, patents, designs, trademarks and other intellectual property (the "Intellectual Property") and any reproductions of copyright works in the thesis, for example graphs and tables ("Reproductions"), which may be described in this thesis, may not be owned by the author and may be owned by third parties. Such Intellectual Property and Reproductions cannot and must not be made available for use without the prior written permission of the owner(s) of the relevant Intellectual Property and/or Reproductions.

iv. Further information on the conditions under which disclosure, publication and commercialisation of this thesis, the Copyright and any Intellectual Property and/or Reproductions described in it may take place is available in the University IP Policy (see http://documents.manchester.ac.uk/DocuInfo.aspx?DocID=2442 0), in any relevant Thesis restriction declarations deposited in the University Library, The University Library's regulations (see http://www.library.manchester.ac.uk/about/regulations/) and in The University's policy on Presentation of Theses.

Journal Format Submission

This thesis is being submitted in a journal format in order to publish the work done in this thesis in peer-reviewed journals as sharing novel research findings might contribute to a better understanding of the field. The format will contain a general introduction, three un-published results chapters in manuscript form including supplementary data, a general discussion for all three results chapters, references, and appendices.

Acknowledgements

First and foremost, praise is to Allah, the greatest of all. I would like to thank Allah for giving me opportunity and strength to complete my thesis.

Now, I would like to thank everyone who contributed in some way to the work presented in this thesis. First of all, I would like to acknowledge my academic supervisor, Professor Clair Baldock and my advisor, Dr. Michael Sherratt, for their patient guidance, help and advice thorough this degree. I would like also to express my gratitude to my lab-mates for their help and support.

To my role model, my father, for his continued support and encouragement which helped me in completion of this work. Many thanks to, my mother, for her love and taking care of my little ones Ghala and Zayed while writing my thesis.

Finally, I would like to express my appreciation to my brothers and sisters for their continued love and support.

Abbreviations

ARCL : Autosomal recissive cutis laxa

ARCL1C : Autosomal recessive cutis laxa type 1 C

ATPase : Adenosine triphosphatase

AUC : Analytical ultracentrifugation

BLI : Biolayer interferometry

cbEGF : Calcium binding epidermal growth factor

CD : Circular dichroism

CL : Cutis laxa

EBP : Elastin binding protein

ECM : Extracellular matrix

EGF : Epidermal growth factor

FBLN4 : Fibulin-4

FBLN5 : Fibulin-5

GAGs : Glycosaminoglycans

KDa : Kilodalton

LAP : Latent associated propeptide

LLC : Large latent complex

LOX : Lysyl oxidase

LTBP : Latent TGFβ binding protein

LTBP4 : Latent TGFβ binding protein 4

LTBP4S: Latent TGFβ binding protein 4 short isoform

LTBP4L: Latent TGFβ binding protein 4 long isoform

MAGP : Microfibril-associated glycoproteins

MALS : Multi-angle light scattering

mRNA : Messenger ribonucleic acid

nM : Nanomolar

NMR : Nuclear magnetic resonance

P5CS/ALDH18A1 : Delta-1-pyrroline-5-carboxylate synthase

PACE : Paired basic amino acid cleaving enzyme

PG : Proteoglycan

PYCR1 : Pyrroline-5-carboxylate reductase-1

RGD : Arginylglycylaspartic acid

SAXS : Small angle X-ray scattering

SLC : Small latent complex

SPR : Surface plasmon resonance

TB : TGFβ binding protein like

TEM : Transmission electron Microscopy

TGFβ : Transforming growth factor beta

URDS : Urban-Rifkin-Davis syndrome

1. Chapter 1

Introduction

1. Introduction

Latent transforming growth factor β binding protein 4 (LTBP4) is a large secreted multidomain glycoprotein that is associated with the major integral microfibril and elastic fibre component, fibrillin-1 (Saharinen et al., 1998, Zilberberg et al., 2012). LTBP4 is essential for promoting elastic fibre assembly by interacting with the elastogenic proteins, fibulin-4 and fibulin-5 (Noda et al., 2013, Bultmann-Mellin et al., 2016). It is also important for regulating TGFβ-bioavailability by mediating its secretion, sequestration by interacting with fibrillin-1 and thus TGFβ activation (Rifkin, 2005). Mutations in the LTBP4 gene cause functional modifications in both the long and short isoforms of LTBP4, leading to an Autosomal Recessive form of Cutis Laxa (CL) type 1C (ARCL1C), initially known as Urban Rifkin Davis Syndrome (URDS) (Urban et al., 2009). ARCL1C is characterised by severely disrupted elastic fibres and life-threatening pulmonary defects. Despite the importance of LTBP4 for intact elastic fibre architecture, the structure of LTBP4 is not yet defined and how LTBP4 point mutations impact on LTBP4 structure and function is not clear, and is the focus of this thesis. This chapter will briefly present the main ECM components of connective tissue and elastic fibre formation. LTBPs family members will be presented with current understanding of how they are involved in regulating TGFβ bioavailability and more detailed introduction on LTBP4 structure, functions and ECM interactions that are important for LTBP4 deposition and its elastogenic role. A brief introduction on CL and more focus on LTBP4-related CL will also be presented.

1.1. Connective Tissues

Connective tissues consist of cells and continuous networks of fibrous proteins, non-fibrous proteins and proteoglycans that are widely distributed throughout the body providing mechanical support and intercellular exchange between cells, organs, and systems. Together they make up the most abundant connective tissue component, the extracellular matrix (Kailashiya et al., 2017).

1.2. The Extracellular matrix (ECM) of Connective Tissue

The ECM is the non-cellular component within tissues and organs that provides an essential scaffold for cells and controls their communication, migration and differentiation. It also provides a tissue specific biochemical and biomechanical properties such as elasticity, tensile

and compressive strength, and homeostasis. The major components of the extracellular matrix are proteoglycans, glycoproteins and fibrous proteins that are produced intracellularly and secreted by exocytosis (Frantz et al., 2010).

1.2.1. Proteoglycans

Proteoglycans (PGs) are glycosaminoglycans that are covalently linked to a protein core (with the exception of hyaluronic acid). PGs participate with other matrix proteins such as, collagen and elastin in organising the ECM. There are different several types of extracellular GAGs including, heparan sulphate/heparin, chondroitin sulphate, keratan sulphate and hyaluronic acid that are composed of linear polysaccharides composed of repeating units of amino acetyl (N-acetyl) disaccharides usually D-galactosamine alternating with uronic acid. In heparan sulphate/heparin, the disaccharides are mostly found as amino sulphate (N-sulphate). All GAGs except hyaluronic acid, contain sulphate groups linked with hydroxyl groups of the amino sugars in an ester linkage. These groups provide GAGs with high negative charge density making them extremely hydrophilic (Kailashiya et al., 2017). PGs are involved in essential biochemical processes such as cell adhesion, migration, proliferation and signaling (Schaefer and Schaefer, 2010).

1.2.2. Glycoproteins

Glycoproteins are proteins that are extensively post-translationally modified in the endoplasmic reticulum (ER) and Golgi apparatus with glycans. There are two types of protein glycosylation, an N- and O-linked glycosylation. While in N-linked glycosylation, the glycans (N-acetylglucosamine) are covalently attached to the side-chain nitrogen atoms of an asparagine residue at the conserved consensus sequence Asn-X-Ser/Thr, where X is any amino acid except proline. Whereas, in the O-linked glycosylation, the glycan (monosaccharide N-acetylglucosamine) is covalently linked to the side-chain an oxygen atom of hydroxyl amino acids such as serine and threonine residues, hydroxyproline side-chains, or to an oxygen atom of lipids (Li et al., 2019). The N-linked glycosylation occurs initially in the ER and further modification occurs in the Golgi apparatus yielding complex glycans. While the O-linked glycosylation occurs in the Golgi only, thus showing little secondary structure. Protein glycosylation is essential and has impact on proteins' folding and stability and function (Moremen et al., 2012, Li et al., 2019).

1.2.3. Fibrous Proteins

Collagen is the most abundant extracellular fibrous protein secreted by fibroblasts and provides tensile strength to the matrix. To date, 28 types of fibrillar and non-fibrillar collagens have been identified, but collagen type I is the major type and expressed in skin, bone, tendon, dentin, and some other tissues. Collagens also play an important role in regulating cell adhesion, migration, and tissue development (Rozario and DeSimone, 2010). Collagen, is synthesized as a propeptide that undergoes posttranslational modification and cleavage of its N- and C-terminal propeptides forming collagen fibrils. The secreted collagen (tropocollagen) then undergoes maturation by covalent crosslinking by lysyl oxidase (LOX) forming mature collagen fibrils (Kailashiya et al., 2017).

Fibrillin is another major ECM fibrillar protein. To date, three fibrillin isoforms have been identified in human tissue, fibrillin-1, -2 and -3, but fibrillin-1 is the major isoform found in the ECM (Kielty et al., 2005). Fibrillin-1 is initially synthesized by many ECM cells including, fibroblasts, smooth muscle cells and osteoblasts as pro-fibrillin-1 with a molecular weight of about 350 KDa that undergoes intracellular calcium dependent processing via furin/PACE convertases leading to the production of fibrillin-1 with a molecular weight of about 330 KDa (Raghunath et al., 1999, Milewicz et al., 1992). Fibrillin-1 monomers undergo aggregation extracellularly into fibrillar structures, microfibrils, with a diameter of 10-12 nm (Kailashiya et al., 2017). These microfibrils undergo maturation process via inter-microfibrillar cross-linking leading to the formation of a framework of microfibrillar bundles (Kailashiya et al., 2017). Fibrillin microfibrils limit tissue elasticity and act as regulators of growth factor signaling events and as a scaffold for elastin deposition during elastogenesis (Handford et al., 2000, Charbonneau et al., 2004, Hubmacher et al., 2006).

Elastin and fibronectin are also important components of ECM connective tissue. Elastin is an amorphous insoluble protein that is tightly associated with collagen. It provides recoil to tissues. It is initially synthesized and secreted by primarily by fibroblasts and smooth muscle cells as the soluble elastin precursor, tropoelastin. The secreted tropoelastin self-assembles (coacervates) and then cross-link via LOX leading to mature elastin that deposit onto fibrillin microfibrils to form elastic fibres (Lucero and Kagan, 2006, Wagenseil and Mecham, 2007).

Fibronectin is secreted as a dimer disulphide bonded via their C-termini and self-assembles into fibronectin fibrils enhanced by integrins. Fibronectin is directly involved in directing and controlling the organization of other extracellular components and plays an essential role in cell adhesion, cell traction forces, and cell migration during development ((Smith et al., 2007, Rozario and DeSimone, 2010, Wierzbicka-Patynowski and Schwarzbauer, 2003).

1.3. Elastic Fibres

Elastic fibres are major insoluble extracellular matrix (ECM) components that provide connective tissues such as blood vessels, lungs, and skin, and other dynamic connective tissues with essential characteristics of elasticity and resiliency that are necessary for the development of multicellular organisms (Li et al., 1998, Wagenseil and Mecham, 2007). Ultrastructural analysis of normal dermal elastic fibres show that elastin and fibrillin microfibrils are the major components of elastic fibres, where its core consists of cross-linked elastin surrounded by a network of fibrillin microfibrils (Figure 1-1).

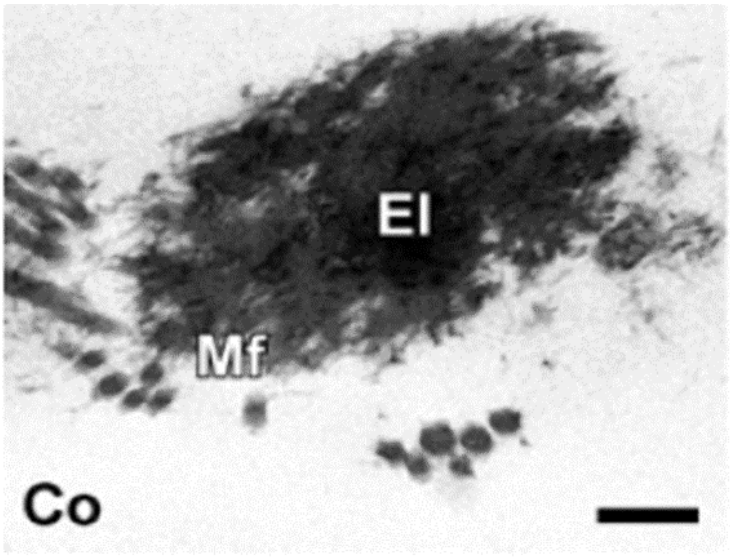

Figure 1-1: Ultrastructure of elastic fibres. Electron microscope image of a normal dermal elastic fibre showing an insoluble elastin core (EI) surrounded by microfibril bundles (Mf). Co, control. Magnification bar represent 0.2 µm. Image was taken from (Urban et al., 2009).

1.3.1. Elastic Fibre Formation (Elastogenesis)

The assembly of elastic fibres is a complicated multi-step process that initially involves synthesis and secretion of fibrillin and elastin precursors, pro-fibrillin and tropoelastin respectively. Then the formation and assembly of mature microfibrils and elastin (Figure 1-2).

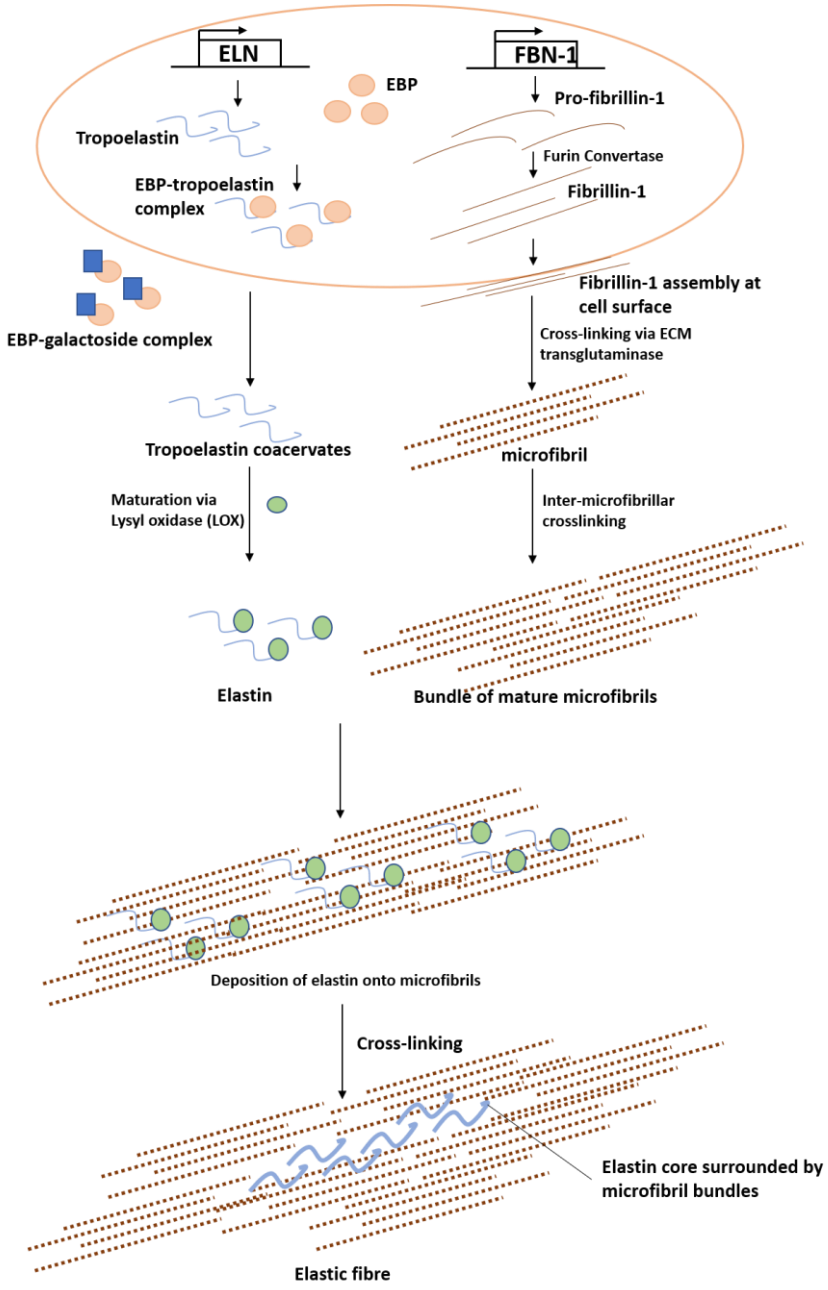

Figure 1-2: Schematic diagram of the stages of elastic fibre formation. Fibrillin-1 is synthesised as pro-fibrillin-1 that is processed by Furin convertase to fibrillin-1. Fibrillin-1 assembles at the cell surface to form the beaded microfibrils that are cross-linked via ECM transglutaminase. The mature microfibrils then form parallel bundles by inter-microfibrillar crosslinking. In elastic tissues, elastin aggregates

deposit on microfibril bundles that act as a scaffold for elastin. Tropoelastin is synthesised and secreted to the extracellular matrix via association with elastin binding protein (EBP). Tropoelastin is then released from EBP-tropoelastin complexes in the presence of galactoside. Tropoelastin coacervates then is cross-linked by lysyl oxidase leading to cross-linked elastin that deposits on microfibrils. The process of deposition and further cross-linking continues to form mature elastic fibres.

Fibrillin microfibrils are widely distributed components in both elastogenic and non-elastogenic ECM of connective tissues. Microfibrils are 10-12 nm in diameter with 56 nm periodicity and are majorly composed of fibrillin-1 molecules (Keene et al., 1991). Newly synthesised fibrillin-1 precursor, pro-fibrillin-1 undergoes intracellular calcium dependent processing via furin/PACE convertases leading to the production of fibrillin-1 (Raghunath et al., 1999, Milewicz et al., 1992). This process is essential for the multimerisation of fibrillin in an aligned linear and lateral manner. The processed C-terminal region of pro-fibrillin, named as asprosin is increased by fasting and involved in regulating glucose homeostasis (Romere et al., 2016). Fibrillins can be multimerised by homotypic and heterotypic interactions between N- terminal and /or C-terminal regions (Kielty et al., 2005). After fibrillin-1 assembly into insoluble microfibrillar arrays at the cell surface it undergoes cross-linking by TG2 (Qian and Glanville, 1997, Ross et al., 1977). Recent ultrastructural analysis revealed that the fibrillin microfibrils are linearly assembled beaded polymers (Figure 1-3) (Godwin et al., 2019, Godwin et al., 2018).

Figure 1-3: Ultrastructure of negatively stained bovine zonular microfibril. Transmission electron microscopy (TEM) image showing the beads on string appearance of the microfibril. Image was taken from (Godwin et al., 2019).

Elastin is initially synthesised as the soluble precursor, tropoelastin with a molecular weight of about 72 KDa (Uitto et al., 1991, Fazio et al., 1988). The intracellular tropoelastin then associates with the elastin binding protein (EBP) in order to prevent intracellular self-association and provide the correct secretion of tropoelastin (Hinek, 1995). Extracellular galactosides can compete for binding to EBP and cause the dissociation of EBP from tropoelastin (Mecham, 1991). The release of EBP from tropoelastin allows the self-association between the hydrophobic domains of tropoelastin. Tropoelastin has the ability to self-associate via a process named coacervation, which concentrates and aligns tropoelastin for cross-linking via LOX and it mainly involves the central hydrophobic domains leading to the formation of mature insoluble elastin (Csiszar, 2001, Siegel et al., 1970). The mature elastin is then deposited onto microfibril scaffolds.

Besides elastin and fibrillins, there are several molecules that have been identified to co-localise with microfibrils and elastic fibres and are required for the association of the elastin core with microfibrils such as, microfibril-associated glycoproteins (MAGPs), fibulins, latent TGFβ binding proteins (LTBP1, 2, 3, and 4) and other ECM proteins reviewed in (Thomson et al., 2019). Among these molecules, fibulin-4, -5, LTBP2 and -4 are the molecules involved in elastogenesis (Kobayashi et al., 2007, Hirai et al., 2007a, Hirai et al., 2007b, Noda et al., 2013)

Fibulins are a family of secreted glycoproteins that function as bridges that stabilise the elastic fibre architecture (Argraves et al., 2003). Fibulin-4 and -5 have been demonstrated to

differently bind tropoelastin, LOX, and fibrillin-1 and have distinct roles in elastic fibre formation (Choudhury et al., 2009, Kobayashi et al., 2007, Papke and Yanagisawa, 2014).

LTBPs are a family of large secreted glycoproteins that are associated with fibrillin microfibrils in the ECM (Todorovic and Rifkin, 2012). Among the LTBPs (LTBP1, 2, 3 and 4) family members, LTBP2 and LTBP4 are involved in elastic fibre formation. LTBP2 is required for the formation of intact microfibril bundles in the ciliary zonules, LTBP4 can compensate LTBP2 and rescue the formation of microfibril bundles in the ciliary zonules by ectopic overexpression in the eye of LTBP2 null mice (Fujikawa et al., 2017).

Genetic defects in one of the elastic fibre constituents may lead to abnormalities in their assembly and loss of function and therefore lead to pathological connective tissue diseases such as cutis laxa (Berk et al., 2012).

1.4. Transforming Growth Factor-β (TGFβ) and Latent TGFβ Binding Proteins (LTBPs)

Transforming growth factor-βs belong to a large superfamily of secreted multipotent growth and differentiation regulators that are implicated in a wide range of biological processes in all tissues of the human body (Weiss and Attisano, 2013, Poniatowski et al., 2015). Three TGFβ isoforms (TGFβ1,2 and 3) have been identified in humans. TGFβ is initially synthesised as a homodimeric proprotein (proTGFβ) associated with its propeptide latency associated propeptide (LAP) forming the small latent complex (SLC) (Figure 1-4). Both proTGFβ and LAP undergo an intracellular cleavage processed via furin. The LAP has strong affinity to the mature TGFβ and thus the proteins are secreted as complex and TGFβ remains inactive (Annes et al., 2003). After SLC intracellular assembly, disulphide exchange occurs between cysteine residues of both LAP and the LTBP leading to the formation of large latent complex (LLC) that is secreted into the extracellular matrix. LTBP binding to the SLC is essential for proper folding and efficient secretion of TGFβ into the extracellular matrix (Saharinen et al., 1999, Rifkin, 2005).

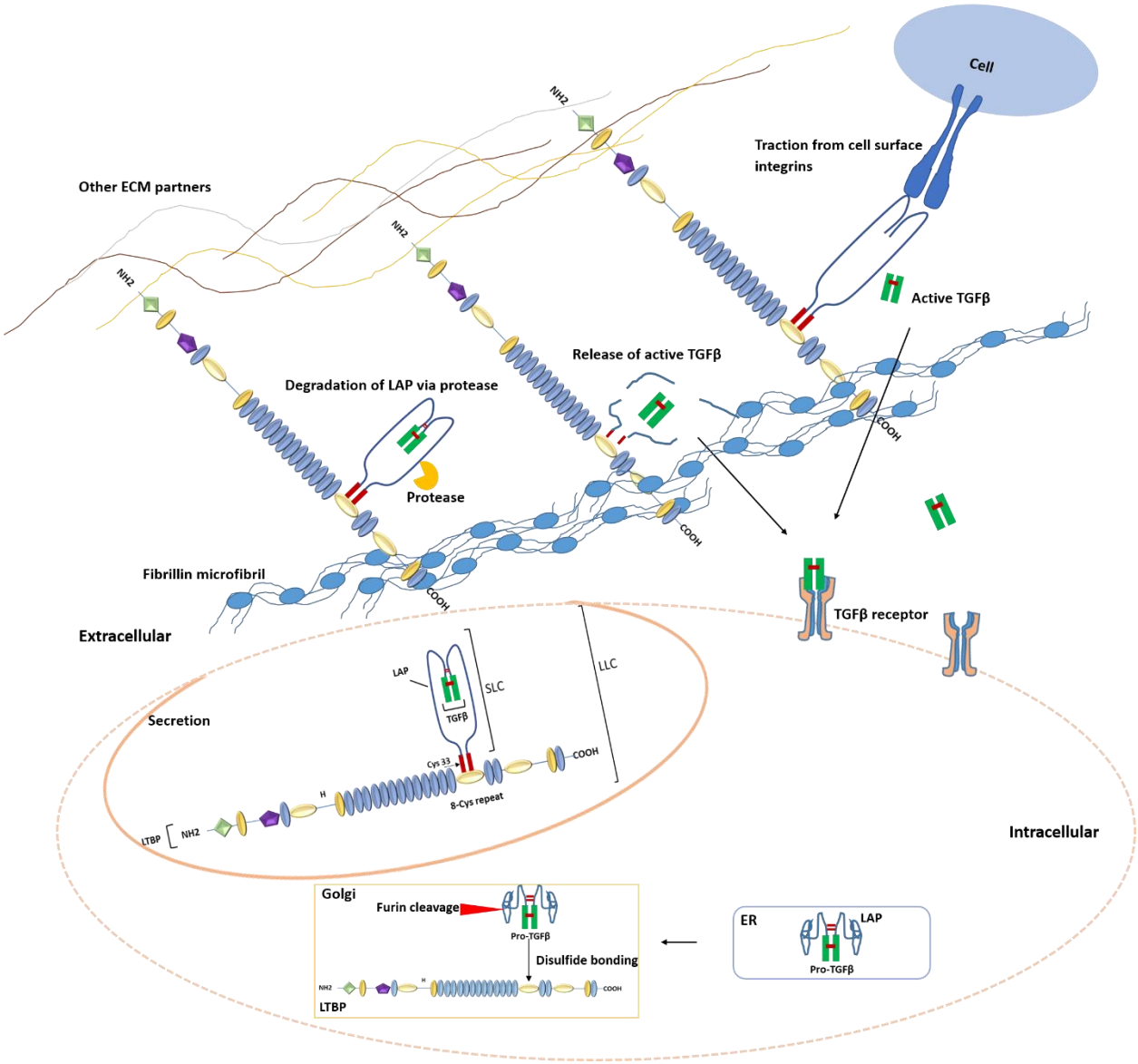

Figure 1-4: Large latent complex (LLC) assembly and TGFβ activation. In the endoplasmic reticulum, pro-TGFβ homodimerizes with its LAP forming the small latent complex (SLC). Then in the trans-Golgi, both Pro-TGFβ and LAP undergo processing via furin, yielding mature TGFβ. The SLC then forms disulphide bonds to LTBP, yielding the LLC. The LLC is then secreted and associates with ECM proteins and the latent TGFβ is activated by proteases or integrins. The activated TGFβ then binds to its receptor.

The domain structures of the LTBPs are highly related to the fibrillins (Figure 1-5). Both LTBPs and fibrillins share two distinct cysteine rich domain types, a six-cysteine domain (Epidermal growth factor-like domain EGF and calcium binding cbEGF-like domain) and eight-cysteine domain (TGFβ binding protein like domain TB) and both perform distinct functions. LTBPs also

exclusively share a four-cysteine domain near their N-terminal region (Todorovic et al., 2005). Each LTBP has three TB domains and a hybrid domain interspersed with EGF-like domains. The hybrid domain is structurally similar to both TB and EGF domains and thus called the hybrid domain (Todorovic and Rifkin, 2012). Moreover, LTBPs have an unstructured hinge region that is susceptible to proteolytic cleavage (Annes et al., 2003, Ge and Greenspan, 2006).

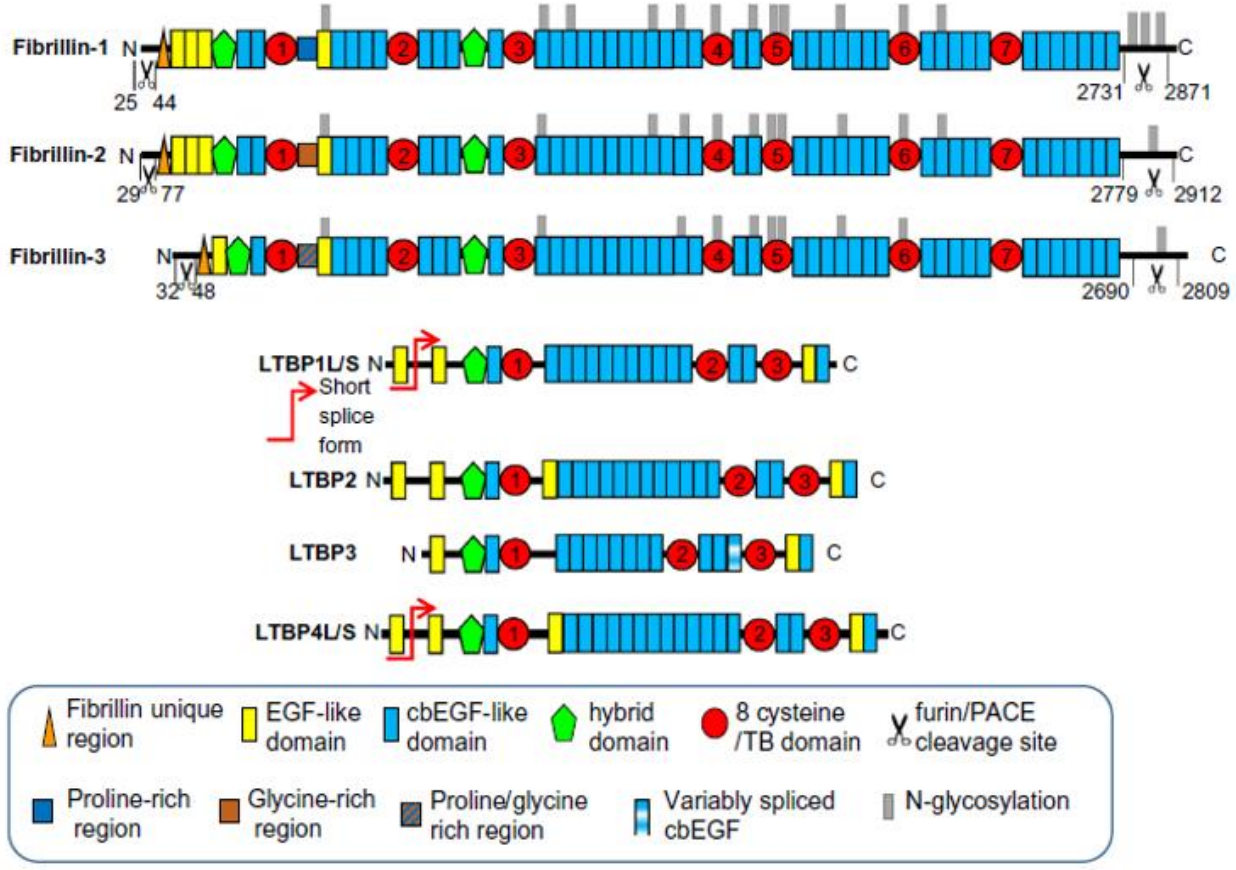

Figure 1-5: Schematic representation of the fibrillins/LTBPs members domain structure. Image was taken from (Godwin et al., 2019).

LTBPs were first identified as a part of the LLC (Kanzaki et al., 1990). All LTBPs except LTBP2, covalently bind to the TGFβ-LAP by disulphide bonding via their TB2 domain (Gleizes et al., 1996, Saharinen et al., 1996, Saharinen et al., 1999). The remaining TB domains of LTBP1, 3, and 4, cannot form covalent bonds with the LAP homodimer of TGFβ. The covalent binding between these LTBPs and the LAP has been demonstrated to be dependent on a specific sequence motif localized between the 6th and 7th conserved cysteine residues within the TB2, that is absent in LTBP2 (Saharinen and Keski-Oja, 2000). Structural studies using nuclear magnetic resonance (NMR) on TB2 domain of LTBP1 has suggested that the dipeptide

insertion before the 7th conserved cysteine leads to the exposure of the sulfhydryl groups of the 2nd and 6th conserved cysteines, allowing the disulphide exchange with the Cys33 of LAP dimer (Lack et al., 2003). This direct disulfide bonding was initially facilitated by a "ring" of five negatively charged amino acids within the third TB2 domain (Chen et al., 2005). In addition to the "ring", four positively charged amino acids surrounding the Cys33 within LAP dimer have been demonstrated to stabilise the disulfide exchange between the SLC and LTBP (Walton et al., 2010).

All LTBPs except LTBP2, bind differently to the TGFβ-LAP. For instance, LTBP1 and LTBP3 bind with strong affinity to all three TGFβ isoforms (TGFβ1, 2, and 3), while LTBP4 binds only TGFβ1 isoform and with weak affinity. The poor interaction between TGFβ1-LAP and LTBP4 has been suggested due to the "ring" within the TB2 domain contained only one negatively charged amino acid (Chen et al., 2005). Indicating that LTBP4 might play less important role in TGFβ extracellular deposition than LTBP1 and LTBP3. Moreover, LTBP4L has been demonstrated to complex more efficiently to TGFβ1-LAP than the LTBP4S (Saharinen and Keski-Oja, 2000). LTBP4L has been also demonstrated to be mainly secreted as part of the LLC, while the LTBPS is mainly secreted free from SLC (Kantola et al., 2010). The difference in binding TGFβ1-LAP between both LTBP4 long and short isoforms suggested isoform specific functions, but no further studies have investigated this hypothesis.

Although, all LTBPs are structurally similar, each possesses different functions in TGFβ biology and homeostasis; this was apparent from the discrete phenotypes linked with their mutations reviewed in (Todorovic and Rifkin, 2012, Robertson et al., 2015, Rifkin et al., 2018). For instance, LTBP1L$^{-/-}$ mice die at birth due to the persistent truncus arteriosis and defective aortic arch (Todorovic et al., 2007). A similar phenotype was observed in LTBP1$^{-/-}$ mice (Horiguchi et al., 2015). To date, no human pathologies have been linked to LTBP1 mutations. Ocular malformations have been linked to LTBP2$^{-/-}$ mutations in humans and mice (Narooie-Nejad et al., 2009, Ali et al., 2009). LTBP3$^{-/-}$ mice and patients display multiple skeletal and craniofacial anomalies including, oligodontia and kyphosis. They also suffer from lung alveolar septation accompanied with decreased levels of TGFβ (Noor et al., 2009, Colarossi et al., 2005, Dabovic et al., 2002). LTBP4$^{-/-}$ mice and patients show complex phenotype that affect craniofacial, musculoskeletal, and visceral organs. They also show skin laxity. Among all LTBPs

associated pathologies, the LTBP4-related phenotype is the most severe human disease. LTBP4 related pathology in mice and humans will be covered in sections 1.5.2 and 1.6.1.

1.5. LTBP4

1.5.1. Domain Structure

LTBP4, as for the other LTBPs, is structurally related to fibrilin-1 (Figure 1-5). It has been demonstrated that the LTBP4 open reading frame codes for a protein that is similar to human LTBP1 and LTBP3 with 1511 amino acids and a molecular mass of 161 KDa (Saharinen et al., 1998). Its domain structure is composed of 20 EGF-like, of which 17 are calcium binding EGF-like repeats (cbEGF), three TB domains, a hybrid domain, and potential protease-sensitive hinge region. It also contains five potential N-linked glycosylation sites and an integrin-mediated cell attachment motif (RGD). Two major isoforms of LTBP4 have been identified in mammalian cells, a long form (LTBP4L) and short form (LTBP4S), produced by alternative splicing (Kantola et al., 2010). LTBP4L and LTBP4S differ in their amino-terminal coding sequence (Saharinen et al., 1998). Both LTBP4 isoforms have distinct tissue expression patterns and are suggested to possess different functions that will be covered in more detail in section 1.5.2.

cbEGF domains contain highly conserved six cysteine residues that form three disulphide bonds in a 1-3, 2-4 and 5-6 pattern. Its secondary structure is mainly composed of β-sheets (Downing et al., 1996). The cbEGF domains of fibrillin-1 have been demonstrated to play a structural role and also protect them from proteolysis by binding to calcium (Smallridge et al., 2003, Reinhardt et al., 1997). TB domains are interspersed between the EGF domains and are characterised by eight conserved cysteines that form four disulphide bonds in a 1-3, 2-6, 4-7 and 5-8 pattern (Yuan et al., 1997). While the hybrid domain has four disulphide bonds conserved in a 1-3, 2-5, 4-6, and 7-8 arrangement (Jensen et al., 2009). The TB domains are composed of β-sheets and a small amount of α-helix. These conserved cysteines in all domain types have been demonstrated to stabilise the domain structures and interdomain interactions in the fibrillin/LTBPs superfamily and substitution of these highly conserved cysteines impact on the conformational integrity of both protein families (Smallridge et al., 2003, Downing et al., 1996, Jensen et al., 2009, Lack et al., 2003).

1.5.2. LTBP4 Functions

LTBP4 has been demonstrated to possess dual independent functions, both TGFβ dependent and independent (Dabovic et al., 2009). Recently, LTBP4 has been shown to compensate for LTBP2 in the ciliary zonule of the eye by restoring the microfibrils in LTBP2$^{-/-}$ mice (Fujikawa et al., 2017). Moreover, LTBP4 has been identified as a genetic modifier for muscular dystrophy (Heydemann et al., 2009). Here we will focus on the role of LTBP4 in TGFβ ECM bioavailability and in elastogenesis that will be covered in sections 1.5.2.1 and 1.5.2.2.

1.5.2.1. ECM TGFβ1 Bioavailability

Both long and short LTBP4 isoforms have been identified as regulators for TGFβ1 bioavailability in the ECM (Saharinen et al., 1998, Saharinen et al., 1999, Lack et al., 2003). The literature on the role of LTBP4 in regulating TGFβ by direct interaction with LAP was inconsistent (Rifkin et al., 2018). However, lung and skin fibroblasts from LTBP4S$^{-/-}$ mice and skin fibroblasts from human were demonstrated to show dysregulated TGFβ signaling, indicating LTBP4 as a regulator for TGFβ signaling (Urban et al., 2009).

LTBP4S$^{-/-}$ mice showed severe pulmonary emphysema, cardiomyopathy and colorectal cancer associated with reduced extracellular deposition of TGFβ1 (Sterner-Kock et al., 2002). The immunohistochemical analysis using anti-TGFβ1 antibodies demonstrated that the lung, colon and heart of these mice, lacked extracellular TGFβ1 but not intracellular TGFβ1. This suggested that LTBP4 is required for the secretion and deposition of the SLC into the ECM. Consistent with the reduced extracellular TGFβ1 deposition, TGFβ1 signaling was significantly reduced in the affected tissues. These data show that LTBP4 is essential for TGFβ1 activity in lung, colon and heart of LTBP4S knockout mice (Sterner-Kock et al., 2002). In line with the previous *in vivo* study (Sterner-Kock et al., 2002), cultured lung fibroblasts from LTBP4S$^{-/-}$ mice showed decreased amounts of active TGFβ1. These data indicate that the loss of LTBP4S causes impaired TGFβ1 secretion and activation. However, further study on these mice showed that TGFβ signaling was increased in skin and lung fibroblasts (Dabovic et al., 2009). A more recent study investigated whether LTBP4 binding to TGFβ1-LAP plays a functional role in regulating TGFβ1 ECM bioavailability (Dabovic et al., 2015), where mice were generated with the two highly conserved cysteine residues (Cys 1235 and 1260 in the TB2 domain of LTBP4) that bind to TGFβ1-LAP were replaced with serine residues. Preventing disulfide bond

formation between LTBP4 and TGFβ1-LAP did not affect the lung development and elastic fibre formation of LTBP4$^{cc>ss}$ mice (Dabovic et al., 2015). This is inconsistent with previous studies on other LTBPs that have shown inhibition of the disulphide bond between TGFβ1-LAP and LTBPs yielded similar pathological phenotypes as observed in TGFβ1$^{-/-}$ mice (Yoshinaga et al., 2008, Shibahara et al., 2013). These data suggested that LTBP4 may play a TGFβ-independent role in the lung.

ARCL1C patients with mutated LTBP4, displayed severely defective pulmonary, gastrointestinal, urinary, musculoskeletal, craniofacial and dermal development (Urban et al., 2009). Skin fibroblasts from these patients showed decreased expression and secretion of LTBP4 accompanied with increased activity of TGFβ1 signaling. Consistent with the normal TGFβ expression observed in LTBP4S knockout mice lung, colon and heart (Sterner-Kock et al., 2002), ARCL1C patients' fibroblasts showed normal TGFβ1 mRNA. This has suggested that decreased expression of LTBP4 causes increased TGFβ ECM bioavailability but not TGFβ biosynthesis (Urban et al., 2009).

1.5.2.2. Elastogenesis

1.5.2.2.1. TGFβ Dependence

Both LTBP4$^{-/-}$ mice and ARCL1C patients show similar phenotype of severely disrupted elastic fibre assembly and die during early infancy due to respiratory failure (Bultmann-Mellin et al., 2015, Urban et al., 2009). Lack of LTBP4 causes the formation of large globular aggregates of elastin adjacent to microfibril bundles in addition to poor incorporation of elastin polymers into microfibril bundles (Urban et al., 2009, Dabovic et al., 2009).

ARCL1C show defective ECM accompanied with dysregulation of TGFβ activity and signaling (Urban et al., 2009). Neutralising the increased TGFβ signaling accompanied with the defective air-sac septation and elastic fibres in the lungs of LTBP4S$^{-/-}$ mice, normalised the TGFβ and rescued the air-sac septation but not elastogenesis. This has suggested that the LTBP4 role in elastogenesis is TGFβ independent (Dabovic et al., 2009). However, the defective air-sac septation was not rescued by normalising TGFβ1 nor TGFβ3, but by lowering TGFβ2 level only, indicating that the abnormal air-sac septation is associated with excessive TGFβ2 level. LTBP4S$^{-/-}$; TGFβ2$^{-/-}$ mice show normal air-sac septation but still have abnormal elastic fibres, indicating that the abnormal elastic fibre formation is caused by LTBP4S

deficiency and is not directly associated with TGFβ2 signaling and that LTBP4 plays an essential structural role. The lack of direct association between elastic fibre formation and TGFβ2 signaling in LTBP4S$^{-/-}$ is consistent with a previous finding that LTBP4 is capable of binding to the TGFβ1 isoform only (Saharinen et al., 1999).

However, human dermal fibroblasts (HDFs) showed normal and linear elastin deposition on microfibrils along with LTBP4. Whereas LTBP4S knockdown cell culture lacked elastin deposition. The defective elastin deposition was rescued by the addition of recombinant LTBP4S (rLTBP4S). Moreover, the rLTBP4S enhanced elastic fibre formation and maturation in a dose-dependent manner. Interestingly, both LTBP4S knockdown or addition of rLTBP4S did not affect the mRNA expression of other elastic fibre components, except elastin. Both the rescued elastin and the added rLTBP4S colocalised with fibrillin-1, suggesting that LTBP4 regulates the deposition of elastin onto the microfibril scaffold (Noda et al., 2013). TGFβ is a multipotent growth factor that increases the expression of elastic fibre proteins (Roberts et al., 1990). Therefore, more studies were needed to investigate whether the elastogenic role of LTBP4 is TGFβ1-dependent. It has been demonstrated that the addition of active TGFβ1 into LTBP4 knockdown HDF culture medium did not rescue the elastic fibre defect. Whereas, the addition of the rLTBP4S + eLAP (empty LAP without TGFβ1) enhanced elastic fibre assembly as effectively as TGFβ-LAP bound rLTBP4S, indicating that the elastogenic role of LTBP4 is TGFβ-independent. Consistent with the previous study that demonstrated that LTBP4S possesses two independent roles in regulating elastogenesis and TGFβ1 signaling in lungs (Dabovic et al., 2009).

1.5.2.2.2. Role of Fibulins on LTBP4-Elastogenesis

Fibulin-5 has been shown to promote elastic fibre formation and maturation in human skin fibroblasts (Hirai et al., 2007a) and LTBP4 has been shown to specifically interact with fibulin-5 and promote elastogenesis (Noda et al., 2013, Bultmann-Mellin et al., 2015). Therefore, the elastogenic role of LTBP4S was further studied using LTBP4 knockdown HDFs and recombinant fibulin-5 and LTBP4S to investigate whether the elastogenic role of LTBP4 is fibulin-5 dependent. These cells lacked elastin deposition that was rescued by addition of rLTBP4 and elastogenesis was enhanced in a dose dependent. While addition of rFibulin-5 into the medium of these cells enhanced elastic fibre formation but in an abnormal punctate pattern, presumably due to the absence of LTBP4S that act as a carrier protein for elastin-fibulin-5 complex leading to defective deposition of the added fibulin-5 (Noda et al., 2013). The punctate pattern of fibulin-5 was also observed in the skin and lung of LTBP4S$^{-/-}$ mice. Using solid-phase binding assays, LTBP4S indirectly interacts with tropoelastin and its elastogenic role is mediated by via fibulin-5 that directly binds tropoelastin (Noda et al., 2013), indicating that the elastogenic role of LTBP4S is fibulin-5 dependent.

LTBP4S$^{-/-}$ mice show non-fibrillar elastin aggregates and short intact elastic fibres (Urban et al., 2009) , while LTBP4S$^{-/-}$; fibulin-5$^{-/-}$ mice show some intact fibrillar elastic fibres (Noda et al., 2013). In contrast, LTBP4S$^{-/-}$; fibulin-4$^{R/R}$ mice show completely fragmented elastic fibres and no intact elastic fibres were present (Bultmann-Mellin et al., 2016). Similar elastic fibre pathology was observed in LTBP4$^{-/-}$ mice (Bultmann-Mellin et al., 2015). However, the formation of intact fibrillar elastin and elastic fibres in LTBP4S$^{-/-}$; fibulin-5$^{-/-}$ mice indicated an alternative elastogenesis pathway likely involving both LTBP4L and fibulin-4 (Dabovic et al., 2015, Bultmann-Mellin et al., 2015).

Fibulin-4 has been demonstrated to aid elastic fibre assembly and maturation by recruiting LOX to tropoelastin in HDFs (Horiguchi et al., 2009). A functional interaction between LTBP4 and fibulin-4 has been reported (Bultmann-Mellin et al., 2015, Bultmann-Mellin et al., 2016, Kumra et al., 2019). LTBP4S$^{-/-}$; Fibulin-4$^{R/R}$ mice that have normal expression of the long isoform of LTBP4, reduced expression of fibulin-4, and normal expression of fibulin-5, showed severely impaired elastogenesis in lungs and the mice died in early postnatal period (Bultmann-Mellin et al., 2016). This indicated that fibulin-5 cannot compensate for fibulin-4

in LTBP4S$^{-/-}$; Fibulin-4$^{R/R}$ mice, while fibulin-4 can partially compensate for fibulin-5 as observed in LTBP4S$^{-/-}$; fibulin-5$^{-/-}$ mice (Bultmann-Mellin et al., 2015, Dabovic et al., 2015). Moreover, the difference in elastic fibre formation between LTBP4S$^{-/-}$; fibulin-5$^{-/-}$ and LTBP4S$^{-/-}$; Fibulin-4$^{R/R}$ mice, led to the speculation that LTBP4L preferentially binds to fibulin-4 rather than fibulin-5 *in vivo*, while LTBP4S preferentially binds to fibulin-5. This was further confirmed by binding studies (Bultmann-Mellin et al., 2015), covered in sections 1.5.3.4 and 1.5.3.5.

1.5.3. LTBP4 Extracellular interactions

The molecular mechanism by which LTBP4 regulates elastic fibre formation is incompletely understood but LTBP4 interacts with other extracellular matrix proteins that are involved in elastic fibre formation and thus enhances elastogenesis. Disruption of LTBP4 interactions with these ECM proteins might lead to the formation of defective elastic fibres.

1.5.3.1. Interaction with Fibronectin

Fibronectin is the first deposited ECM component that regulates and directs the assembly and deposition of other ECM proteins (Wierzbicka-Patynowski and Schwarzbauer, 2003, Zilberberg et al., 2012).

Previous research has demonstrated that FN$^{-/-}$ mouse fibroblast matrix lacked ECM deposition of LTBP4 (Kantola et al., 2008). Although early FN$^{-/-}$ cell culture mainly lacked LTBP4, minor quantities of LTBP4 were detected occasionally in these cells' matrices, indicating that there might be another protein that may mediate LTBP4 matrix incorporation. Addition of exogenous FN into FN$^{-/-}$ cell culture rescued the matrix deposition of LTBP4. Interestingly, LTBP4 deposits and colocalises with fibronectin in early fibroblast ECM then it colocalised with fibrillin-1 in matured cultures (Kantola et al., 2008). This finding was in line with an earlier study that showed that LTBP4 deposits after 7 days from fibronectin meshwork in human lung fibroblast culture then it colocalises with fibrillin-1 after matrix maturation in a fibronectin independent manner (Koli et al., 2005), indicating the requirement of fibronectin for the early ECM assembly and deposition of LTBP4. However, more recent study demonstrated that fibrillin-1$^{-/-}$ fibroblasts matrix that normally produce and deposit fibronectin, lacked LTBP4 deposition (Zilberberg et al., 2012).

Using solid-phase binding assays, LTBP4S has been demonstrated to directly bind with fibronectin via its N-terminal region (Kantola et al., 2008). Deletion of LTBP4 N-terminal region containing the 1st and 2nd 8-cys domain prevented this direct interaction, indicating that these two domains might be involved in the interaction with fibronectin.

No further studies have investigated the LTBP4 interaction with fibronectin. Fibroblast cultures from patients with a frameshift mutation in LTBP4 showed reduced colocalisation with fibronectin and abnormal microfibrils (Callewaert et al., 2013). However, the deposition of fibronectin was normal in all fibroblast cultures from patients with other mutations in LTBP4 (Urban et al., 2009) and lung fibroblast cultures from LTBP4S$^{-/-}$ and LTBP4$^{-/-}$ mice also showed normal fibronectin matrix deposition (Bultmann-Mellin et al., 2015).

1.5.3.2. Interaction with Heparan Sulphate

Heparan sulphate (HS) is a ubiquitous GAG that is expressed in the ECM and on the cell surface. It is synthesised in the Golgi apparatus of several different cells. Heparin is highly structurally related to HS and is a more sulphated variant that is produced by mast cells. Both HS and heparin are involved in the regulation of several biological processes such as cell adhesion and cell matrix assembly and immunity via their interaction with several proteins (Meneghetti et al., 2015, Dreyfuss et al., 2009, Simon Davis and Parish, 2013).

The heparin binding of LTBP4S has been demonstrated using heparin affinity chromatography (Kantola et al., 2008). LTBP4S possesses heparin binding sites at both its N- and C-termini, but the N-terminal region shows stronger binding than the C-terminal region. This interaction was increased with the addition of exogeneous human plasma fibronectin, but was inhibited with the addition of soluble heparin, indicating the specificity of this interaction (Kantola et al., 2008)

It has been shown that the LTBP4S C-terminal region mediated both human and mouse lung fibroblast adhesion (Kantola et al., 2008). Further analysis has been done to investigate the significance of the LTBP4 C-terminal region heparin binding site on cell adhesion. While cell adhesion to LTBP4 C-terminal was inhibited by the addition of soluble heparin, confirming the involvement of LTBP4S C-terminal region heparin binding site in supporting fibroblast adhesion. In contrast, the N-terminal region heparin binding sites did not support cell adhesion but were suggested to mediate LTBP4 ECM targeting, as addition of soluble heparin

inhibited LTBP4 matrix deposition in dose dependent manner (Kantola et al., 2008). To our knowledge, no studies have further investigated this interaction.

1.5.3.3. Interaction with Fibrillin-1

Fibrillin-1 is an essential ECM glycoprotein in both elastic and non-elastic tissues. It is the major component of the microfibrils that are required for the normal fibrillogenesis of the connective tissues. Fibrillin-1 microfibrils also act as anchors in non-elastic tissues (Kielty et al., 2005). Several ECM proteins interact with fibrillin-1 and regulate the formation of elastic fibres (Thomson et al., 2019).

Previous studies have shown that LTBP4 associates with fibrillin-1 in mature fibroblast cultures (Koli et al., 2005, Kantola et al., 2008). An *in vitro* study has demonstrated that, fibrillin-$1^{-/-}$ dermal fibroblasts lacked fibrillin-1 and LTBP4 matrix deposition even after matrix maturation but showed normal expression of LTBP4 (Ono et al., 2009). In contrast, fibrillin-$2^{-/-}$ fibroblasts showed normal deposition of fibrillin-1 and LTBP4. Moreover, immunostaining using LTBP4 antibodies on wildtype, fibrillin-$1^{-/-}$ and fibrillin-$2^{-/-}$ mice skin tissue, demonstrated fibrillar patterns similar to that of fibrillin-1 fibrillar patterns in both wildtype and fibrillin-$2^{-/-}$ but significantly reduces LTBP4 staining in fibrillin-$1^{-/-}$ compared with the wild type tissue (Ono et al., 2009). These data suggested that fibrillin-1 is required for the matrix assembly and deposition of LTBP4. The association between LTBP4 and fibrillin-1 is mediated by the C-terminal region of LTBP4 and the N-terminal region of fibrillin-1 (Ono et al., 2009, Isogai et al., 2003).

Further investigations on the interaction between LTBP4 and fibrillin-1 have been performed using surface plasmon resonance (SPR) binding and the 1^{st} hybrid domain of fibrillin-1 has been shown to majorly contribute to this direct interaction with binding affinity of 24 nM, and deletion of this domain prevented interaction with LTBP4 C-terminal (Choi et al., 2009). Moreover, the N164S fibrillin-1 mutation that is associated with dominant ectopia lentis (Comeglio et al., 2002, Ono et al., 2009), showed reduced binding to the LTBP4 C-terminal region compared with wildtype fibrillin-1, suggesting that the disruption of this interaction might contribute to ectopia lentis (Ono et al., 2009).

Skin fibroblasts from patients with homozygous premature termination mutations in LTBP4, showed normal and robust deposition of fibrillin-1 but lacked LTBP4 ECM deposition (Urban

et al., 2009, Callewaert et al., 2013). However, no study to date has examined the impact of LTBP4 mutations on the interaction with fibrillin-1.

1.5.3.4. Interaction with Fibulin-5

Fibulin-5 is an elastin binding ECM protein that promotes elastogenesis by acting as chaperone and directing elastin deposition onto microfibrils scaffolds (Choudhury et al., 2009). Impaired matrix deposition of fibulin-5 causes the formation of abnormal elastin aggregates that are poorly deposited onto microfibrils (Hirai et al., 2007a, Choi et al., 2009).

Fibulin-5 has been shown to specifically colocalise with LTBP4 in mice lung and skin tissues (Noda et al., 2013, Dabovic et al., 2015). LTBP4 knockdown abolished fibulin-5 deposition, while the addition of recombinant LTBP4S rescued the linear deposition of fibulin-5. In contrast, the addition of recombinant fibulin-5 into LTBP4 knockdown culture, did not deposit linearly on microfibrils, indicating the requirement of LTBP4 for fibulin-5 ECM deposition (Noda et al., 2013).

In vitro and *in vivo* studies on lungs and skin tissues of LTBP4S$^{-/-}$ and LTBP4$^{-/-}$ mice demonstrated that lack of LTBP4S and or LTBP4 disrupted the matrix assembly of the fibulin-5-elastin complex and showed punctate globular patterns rather than fibrillar patterns of deposited fibulin-5-elastin complex compared to wildtype, suggesting the requirement of LTBP4 for normal ECM deposition of fibulin-5 and elastin (Dabovic et al., 2015, Noda et al., 2013, Bultmann-Mellin et al., 2015).

In vitro binding assays by immunoprecipitation and solid-phase binding using shortened fragments of both LTBP4 short and long isoforms, and showed that only the N-terminal region fragment of both LTBP4 isoforms directly interact with fibulin-5. Fibulin-5 binding site in LTBP4 isoforms was defined, where the four-cysteine domain within the N-terminal region was involved and the binding site on fibulin-5 was the C-terminal region, as deletion of this region ablated the interaction (Noda et al., 2013).

Further study has investigated the direct interaction between LTBP4 and fibulin-5 using SPR analysis to measure the binding affinity (Bultmann-Mellin et al., 2015). SPR analysis showed that the N-terminal region of LTBP4 isoforms directly interact with the full length fibulin-5 with different binding affinities. The long isoform of LTBP4 showed stronger binding to fibulin-

5 than the short isoform (K_D of 2.4 and 15.8 nM, respectively) (Bultmann-Mellin et al., 2015). However, no study to date has tested whether LTBP4 mutations impact on the interaction with fibulin-5.

1.5.3.5. Interaction with Fibulin-4

Fibulin-4 has been demonstrated to enhance elastic fibre formation by tethering lysyl oxidase (LOX) to tropoelastin leading to the maturation of elastic fibres. Lack of fibulin-4 matrix deposition in fibulin-$4^{-/-}$ mice and reduced expression of fibulin-4 in fibulin-$4^{R/R}$ mice caused the formation of defective elastic fibres (Horiguchi et al., 2009, McLaughlin et al., 2006).

Fibulin-4 has been shown to colocalise with LTBP4 and deposit linearly in lung fibroblasts of wildtype mice (Bultmann-Mellin et al., 2015). Fibulin-4 deposition in $LTBPS^{-/-}$ was comparable to that in wildtype mice, whereas fibulin-4 deposition in $LTBP4^{-/-}$ mice was defective in a punctate pattern rather than fibrillar. The difference in fibulin-4 deposition between these strains supported an interaction between LTBP4 and fibulin-4. A direct interaction between LTBP4 and fibulin-4 has been demonstrated using SPR binding assays where the N-terminal region of both LTBP4 isoforms bound to full-length fibulin-4.The long isoform showed higher binding affinity than the short isoform to fibulin-4 with a K_D of 3.1 and 15.4 nM, respectively (Bultmann-Mellin et al., 2015). However, no previous study has examined the impact of LTBP4 mutations on the interaction with fibulin-4.

1.6. Cutis Laxa (Elastolysis)

Cutis laxa (CL), is a group of rare inherited or acquired disorders, characterised by generalised loose and redundant skin with loss of elasticity and resilience creating a premature ageing appearance as a result of abnormal elastic fibres (Berk et al., 2012). This group of disorders has a wide range of symptoms and clinical features (Uitto et al., 2013). CL may be inherited in autosomal dominant, autosomal recessive or X-linked recessive manners. To date, mutations in 13 genes have been reported to cause CL (Mohamed et al., 2014, Van Damme et al., 2017). Acquired CL cases associated with inflammatory reactions or hematological malignancies have also been reported (McCarty et al., 1996, Timmer et al., 2009, Lewis et al., 2004). Although the inherited forms of CL are rare, the autosomal recessive cutis laxa (ARCL) is the

most prevalent and heterogeneous type due to the clinical overlap between the subtypes of this form (Berk et al., 2012, Morava et al., 2009).

Autosomal recessive cutis laxa (ARCL) is divided into types (ARCL1-3) based on specific symptoms and the causative gene. And each type is further divided into subtypes. ARCL1 includes ALCL1A, ARCL1B, and ARCL1C that are caused by mutations in fibulin5 (FBLN5), fibulin4 (FBLN4), and Latent TGFβ binding protein 4 (LTBP4) genes, respectively (Loeys et al., 2002, Hucthagowder et al., 2006, Urban et al., 2009). ARCL2 includes ARCL2A and ARCL2B caused by mutations in ATPase, H+ transporting, lysosomal V0 subunit a2 (ATP6V0A2) and Pyrroline-5-carboxylate reductase 1 (PYCR1), respectively (Kornak et al., 2008, Reversade et al., 2009). Finally, the ARCL3 overlaps with the ARCL2 subtypes is also caused by same mutations as ARCL2 or by mutations in Delta-1-pyrroline-5-carboxylate synthetase (P5CS)/ALDH18A1 gene (Bicknell et al., 2008, Guernsey et al., 2009, Leao-Teles et al., 2010).

LTBP4 is the focus of this thesis, thus the LTBP4-related cutis laxa will be covered in more detail in section 1.6.1.

1.6.1. LTBP4-Related Cutis Laxa (ARCL1C)

The LTBP4-related cutis laxa, is an autosomal recessive form of CL type 1C (ARCL1C), also known as Urban Rifkin Davis Syndrome (URDS), caused by mutations in the LTBP4 gene in humans reviewed in (Ritelli et al., 2019) summarized in Table 1-1.

Table 1-1: ARCL1C-causing mutations of LTBP4.

Patient	Cons.	Status	Exon	cDNA	Protein	Type	Domains	References
P1	+	Hom	12	c.1450del	p.(Arg484Glyfs*290)	Frameshift-PTC	-	(Ritelli et al., 2019)
P2	+	Hom	28	c.3554del	p.(Gln1185Argfs*27)	Frameshift-PTC	Second 8-Cys domain	(Urban et al., 2009)
P3	–	Comp. Het	9	c.791del	p.(Pro264Argfs*37)	Frameshift-PTC	Hybrid domain	
			22	c.2570_2571delGCinsAA	p.(Cys857*)	Frameshift-PTC	Eleventh EGF-like domain	
P4	+	Hom	9	c.820T>G	p.(Cys274Gly)	Missense	Hybrid domain	
P5	–	Comp. Het	22	c.2570_2571delGCinsAA	p.(Cys857*)	Frameshift-PTC	Eleventh EGF-like domain	
			33	c.4127dup	p.(Arg1377Alafs*27)	Frameshift-PTC	Third 8-Cys domain	
P6	–	Comp. Het	11	c.1342C>T	p.(Arg448*)	Nonsense	First 8-Cys domain	(Callewaert et al., 2013)
			31	c.4115dup	p.(Tyr1373Ilefs*2)	Frameshift-PTC	Third 8-Cys domain	
P7	+	Hom	19	c.2408C>A	p.(Ser803*)	Nonsense	Seventh EGF-like domain	
P8	–	Comp. Het	28	c.3661C>T	p.(Gln1221*)	Nonsense	Second 8-Cys domain	
			29	c.3886C>T	p.(Gln1296*)	Nonsense	Fourteenth EGF-like domain	
P9		Homo	6	c.780+2T>G	-	Splicing	-	
P10	+	Homo	11	c.1263del	p.(Cys422Alafs*352)	Frameshift-PTC	First 8-Cys domain	
P11	+	Homo	15	c.1851C>A	p.(Cys617*)	Nonsense	Second EGF-like domain	
P12	+	Homo	31	c.4127dup	p.(Arg1377Alafs*27)	Frameshift-PTC	Third 8-Cys domain	
P13	+	Homo	31	c.4128C>T	p.(Arg1377*)	Nonsense	Third 8-Cys domain	
P14	+	Homo	26	c.3556T>C	p.(Cys1186Arg)	Missense	Second 8-Cys domain	
P15	–	Comp. Het	7	c.883+1G>T	-	Splicing	Hybrid domain	(Su et al., 2015)
			17	c.2161C>T	p.(Arg721*)	Nonsense	Eighth EGF-like domain	
P16	–	Comp. Het	18	c.2377_2378insA	p.(Gly793Glufs*5)	Frameshift-PTC	Ninth EGF-like domain	
			29	c.3856T>A	p.(Cys1286Ser)	Missense	Eighteenth EGF-like domain	
P17	–	Comp. Het	20	c.2632G>T	p.(Gly878*)	Nonsense	Eleventh EGF-like domain	
			31	c.4113dup	p.(Ala1372Argfs*3)	Frameshift-PTC	Third 8-Cys domain	
P18	+	Hom	5	c.341−1G>C	-	Splicing	First EGF-like domain	

Table 1-1: Exons and mutations numbering are based on transcript NM_003573.2, NP_003564.2; Cons, consanguinity; Comp. het., compound heterozygous, Hom, homozygous, PTC, premature termination codon. The table was modified from (Ritelli et al., 2019).

ARCL1C, as other cutis laxa forms, is characterised by generalised skin laxity as a result of defective elastic fibres, but is also accompanied with other manifestations such as craniofacial, pulmonary, gastrointestinal and genitourinary anomalies.

ARCL1C patients usually die during infancy due to respiratory failure (Urban et al., 2009, Callewaert et al., 2013, Ritelli et al., 2019). *LTBPS* $^{-/-}$ mice also have elastic fibre pathology similar to that of ARCL1C patients (Figure 1-6) (Urban et al., 2009). These mice also have severe pulmonary and gastrointestinal defects but survive to adulthood. The milder phenotype seen in *LTBPS* $^{-/-}$ mice may be due to the expression of *LTBP4L* in these mice (Dabovic et al., 2009, Sterner-Kock et al., 2002). Indeed, *LTBP4*$^{-/-}$ mice nearly replicate the phenotype of ARCL1C (Bultmann-Mellin et al., 2015).

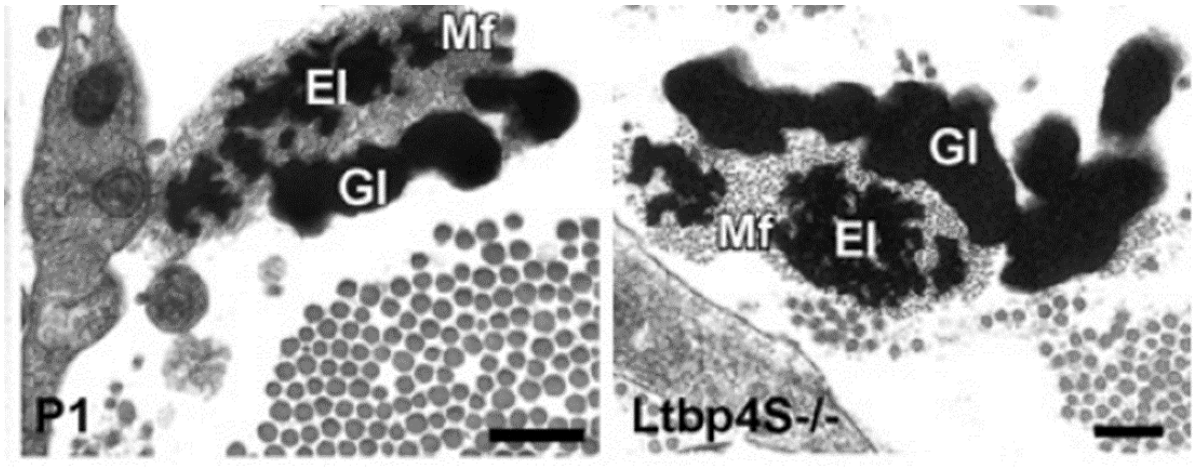

Figure 1-6: Ultrastructure of elastic fibres in ARCL1C patient and LTBP4S$^{-/-}$ mouse. Electron microscope images of defective dermal elastic fibre showing diminished elastin core (EI) and large aggregates of globular elastin (GI) that are adjacent to microfibril bundles (Mf) in ARCL1C patient (left panel) and in LTBP4S-/- mice (right panel). Magnification bar represent 0.2 µm. Images were taken from (Urban et al., 2009).

To date, only 18 ARCL1C patients have been reported (Callewaert et al., 2013, Urban et al., 2009, Ritelli et al., 2019, Su et al., 2015). Frameshift, nonsense, and splice mutations are the most frequent LTBP4 mutations that lead to premature termination and severely reduced LTBP4 mRNA expression. Missense mutations in LTBP4 were also reported (reviewed by (Ritelli et al., 2019)).

LTBP4 missense mutations, the focus of this thesis, affect highly conserved cysteine residues within the hybrid (Urban et al., 2009), the 16th cbEGF (Su et al., 2015), and the 3rd 8-Cys/TB2 (Callewaert et al., 2013) domains. Substitution of these cysteines has been demonstrated to interfere with the structure and function of LTBPs and fibrillin (Jensen et al., 2009, Lack et al., 2003). Therefore, this thesis will focus on the structure of LTBP4, its interactions with other ECM partners and the impact of LTBP4 point mutations.

1.7. Biophysical Characterisation of LTBP4 Monomers

The structure and hydrodynamic properties of LTBP4 is not known yet. Here a number of complementary biophysical techniques was used to structurally characterise LTBP4 N- and C-termini monomers to gain information on its structure, dynamics and function. LTBP4 binding with other ECM protein was investigated using surface-based binding techniques that determine binding kinetics in real-time.

1.7.1. Size-Exclusion Chromatography with Multi-Angle Laser Light Scattering (SEC-MALS)

SEC-MALS is widely used static light scattering technique to separate proteins based on hydrodynamic size and to determine the concentration and the absolute molecular mass of the separated proteins by measuring the absorbance at 280 nm and the differential refractive index (dRI) of the scattered light of a protein sample that hit by intense laser beam. As the measured intensity of scattered light is proportional to molecular mass and concentration. It also can be used to measure the radius of gyration (R_g) in an angular dependence for proteins larger than 10 nm. The R_g of proteins smaller than 10 nm can be measured by small-angle X-ray scattering. SEC-MALS can use a detector that detects the fluctuations in the intensity of the scattered light over time and estimate the hydrodynamic radius of the protein (R_h). Both R_g and R_h describe the size but use different means. R_g is defined as the mass weighted average distance from the core of a molecule to each mass element in the molecule. While, R_h is the apparent size adopted by solvated molecule. The ratio of R_g/R_h can provide information about the shape of the molecule. Globular proteins have a ratio of 0.775, if proteins deviate from this ratio then they are considered as non-globular proteins (Beirne et al., 2011, Espinosa-de la Garza et al., 2015).

The advantages of SEC-MALS, widely used and accepted for quantitative assessment of oligomers and aggregates, it directly determines the molecular mass and overcomes limitations of column calibration. The disadvantages of SEC-MALS, limited size range and is invaluable for characterising peptides and heterogeneous polymers (Espinosa-de la Garza et al., 2015, Beirne et al., 2011).

1.7.2. Analytical Ultracentrifugation (AUC)

AUC is a hydrodynamic technique that separates protein species in solution, without the use of stationary phase as in SEC, under a strong centrifugal force. It also determines the sedimentation rate of the protein by real-time continues monitoring the UV absorbance to provide size distribution profile of the protein species. Two methods can be applied, the sedimentation velocity that provides hydrodynamic information and equilibrium velocity that provides thermodynamic information (Howlett et al., 2006, Laue, 1995). Here sedimentation velocity (SV-AUC) at 20^{o}C was used to provide information about LTBP4 proteins homogeneity/heterogeneity and to detect the presence of aggregates. SV-AUC provides information about, size, shape, and approximate molecular mass of the studied protein (Howlett et al., 2006). The principle of SV-AUC is based on three forces that act on the molecule; the sedimentation force and the opposing forces, the buoyant and frictional forces. The sedimentation force of a molecule must be stronger than the opposing forces to be sedimented at the bottom of the cell, therefore gravitational force is used to allow for protein particles to migrate according to their mass. The sedimentation coefficient (s), the ratio of the velocity to the centrifugal field can be determined by balancing the applied forces using the Svedberg equation;

$$s = v/ \omega^2 r = M_b/ f$$

Where v is the partial specific volume of the particle, ω is the rotor speed in radians per second, r is the distance from the centre of the rotor, M_b , the buoyant mass of the particle, and ƒ is the frictional coefficient (Fujita, 1975, Williams et al., 1958). This equation indicates that s is proportional to the buoyant molar mass, M_b, and inversely proportional to the frictional coefficient, ƒ. Diffusion is another force that opposes S and ƒ. Diffusion causes the sedimenting boundary to spread with time.

Lamm equation (sedimentation boundary modle) describes the sedimentation and diffusion of a molecule under centrifugal force. It shows the evolution of concentration distribution variations of a molecule in a centrifugal field as a function of time with two competing forces; diffusion and sedimentation.

$$\frac{\partial c}{\partial t} = D\left[\frac{\partial^2 c}{\partial r^2} + \frac{1}{r}\frac{\partial c}{\partial r}\right] - s\omega^2\left[r\frac{\partial c}{\partial r} + 2c\right]$$

Where c is the weight concentration of macromolecules and t is time. The optical systems on the analytical ultracentrifuge provides the radial concentration distribution at time intervals during the experiment. By taking the ratio of s/D through Svedberg equation that describes the sedimentation rate of a macromolecule;

$s/D = M_b/RT$

where R is the gas constant and T is the absolute temperature. This indicates that the s/D ratio is proportional to the buoyant molar mass (Philo, 1994). The sedimentation coefficient is expressed in Svedberg (Schuck, 2000). There are different meddles can be used for data analysis. Here the sedimentation coefficient distribution c (s) analysis was used to calculate the sedimentation distribution of protein species based on the Lamm equation, where the differential sedimentation distribution c (s) is plotted against the sedimentation coefficient which was determined by the mathematical data analysis program SEDFIT (Schuck, 2000, Philo, 1994). Advantages of the AUC, it is direct and native proteins can be used with minimal sample preparation. The disadvantages of this technique, is low throughput and impractical to use as a routine method (Liu et al., 2006).

1.7.3. Circular Dichroism (CD)

CD measures the difference in absorption of circularly polarised light that arise from structural asymmetry (Greenfield, 2006). Here, the Far-UV (195-260), that is dependent on peptides, was used. A beam of light that has a time dependent electric and magnetic fields is associated with the CD instrument (Jasco). The obtained CD data was reported in milli degree was deconvoluted to estimate the secondary structure content of LTBP4 N- and C-termini. Each secondary structure content has characterised CD spectra for instance, α-helix has negative

peaks at 222 and 208 nm and a positive peak at 193 nm, β-pleated sheets (β-helices) have negative peak at 218 nm and positive peak at 195 nm5, while disordered structure has very low spectra above 210 nm and negative peak near 195 nm (Holzwarth and Doty, 1965, Greenfield and Fasman, 1969, Venyaminov et al., 1993). CD spectra are collected in high transparency quartz cuvettes with path length ranging from 0.01 – 1 cm. Different methods can be used to analyse CD data, here CONTIN and CDSSTR that gave me the best fit were used (Sreerama and Woody, 2000). CD is rapid and sensitive to asymmetry in sample structure, while its limitations are, provides qualitative data only, cannot be used for atomic level structure analysis (Greenfield, 2006).

1.7.4. Small-Angle X-ray Scattering (SAXS)

SAXS is a powerful analytical technique used for nanostructure analysis. It measures the intensities of X-rays scattered by a solution of particles usually placed in a quartz capillary illuminated by a collimated monochromatic X-ray beam as a function of the scattering angle. Here a pure monodisperse protein samples were used to characterise LTBP4 structure. The scattering pattern of the solvent must be subtracted from the scattering data of the protein solution leaving only the scattering data from the protein particles that can be used to determine the structural parameters of the particle including, size, molecular mass, shape, and flexibility. SAXS data can also be used to determine a low revolution reconstruction of the protein structure (Svergun, 1999, Svergun et al., 2001, Kikhney and Svergun, 2015). Due to the randomly oriented protein articles in a solution, the scattering pattern is isotropic, thus the scattering is recorded by 2-dimentional detector that is averaged. The scattering intensity I is represented as a function of momentum transfers;

$I = 4\pi \sin \theta / \lambda$

Where λ is the beam wavelength and 2θ is the scattering angle. The Rg of the protein particle can be estimated from SAXS data using the Guinier approximation at very small angles (Mertens and Svergun, 2010). The averaged data can be transformed using indirect Fourier transform (IFT) to distance distribution function p (r) that provides the inter-atomic distance in real space and the maximum dimension D_{max} of the particle. SAXS data provides several indicators of the presence of protein flexibility using the Kratky plot that provide sensitive means of monitoring the degree of compactness (Uversky and Dunker, 2010). The low-

resolution solution structure of the protein molecule can be modelled *ab initio* using Dummy Atom Model Minimisation (DAMMIN/DAMMIF) program and DAMAFVER is used to average the ab initio models (Franke and Svergun, 2009, Svergun, 2003). The advantages of SAXS, is a versatile technique for quantitative structural characterisation, no size limitation, native proteins can be used with minimal sample preparation, it ideally complements electron microscopy and nuclear magnetic resonance methods because it provides representative structural information, while the main limitation is the complexity in data fitting and analysis (Tuukkanen et al., 2017).

1.7.5. Surface Plasmon Resonance (SPR)

SPR is a label-free biomolecular interaction technique that measures real-time binding affinities, kinetics and thermodynamic parameters of interacting molecules. SPR uses thin gold films as biosensors. The SPR signal originates from changes in the refractive index (RI) at the surface of the gold biosensor chip. The increase in mass at the surface of the sensor associated with the binding event causes proportional increase in the RI, observed as change in response. The changes in RI are measured as changes in response angle of the refracted light when the analyte binds to the ligand and thus increasing the density at the sensor chip. Several different concentrations of analyte are used to obtain the binding curves that are fit to a binding modle to determine the kinetic binding constants including the binding affinity (K_D), association rate constant K_a, and dissociation rate constant K_d (Nguyen et al., 2015, Souto et al., 2019). The benefits of SPR are, label-free detection, real-time quantitative data, sensitivity and accuracy, small sample quantity is required. While its limitations are, expensive sensors and maintenance, surface preparation is required, air-bubble using the fluidic system, immibilisation of one ligand so its not very practical, the amine coupling is a multi-step and requires reagents that must be freshly prepared with each immobilisation, and its moderate throughput (Drescher et al., 2009, Li et al., 2006, Wang and Fan, 2016).

1.7.6. Biolayer Interferometry (BLI)

BLI is another label-free biomolecular interaction technique that measures real-time binding affinities and kinetics (K_D, K_a, and K_d) of interacting molecules. It analyses the interference pattern of white light reflected from two optical surfaces; a layer of immobilised ligand on the biosensor tip and an internal reference layer. The binding event between a ligand and an

analyte results in an increase in the density (optical thickness) at the biosensor tip resulting in a shift in the interference pattern (Concepcion et al., 2009). As in SPR, several different concentrations of analyte are used to obtain the binding curves. The benefits of this technique are, label-free detection, real-time data, high throughput, fluidic-free system so less maintenance needed, no surface preparation, biotinylated proteins can be stored and reused, and small sample quantity is required. The disadvantage of BLI is its less sensitivity compared to SPR and expensive biosensor tips (Sanders et al., 2016, Sun et al., 2013).

1. 8. Project Aims

Despite the importance of LTBP4 for intact elastic fibre architecture, its structure is not yet defined and the molecular mechanism by which it regulates elastic fibre assembly is poorly understood. Moreover, the structural and functional outcome of ARCL1C causing missense mutations that lead to severely defective elastic fibre assembly was not investigated. Three ARCL1C missense mutations have been reported (Urban et al., 2009, Su et al., 2015, Callewaert et al., 2013), C244G, C1186S and C1286R, where highly conserved cysteines have been replaced within the hybrid, the cbEGF16, and the TB2 domains, respectively. However, only clinical characterization studies have been published on these mutations. The main hypothesis of this thesis was that the substitution of the highly conserved cysteines affects LTBP4 structure and molecular interactions that are involved in elastic fibre assembly and LTBP4 matrix deposition.

LTBP4 shows sequence similarity with LTBP1 and both LTBP4 and LTBP1 bind equally to the C-terminal region of fibrillin-1 (Isogai et al., 2003). LTBP1 has the capacity to self-assemble and cross-link via TG2 forming filamentous structures (Troilo et al., 2016). LTBP1 can be cross-linked to fibrillin-1 by TG2 cross-linking assays (Steer, 2014). Moreover, both LTBP4 and LTBP1 are covalently linked to the ECM. It has been shown that LTBP1 cross-links to fibronectin, while it is not known yet to which ECM proteins LTBP4 is covalently linked and whether TG2 is implicated in this cross-linking (Zilberberg et al., 2012). It has been demonstrated that LTBP4 associates with fibrillin-1 and that fibrillin-1 is essential for LTBP4 matrix deposition (Zilberberg et al., 2012). LTBP1 also has been demonstrated to interact with SLC non-covalently (Saharinen and Keski-Oja, 2000). This data led to the hypothesis that LTBP4 may

also self-interact or interact with LTBP1, LTBP4 may self-cross-link or cross-link to fibrillin-1 by TG2, and LTBP4 may non-covalently interact with SLC.

Therefore, this thesis aimed to understand how ARCL1C causing mutations impact on LTBP4 structure and molecular interaction with other matrix partners and to investigate whether LTBP4 can self-interact or cross-link, whether LTBP4 can be cross-linked to fibrillin-1 by TG2, and whether LTBP4 can interact non-covalently with SLC.

This will be addressed via the following aims:

1. To express and purify wildtype and mutant recombinant human LTBP4 in HEK293-EBNA cells to yield sufficient protein for characterisation.
2. To determine the LTBP4 structure and how this is disturbed in ARCL1C using complementary methods including, multi-angle light scattering (MALS), small angle X-ray scattering (SAXS), circular dichroism (CD) and analytical ultracentrifugation (AUC). Wildtype human LTBP4 will be compared with ARCL1C mutants to analyze differences in their behavior and conformation.
3. To investigate LTBP4 interactions with other extracellular proteins, and determine if the interactions are disrupted when introducing ARCL1C mutations, using surface plasmon resonance (SPR) and biolayer interferometry (BLI). Interactions with ECM proteins will be compared for both wildtype LTBP4 and ARCL1C mutations.
4. To investigate LTBP4 self-interaction using SPR and self-cross-linking and cross-linking with fibrillin-1 by TG2 using cross-linking assays.
5. To investigate LTBP4 non-covalent interaction with SLC using SPR.

The studies in this thesis have been written as a paper draft and the aims will be addressed in three separate paper drafts.

1.8.1. Paper draft 1: Autosomal recessive Cutis Laxa 1C Mutations Disrupt the Structure and Interactions of Latent TGFβ binding protein 4 (LTBP4)

This paper draft aims to characterize LTBP4 C-terminal region and compare its hydrodynamic properties to LTBP4 C-terminal region ARCL1C-causing point mutations. This paper draft also aimed to investigate whether ARCL1C mutations impact on LTBP4 interaction with fibrillin-1.

1.8.2. Structural and Functional Consequences of a Point mutation in the N-terminal region of LTBP4 in Autosomal Recessive Cutis Laxa type 1C

Continuing on paper draft 1, this paper aims to determine the hydrodynamic properties of LTBP4 N-terminal region and compare it to that one of the LTBP4 N-terminal region ARCL1C-causing point mutation. This paper draft also investigates whether ARCL1C N-terminal point mutation interferes with LTBP4 interaction with fibulin-4, fibulin-5, fibronectin and heparan sulphate.

1.8.3. Functional similarities and interaction between Latent TGFβ binding protein 4 and Latent TGFβ binding protein 1

Since LTBP1 is the most studied LTBP member and LTBP4 is highly structurally related to it, this paper draft aims to compare LTBP4 to LTBP1 on its capacity to self-assemble or cross-link. This paper draft also investigated whether LTBP4 cross-link to fibrillin-1. Moreover, this paper aimed to investigate whether LTBP4 non-covalently interacts with TGFβ.

1.9. Author Contributions

1.9.1. Autosomal recessive Cutis Laxa 1C Mutations Disrupt the Structure and Interactions of Latent TGFβ binding protein 4 (LTBP4)

Status: Un-published

Authors: Yasmene F. Alanazi, Michael P. Lockhart-Cairns, Anthony S. Weiss and Clair Baldock

Contributions: The original idea for this study was convinced by Clair Baldock. I performed all the experiments in this paper draft including the supplementary experiments, except loading protein sample in the SEC-SAXS column that was performed by Michael P. Lockhart-Cairns. Michael P. Lockhart-Cairns also provided me a training for SAXS data processing. Anthony S. Weiss provided the tropoelastin for binding experiments. I wrote the paper draft with Clair Baldock guidance and revision.

1.9.2. Structural and Functional Consequences of a Point mutation in the N-terminal region of LTBP4 in Autosomal Recessive Cutis Laxa type 1C

Status: Un-published

Authors: Yasmene F. Alanazi, Michael P. Lockhart-Cairns, and Clair Baldock

Contributions: The original idea for this study was convinced by Clair Baldock. I performed all the experiments in this paper draft including the supplementary experiments, except loading protein sample in the SEC-SAXS column that was performed by Michael P. Lockhart-Cairns. I wrote the paper draft with Clair Baldock guidance.

1.9.3. Functional similarities and interaction between Latent TGFβ binding protein 4 and Latent TGFβ binding protein 1

Status: Un-published

Authors: Yasmene F. Alanazi, Thomson J, and Clair Baldock

Contributions: The original idea for this study was convinced by Clair Baldock. I performed all the experiments in this paper draft including the supplementary experiments except the SPR of the LTBP1 C-terminal interaction with fibrillin-1 (PF3) fragment was done by Thomson J. I wrote the paper draft with Clair Baldock guidance.

2. Chapter 2

Materials and Methods

2. Materials and Methods

2.1. Materials

2.1.1. Plasmid Vectors

The vectors utilized were, the pCEP-Pu/Ac7 vector, a derivative of the pCEP4 mammalian expression vector (Appendix 2) (Life Technologies). These vectors contain the BM40 signal sequenced that allows for increased protein expression. Moreover, these vectors acquired puromycin resistance from the transformed cells.

2.1.2. Bacterial strains

The bacterial strains used were, NEB 10-beta Competent E. coli, a derivative of the DH10B (New England Biolabs).

2.1.3. Mammalian expression cell lines

Human embryonic kidney (HEK) 293 cells that stably express the Epstein-Barr virus nuclear antigen-1 (EBNA) were available in the lab prior to the start of this project (Troilo et al., 2014). The expression of the EBNA-1 gene is constrictively controlled by the CMV promoter. The HEK293-EBNA cells were transfected with pCEP-Pu/AC7 expression vector containing C-terminally tagged with a thrombin cleavage site (LVPRGS) and six-histidine residue tag (6x His-tag) wildtype N-terminal LTBP4S (residues 29-394), mutant C244G, wildtype C-terminal (residues 1114-1557), mutants C1286S and C1186R that were available in the lab.

2.1.4. Antibodies

Anti-His_6 tag primary antibodies (R & D Systems) and donkey anti-mouse secondary antibodies (LI-COR). 2.2. Basic Molecular Biology

2.2.1. NEB 10-beta competent E. coli transformation of LTBP4 constructs and isolation of Positive colonies from LB Agar Plates

2 µL of each wildtype LTBP4 and mutant constructed vector was transformed into 20 µL of 10-Beta Competent E. coli cells, incubated on ice for 30 minutes then heat-shocked at 42°C for 45 seconds. Cells were immediately placed back on ice for 2 minutes. 500 µL of warmed

Super Optimal broth (SOC) media (Thermo Fisher Scientific) were added to the transformations and grown in 37°C shaking incubator for an hour. The mixture was centrifuged at 200 x *g* for a minute and 250 µL of the SOC media was discarded. The cells were re-suspended with the remaining 250 µL of SOC media. 75µL of the transformed cells were then plated onto solidified LB agar plates containing ampicillin (100 µg/mL). finally, the plates were incubated at 37°C overnight to allow for selection.

2.2.2. Inoculation and growth of bacterial culture

Using sterile inoculating loop, a single colony from the ampicillin containing LB agar plate was picked and transferred into 50 mL centrifuge tube (Corning) containing 15mL Luria broth (LB) media supplemented with ampicillin (100 µg/ml). The LB bacterial culture was then grown overnight in a 37°C shaking incubator to grow up sufficient numbers of bacteria necessary to isolate plasmid DNA.

2.2.3. Miniprep purification of LTBP4 expression vectors

Minipreps were performed on the overnight cell cultures to isolate the expression vectors using QIAprep Spin Miniprep Kit according to the manufacture's protocol (Qiagen). Briefly, a 15 mL of the overnight cell culture was pelleted by centrifugation at 10000 x *g.* The pelleted cells were then re-suspended in a 250 µL of re-suspension buffer P1 (with added RNase) and then transferred to a 1.5 mL microcentrifuge tube. 250 µL of lysis buffer P2 was added, mixed thoroughly and allowed for the lysis reaction to proceed for 5 minutes. 350 µL of the neutralizing buffer N3 was added and immediately mixed gently. The precipitant was pelleted by centrifugation at 10000 x *g* for 10 minutes. The supernatant was transferred into the QIAprep spin column and centrifuged for 60 seconds. The bound DNA was washed with 750 µL of the washing buffer PE and centrifuged for 60 seconds followed by an additional step of 1-minute centrifugation to remove the excess material. The purified DNA was eluted from the spin column by 50 µL of sterile water that was incubated for 1 minute before centrifugation for 1 minute. The purified DNA was quantified using nanodrop instrument. The DNA was stored at -20 °C.

2.3. Recombinant protein expression in HEK293-EBNA

2.3.1. HEK-293 EBNA cell culture

HEK-293 EBNA cells were initially seeded in T75 culture flasks (Corning) using 15 mL growth media (Dulbecco's modified Eagle's medium DMEM (Sigma-Aldrich) supplemented with 1% glutamine, 1% penicillin/streptomycin, and 10% fetal bovine serum). Cells were grown for 48 h at 37°C and 5% CO2, until confluent. Cells were passaged by removing the growth media and washing the cells in the T75 cell culture flask (Corning) (with 10 mL Phosphate buffered saline (PBS) (Sigma). Cells were then trypsinised by adding 2 mL of trypsin-EDTA (Sigma), leaving it for 2-3 min to allow adherent cells to detach. Trypsin was inhibited and cells were suspended by adding 10 mL of growth media. Trypsinised cells were centrifuged at 1000 *g* and resuspended in 5ml of growth media in a T27 cell culture flask. Suspended cells were then passaged and seeded at a 1:10 dilution.

2.3.2. Stable Episomal vector transfection of HEK293-EBNA cells

Mammalian expression vector pCEP-Pu/AC7 containing the His-tagged LTBP4 constructs were transfected into 70-80 % confluent HEK-293 EBNA cell culture using Lipofectamine 3000 reagent according to the manufacture's protocol (Invitrogen). Briefly, LTBP4 construct was mixed with diluted P3000 reagent with 125 µL of serum free Opti-MEM media (DMEM4 mixed in a 1:1 ratio with F12-HAMS supplemented with 5% (v/v) of Penicillin/Streptomycin mixture). Lipofectamine 3000 reagent was also diluted with serum free media. The diluted mixtures were then combined and incubated at room temperature for 5 minutes. The mixture was then added to the semiconfluent cell culture and incubated overnight at 37°C and 5% CO2. The cells then were passaged as previously described in (section 2.3.1.) using media supplemented with 2 µg/mL of puromycin (Gibco) to select the transfected cells. Cell selection last for a period of 2-3 weeks.

2.3.3. Storage of transfected HEK293-EBNA cells

Following successful stable Episomal transfection of the HEK293-EBNA cells, cells were grown until 90-100% confluency. The confluent culture was then trypsinised and centrifuged as previously described in (section 2.3.1.). The centrifuged cells were resuspended using freezing media (Thermo Fisher SCIENTIFIC), aliquoted in 1mL and frozen at -80^{O}C.

2.3.4. Expression of recombinant LTBP4 constructs in HEK293-EBNA cells

Stored transfected HEK293-EBNA cells were thawed at 37^{o}C and resuspended in 9 mL growth media and seeded in T75 cell culture flask. Cells were grown at same conditions mentioned in (section 2.3.1.) until 100% confluency. Cells were then passaged to larger culture flask T225 followed by HYPER flasks using growth media. 100 % confluent cells were then washed with 200-300 mL of serum free Opti-MEM media (DMEM4 mixed in a 1:1 ratio with F12-HAMS supplemented with 5% (v/v) of Penicillin/Streptomycin mixture). After washing, confluent cells were incubated at 37°C and 5% CO2 with serum free media.

2.3.5. Expression media harvest

Serum free expression media from confluent transfected HEK293-EBNA cells was collected every 3-4 days. The collected media was replaced with fresh serum free media. The collected serum free media was stored at -20^{o}C. For protein purification, the stored media was thawed at room temperature, filtered using vacuum and 65µm (Whatmann N. 1) filter paper to remove cellular debris.

2.4. Purification of recombinant proteins from harvested media

2.4.1. Nickle affinity chromatography

Filtered media was purified using 5 mL His-Trap column (GE Healthcare). The column was washed with water then equilibrated with 10 column volume of binding buffer (10 mM Tris, 500 mM NaCl, 10mM imidazole, pH 7.8). The media was passed through the column overnight at 2ml/min. the column was then washed using 50-60 mL of binding buffer at 1 mL/min. For protein elution, 50 mL of elution buffer (10 mM Tris, 500 mM NaCl, 500 mM imidazole) was used at a flow rate of 0.5 mL/min. 0.5 mL eluates were collected and protein yield and purity were

assessed by Sodium Dodecyl Sulphate-Polyacrylamide gel electrophoresis. The highest protein fractions were further purified using Size-exclusion chromatography.

2.4.2. Size exclusion chromatography

The most concentrated protein fractions further purified by size-exclusion chromatography on an AKTA purifier FPLC using a Superdex 200 10/300GL column (GE Healthcare), that was equilibrated with buffer containing 10 mM Tris, 150 mM NaCl, pH 7.8 at a flow rate of 0.5 ml/min. 1mL of protein sample was injected into the column at a flow rate of 0.5 ml/min. Eluates were collected in 0.5 mL fractions monitored by absorbance at 280 nm. Protein purity was assesed by SDS-PAGE under reducing and non-educing conditions. Protein concentration was determined using Bicinchoninic acid (BCA) protein assay.

2.5. Purity assessment and concentration determination of purified proteins

2.5.1. Purity assessment by SDS-PAGE

Using precast 4-12% NuPAGE SDS-PAGE gel (Thermo Fisher SCIENTIFIC), (4x) LDL NuPAGE buffer (Life Technologies) was diluted with protein sample in a ratio of 1:4 was loaded under either non-reducing and reducing (2-Mercaptoethanol) conditions. Electrophoresis was performed at 180V at room temperature for 50 min – 1hour using 50mM MOPS or MES running buffer (Thermo Fisher SCIENTIFIC) in X-Cell Surelock Minicell electrophoresis system (Thermo Fisher SCIENTIFIC). See-blue Plus2 pre-stained standard (Thermo Fisher SCIENTIFIC) was used for molecular weight assessment. Protein bands were visualized using instant Blue following the manufacture's protocol (Expendion).

2.5.2. Concentration determination by BCA

Purified recombinant wildtype and mutant protein concentration was determined using the BCA assay according to the manufacture's protocol (Thermo Fisher SCIENTIFIC). Bovine serum albumin (BSA) protein standards at known range of concentration (0 – 2 mg/mL) was used. The assay was carried out in a 96 well microplate, where the known protein sample (10 µL/well) and the BSA standard (10 µL/well) were separately added to the BCA reagent (200 µL/well). The plate was incubated at 37°C for 30 minutes and the absorbance at 570 nm was measured using a Dynex MRX II microtitre plate reader with Revolution software.

2.6. De-glycosylation of recombinant protein

Purified recombinant wildtype and mutant proteins were digested using PNGase-F according to the manufacturer's protocol (New England's Biolabs). 20 µg of protein was incubated with 2 µL of GlycoBuffer 2 (10X) and 5 µL of PNGase F at 37^{o}C for 24 hours. The removal of glycans was verified using SDS-PAGE as previously described in (section 2.5.1.).

2.7. Cross-linking

Cross-linking assay was performed using guinea pig liver-derived commercial transglutaminase-2 (TG2) (Sigma-Aldrich). Cross-linking assays of LTBP4 with tropoelastin, fibulin-5, fibrillin-1 were performed with TG2. TG2 was incubated with proteins in a ratio of 0.1:1 for 2 hours at 30 °C in 10 mM HEPES, 150 mM NaCl pH 7.4 buffer containing 1 mM CaCl2. Equal molar ratios of cross-linking proteins were used. Cross-linked proteins were then analysed by SDS-PAGE as previously described in (section 2.5.1.).

2.8. Biophysical characterisation of recombinant protein

2.8.1. Multi-angle Light Scattering (MALS)

Purified recombinant wildtype and mutant protein samples (0.5 ml at approximately 0.4 - 1 mg/ml) were passed into a Superdex 200 10/300GL column (GE Healthcare) running at a flow rate of 0.5 ml/min using a buffer containing 10 mM Tris, 150 mM NaCl, pH 7.8. Eluted protein fractions were passed from the column into a Wyatt DAWN Heleos II EOS 18 angle laser photometer that measures the intensity of scattered light at 18 angles with QELS detector (Wyatt Technologies) that detects the fluctuations in the intensity of scattered light to determine the hydrodynamic radius (R_h) of the protein. The QELS is connected to an Optilab T-rEX refractive index detector that detects the absolute refractive index to determine the absolute molecular mass. The absolute molar mass, concentration and hydrodynamic radius of the resulting peaks were analyzed using ASTRA 6.

2.8.2. Sedimentation Velocity Analytical Ultracentrifugation (SV-AUC)

Monomeric recombinant wildtype and mutant protein samples (0.4 - 1 mg/ml) in the same buffer as used in MALS (section 2.7.1.) were characterised by sedimentation velocity SV-AUC

using Beckman XL-A analytical ultracentrifuge with an An60Ti 4-hole rotor running at 45,000 rpm at 20°C. The sedimenting boundary was monitored at either 280 or 230 nm for 200 scans. Data were analyzed by continuous model-based distribution C(s) of Lamm equation solutions method using SEDFIT software (Schuck, 2000). The resulting sedimentation coefficients were corrected to standard conditions using SEDNTERP software (Philo, 2000).

2.8.3. Small-angle Light Scattering (SAXS)

In-line SEC-SAXS was performed on purified wildtype and mutant proteins at a concentration range of 1 - 2 mg/ml in the same buffer used for MALS and SV-AUC. Wildtype LTBP4 N- and C-termini and C1286S SAXS data were collected at 1 second intervals using 45 µL purified protein sample passed through a Superdex 200 3.2/300 column at beamline BM29, European synchrotron radiation facility (Grenoble, France), while SAXS data for C1186R were collected at B21 at Diamond. SAXS data were pre-processed and reduced by EDNA, inhouse ESRF software(http://www.esrf.eu/home/UsersAndScience/Experiments/MX/About_our_beamlines/bm29/computing-environment/edna.html; last accessed September 2017). For each frame with a consistently similar radius of gyration (Rg) across the elution peak, the protein scattering intensities were merged. SAXS data were then analyzed and buffer scattering subtracted from that of the sample using ScAtter software (http://www.bioisis.net/tutorial/9; last accessed October 2018). The Rg of the protein was estimated by Guinier analysis and the intraparticle distance distribution function P(r) in real space were evaluated using the Indirect Fourier transform (IFT) program GNOM, and particle shapes were modelled *ab initio* using DAMMIN software in slow mode (Franke and Svergun, 2009). Ten *ab initio* models were generated and aligned and superimposed to generate a single model using the DAMAVER suite (Svergun, 2003). The goodness of the superimpositions of the 10 models compared using DAMSEL was estimated by the normalized spatial discrepancy (NSD).

2.8.4. Circular Dichroism (CD)

The purified wildtype and mutant proteins, at a concentration range of 0.5 - 1 mg/ml in 10 mM Tris, 150 mM NaCl, pH7.8 buffer, were analysed by circular dichroism (CD) using the Far-UV spectral region (190-260 nm). The Far-UV spectra were recorded in millidegrees (mdeg) by Jasco-J810 spectropolarimeter. Measurements were taken every 0.2 mm in a 0.5 cm path

length cell at 25 °C. 10 accumulated scans were recorded, averaged, and corrected for each construct. The secondary structure content was quantitatively analyzed by the online tool Dichroweb (http://dichroweb.cryst.bbk.ac.uk/html/home.shtml; last accessed October 2018) using CDSSTR and CONTIN algorithms.

2.9. Interaction characterisation of recombinant protein

2.9.1. Surface Plasmon Resonance (SPR)

Kinetics of fibrillin-1 PF3 fragment (residues 1-722) (Rock et al., 2004) and LTBP4 wildtype and mutant C-terminal region binding were measured in real time using SPR ProteOn system at 25 °C. Fibrillin-1 was diluted in 10 mM HEPES, 150mM NaCl, pH7.4 supplemented with 0.005% (v/v) Tween-20 and then injected at a range of concentrations from 100-0 nM over a constant concentration of immobilised LTBP4 on amine coupling GLC sensor chip using the manufacturer's instructions (Bio-Rad). All binding experiments for each LTBP4 construct were performed at least 2 times. The sensor chip surface was regenerated using 10 mM glycine at pH 2.5. Equilibrium analysis was used to determine kinetic parameters.

2.9.2 Bio-layer interferometry (BLI)

BLI using OctetRED96 (ForteBio) system was performed for measuring the kinetics of the interaction of wildtype and mutant LTBP4 with full-length tropoelastin, fibronectin, fibulin-4, fibulin-5, heparan sulphate, LTBP1 and SLC in real time. Biotinylated proteins were diluted in 10 mM HEPES, 150 NaCl, pH7.4 buffer supplemented with 0.005% (v/v) Tween-20 and then immobilized at 200nM constant concentration on Streptavidin biosensors tips surface. The biosensors immobilized with biotinylated proteins were then incubated with the analyte diluted at a range of concentrations. The biosensor surface was regenerated using 10 mM glycine at pH 2.5. The binding kinetics was analyzed using Octet software version 7 (ForteBio). The goodness of binding data fitting was assessed by X2 and R2 values. All binding experiments were performed in solid-black 96 well plates at 25C° with an agitation speed of 1000 rpm and repeated at least 2-3 times.

3. Chapter 3

Autosomal recessive Cutis Laxa 1C Mutations Disrupt the Structure and Interactions of Latent TGFβ binding protein 4 (LTBP4)

Autosomal recessive Cutis Laxa 1C Mutations Disrupt the Structure and Interactions of Latent TGFβ binding protein 4 (LTBP4)

Yasmene F. Alanazi[1], Michael P. Lockhart-Cairns[1], Anthony S. Weiss[2,3,4] and Clair Baldock[1]

Wellcome Trust Centre for Cell Matrix Research, Division of Cell Matrix Biology and Regenerative Medicine, School of Biological Science, Faculty of Biology, Medicine and Health, Manchester Academic Health Science Centre, University of Manchester, UK[1]

Charles Perkins Centre, University of Sydney, NSW 2006 Australia[2]

School of Life and Environmental Sciences, University of Sydney, NSW 2006 Australia[3]

Bosch Institute, University of Sydney, NSW 2006 Australia

Abstract

Latent TGFβ binding protein 4 (LTBP4) mutations are linked to autosomal recessive cutis laxa type 1C (ARCL1C), a rare congenital disease characterised by high mortality and severely disrupted elastic fibres. LTBP4, a multi-domain glycoprotein, is essential for regulating elastic fibre assembly and the bioavailability of TGFβ. Despite the importance of LTBP4, its structure is not known and the molecular mechanism by which it regulates elastogenesis is poorly understood. Therefore, we analysed the structural and functional consequences of two ARCL1C-causing point mutations, C1286S and C1186R, which both effect highly conserved cysteine residues to result in either a mild or severe pathology, respectively. Our structural and biophysical data show that the LTBP4 C-terminal region is monomeric in solution and adopts an extended and flexible conformation. The C1186R mutation results in a more unordered structure whereas, the C1286S mutation results in a more compact conformation which demonstrates the importance of conserved cysteine residues in stabilising the structure of LTBP4. Binding studies show that the C1186R but not the C1286S mutation, slightly decreases binding to fibrillin-1. We found that the LTBP4 C-terminal region directly interacts with tropoelastin which is also disrupted by C1286R and C1186S mutations. Our results suggest that both mutations contribute to ARCL1C by disrupting the structure of LTBP4.

Introduction

Latent TGFβ Binding Protein 4 (LTBP4) is a large secreted multidomain glycoprotein that is associated with fibrillin-rich microfibrils in the extracellular matrix (ECM). The LTBP4 domain structure, as for other LTBP family members (LTBP1, 2 and 3), is highly structurally related to the major component of extracellular matrix microfibrils, fibrillin. Both LTBPs and fibrillin share two types of cysteine-rich domains, the six-cysteine Epidermal growth factor-like domains (EGF) that form disulphide bonds in a conserved 1-3, 2-4 and 5-6 pattern and an eight cysteine domain TGFβ binding protein-like (TB) domains that form disulphide bonds in a conserved 1-3, 2-6, 4-7 and 5-8 pattern (Lack et al., 2003, Saharinen et al., 1999, Yuan et al., 1997, Oklu and Hesketh, 2000). The LTBPs also share a 4-cysteine domain near their N-terminus. LTBP4 has 20 EGF-like domains, of which 17 are calcium-binding, a hybrid domain, three TB domains, and a proline-rich interdomain region. Two major isoforms of LTBP4 are expressed in mammalian cells, a long (LTBP4L) and short form (LTBP4S) (Saharinen et al., 1998), produced by independent promoters (Kantola et al., 2010). Both isoforms share similar domain structure, but LTBP4L has an additional amino-terminal 4-Cysteine domain compared with LTBP4S. The long and short LTBP4 isoforms have overlapping expression in the lung and aorta, whereas, in the skin and heart, LTBP4S is the major expressed isoform (Bultmann-Mellin et al., 2015). Moreover, LTBP4S has higher expression in lung during late embryonic and postnatal periods (Bultmann-Mellin et al., 2017). Mutations in both LTBP4 isoforms lead to an autosomal recessive cutis laxa type 1C (ARCL1C), initially named as Urban-Rifkin-Davis Syndrome, and an autosomal recessive cutis laxa type 1C-like phenotype is seen in LTBP4S deficient mice (Urban et al., 2009, Bultmann-Mellin et al., 2015, Sterner-Kock et al., 2002). ARCL1C patients share similar clinical and pathological features of craniofacial, pulmonary, gastrointestinal, genitourinary anomalies accompanied with generalised cutis laxa. Both ARCL1C patients and LTBP4 deficient mice have high postnatal mortality due to respiratory failure caused by severely disrupted pulmonary elastic fibre architecture (Urban et al., 2009, Bultmann-Mellin et al., 2015), indicating a crucial role for LTBP4 in elastic fibre assembly. LTBP4 modulates elastic fibre assembly by interacting with other extracellular partners such as fibulin-4 (Bultmann-Mellin et al., 2015, Bultmann-Mellin et al., 2016), fibulin-5 (Noda et al., 2013) and fibrillin-1 (Ono et al., 2009) and regulates extracellular TGFβ bioavailability by covalent interaction with the small latent complex (Annes et al., 2004, Robertson and Rifkin, 2016, Saharinen and Keski-Oja, 2000).

LTBP4 is primarily involved in the regulation of elastic fibre assembly in a TGFβ independent manner (Dabovic et al., 2009). The LTBP4 C-terminal region binds directly to the N-terminal region of fibrillin-1 (Isogai et al., 2003, Ono et al., 2009) and this interaction is essential for LTBP4 matrix deposition LLC (Ono et al., 2009, Zilberberg et al., 2012). These studies have confirmed the requirement of fibrillin-1 for LTBP4 to be incorporated into the extracellular matrix. Moreover, it has been suggested that the disruption of this interaction in Marfan syndrome might contribute to ectopia lentis (Ono et al., 2009, Comeglio et al., 2002). LTBP4 has also been demonstrated to compensate LTBP2 in forming microfibrils of the ciliary zonules in LTBP2 null mice (Fujikawa et al., 2017).

Here we focused on two missense mutations p.C1186R (Callewaert et al., 2013) and p.C1286S (Su et al., 2015) in the C-terminal region of LTBP4 that affect highly conserved cysteine residues within the 2nd TB and the 16th cbEGF domains, respectively. A cutis laxa (CL) patient with homozygous LTBP4 p.C1186R mutations, suffered a life-threatening pulmonary defect, hydronephrosis with generalised skin laxity (Callewaert et al., 2013). The p.C1286S mutation was reported in a 14-year-old female heterozygous for c.3856T>A and p.C1286S with the clinical and pathological characteristics of CL. Skin biopsies show large globular elastin aggregates and poor integration into the fibrillin microfibrils (Su et al., 2015). Whereas the p.C1186R mutation resulted in severe ARCL1C, the C1286S mutation resulted in mild to moderate pulmonary disease (Su et al., 2015).

To determine whether ARCL1C mutations interfere with LTBP4 structure and molecular interactions, we analysed the structure of the LTBP4 C-terminal region using complementary structural and biophysical methods and compared its structural features with the ARCL1C mutants. We identified tropoelastin as a new interaction partner for LTBP4 and investigated the impact of ARCL1C mutations on the interactions with tropoelastin and fibrillin-1 to further understand the role of LTBP4 in elastic fibre assembly and disruption in ARCL1C.

Material & Methods

Expression and Purification of Recombinant LTBP4 Constructs

Human wildtype and mutant LTBP4 C-terminal region constructs were purchased as gene strings (residues 1114-1557) and ligated into a modified version of the mammalian expression

vector pCEP4 (Invitrogen), pCEP-Pu/AC7 that contains a C-terminal six-histidine residue tag (6x His-tag). The recombinant human wildtype and mutant LTBP4 C-terminal constructs were stably transfected and expressed in Human Embryonic Kidney (293)-EBNA cells. The proteins were then purified using nickel affinity column (GE Healthcare) followed by size-exclusion chromatography on fast protein liquid chromatography (FPLC) (AKTApurifier) using a Superdex 200 10/300GL column (GE Healthcare) equilibrated with buffer containing 10 mM Tris, 150 mM NaCl, pH 7.8 at a flow rate of 0.5 ml/min. Protein identity was confirmed by mass spectrometry (MS) and Western immunoblotting and concentration determined using BCA protein assay (Thermo Fisher Scientific).

Multi-angle Light Scattering (MALS)

Purified native protein samples (0.5 ml at approximately 0.4 - 1 mg/ml) were loaded onto a Superdex 200 10/300GL column (GE Healthcare) running at a flow rate of 0.5 ml/min using a buffer containing 10 mM Tris, 150 mM NaCl, pH 7.8. Eluted protein fractions were passed from the column into a Wyatt DAWN Heleos II EOS 18 angle laser photometer with QELS detector (Wyatt Technologies) connected to an Optilab T-rEX refractive index detector. The absolute molar mass, concentration and hydrodynamic radius of the resulting peaks were analysed using ASTRA 6.

De-glycosylation:

Purified proteins were digested using PNGase-F according to the manufacturer's protocol (New England's Biolabs). The removal of glycans was verified using SDS-PAGE.

Sedimentation Velocity Analytical Ultracentrifugation (SV-AUC)

Native monomeric protein samples (0.4 - 1 mg/ml) in the same buffer as used in MALS were characterised by sedimentation velocity SV-AUC using Beckman XL-A analytical ultracentrifuge with an An60Ti 4-hole rotor running at 45,000 rpm at 20°C. The sedimenting boundary was monitored at either 280 or 230 nm for 200 scans. Data were analysed by continuous model-based distribution C(s) of Lamm equation solutions method using SEDFIT software (Schuck, 2000), and the resulting sedimentation coefficients were corrected to standard conditions using SEDNTERP software (Philo, 2000).

Small-angle Light Scattering (SAXS)

In-line SEC-SAXS was performed on purified proteins at a concentration range of 1 - 2 mg/ml in the same buffer used for MALS and SV-AUC. Wildtype LTBP4 C-terminal and C1286S SAXS data were collected at 1 second intervals using 45 µL purified protein sample passed through a Superdex 200 3.2/300 column at beamline BM29, European synchrotron radiation facility (Grenoble, France), while SAXS data for C1186R were collected at B21 at Diamond. SAXS data were pre-processed and reduced by EDNA, inhouse ESRF software (http://www.esrf.eu/home/UsersAndScience/Experiments/MX/About_our_beamlines/bm29/computing-environment/edna.html; last accessed September 2017). For each frame with a consistently similar radius of gyration (Rg) across the elution peak, the protein scattering intensities were merged. SAXS data were then analysed and buffer scattering subtracted from that of the sample using ScAtter software (http://www.bioisis.net/tutorial/9; last accessed October 2018). The Rg of the protein was estimated by Guinier analysis and the intraparticle distance distribution function P(r) in real space were evaluated using the Indirect Fourier transform (IFT) program GNOM, and particle shapes were modelled *ab initio* using DAMMIN software in slow mode (Franke and Svergun, 2009). Ten *ab initio* models were generated and aligned and superimposed to generate a single model using the DAMAVER suite (Svergun, 2003). The goodness of the superimpositions of the 10 models compared using DAMSEL was estimated by the normalised spatial discrepancy (NSD).

Circular Dichroism (CD)

The purified wildtype and mutant LTBP4 C-terminal regions, at a concentration range of 0.5 - 1 mg/ml in 10 mM Tris, 150 mM NaCl, pH7.8 buffer, were analysed by circular dichroism (CD) using the Far-UV spectral region (190-260 nm). The Far-UV spectra were recorded in millidegrees (mdeg) by Jasco-J810 spectropolarimeter. Measurements were taken every 0.2 mm in a 0.5 cm path length cell at 25 ^{o}C. Ten accumulated scans were recorded, averaged, and corrected for each construct. The secondary structure content was quantitatively analysed by the online tool Dichroweb (http://dichroweb.cryst.bbk.ac.uk/html/home.shtml; last accessed October 2018) using CDSSTR and CONTIN algorithms.

Surface Plasmon Resonance (SPR)

Kinetics of fibrillin-1 PF3 fragment (residues 1-722) (Rock et al., 2004) and the LTBP4 C-terminal region binding were measured in real time using SPR ProteOn system at 25 ^{o}C. Fibrillin-1 was diluted in 10 mM HEPES, 150mM NaCl, pH7.4 supplemented with 0.005% (v/v) Tween-20 and then injected at a range of concentrations from 100-0 nM over a constant concentration of immobilised LTBP4 C-terminal region on amine coupling GLC sensor chip using the manufacturer's instructions (Bio-Rad). All binding experiments for each LTBP4 construct were performed at least twice. The sensor chip surface was regenerated using 10 mM glycine at pH 2.5. Equilibrium analysis was used to determine kinetic parameters.

Bio-layer interferometry (BLI)

BLI using OctetRED96 (ForteBio) system was performed for measuring the kinetics of the interaction between full-length tropoelastin and the LTBP4 N- (residues 29-394) and C-terminal regions in real time. Biotinylated full-length tropoelastin was diluted in 10 mM HEPES, 150 NaCl, pH7.4 buffer supplemented with 0.005% (v/v) Tween-20 and then immobilised at 200nM constant concentration on Streptavidin biosensors tips surface. The biosensors immobilised with biotinylated tropoelastin were then incubated with the LTBP4 C-terminal wildtype or mutant constructs diluted at a range of concentrations in the same buffer used for tropoelastin. The biosensors surface was regenerated using 10 mM glycine at pH 2.5. The binding kinetics was analyzed using Octet software version 7 (ForteBio). The goodness of binding data fitting was assessed by X2 and R2 values. All binding experiments were performed in solid-black 96 well plates at 25^{o}C with an agitation speed of 1000 rpm and repeated at least twice. The interaction was also performed in the other orientation with immobilized biotinylated LTBP4 and tropoelastin as the analyte.

Results

Expression and Purification of Recombinant Human LTBP4 C-terminal region

To structurally characterise the LTBP4 C-terminal region, HEK293-EBNA cells stably expressing the wildtype LTBP4 C-terminal region and ARCL1C mutants were generated (Figure 3-1A). The LTBP4 proteins were purified using nickel affinity followed by size exclusion chromatography (SEC), which yielded a single prominent peak with similar elution volumes (Supplementary Figure 3-1). The purified proteins were analysed by non-reduced SDS-PAGE (Figure 3-1B),

based on the sequence predicted mass, the main species corresponded to a monomer which appeared slightly larger than the sequence predicted size of 51 kDa. LTBP4 has eight potential glycosylation sites, of which six asparagine residues were predicted to be N-glycosylated and three threonine residues to be O-glycosylated (Saharinen et al., 1998, Bultmann-Mellin et al., 2015). Our C-terminal construct was predicted to contain two potential N-linked glycan. This post-translational modification could explain the slight increase in the molecular mass. The presence of sugars was verified using PNGase F deglycosylation assay by increased protein mobility on SDS-PAGE and a shift to lower molecular weight for all LTBP4 constructs shown in Figure 3-1B. To determine whether the loss of a cysteine residue resulted in abnormal dimerisation for the mutants, fractions of each peak were analysed under both non-reducing and reducing conditions but only monomeric species were observed for both the wildtype and mutants indicating that the free cysteine residue in the mutants de not induce dimerisation (Figure 3-1C).

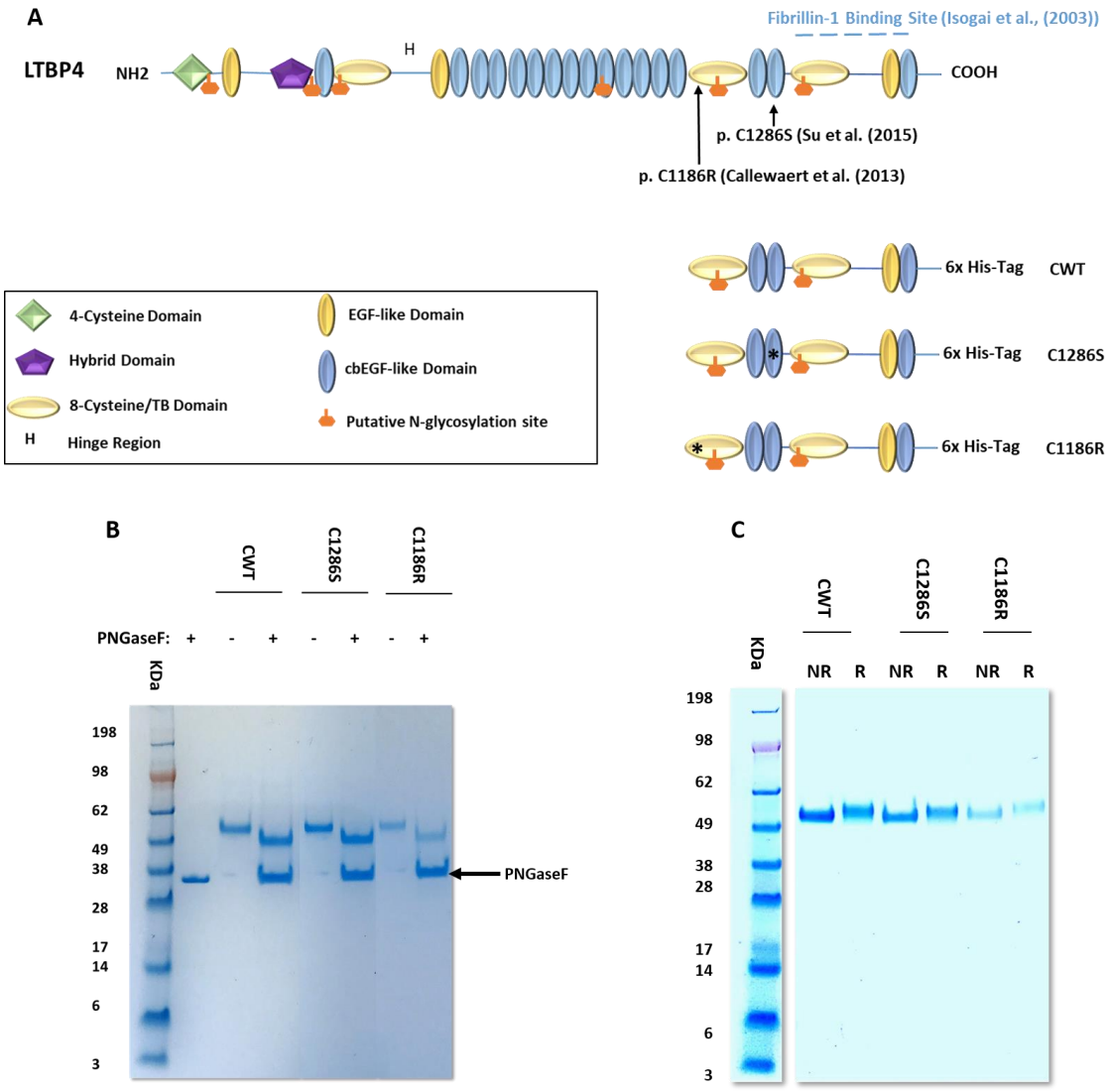

Figure 3-1: Expression and purification of recombinant LTBP4**.** (A) Schematic diagram of the domain organization of full-length LTBP4S, with fibrillin-1 interaction site, and the human LTBP4 C-terminal constructs with C-terminal 6x-His-tag used in this study. Arrows and asterisks indicate the positions of the ARCL1C mutations. (B) Non-reduced Coomassie blue stained SDS-PAGE gel showing the purified LTBP4 C-terminal constructs: CWT, C1286S and C1186R before and after deglycosylation. (C) SDS-PAGE for the purified LTBP4 C-terminal constructs: CWT, C1286S and C1186R under (NR: non-reducing) and (R: reducing using 2-Mercabtoethanol) conditions.

The C-terminal of Latent TGFβ Binding Protein 4 is Monomeric in Solution

Multi-angle light scattering (MALS) in combination with size exclusion chromatography (SEC) and sedimentation velocity analytical ultracentrifugation (SV-AUC) were used to determine the native state, size and absolute molar mass of LTBP4 C-terminal region in solution. SEC-MALS data showed a single peak with an estimated hydrodynamic radius of 4.7 nm and

absolute molecular mass of 58 KDa for both CWT and C1286S and a hydrodynamic radius of 5 nm and absolute molecular mass of 58 kDa for the C1186R. These results indicate that all LTBP4 C-terminal proteins are monomeric in solution (Figure 3-2A). Consistent with SEC-MALS data, the SV-AUC profile showed that both the wildtype and mutant C-terminal region behaved as monomers in solution, but the SV-AUC profile for the ARCL1C C1286S mutant was asymmetric, indicating the presence of higher ordered species (Figure 3-2B). Based on the sedimentation profile from SV-AUC data, the wildtype LTBP4CT sediments at 4.15 Svedberg (S) with a frictional ratio of 1.39, that deviates from that expected for a globular protein (theoretically f/f0 of 1.2) (Schuck, 2000). This suggests a moderate elongation of this region. However, the C1286S mutant was more compact than the WT and sedimented faster at 4.70 S with a lower friction ration of 1.31. In contrast, the C1186R mutant sedimented slower at 3.61 S with a higher friction ratio of 1.69, indicating a more extended protein conformation.

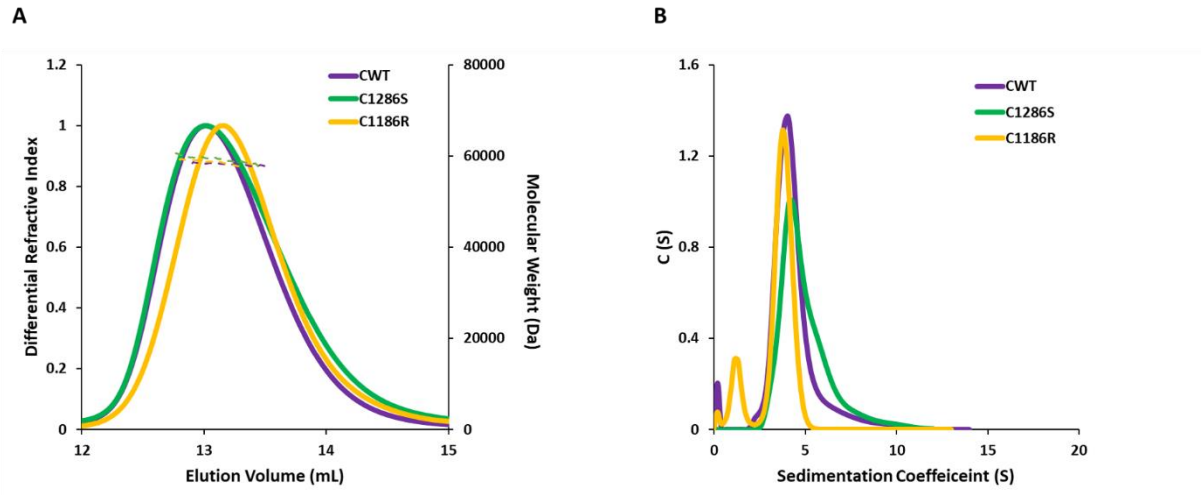

Figure 3-2: Structural characterisation of LTBP4CT region. (A) SEC-MALS chromatograms of LTBP4 C-terminal constructs showing that all LTBP4 constructs are monomeric in solution with mass of 58KDa and (B) Sedimentation coefficient profile of LTBP4 C-terminal constructs showing a prominent single peak for each construct.

Table 3-1: Experimental hydrodynamic results for LTBP4 C-terminal region constructs

Hydrodynamic Properties	CWT	C1286S	C1186R
Molecular Mass (kDa) [a]	58	58	58
Hydrodynamic Radius R_h (nm) [a]	4.7	4.7	5.0
Sedimentation Coefficient (Sw) [b]	4.30	4.98	3.82
Sedimentation Coefficient (Sw,20) [b]	4.15	4.70	3.61
Frictional Ratio [b]	1.39	1.31	1.69
Stokes Radius (nm) [b]	3.70	3.61	4.63
Radius of Gyration R_g (nm) [c]	3.97	4.02	4.28
Maximum Dimension Dmax (nm) [c]	13.0	12.3	13.7
R_g/R_h	0.84	0.85	0.84

[a] Multi-Angle Light Scattering (MALS)

[b] Sedimentation Velocity Analytical Ultracentrifugation (SV-AUC)

[c] Small-Angle X-ray Scattering (SAXS)

The LTBP4 C-terminal Region has an Elongated and Flexible Nanostructure

Small angle X-ray scattering was performed to obtain more detailed structural information on LTBP4. SAXS data were collected directly from SEC eluates to ensure the monodispersity of LTBP4 in solution. The 1D scattering intensity data of each LTBP4CT construct are plotted as a function of q (Figure 3-3A). The Guinier approximation was used for sample quality assessment. Guinier plots for both wildtype and ARCL1C mutants showed linearity which indicates that no aggregation present (Supplementary Figure 2Ai, Bi and Ci for LTBP4CWT, C1286S and C1186R, respectively). The structural parameters including Rg and Dmax obtained from the experimental data are summarised in Table 3-1.

The radius of gyration (Rg) was similar for the WT and the C1286S mutant, 3.97 nm and 4.02 nm, respectively. Whereas the Rg for the C1186R mutant was slightly larger (4.28 nm) consistent with the more elongated conformation shown by SV-AUC. The flexibility of the LTBP4 C-terminal region was assessed (Supplementary Figure 2Aii, Bii and Cii for LTBP4CWT, C1286S and C1186R, respectively) and the normalised Kratky plots in Figure 3-3B show a

single peak, with maxima slightly deviating from the expected peak position for a globular protein, with tail extending to high q values, indicating that this region has an elongated structure with some flexibility rather than a compact and globular conformation. The distance distribution function P(r) shown in Figure 3-3C, is also consistent with an extended conformation for the LTBP4 C-terminal region. The maximum particle dimension was 13.0 nm, 12.3 nm and 13.7 nm for the CWT, C1286S and C1186R, respectively, again consistent with the SV-AUC data in figure 3-2B where the C1286S mutant is more compact and the C1186R mutant more extended than the WT.

3-dimensional *ab initio* models of the wildtype and mutants were generated using the DAMMIN (Supplementary Figure 3) and DAMAVER suite (Figure 3-3D) of programmes. The determined Normalized spatial discrepancy (NSD) was 0.666 ± 0.028, 0.857 ± 0.022 and 0.694 ± 0.017 for LTBP4CWT, C1286S and C1186R, respectively suggestive of a unique solution. The *ab initio* models are consistent with the elongated conformation adopted by the LTBP4 C-terminal region. The models of the wildtype and mutant constructs highlighted differences in their 3D-dimensional structures. The nanostructure of the C1286S mutant was more compact compared with the wildtype LTBP4 C-terminal, while the C1186R mutant was wider and more extended than the wildtype again consistent with the SV-AUC results.

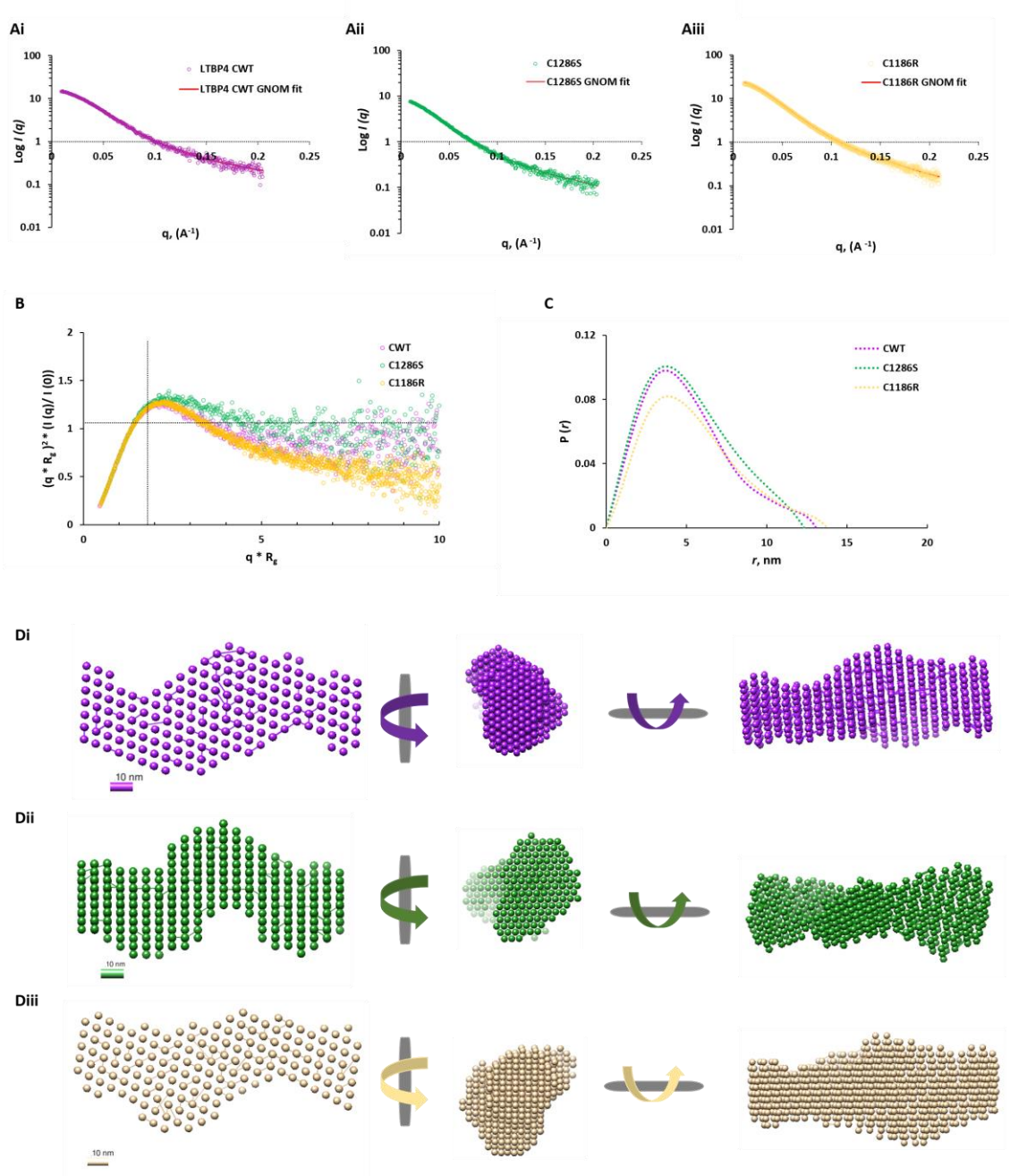

Figure 3-3: Structural characterisation of LTBPCT region in solution Using Small Angle X-ray Scattering (SAXS). The experimental 1D scattering intensity I plotted as a function of q for (Ai) WT, (Aii) C1286S and (Aiii) C1186R constructs used for analysis and modelling. (B) The dimensionless Kratky plot for wildtype and mutants show a peak deviating from the expected peak position for globular particles (cross-hair marks the Guinier-Kratky point (1.732, 1.1)), indicating that the proteins are folded and have a non-globular conformation but rather are elongated with some flexibility. (C) The indirect Fourier transform of I vs. q using GNOM, P(r) vs. r indicates the maximum dimensions in real space. The averaged DAMFILT model of (Di) LTBP4CWT, (Dii) C1286S and (Diii) C1186R shown in three orthogonal views.

ARCL1C mutation alters the Secondary Structure of the LTBP4 C-terminal region

To gain more information on the structure of the LTBP4 C-terminal region, we performed circular dichroism (CD). The secondary structure of LTBP4 wildtype C-terminal and ARCL1C mutants were analysed using Far UV-CD. The far-UV spectra for the WT showed a negative maximum at 209 nm, which is characteristic for proteins with a high content of β–sheet and unordered regions (Figure 3-4). To investigate possible conformational changes caused by ARCL1C mutations, the far-UV spectra of ARCL1C mutants were analysed and compared to the WT. The C1286S substitution had little impact on the far UV-CD spectra and showed a shift of three nm in the position of the negative peak (Figure 3-4). A more substantial change in the far UV-CD spectra was observed for the C1186R substitution, resulted in a shift of six nm in the position of the negative peak towards 200 nm, which is characteristic for a more unordered structure (Figure 3-4). These changes indicated a secondary structural transition. Using the online tool Dichroweb, the secondary structure components were quantitatively analysed and summarised in Table 3-2. The estimated α–helix content was generally low (4.5-7.8%) for all LTBP4 C-terminal constructs whereas there was a high content of β–sheet (32.2-40.15 %) and unordered conformations (60.8-61.4 %) consistent with the secondary structure of cbEGF/TB domains of fibrillin-1 (Rao et al., 1995, Downing et al., 1996). The C1186R mutant had a decrease in the β–sheet content to 26.6% and an increase in the unordered structure to 64%. These data indicate that the ARCL1C cysteine substitution, C1186R alters the secondary structure of the LTBP4 C-terminal and possibly results in a less stable protein.

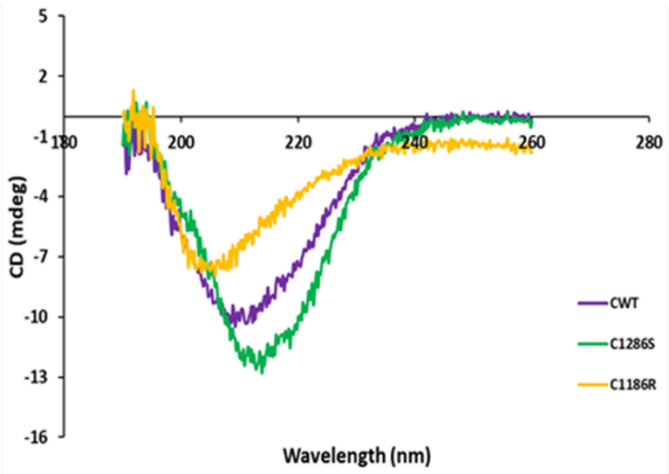

Table 3.2.

LTBP Construct	α–Helix %	β–Sheet %	Turns & Unordered %
CWT	6.35	32.2	61.4
C1286S	4.55	40.15	60.85
C1186R	7.8	26.65	64.05

Figure 3-4: Circular Dichroism using the Far UV-CD spectra in the 260-190 nm range of LTBP4 CWT and mutants. LTBP4 CWT spectra showed a negative maximum at 209 nm, which is characteristic for proteins with a high content of β-sheet and unordered conformations. The C1286S substitution had little impact on the spectra. Whereas a more significant change in the spectra was observed for the C1186R substitution, resulting in a shift of six nm in the position of the negative peak towards 200 nm, indicating a secondary structural transition to a less β-sheet and more unordered conformation. Table 3-2: Secondary structure content of LTBP4 C-terminal region constructs.

ARCL1C Mutation reduces Binding to Fibrillin-1

LTBP4 binds to fibrillin-1 as has been previously shown by solid phase and surface-based binding studies (Isogai et al., 2003, Ono et al., 2009). These studies demonstrated that binding was via the TB3, EGF3 and cbEGF17 domains in LTBP4 (domains indicated in Figure 3-1A). The LTBP4-fibrillin-1 interaction is essential for matrix assembly and incorporation of LTBP4 (Ono et al., 2009, Zilberberg et al., 2012) so ARCL1C causing mutations might interfere with this important interaction. Therefore, to investigate the impact of ARCL1C mutations on the interaction with fibrillin-1, surface plasmon resonance binding analysis was performed. An N-terminal region of fibrillin-1 (PF3 fragment as previously described (Rock et al., 2004)) encompassing the LTBP4 binding site was used. Fibrillin-1 was injected at different concentrations over immobilised LTBP4. The kinetic analysis demonstrated that fibrillin-1 strongly interacted with both WT and mutant LTBP4 C-terminal regions with low nanomolar affinity (K_D). The calculated binding affinities for fibrillin-1 to both WT and the C1286S mutant were equivalent (15.81 and 12.23 nM, respectively), indicating that C1286S substitution did

not affect this interaction. Whereas the C1186R mutant had a slightly weaker binding affinity with a K_D of 40.22 nM, indicating that C1186R substitution slightly interfered with the fibrillin-1 interaction. Moreover, this data suggests that the 2nd TB domain in LTBP4 where cystine residue 1186 is located might be involved in this important interaction or that the conformational change induced by the mutation may have longer-range effects (Figure 3-5).

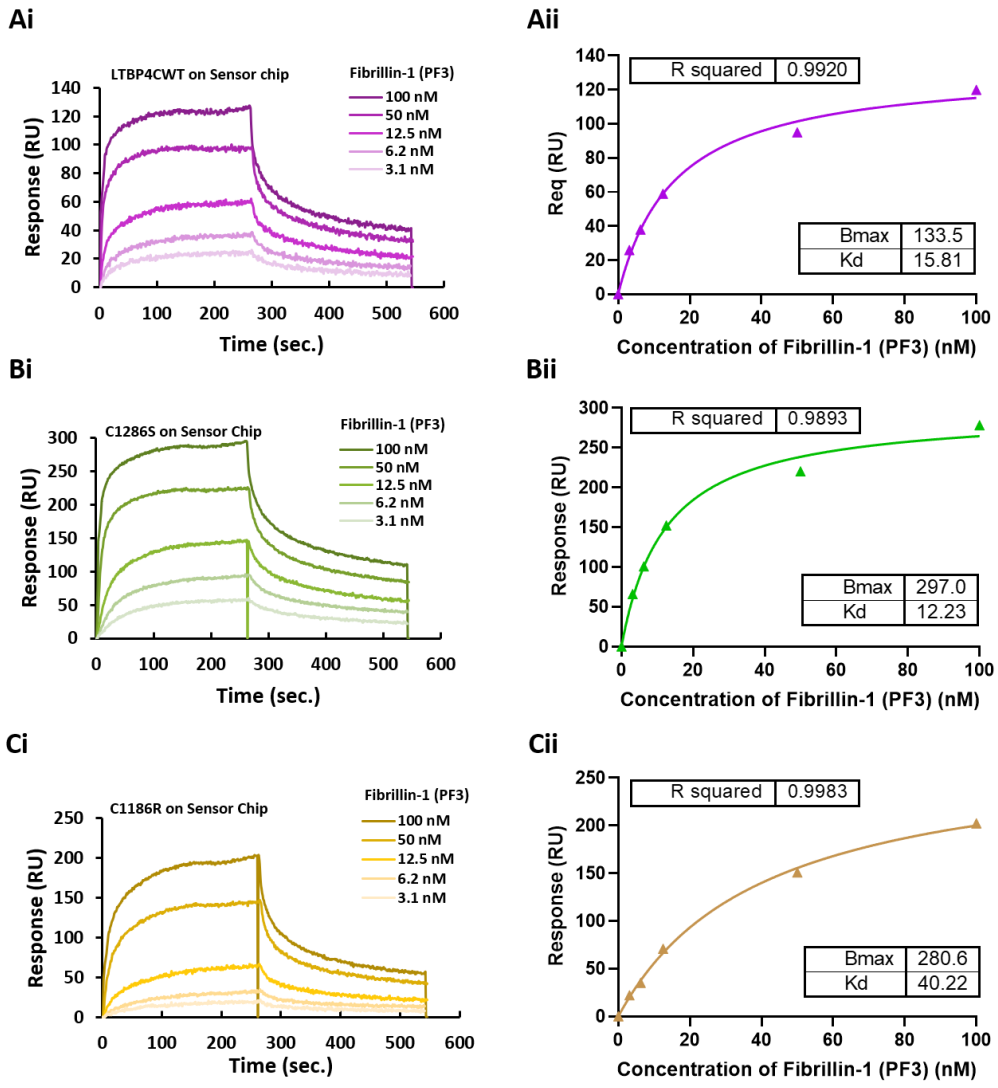

Figure 3-5: Surface Plasmon Resonance (SPR) analysis of the fibrillin-1 PF3 construct binding to LTBP4. (Ai) WT, (Bi) C1286S) and (Ci) C1186R. LTBP4 was immobilised on the sensor chip (GLC) using amine-coupling and purified fibrillin-1 (PF3) was injected as analyte at different concentrations (100 – 3.1 nM) over the immobilised LTBP4. The binding affinity was determined by steady state with equilibrium response plotted against fibrillin-1 concentration for (Aii) WT, (Bii) C1286S) and (Cii) C1186R mutants. All experiments were performed in duplicates and representative results are shown.

The C-terminal region of LTBP4 Directly Interacts with Tropoelastin which is perturbed by ARCL1C Mutation

A previous study showed that LTBP4 knockdown prevented elastin deposition in human dermal fibroblasts and LTBP4 has also been shown to interact with tropoelastin indirectly using solid phase and surface based binding assays (Noda et al., 2013). This led us to speculate that LTBP4 might interact directly with tropoelastin. To examine whether LTBP4 interacts directly with tropoelastin, binding studies using Biolayer interferometry (BLI) were performed using the N- and C- terminal region constructs of LTBP4 to define which region of LTBP4 binds to tropoelastin. The OctetRED96 sensorgrams for the C-terminal but not the N-terminal region, showed a binding response to immobilised tropoelastin (Figure supplementary 4). The kinetics of the interaction between the C-terminal region with tropoelastin were then studied. Full-length tropoelastin was immobilised and then incubated with increasing concentrations of the LTBP4 C-terminal region. The kinetic analysis demonstrated that the LTBP4 C-terminal region binds to tropoelastin with binding affinity of 56.98 nM. The effect of ARCL1C mutations on this interaction was also investigated. Both mutants C1286S and C1186R showed weaker binding affinity to tropoelastin with a K_D of 151.1 and 154.1 nM, respectively. Although the steady state for both mutants resulted in a similar dissociation constant for binding to tropoelastin, the kinetic analysis demonstrated a highly biphasic association and slower dissociation steps for C1186R binding to tropoelastin (Figure 3-6). We further confirmed the direct interaction between the C-terminal region of LTBP4 and tropoelastin by performing binding studies in the opposite orientation immobilizing the LTBP4 C-terminal region constructs and using tropoelastin as the analyte (Supplementary Figure 5).

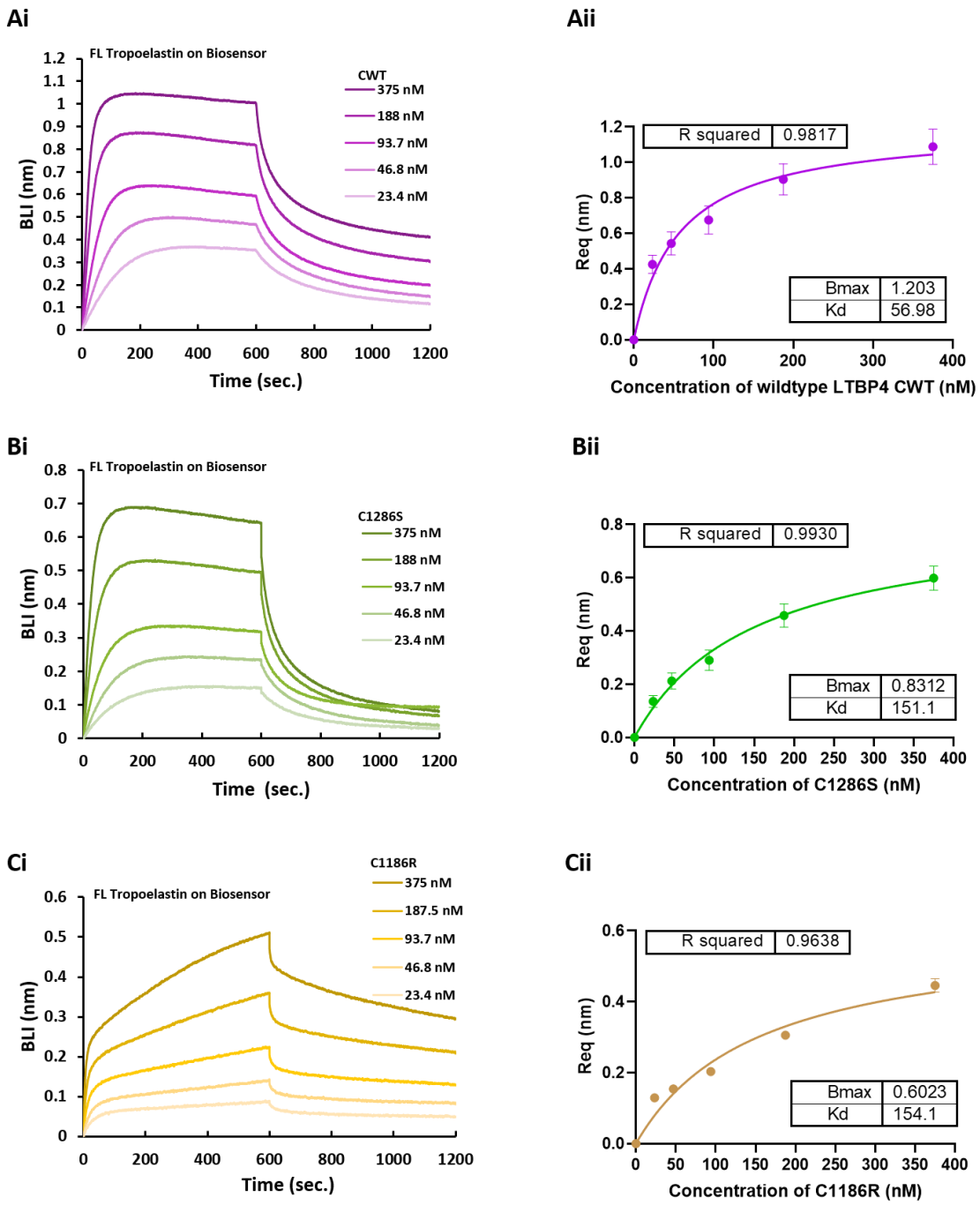

Figure 3-6: Biolayer interferometry (BLI) analysis of LTBP4CT binding to full-length tropoelastin using OctetRED96. OctetRED analysis show that all LTBP4 (A) CWT, (B) C1286S and (C) C1186R at different concentrations (375 – 23.4 nM) directly bind to immobilised full-length tropoelastin. The binding affinity was determined by steady state analysis (equilibrium) plotted against LTBP4 (Aii) CWT, (Bii) C1286S and (Cii) C1186R concentration. All experiments were performed in duplicates and averaged Kd are presented. Error bars represent standard error of the mean.

Discussion

LTBP4 is important for the correct formation of an intact elastic fibre network with mutations resulting in ARCL1C, confirming its biological significance in elastogenesis (Urban et al., 2009). ARCL1C missense mutations C1286S and C1186R result in the substitution of highly conserved cysteine residues located in the 16th cbEGF and 2nd TB domains, respectively. Our hypothesis was that mutant LTBP4 may result in structural changes and altered molecular interactions of LTBP4 to result in defective elastic fibre assembly.

In our study, we have provided novel structural and functional information on the wildtype LTBP4 C-terminal region. Using SEC-MALS and SV-AUC, we show that the wildtype LTBP4 C-terminal region is stable and is a monomer in solution. This is consistent with our previous study on LTBP1 where the LTBP1 C-terminal region is also a monomer in solution (Troilo et al., 2016). The ARCL1C-causing mutants C1286S and C1186R are also monomers, but the C1286S mutant shows a tendency to form higher-order aggregates, suggesting the production of a less stable protein. The molecular masses for all C-terminal fragments determined by MALS were slightly larger than expected from sequence, consistent with the presence of N-linked glycans (Saharinen et al., 1998, Bultmann-Mellin et al., 2015). This post-translational modification is vital in a wide range of biological processes, including protein folding, stability and protein-protein interaction (Dalziel et al., 2014). SV-AUC analysis of the wildtype LTBP4 C-terminal region suggested a moderately elongated conformation. However, the C1286S mutant adopted a more compact conformation compared with the wildtype LTBP4 C-terminal region. In contrast, the C1186R mutant had a more extended conformation. In line with SV-AUC analysis, SAXS data showed that the C-terminal region has a non-globular structure but is elongated with some flexibility. This is consist with our recent study on the C-terminal region of LTBP1 which also adopts an elongated and flexible conformation (Troilo et al., 2016). The 3D *ab initio* models for the LTBP4 C-terminal region generated from SAXS data supported an elongated conformation for this region. Consistent with the SV-AUC findings, the C1286S mutant resulted in a more compact and shorter protein structure and the C1186R mutant resulted in a more elongated protein compared with the WT. The secondary structure of wildtype LTBP4 C-terminal region contained low α-helix content (6.3 %), high β-sheet (32.2%) and unordered conformation (61.4 %). These data are consistent with previous structural studies on the TB and cbEGF domains of the LTBP4 homolog, fibrillin-1, which are mainly

composed of β-sheets and small amount of α-helix (Rao et al., 1995, Downing et al., 1996). The C1286S mutant resulted in a slight increase in the β-sheet content (to 40.15%), while the C1186R mutant resulted in a conformation transition with lower β-sheet content (26.65%) and slightly higher random structure content (64 %). Our structural characterisation suggests that substitution of highly conserved cysteines within the TB or cbEGF domain, impacts on the conformational integrity of LTBP4.

The observed structural differences caused by the mutations led us to hypothesise that these mutations might also interfere with LTBP4 molecular interactions with extracellular proteins. Our SPR binding studies demonstrate that the wildtype LTBP4 C-terminal region and C1286S mutant showed similar binding affinities to fibrillin-1, indicating that the substitution of Cysteine with Serine in the cbEGF16 domain of LTBP4 had little impact on fibrillin-1 binding. Conversely, the C1186R mutation resulted in a slight reduction in the binding to fibrillin-1, indicating that this substitution in the 2nd TB domain of LTBP4 interferes with fibrillin-1 binding which could either be due to the secondary structure transition caused by this mutation or that the 2nd TB domain in LTBP4 contributes to the interaction with fibrillin-1. It has been demonstrated that fibrillin-1 is required for LTBP4 deposition (Ono et al., 2009, Zilberberg et al., 2012) and so perturbing this interaction may result in less LTBP4 deposited in the matrix. Indeed, it has been demonstrated that disruption of this interaction, caused by mutation in fibrillin-1 N-terminal region (N164S), results in reduced matrix deposition of LTBP4. Therefore, we hypothesised that ARCL1C causing mutations might impair LTBP4 matrix deposition leading to defective elastic fibres. Future work using *in vivo* studies are required to confirm this hypothesis.

Using BLI binding assays, we show that the LTBP4 C-terminal region but not the N-terminal region interacts with tropoelastin. A previous study was not able to detect an interaction between full-length LTBP4S and tropoelastin using solid phase binding assays (Noda et al., 2013). However, recently, full length LTBP4L has been shown to adopt a compact conformation that turns to a more open and extended conformation after binding with fibulin-4 (Kumra et al., 2019). Therefore, the tropoelastin binding site in full-length LTBP4 might be hidden, whereas the binding site for tropoelastin might be more accessible in our shortened LTBP4 construct. Noda et al., 2019 also showed that fibulin-5 mediates an interaction between LTBP4 and tropoelastin but it may also be that fibulin-5 induces a

conformational change in LTBP4S exposing a cryptic tropoelastin binding site. Both LTBP4 C-terminal mutants, C1186R and C1286S, impacted on tropoelastin binding. Our BLI binding studies identify tropoelastin as a new interaction partner for LTBP4. Elastic fibre formation might require both the indirect and direct molecular interactions between LTBP4 and tropoelastin (Figure 3-7). This is consistent with previous studies that observed distinguishable elastic fibre ultrastructural anomalies in patients with fibulin-5 mutations *(FBLN5$^{-/-}$)* and patients with LTBP4 mutations *(LTBP4S$^{-/-}$)*. Both patients showed globular elastin deposits that were poorly integrated into the microfibrils in their skin, but the LTBP4 mutants showed larger elastin deposits and more patchy elastic fibres than fibulin-5 mutants (Callewaert et al., 2013), in line with the immunolocalisation studies of fibulin-5 and LTBP4 knockdown cells (Noda et al., 2013). Moreover, it has been demonstrated that fibulin-5$^{-/-}$ mice show some incorporated elastic fibres into microfibrils, suggesting an alternative elastogenesis likely involving LTBP4 and fibulin-4 (Dabovic et al., 2015). With our demonstrated direct interaction between LTBP4 and tropoelastin, we hypothesise that LTBP4 may directly facilitate tropoelastin deposition onto microfibrils. Future work should be conducted to confirm the direct binding using *in vitro* binding studies and to investigate the significance of this interaction in elastic fibre formation using in vivo studies.

Our data also demonstrated that the C1186R mutation has more dramatic consequences to both structure and interactions than the C1286S mutation. The difference in these mutations might be attributed to the position of the replaced cysteine residue. From the sequence of the 2nd TB domain of LTBP4 in Figure 3-8A, the C1186R disrupts the C4-C7 disulphide bond that is involved in stabilising the intramolecular folding. It is well studied that there is an important hydrophobic area between the C6 and C7 shown in Figure 3-8A that is responsible for binding of TGFβ-LAP (Saharinen and Keski-Oja, 2000). Therefore, the C7 substitution in TB2 might also disturb this area leading to less functional protein. While the C1186S mutation disrupts the C5-C6 disulphide bridge in the 16th cbEGF domain. The disulphide bridges in the cbEGFs of fibrillin-1, to stabilise an antiparallel β-sheet that increases binding to calcium (Figure 3.9B) (Iain D. Campbell, 1993, Downing et al., 1996, Schrijver et al., 1999). Additionally, a cysteine to serine substitution might not cause such a dramatic change as cysteine to arginine substitution due to the comparative size of cysteine and serine. While the arginine side-chain is much larger than cysteine and positively charged which could account for the

more dramatic effect of this substitution both in terms of structural alterations and perturbed interactions with binding partners. In summary, we have provided the solution structure of the C-terminal region of LTBP4 and shown the impact of ARCL1C causing point mutations. These data demonstrate the importance of the conserved cysteine residues in maintaining the structure and function of the LTBP4 C-terminal region.

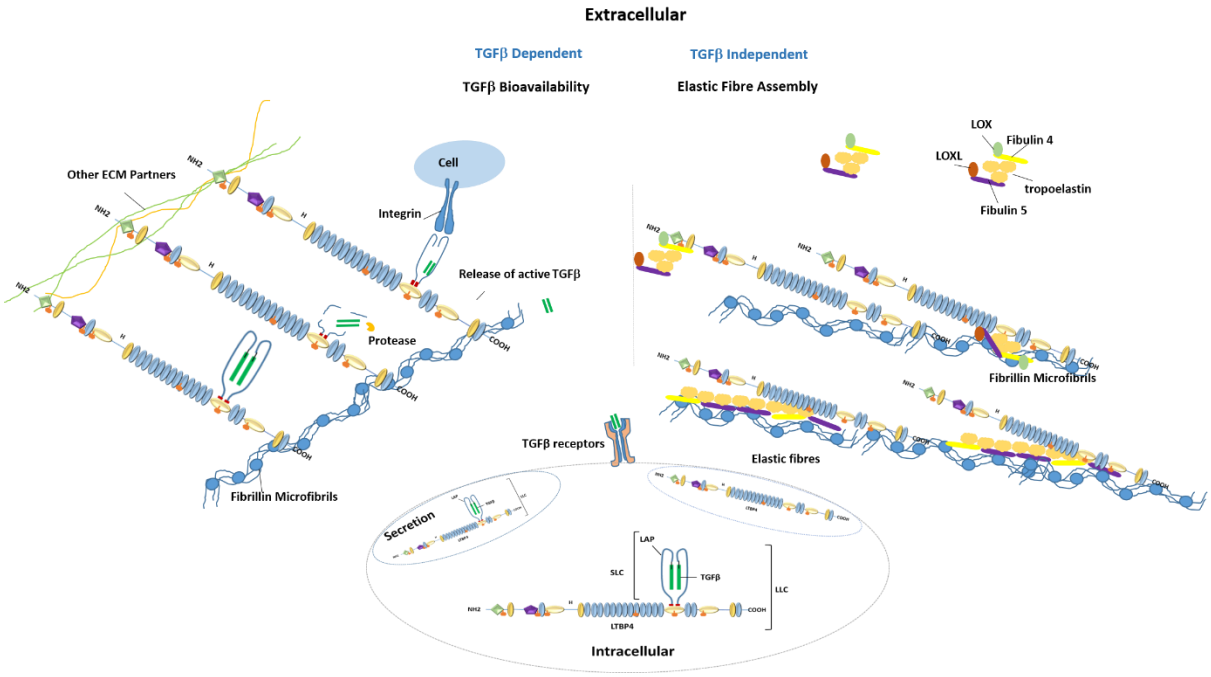

Figure 3-7: Model of LTBP4 role in health. In TGFβ dependent functionality, LTBP4 regulates TGFβ bioavailability by facilitating its secretion, ECM targeting and assisting in latent TGFβ activation by proteases or integrins (Todorovic and Rifkin, 2012). Active TGFβ then binds to its receptor and promotes the expression of many extracellular matrix components. LTBP4 also regulates elastic fibre assembly in a TGFβ independent manner by direct interaction with fibulin-4 and fibulin-5 via its N-terminal region to facilitate the deposition of elastin-fibulin-4/-5 complex onto fibrillin microfibrils by direct interaction with Fibrillin-1 via its C-terminal region involving TB3, EGF3 and cbEGF18 domains (Bultmann-Mellin et al., 2015, Bultmann-Mellin et al., 2016, Noda et al., 2013). Moreover, it might help in the deposition of tropoelastin by direct interaction maybe involving TB2 and 16th cbEGF with tropoelastin onto microfibrils via direct interaction with fibrillin-1 involving TB3, EGF3 and cbEGF18 domains.

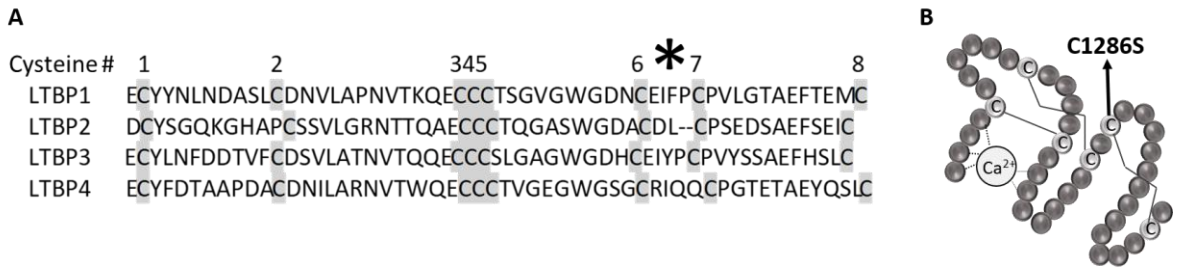

Figure 3-8: TB and cbEGF domains conserved Cysteine residues. (A) Aligned amino acid sequence of LTBPs 2nd TB domain showing the conserved eight cysteine residues (highlighted by black) and the hydrophobic area that is involved in the interaction with TGFβ-LAP between C6 and C7 (indicated by black asterisk). (B) A schematic diagram of a cbEGF domain with the conserved cysteine residues (shaded light grey) and disulphide bonds illustrated by (bold black lines) and the position of substituted cysteine, C5, indicated by an arrow.

References

ANNES, J. P., CHEN, Y., MUNGER, J. S. & RIFKIN, D. B. 2004. Integrin alphaVbeta6-mediated activation of latent TGF-beta requires the latent TGF-beta binding protein-1. J Cell Biol, 165, 723-34.

BERNADO, P., MYLONAS, E., PETOUKHOV, M. V., BLACKLEDGE, M. & SVERGUN, D. I. 2007. Structural characterization of flexible proteins using small-angle X-ray scattering. J Am Chem Soc, 129, 5656-64.

BULTMANN-MELLIN, I., CONRADI, A., MAUL, A. C., DINGER, K., WEMPE, F., WOHL, A. P., IMHOF, T., WUNDERLICH, F. T., BUNCK, A. C., NAKAMURA, T., KOLI, K., BLOCH, W., GHANEM, A., HEINZ, A., VON MELCHNER, H., SENGLE, G. & STERNER-KOCK, A. 2015. Modeling autosomal recessive cutis laxa type 1C in mice reveals distinct functions for Ltbp-4 isoforms. Dis Model Mech, 8, 403-15.

BULTMANN-MELLIN, I., DINGER, K., DEBUSCHEWITZ, C., LOEWE, K. M. A., MELCHER, Y., PLUM, M. T. W., APPEL, S., RAPPL, G., WILLENBORG, S., SCHAUSS, A. C., JUNGST, C., KRUGER, M., DRESSLER, S., NAKAMURA, T., WEMPE, F., ALEJANDRE ALCAZAR, M. A. & STERNER-KOCK, A. 2017. Role of LTBP4 in alveolarization, angiogenesis, and fibrosis in lungs. Am J Physiol Lung Cell Mol Physiol, 313, L687-L698.

BULTMANN-MELLIN, I., ESSERS, J., VAN HEIJINGEN, P. M., VON MELCHNER, H., SENGLE, G. & STERNER-KOCK, A. 2016. Function of Ltbp-4L and fibulin-4 in survival and elastogenesis in mice. Dis Model Mech, 9, 1367-1374.

CALLEWAERT, B., SU, C. T., VAN DAMME, T., VLUMMENS, P., MALFAIT, F., VANAKKER, O., SCHULZ, B., MAC NEAL, M., DAVIS, E. C., LEE, J. G., SALHI, A., UNGER, S., HEIMDAL, K., DE ALMEIDA, S., KORNAK, U., GASPAR, H., BRESSON, J. L., PRESCOTT, K., GOSENDI, M. E., MANSOUR, S., PIERARD, G. E., MADAN-KHETARPAL, S., SCIURBA, F. C., SYMOENS, S., COUCKE,

P. J., VAN MALDERGEM, L., URBAN, Z. & DE PAEPE, A. 2013. Comprehensive clinical and molecular analysis of 12 families with type 1 recessive cutis laxa. Hum Mutat, 34, 111-21.

DABOVIC, B., CHEN, Y., CHOI, J., VASSALLO, M., DIETZ, H. C., RAMIREZ, F., VON MELCHNER, H., DAVIS, E. C. & RIFKIN, D. B. 2009. Dual functions for LTBP in lung development: LTBP-4 independently modulates elastogenesis and TGF-beta activity. J Cell Physiol, 219, 14-22.

DALZIEL, M., CRISPIN, M., SCANLAN, C. N., ZITZMANN, N. & DWEK, R. A. 2014. Emerging principles for the therapeutic exploitation of glycosylation. Science, 343, 1235681.

DOWNING, A. K., KNOTT, V., WERNER, J. M., CARDY, C. M., CAMPBELL, I. D. & HANDFORD, P. A. 1996. Solution structure of a pair of calcium-binding epidermal growth factor-like domains: implications for the Marfan syndrome and other genetic disorders. Cell, 85, 597-605.

FRANKE, D. & SVERGUN, D. I. 2009. DAMMIF, a program for rapid ab-initio shape determination in small-angle scattering. J Appl Crystallogr, 42, 342-346.

FUJIKAWA, Y., YOSHIDA, H., INOUE, T., OHBAYASHI, T., NODA, K., VON MELCHNER, H., IWASAKA, T., SHIOJIMA, I., AKAMA, T. O. & NAKAMURA, T. 2017. Latent TGF-beta binding protein 2 and 4 have essential overlapping functions in microfibril development. Sci Rep, 7, 43714.

IAIN D. CAMPBELL, P. B. 1993. Epidermal growth factor-like modules. Current Opinion in Structural Biology, Volume 3, , 385-392.

ISOGAI, Z., ONO, R. N., USHIRO, S., KEENE, D. R., CHEN, Y., MAZZIERI, R., CHARBONNEAU, N. L., REINHARDT, D. P., RIFKIN, D. B. & SAKAI, L. Y. 2003. Latent transforming growth factor beta-binding protein 1 interacts with fibrillin and is a microfibril-associated protein. J Biol Chem, 278, 2750-7.

KANTOLA, A. K., RYYNANEN, M. J., LHOTA, F., KESKI-OJA, J. & KOLI, K. 2010. Independent regulation of short and long forms of latent TGF-beta binding protein (LTBP)-4 in cultured fibroblasts and human tissues. J Cell Physiol, 223, 727-36.

KUMRA, H., NELEA, V., HAKAMI, H., PAGLIUZZA, A., DJOKIC, J., XU, J., YANAGISAWA, H. & REINHARDT, D. P. 2019. Fibulin-4 exerts a dual role in LTBP-4L–mediated matrix assembly and function. 116, 20428-20437.

LACK, J., O'LEARY, J. M., KNOTT, V., YUAN, X., RIFKIN, D. B., HANDFORD, P. A. & DOWNING, A. K. 2003. Solution structure of the third TB domain from LTBP1 provides insight into assembly of the large latent complex that sequesters latent TGF-beta. J Mol Biol, 334, 281-91.

NODA, K., DABOVIC, B., TAKAGI, K., INOUE, T., HORIGUCHI, M., HIRAI, M., FUJIKAWA, Y., AKAMA, T. O., KUSUMOTO, K., ZILBERBERG, L., SAKAI, L. Y., KOLI, K., NAITOH, M., VON MELCHNER, H., SUZUKI, S., RIFKIN, D. B. & NAKAMURA, T. 2013. Latent TGF-beta binding protein 4 promotes elastic fiber assembly by interacting with fibulin-5. Proc Natl Acad Sci U S A, 110, 2852-7.

OKLU, R. & HESKETH, R. 2000. The latent transforming growth factor beta binding protein (LTBP) family. Biochem J, 352 Pt 3, 601-10.

ONO, R. N., SENGLE, G., CHARBONNEAU, N. L., CARLBERG, V., BACHINGER, H. P., SASAKI, T., LEE-ARTEAGA, S., ZILBERBERG, L., RIFKIN, D. B., RAMIREZ, F., CHU, M. L. & SAKAI, L. Y. 2009. Latent transforming growth factor beta-binding proteins and fibulins compete for fibrillin-1 and exhibit exquisite specificities in binding sites. J Biol Chem, 284, 16872-81.

RAO, Z., HANDFORD, P., MAYHEW, M., KNOTT, V., BROWNLEE, G. G. & STUART, D. 1995. The structure of a Ca(2+)-binding epidermal growth factor-like domain: its role in protein-protein interactions. Cell, 82, 131-41.

ROBERTSON, I. B. & RIFKIN, D. B. 2016. Regulation of the Bioavailability of TGF-beta and TGF-beta-Related Proteins. Cold Spring Harb Perspect Biol, 8.

ROCK, M. J., CAIN, S. A., FREEMAN, L. J., MORGAN, A., MELLODY, K., MARSON, A., SHUTTLEWORTH, C. A., WEISS, A. S. & KIELTY, C. M. 2004. Molecular basis of elastic fiber formation. Critical interactions and a tropoelastin-fibrillin-1 cross-link. J Biol Chem, 279, 23748-58.

SAHARINEN, J., HYYTIAINEN, M., TAIPALE, J. & KESKI-OJA, J. 1999. Latent transforming growth factor-beta binding proteins (LTBPs)--structural extracellular matrix proteins for targeting TGF-beta action. Cytokine Growth Factor Rev, 10, 99-117.

SAHARINEN, J. & KESKI-OJA, J. 2000. Specific sequence motif of 8-Cys repeats of TGF-beta binding proteins, LTBPs, creates a hydrophobic interaction surface for binding of small latent TGF-beta. Mol Biol Cell, 11, 2691-704.

SAHARINEN, J., TAIPALE, J., MONNI, O. & KESKI-OJA, J. 1998. Identification and characterization of a new latent transforming growth factor-beta-binding protein, LTBP-4. J Biol Chem, 273, 18459-69.

SCHRIJVER, I., LIU, W., BRENN, T., FURTHMAYR, H. & FRANCKE, U. 1999. Cysteine substitutions in epidermal growth factor-like domains of fibrillin-1: distinct effects on biochemical and clinical phenotypes. Am J Hum Genet, 65, 1007-20.

SCHUCK, P. 2000. Size-distribution analysis of macromolecules by sedimentation velocity ultracentrifugation and lamm equation modeling. Biophys J, 78, 1606-19.

STERNER-KOCK, A., THOREY, I. S., KOLI, K., WEMPE, F., OTTE, J., BANGSOW, T., KUHLMEIER, K., KIRCHNER, T., JIN, S., KESKI-OJA, J. & VON MELCHNER, H. 2002. Disruption of the gene encoding the latent transforming growth factor-beta binding protein 4 (LTBP-4) causes abnormal lung development, cardiomyopathy, and colorectal cancer. Genes Dev, 16, 2264-73.

SU, C. T., HUANG, J. W., CHIANG, C. K., LAWRENCE, E. C., LEVINE, K. L., DABOVIC, B., JUNG, C., DAVIS, E. C., MADAN-KHETARPAL, S. & URBAN, Z. 2015. Latent transforming growth factor binding protein 4 regulates transforming growth factor beta receptor stability. Hum Mol Genet, 24, 4024-36.

SVERGUN, V. V. V. A. D. I. 2003. Uniqueness of ab-initio shape determination in small-angle scattering. J. Appl. Cryst., 36, 860-864.

TRIA, G., MERTENS, H. D., KACHALA, M. & SVERGUN, D. I. 2015. Advanced ensemble modelling of flexible macromolecules using X-ray solution scattering. IUCrJ, 2, 207-17.

TROILO, H., STEER, R., COLLINS, R. F., KIELTY, C. M. & BALDOCK, C. 2016. Independent multimerization of Latent TGFβ Binding Protein-1 stabilized by cross-linking and enhanced by heparan sulfate. Scientific Reports, 6, 34347.

URBAN, Z., HUCTHAGOWDER, V., SCHURMANN, N., TODOROVIC, V., ZILBERBERG, L., CHOI, J., SENS, C., BROWN, C. W., CLARK, R. D., HOLLAND, K. E., MARBLE, M., SAKAI, L. Y., DABOVIC, B., RIFKIN, D. B. & DAVIS, E. C. 2009. Mutations in LTBP4 cause a syndrome of impaired pulmonary, gastrointestinal, genitourinary, musculoskeletal, and dermal development. Am J Hum Genet, 85, 593-605.

WATERHOUSE, A., BERTONI, M., BIENERT, S., STUDER, G., TAURIELLO, G., GUMIENNY, R., HEER, F. T., DE BEER, T. A. P., REMPFER, C., BORDOLI, L., LEPORE, R. & SCHWEDE, T. 2018. SWISS-MODEL: homology modelling of protein structures and complexes. Nucleic Acids Res, 46, W296-W303.

YUAN, X., DOWNING, A. K., KNOTT, V. & HANDFORD, P. A. 1997. Solution structure of the transforming growth factor beta-binding protein-like module, a domain associated with matrix fibrils. EMBO J, 16, 6659-66.

ZILBERBERG, L., TODOROVIC, V., DABOVIC, B., HORIGUCHI, M., COUROUSSE, T., SAKAI, L. Y. & RIFKIN, D. B. 2012. Specificity of latent TGF-beta binding protein (LTBP) incorporation into matrix: role of fibrillins and fibronectin. J Cell Physiol, 227, 3828-36.

Supplementary

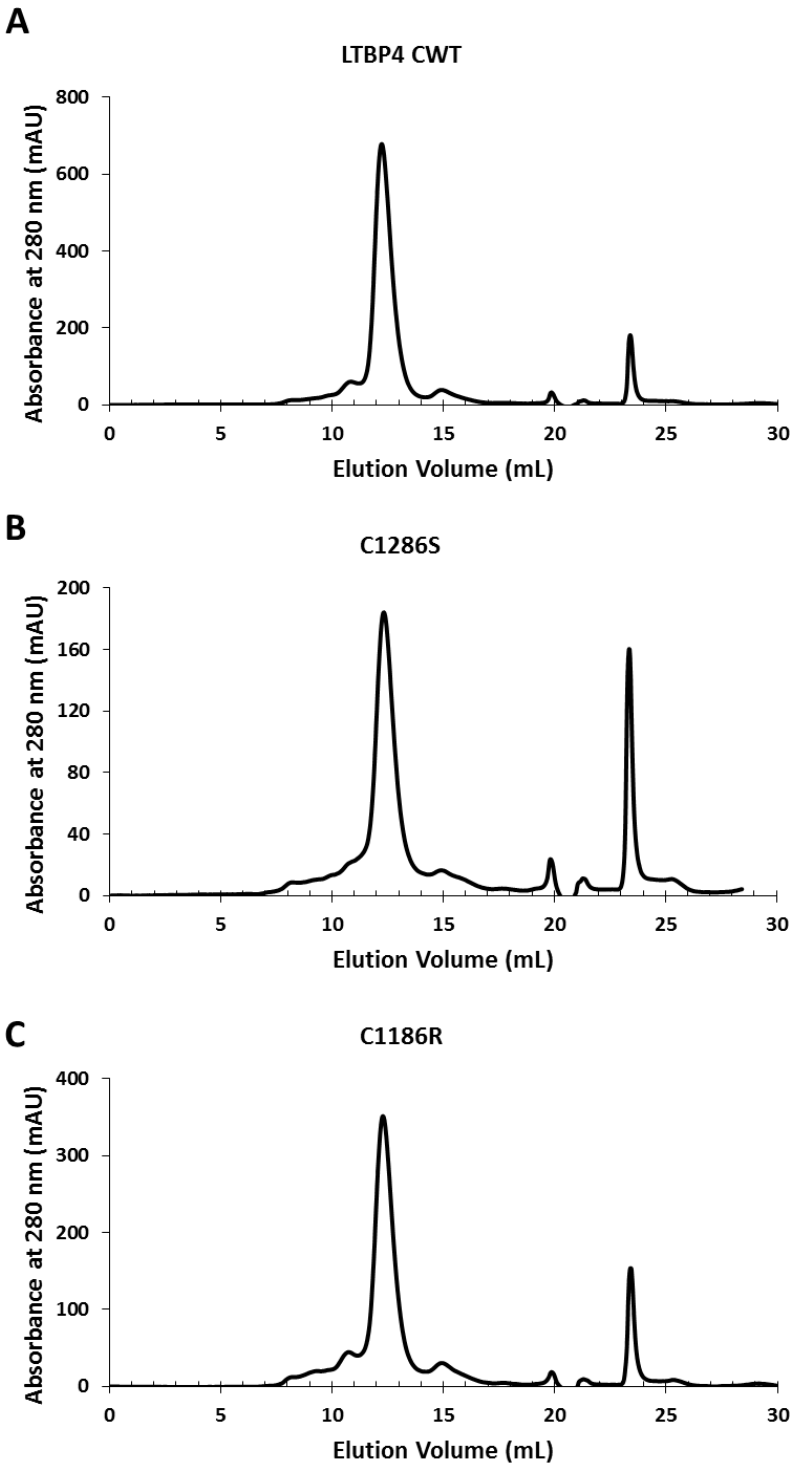

Figure 1: Purification of LTBP4 C-terminal constructs. Size exclusion chromatograms of the **(A)** wildtype LTBP4 C-terminal, **(B)** C1286S and **(C)** C1186R showing similar elution volumes of the monomer species for each construct. All proteins were in buffer containing 10 mM Tris and 150 mM NaCl at pH 7.8 and eluted at a flow rate of 0.5 ml/min.

Ai

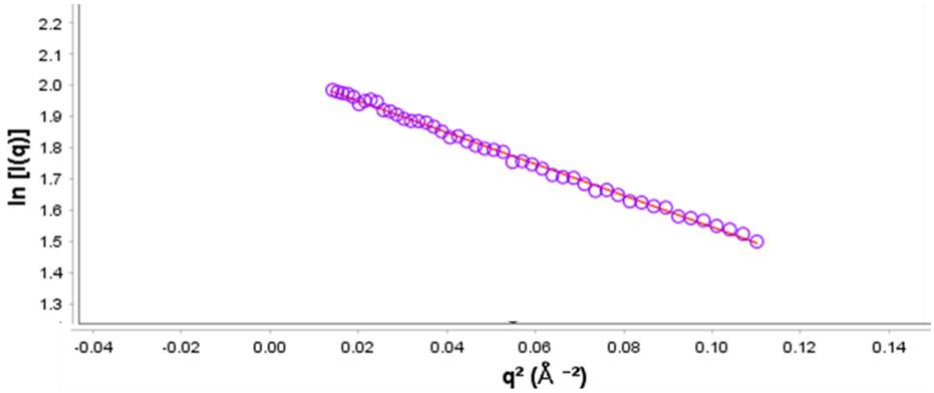
ln [I(q)]
2.2
2.1
2.0
1.9
1.8
1.7
1.6
1.5
1.4
1.3
-0.04
-0.02
0.00
0.02
0.04
0.06
0.08
0.10
0.12
0.14
q² (Å ⁻²)

Aii

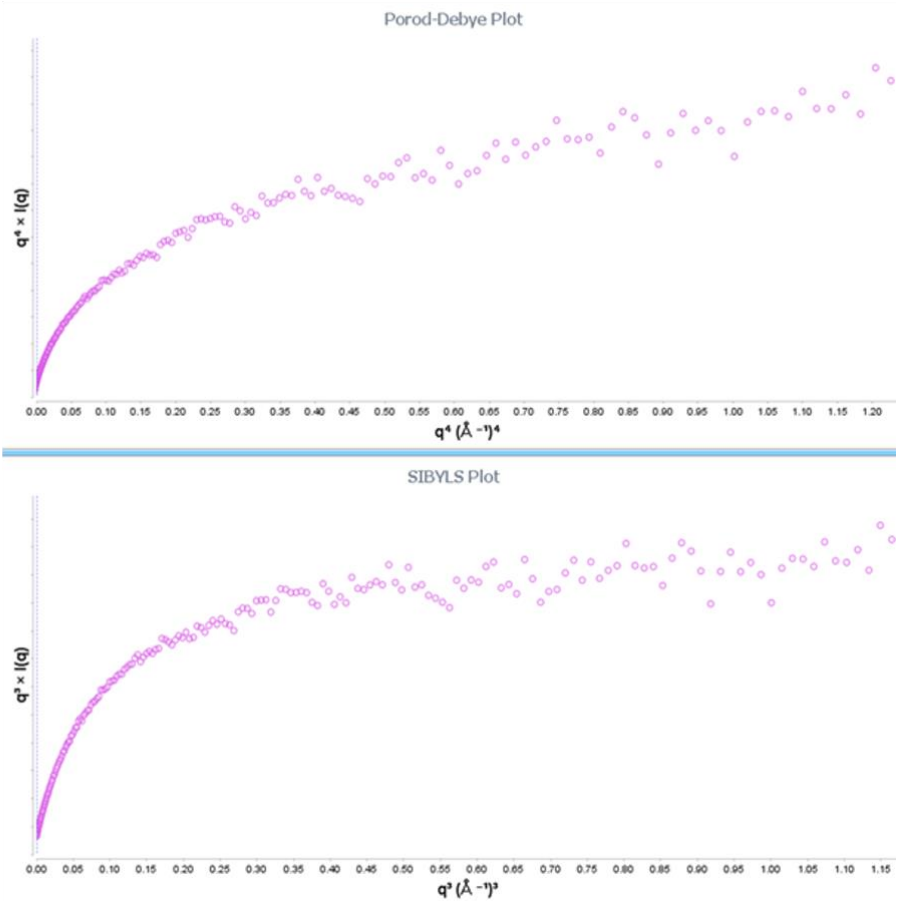
Porod-Debye Plot
q⁴ × I(q)
q⁴ (Å⁻¹)⁴
SIBYLS Plot
q³ × I(q)
q³ (Å⁻¹)³

Bi

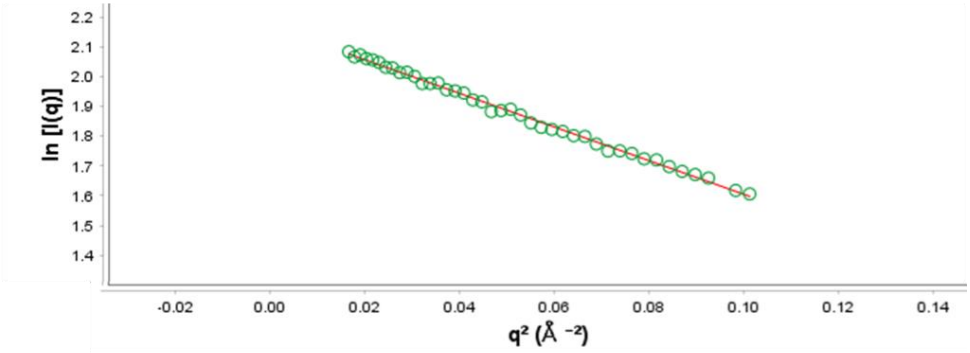
ln [I(q)]
2.2
2.1
2.0
1.9
1.8
1.7
1.6
1.5
1.4
-0.02
0.00
0.02
0.04
0.06
0.08
0.10
0.12
0.14
q² (Å ⁻²)

Bii

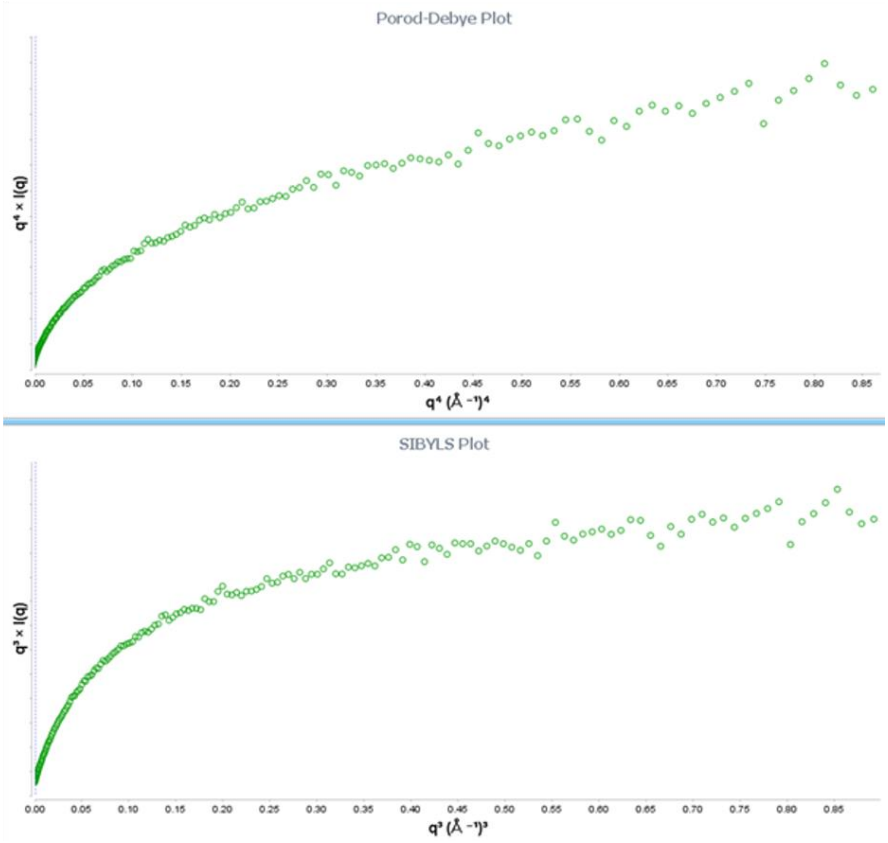
Porod-Debye Plot
q⁴ × I(q)
q⁴ (Å⁻¹)⁴
SIBYLS Plot
q³ × I(q)
q³ (Å⁻¹)³

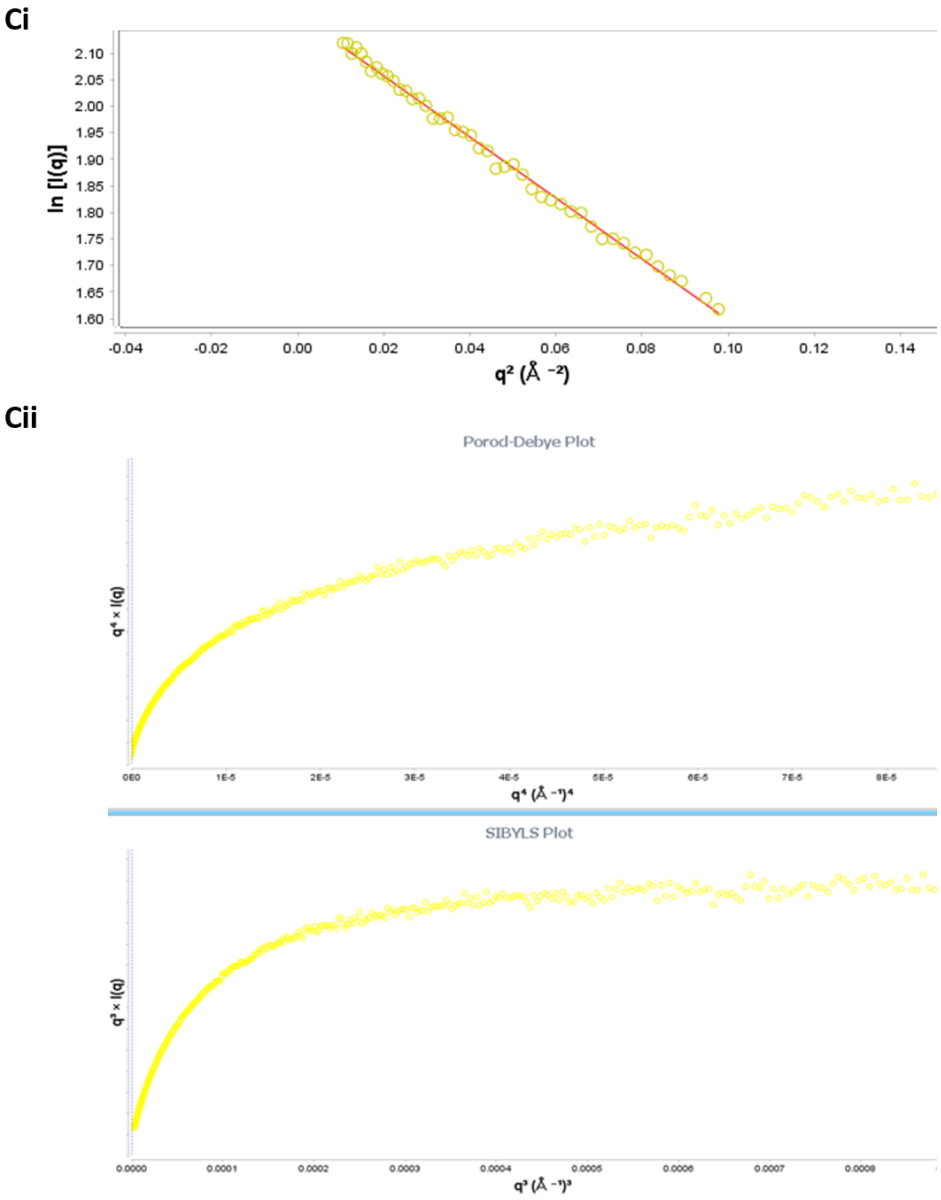

Figure 2: SAXS analysis of LTBP4 C-terminal constructs. Guinier plot of the low q region for the **(Ai)** wildtype LTBP4 C-terminal**, (Bi)** C1286S and **(C)** C1186R showing linearity. Nicer plateau in the SIBYLS plot than in the Porod-Debye plot for the **(Aii)** wildtype LTBP4 C-terminal**, (Bii)** C1286S and **(Cii)** C1186R suggesting flexibility in their structures.

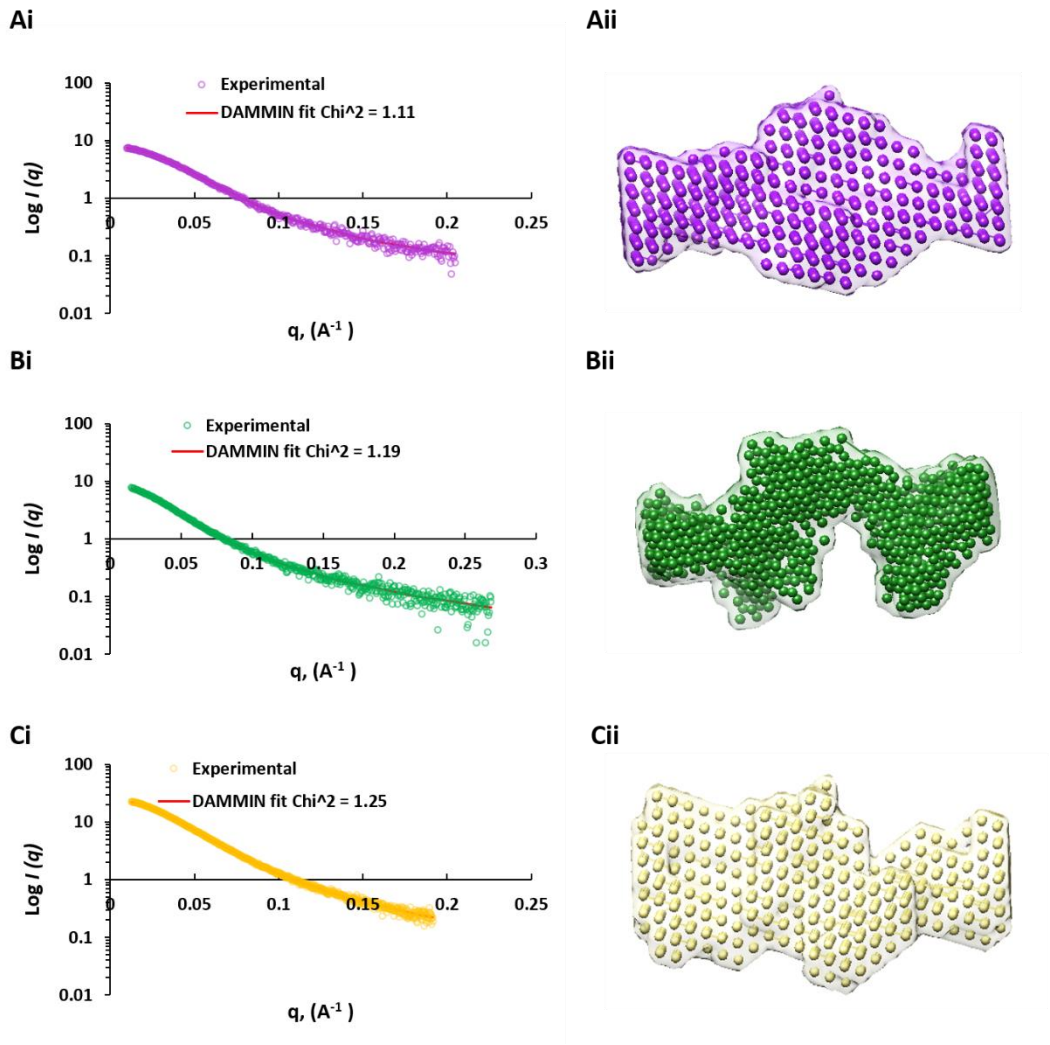

Figure 3: *ab initio* modeling of LTBP4 C-terminal constructs. The experimental 1D scattering intensity I plotted as a function of q for the **(Ai)** wildtype LTBP4 C-terminal , **(Bi)** C1286S and **(Ci)** C1186R used for analysis and modelling with the DAMMIN best fit to the experimental data and discrepancy factor χ^2 of (1.1) for the LTBP4CWT, (1.19) for the C1286S and (1.2). Bead model of one of the ten generated DAMMIF's showing an elongated conformation for the (Aii) wildtype LTBP4 C-terminal, (Bii) C1286S and (Cii) C1186R.

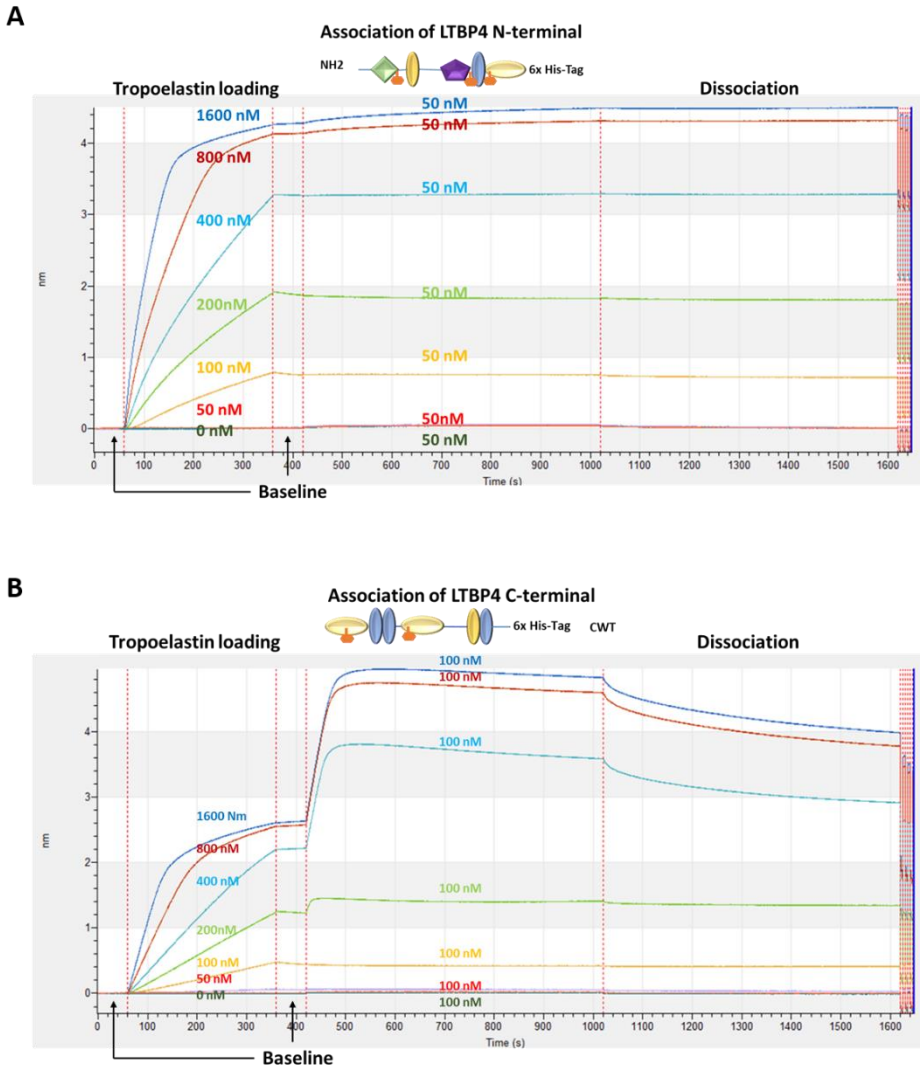

Figure 4: LTBP4 binding to tropoelastin. (A) OctetRED96 analysis of 50 nM of the wildtype LTBP4 N-terminal binding to immobilized tropoelastin at different concentrations (1600 – 0 nM) showing no binding. **(B)** OctetRED96 analysis of 100 nM of the wildtype LTBP4 C-terminal binding to immobilized tropoelastin at different concentrations (1600 – 0 nM) showing specific binding.

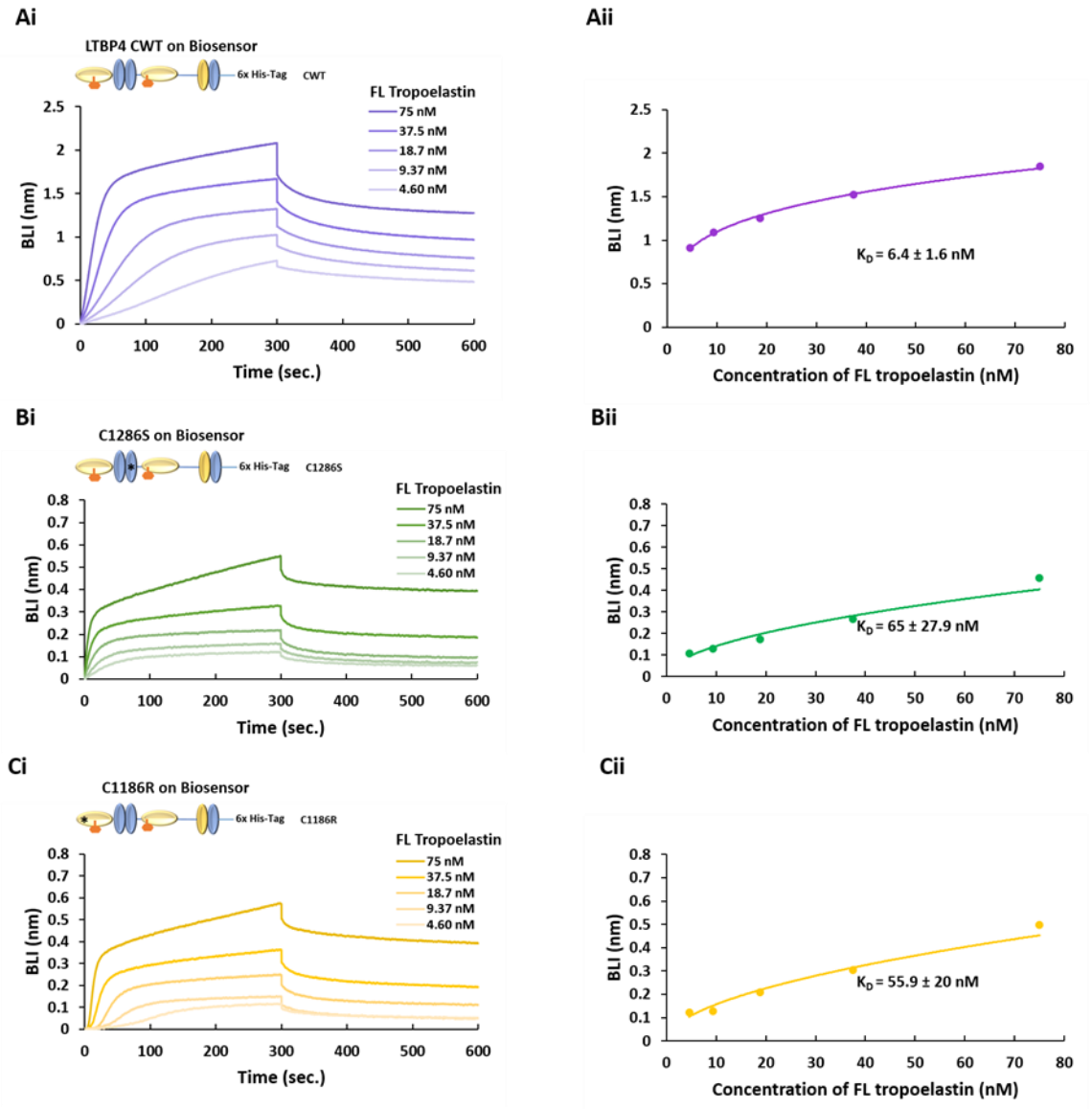

Figure 5: Biolayer interferometry (BLI) analysis of full length tropoelastin binding to LTBP4 C-terminal constructs using OctetRED96. OctetRED analysis show that different concentrations (75 – 4.60 nM) of full length tropoelastin directly bind to immobilized **(Ai)** CWT, **(Bi)** C1286S and **(Ci)** C1186R. The binding affinity was determined by steady state (equilibrium) plotted against full length tropoelastin concentration with the determined averaged binding affinity K_D for the interaction with the LTBP4 **(Aii)** CWT, **(Bii)** C1286S, and **(Cii)** C1186R. All experiments were performed in duplicates and representative results are shown.

4. Chapter 4: Results

Structural and Functional Consequences of a Point mutation in the N-terminal region of LTBP4 in Autosomal Recessive Cutis Laxa type 1C

Structural and Functional Consequences of a Point mutation in the N-terminal region of LTBP4 in Autosomal Recessive Cutis Laxa type 1C

Yasmene F. Alanazi, Michael P. Lockhart-Cairns, and Clair Baldock

Wellcome Trust Centre for Cell Matrix Research, Division of Cell Matrix Biology and Regenerative Medicine, School of Biological Science, Faculty of Biology, Medicine and Health, Manchester Academic Health Science Centre, University of Manchester, UK

Abstract

Latent TGFβ binding protein 4 (LTBP4) is essential for the formation of intact elastic fibres and extracellular regulation of TGFβ bioavailability. Mutations in LTBP4 result in Autosomal Recessive Cutis Laxa type 1 C (ARCL1C) in humans, that severely disrupts elastic fibre assembly in multiple organs including the lung, leading to high mortality. The multi-organ involvement associated with LTBP4 mutations emphasises its biological importance in elastogenesis. Despite the importance of LTBP4, its structure is not yet defined and little is known about the molecular mechanism by which it regulates elastogenesis. The N-terminal region of LTBP4 is functionally important in extracellular matrix deposition and elastogenesis. Mutations in this region could impair its matrix deposition and hamper its involvement in elastic fibre assembly leading to defected elastic fibres. Here we show that the LTBP4 N-terminal region is monomeric in solution and adopts an extended inflexible structure. We also demonstrate that the ARCL1C causing point mutation, within the hybrid domain of LTBP4, induces a conformational change resulting in a more compact conformation. Binding studies show that this mutation increased binding to fibulin-4 and decreased binding to heparan sulphate. We also show that the N-terminal region of LTBP4 does not directly bind to fibronectin. Together, these data demonstrate the importance of the hybrid domain in stabilising the structure and maintaining the function of LTBP4.

Introduction

Latent TGFβ binding protein 4 (LTBP4) belongs to a family of four large secreted extracellular matrix glycoproteins (LTBP1-4) that are structurally homologous to the integral extracellular matrix protein fibrillin-1 (Todorovic and Rifkin, 2012). Both LTBPs and fibrillin-1, share

disulphide-rich epidermal growth factor-like domains (EGF) and TGFβ binding protein-like domains (TB) (Saharinen et al., 1999, Oklu and Hesketh, 2000, Robertson et al., 2011). LTBP4 has 20 EGF-like domains, of which 17 are calcium-binding, three TB domains and a hybrid domain, named due to its sequence similarity to both TB and cbEGF domains, and proline-rich interdomain regions (Saharinen et al., 1998, Giltay et al., 1997). LTBP4 assists in TGF-β folding and secretion by disulphide bonding with TGFβ latency associated propeptide (LAP) via the 2nd TB domain to form the large latent complex. The Latent complex is targeted into the extracellular matrix via the N-terminal region of LTBP4 where it is accessible for activation (Saharinen and Keski-Oja, 2000, Rifkin, 2005, Robertson and Rifkin, 2016, Koli et al., 2005). In addition to the TGFβ related function, LTBP4 has also been shown to regulate elastic fibre assembly in a TGFβ independent manner (Dabovic et al., 2009) by direct interaction with fibulin-4 and fibulin-5 via the N-terminal region (Noda et al., 2013, Bultmann-Mellin et al., 2016, Dabovic et al., 2015) and fibrillin-1 via the C-terminal region (Isogai et al., 2003, Ono et al., 2009).

In mammalian cells, two LTBP4 isoforms are expressed, a long form LTBP4L and a short form LTBP4S (Saharinen et al., 1998). Both isoforms have similar domain structure, but an additional N-terminal 4-Cys domain was found in the long form (Kantola et al., 2010). Each LTBP4 isoform is produced by an independent promoter and possesses distinct functions (Kantola et al., 2010). Both LTBP4 isoforms show overlapping expression in lung and aorta in mice. Whereas, the short form of LTBP4 is the major expressed isoform in heart and skin (Bultmann-Mellin et al., 2015). Interestingly, LTBP4S is the major expressed form in lung during late embryonic and postnatal periods (Bultmann-Mellin et al., 2017). Mutations in both LTBP4 isoforms cause Autosomal Recessive Cutis Laxa type 1C (ARCL1C) in humans. This rare congenital connective tissue disease is characterised by craniofacial anomalies and high mortality, lung and several visceral organs are severely involved due to the severe disruption of elastic fibres (Callewaert et al., 2013, Urban et al., 2009). LTBP4 deficient (*LTBP4* $^{-/-}$) mice replicate the phenotype of ARCL1C (Bultmann-Mellin et al., 2015). *LTBP4S* $^{-/-}$ mice that express the long isoform of LTBP4, have a milder phenotype of ARCL1C, ARCL1C-like (Dabovic et al., 2009, Sterner-Kock et al., 2002). The homozygous point mutation p. C274G, where a highly conserved cysteine residue is substituted with glycine in the hybrid domain of LTBP4, was first reported in a 4-month old male with generalised LTBP4-related cutis laxa (CL) (Urban et al., 2009) and severe pulmonary emphysema caused by severely disrupted elastic fibres

(Ritelli et al., 2019). Hybrid domains of both fibrillins and LTBPs play a major role in stabilising their folding and structure (Jensen et al., 2009, Lack et al., 2003).

To our knowledge, only a clinical characterisation and mutational analysis studies were reported for this mutant. Thus, the purpose of this study was to characterise the structural and functional properties of wildtype human LTBP4 N-terminal region and to investigate the structural and functional consequences caused by the ARCL1C mutation on LTBP4, thus improving our knowledge on the role of LTBP4 in elastic fibre assembly.

Material & Methods

Expression and Purification of Recombinant Proteins

Human wildtype and mutant LTBP4 N-terminal region fragments were purchased as gene strings (residues 29-394) and expressed in Human Embryonic Kidney (293)-EBNA cells using a modified mammalian expression vector pCEP4 (Invitrogen), pCEP-Pu/AC7 that contains a C-terminal six-histidine residue tag (6x His-tag). The recombinant human wildtype and mutant LTBP4 N-terminal constructs were then purified using nickel affinity column (GE Healthcare) followed by size-exclusion chromatography on FPLC (AKTA purifier) using a Superdex 200 10/300GL column (GE Healthcare). The Superdex 200 10/300GL column was equilibrated with buffer containing 10 mM Tris and 150 mM NaCl at pH 7.8 at a flow rate of 0.5 ml/min. Protein identity was confirmed by mass spectrometry (MS) and Western immunoblotting, and concentration determined using BCA protein assay (Thermo Fisher Scientific). Full length fibulin-5, fibulin-4 and fibronectin were expressed and purified as previously describe (Choudhury et al., 2009, Cheng et al., 2018).

Multi-angle Light Scattering (MALS)

Purified protein samples 0.5 ml at approximately 0.4 - 1 mg/ml were loaded onto a Superdex 200 10/300GL column (GE Healthcare) at a flow rate of 0.5 ml/min using a buffer containing 10 mM Tris and 150 mM NaCl at pH 7.8. Protein samples were then passed from the column into a Wyatt DAWN Heleos II EOS 18 angle laser photometer with QELS detector (Wyatt Technologies) coupled to an Optilab T-rEX refractive index detector. The absolute molar mass, hydrodynamic radii and concentration of the resulting peaks were analyzed using ASTRA 6 software.

De-glycosylation:

Deglycosylation of the purified proteins were performed using PNGase-F under according to the manufacturer's protocol (New England Biolabs). The removal of sugars was verified using SDS-PAGE electrophoresis.

Sedimentation Velocity Analytical Ultracentrifugation (SV-AUC)

Sedimentation velocity AUC was performed using Beckman XL-A analytical ultracentrifuge with an An60Ti 4-hole rotor running at 45,000 rpm at 20°C on native monomeric protein samples (0.4 - 1 mg/ml) in the same buffer as used in MALS. Continuous model-based distribution C(s) method was used for analysis by SEDFIT software (Troilo et al., 2016). The obtained sedimentation coefficients were corrected to standard conditions using the software, SEDNTERP (Philo, 2000).

Small-angle Light Scattering (SAXS)

In-line SEC-SAXS data were collected at 1 - 2 mg/ml on native monodisperse sample of wildtype and mutated LTBP4 N-termini in the same buffer as used in MALS and AUC at the Diamond Light Source on beamline B21. SAXS data were collected at 1 second intervals using 45uL purified protein sample passed through a Superdex 200 3.2/300 column. The initial SAXS data were spherically averaged reduced by an in-house software then were processed and analysed using ScAtter software (http://www.bioisis.net/tutorial/9; last accessed November 2019). The collected scattering data from buffer was subtracted from that of the sample. Guinier approximation was used to determine the radius of gyration R_g of the protein. Indirect Fourier transform (IFT) method, GNOM, was used to determine the pair distance distribution P (r) in real space and particle shapes of the protein were generated in slow mode using DAMMIN software (Franke and Svergun, 2009). Ten *ab initio* models were generated separately and aligned and then superimposed to obtain a final filtered model using the DAMAVER suite. Goodness of the superimpositions of the separate DAMMIN models compared using DAMSEL was assessed by the normalised spatial discrepancy (NSD).

Circular Dichroism (CD)

Purified wildtype and mutant LTBP4 proteins at a concentration range of 0.5 - 1 mg/ml in 10 mM Tris, 150 mM NaCl, pH7.8 buffer were analysed by circular dichroism (CD) using the Far-UV spectral region (190-260 nm). The Far-UV spectra were recorded in millidegrees (mdeg)

by Jasco-J810 spectropolarimeter. Measurements were taken every 0.2 mm in a 0.5 cm path length cell at 25^{o}C. Ten accumulated scans were recorded, averaged, and then corrected for each LTBP4 N-terminal construct. The online tool Dichroweb was used to quantitatively analyze the secondary structure content of each construct.

Bio-layer interferometry (BLI)

Binding studies were performed on an OctetRED96 system (ForteBio) using biolayer interferometry (BLI). Streptavidin biosensors were first hydrated with buffer containing 10 mM HEPES, 150 NaCl, pH7.4 buffer supplemented with 0.005% (v/v) Tween-20 for 10 minutes then were loaded with the biotinylated ligands at constant concentration. The loaded biosensors were then incubated with the analyte diluted at different concentrations in the same buffer used for hydration. The biosensors were regenerated using 10 mM glycine at pH 2.5. The binding kinetics were analyzed using Octet software version 7 (ForteBio). The goodness of binding data fitting was assessed by X^2 and R^2 values. Background response has been subtracted from all binding sensorgrams. All binding experiments were performed in solid-black 96 well plates at 25C^{o} with an agitation speed of 1000 rpm and repeated at least 2 times. Both ligand and analyte were diluted in the same buffer used for biosensors hydration. Biotinylated human long chain heparan sulphate was kindly provided by the Biomolecular analysis facility in the University of Manchester.

Results

Expression and Purification of Recombinant Human LTBP4 N-terminal region

The wildtype and mutant N-terminal region of human LTBP4S were stably expressed in HEK293-EBNA cells (Figure 4-1A). The expressed and secreted LTBP4S N-terminal wildtype and mutant were then purified using nickel affinity chromatography followed by size-exclusion chromatography (SEC). The SEC chromatograms for both wildtype and mutant showed a single prominent peak which eluted at similar elution volume (Figure supplementary 1). The non-reducing SDS-PAGE of the purified prominent species presented in Figure 4-1B & C showed a single band of approximately 50 KDa for both the wildtype and mutant, respectively, which is larger than expected from sequence (41 KDa). However, there are three potential N-linked glycosylation sites predicted in the N-terminal region of LTBP4S (Saharinen et al., 1998). The presence of N-glycans on full-length LTBP4S was previously

shown using PNGaseF (Bultmann-Mellin et al., 2015) so the presence of N-glycans on the shorter constructs was verified using PNGaseF deglycosylation assays. Following PNGase treatment, wildtype and mutant proteins migrated at the expected size, confirming the presence of N-linked sugars (Figure 4-1D). Since the ARCL1C mutation changes a conserved cysteine residue involved in disulphide bond formation, purified wildtype and mutant proteins were analysed using SDS-PAGE under reducing and non-reducing conditions to determine whether the presence of a free cysteine in the mutant altered disulphide bond formation or allowed the formation of disulphide-bonded dimers. Upon reduction the mobility of the LTBP4 N-terminal regions decreased, consistent with intramolecular disulphide bridges maintaining the domain fold even in denaturing conditions but no higher ordered species were present for either the wildtype or mutant N-terminal regions under non-reducing conditions, indicating the absence of intermolecular interactions between LTBP4 monomers (Figure 4-1B & C).

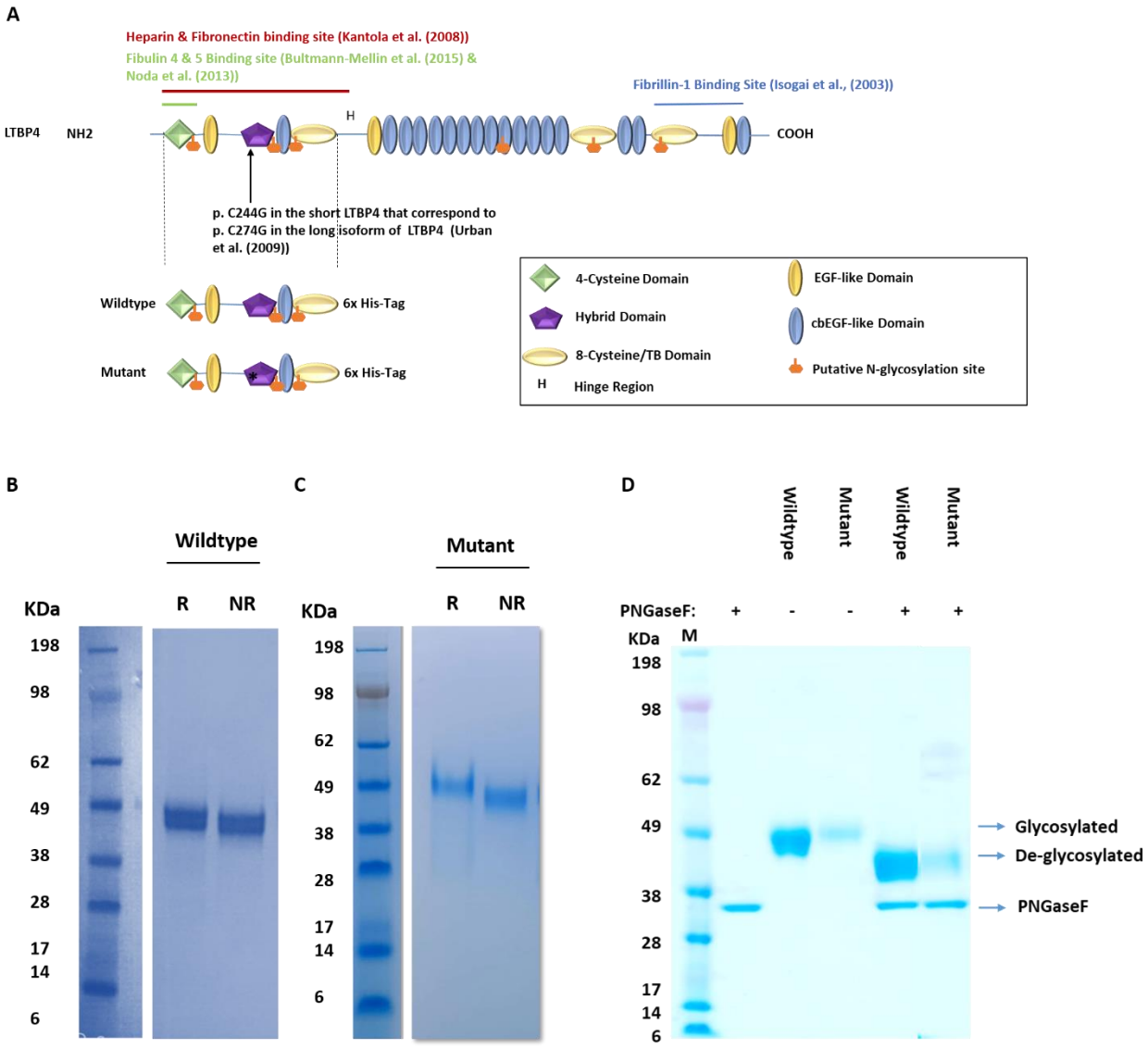

Figure 4-1: Expression and purification of recombinant LTBP4 N-terminal region. (A) Schematic diagram of the domain organisation for full-length LTBP4S with N- and C-terminal binding sites indicated and the shorter constructs used in this study. Arrows indicate the location of the ARCL1C causing mutation studied. (B & C) SDS-PAGE gel showing purified LTBP4 N-terminal constructs: wildtype and mutant, respectively, under reducing (R) and non-reducing (NR) conditions. (D)Non-reduced SDS-PAGE gel showing the purified LTBP4 N-terminal constructs before and after deglycosylation with PNGaseF.

The N-terminal region of Latent TGFβ Binding Protein 4 is Monomeric in Solution

Our recent study on human LTBP1 demonstrated that the wildtype N-terminal terminal region tends to oligomerise into dimers and higher ordered species in a calcium-dependent manner [28]. Therefore, we used complementary methods including SEC-MALS and SV-AUC to

investigate the oligomeric state and the hydrodynamic properties of LTBP4. The ARCL1C causing mutant was also characterised to investigate possible structural consequences caused by this mutation. SEC-MALS data showed a single peak eluted at similar volume for both the wildtype and mutated LTBP4 N-termini (Figure 4-2A). An absolute molar mass of 47 KDa and 51 KDa were estimated for the LTBP4 N-terminal wildtype and mutant, respectively. The estimated absolute molar mass for each construct indicates that both the wildtype and mutated LTBP4 N-termini are monomeric in solution. The sedimentation profile from the AUC (Figure 4-2B) further confirmed the monomeric state of both the wildtype and mutant LTBP4 N-termini, with estimated molecular weight of 42 KDa for the wildtype LTBP4 N-terminal and 45 KDa for the mutant. Moreover, the SV-AUC data for the mutant showed small amounts of higher sedimenting species, indicating an increased tendency to form larger species. Based on the sedimentation profile (Figure 4-2B), the wildtype LTBP4 N-terminal region sediments at 3.25 Svedberg (S) with a frictional ratio of 1.40, higher than that expected for a globular protein (theoretically f/f0 of 1.2) (Schuck, 2000), suggesting a moderate elongation for this region. While the mutant sediments slightly faster at 3.61 (S) with slightly lower frictional ratio of 1.33, indicating that the mutation induces a more compact conformation. Table 4-1 summarises the hydrodynamic properties of LTBP4 N-terminal region constructs.

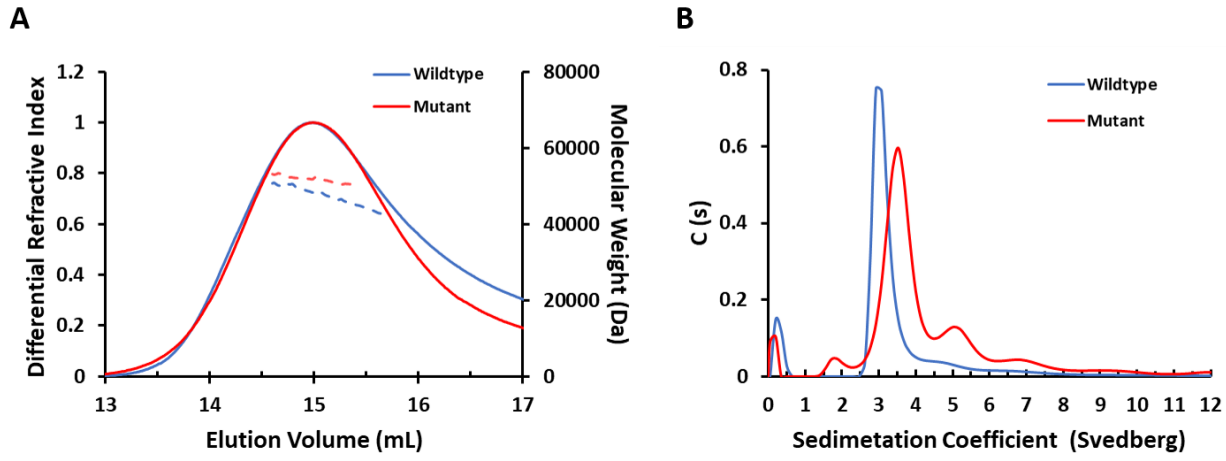

Figure 4-2: Structural characterisation of LTBP4 N-terminal region. (A) SEC-MALS chromatograms of the LTBP4 N-terminal constructs, in which the differential refractive index (solid lines) and molecular weight (dashed lines) are plotted as a function of elution volume (mL), showing both wildtype and mutant constructs are monomeric in solution with mass of 47 and 51 KDa for LTBP4 N-terminal region wildtype and mutant, respectively and (B) Sedimentation coefficient profile of the LTBP4 N-terminal

region constructs showing a prominent single peak for each construct with smaller amounts of larger sedimenting species.

Table 4-1: Experimental hydrodynamic results for LTBP4 N-terminal region constructs

Hydrodynamic Properties	**Wildtype**	**Mutant**
Molecular Mass (KDa) [a]	47	51
Molecular Mass (KDa) [b]	41	45
Sedimentation Coefficient (Sw) [b]	3.15	3.54
Sedimentation Coefficient (Sw, 20) [b]	3.25	3.61
Frictional Ratio (f/f_0) [b]	1.40	1.33
Stokes Radius [b]nm	3.20	3.14
Radius of gyration R_g (nm)[c]	3.8	3.5
Maximum Dimension D_{max} (nm)[c]	ND	11.1
R_g/R_h	1.18	1.11

[a] Multi-Angle Light Scattering (MALS)

[b] Sedimentation Velocity Analytical Ultracentrifugation (AUC)

[c] Small angle X-ray Scattering

LTBP4 N-terminal Monomer has an Elongated and inflexible Nanostructure

To gain more information on the size and shape of the LTBP4 N-terminal region, small angle X-ray scattering (SAXS) was performed. SAXS data were collected directly from in-line SEC eluates of purified wildtype and mutant LTBP4 N-terminal region to ensure their monodispersity in solution. The experimental 1D scattering intensity curve of each LTBP4 N-terminal region construct is plotted as a function of q (Figure 4-3A & B). SAXS data quality was assessed using Guinier plots of each LTBP4 N-terminal region construct. Guinier plots for both wildtype and mutated LTBP4 N-termini showed linearity, indicating no aggregation present (Figure supplementary 2A and B for LTBP4 N-termini wildtype and mutant, respectively). The Guinier approximation was also used to determine the radius of gyration R_g which was 3.8 and 3.5 nm for the wildtype and mutant, respectively. The scattering intensity at higher angles was insufficient for the wildtype to perform further data analysis or ab initio modelling so the data for the mutant was analysed. The maximum particle dimension D_{max} for the mutant was 11.1 nm determined by indirect Fourier transformation using GNOM (Svergun, 2003). The

flexibility of the mutant was assessed, the Porod-Debye plot plateaued at high q range, indicating that this region is not flexible (Figure supplementary 2C). The normalised Kratky plot for the mutant (Figure 4-3C) displayed single peak with maxima slightly deviating from globularity point, indicating that this region is asymmetric and elongated. The obtained distance distribution function P(r) shown in Figure 3-3D, also suggests an extended conformation for the mutant. Ten 3-D *ab initio* models were independently generated using DAMMIN. A representative DAMMIN model confirmed the elongated structure with the best fit to the experimental SAXS data χ^2 of 1.5 (Figure supplementary 2). An average *ab initio* model was generated by DAMAVER (Figure 4-3E), with normalised special discrepancy (NSD) of 0.655 ± 0.030 which indicates a unique solution. The structural parameters including Rg and Dmax obtained from the experimental data are summarised in Table 4.1.

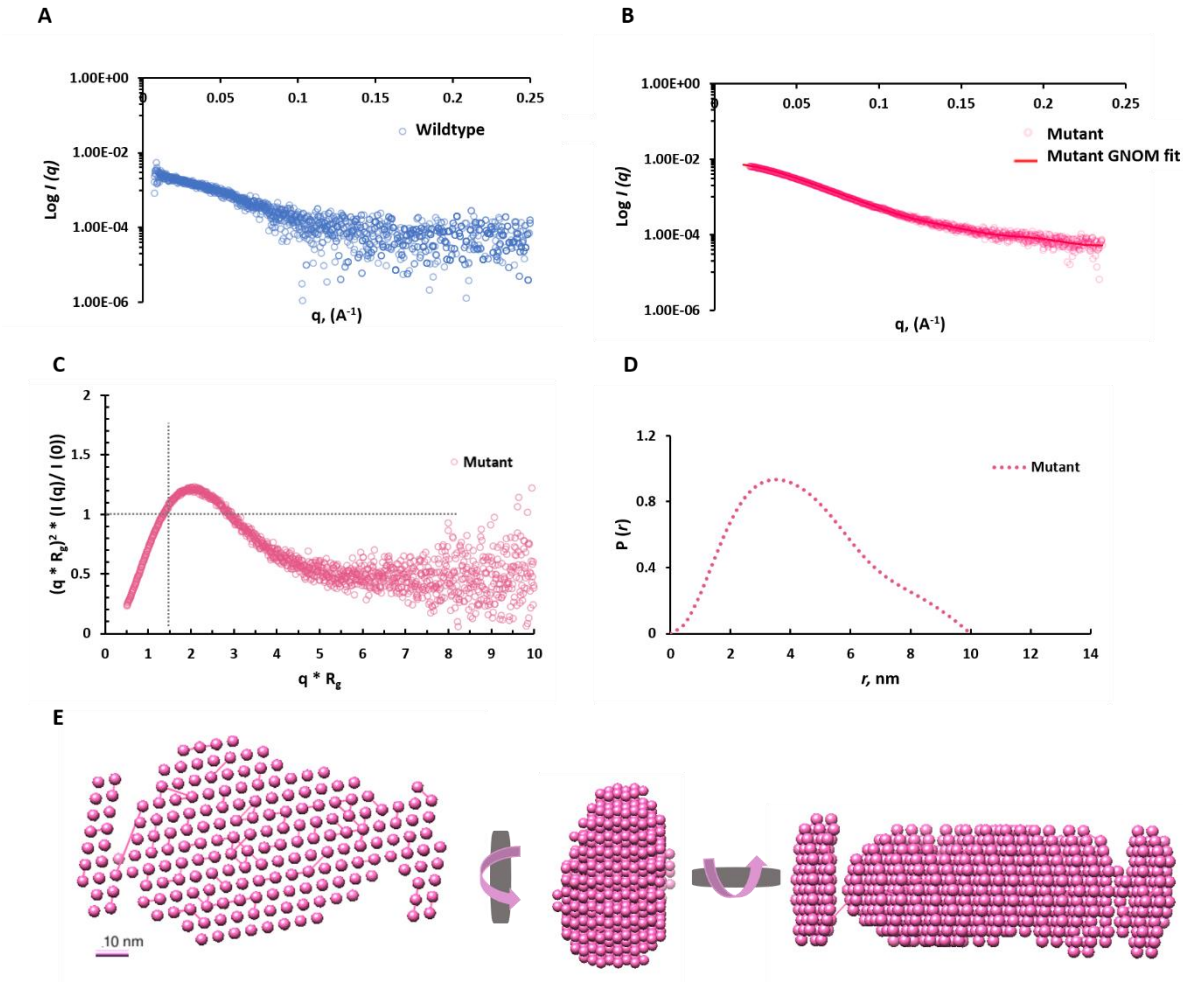

Figure 4-3: Structural characterisation of the LTBP4 N-terminal region in solution using Small Angle X-ray Scattering (SAXS).Experimental 1D scattering intensity I plotted as a function of q for (A) wildtype LTBP4and (B) mutant LTBP4 N-terminal constructs used for analysis. (C) The normalised Kratky plot

for the mutant shows the peak slightly deviating from the globular point (cross-hair indicates the Guinier-Kratky point (1.732, 1.1)), indicating that the protein has a folded but extended conformation. (D) The indirect Fourier transform of I vs. q using GNOM, P(r) vs. r indicating the maximum dimension in real space. (E) The averaged DAMFILT model of the mutant LTBP4 N-terminal region shown in three orthogonal views.

Secondary Structure Analysis of Wildtype and mutant LTBP4 N-terminal region

The secondary structure of the wildtype and ARCL1C mutant LTBP4 N-terminal region was analysed using Far UV-CD to determine whether the mutation causes structural changes. The CD spectra displayed a minima at 205 nm for both wildtype and mutant (Figure 4-4). The estimated secondary structure content for both wildtype and mutant LTBP4 N-termini were similar, indicating that the ARCL1C point mutation did not cause a conformational transition. Both contained 16 – 17 % of α-helix, 23 – 24 % of β-sheet, 19 – 20 % turns, and 40 % of unordered structure.

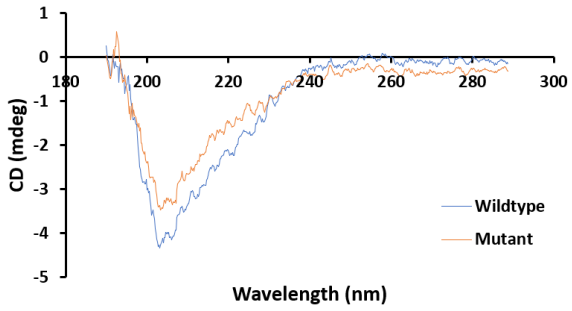

Table 4-2

LTBP4 N-terminal Construct	α-Helix %	β-Sheet %	Turns %	Unordered %
Wildtype	17	24	19	40
Mutant	16	23	20	40

Figure 4-4: Circular Dichroism and secondary structure prediction of LTBP4 N-terminal region. The Far-UV-CD spectra in the 260-190 nm range for the wildtype and mutant LTBP4 N-terminal regions show a negative peak with a strong intensity at 205 nm. Table 4-2: Secondary structure content of LTBP4 N-terminal region constructs.

The Effect of ARCL1C Causing Point Mutation on Binding to Fibulin-4

LTBP4 has been previously shown to interact with fibulin-4 to support elastogenesis where both LTBP4 long and short isoforms bind to fibulin-4 (Bultmann-Mellin et al., 2016, Bultmann-Mellin et al., 2015, Kumra et al., 2019). However, since the elastogenic role of LTBP4 is driven by its N-terminal region, we hypothesised that the ARCL1C causing mutation might interfere with the interaction with fibulin-4. To test whether the interaction of the LTBP4 N-terminal region with fibulin-4 is affected by the C244G mutation, we performed kinetic analysis using

OctetRED96 biolayer interferometry. As shown in Figure 4-5, both wildtype and mutant bound to immobilised full-length fibulin-4. Interestingly, the ARCL1C causing mutation resulted in an increase in binding affinity to fibulin-4 with a K_D of 177.3 nM compared to the wildtype that binds with a K_D of 1294 nM. From the binding profile, faster association and dissociation steps were observed for the wildtype compared with the mutant (Figure 4-5Ai). Since fibulin-5 is also vital for the elastogenic role of LTBP4 and mutations in LTBP4 might also interfere with the interaction of fibulin-5, we attempted to test this hypothesis but we were unable to detect direct binding response between the N-terminal region of LTBP4S and fibulin-5 (Figure supplementary 4).

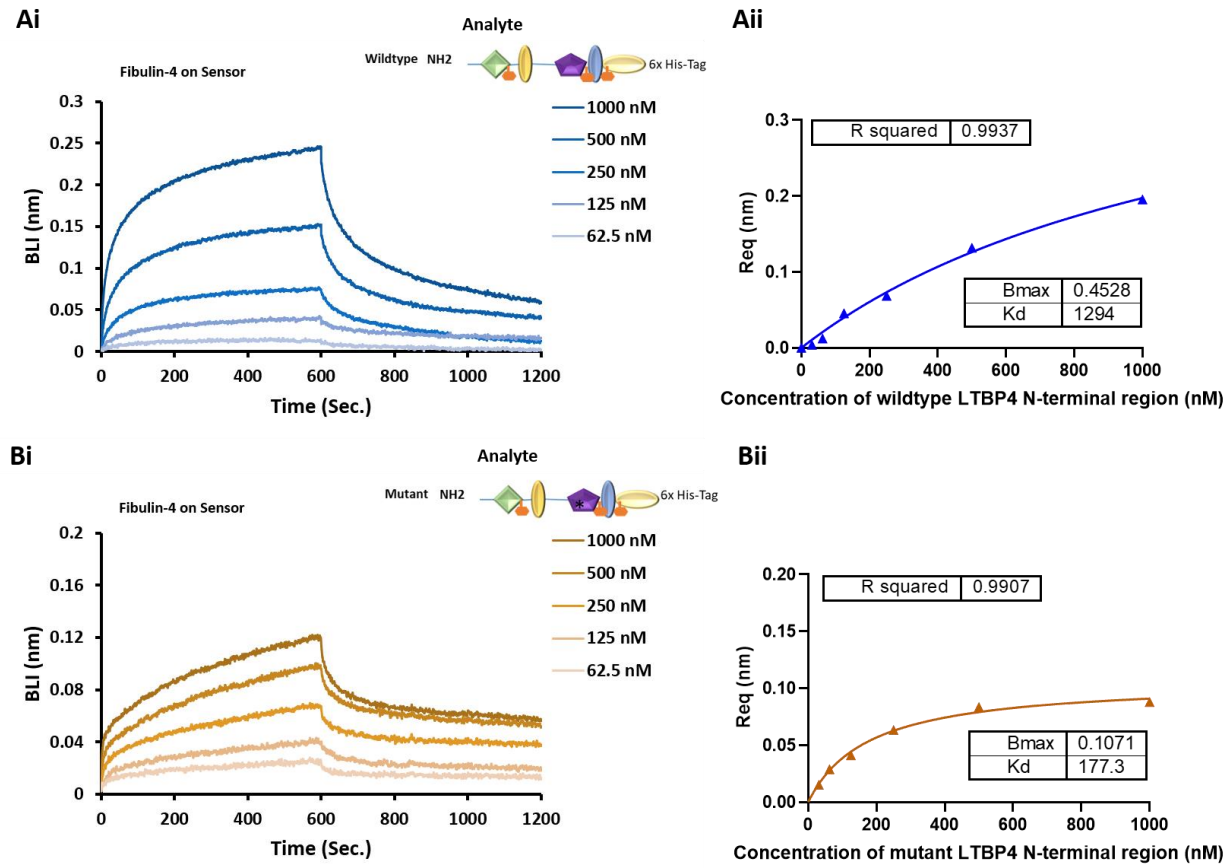

Figure 4-5: The Impact of ARCL1C-causing point mutation on LTBP4 N-terminal region Interaction with fibulin-4. Binding studies using Biolayer interferometry (BLI) were performed using OctetRED analysis. Representative Octet sensorgrams showing both (A) wildtype and (B) the mutant at a range of concentrations (1000 – 62.5 nM) bind to immobilised fibulin-4. The binding affinity K_D was determined by steady state (equilibrium) for (Aii) the wildtype and (Bii) Mutant. All experiments were performed in duplicates and representative results are shown.

LTBP4 N-terminal region Monomer does not Directly Bind to Fibronectin but it Does with Heparan Sulphate

Fibronectin regulates and directs the assembly and deposition of other ECM proteins (Wierzbicka-Patynowski and Schwarzbauer, 2003, Hielscher et al., 2016). LTBP4 ECM association has been thought to be mediated via its N-terminal region binding to fibronectin (Kantola et al., 2008). An LTBP4 N-terminal region direct interaction with plasma fibronectin has previously demonstrated using solid phase binding assay (Kantola et al., 2008) and deletion of the LTBP4 N-terminal region prevented interaction with fibronectin. This interaction has been suggested to be important for LTBP4 deposition into early extracellular matrix. To our knowledge, no previous studies have examined this interaction using real-time binding methods. To determine whether LTBP4S N-terminal was able to bind fibronectin we performed binding studies using OctetRED96 biolayer interferometry (BLI). Purified wildtype LTBP4 N-terminal region was biotinylated and immobilised on streptavidin biosensors. The wildtype LTBP4 N-terminal region loaded biosensors were then incubated in a range of concentrations from (100 -0 nM) of purified full-length fibronectin. The obtained sensorgrams (Figure 4-6A), show flat association/dissociation steps, indicating no direct binding was detected between wildtype LTBP4 N-terminal region and full-length fibronectin. Heparan Sulphate (HS) has been reported to mediate binding between LTBP1 and fibronectin (Chen et al., 2007) and no direct binding was observed between LTBP1 and fibronectin. Therefore, we hypothesised that HS might also mediate the interaction between LTBP4 and fibronectin. The importance of heparin/heparan Sulphate (HS) interaction in mediating cell adhesion has been previously studied (Bax et al., 2007, Vehvilainen et al., 2003). They are also important in mediating protein-protein interactions (Chen et al., 2007). Using heparin affinity chromatography, an interaction between the LTBP4 N-terminal region and heparin has previously been demonstrated (Kantola et al., 2008). Heparin is an analogue of the highly sulphated polysaccharide, HS (Liu and Pedersen, 2007). No studies have examined whether there is a direct interaction between LTBP4 and HS. To determine whether they interact and if the ARCL1C causing mutation interferes with this interaction, we first examined binding using biolayer interferometry OctetRED system and investigated the impact of this mutation on the interaction with HS. Biotinylated HS was immobilised on streptavidin biosensors then incubated with different dilutions of the LTBP4 N-terminal region. The sensorgrams showed

that the wildtype LTBP4 N-terminal region interacted with HS with high affinity K_D = 53.4 nM (Figure 4-6Bi). The mutant LTBP4 N-terminal region also binds to HS with similar affinity K_D = 52.6 nM (Figure 4-6Bii).

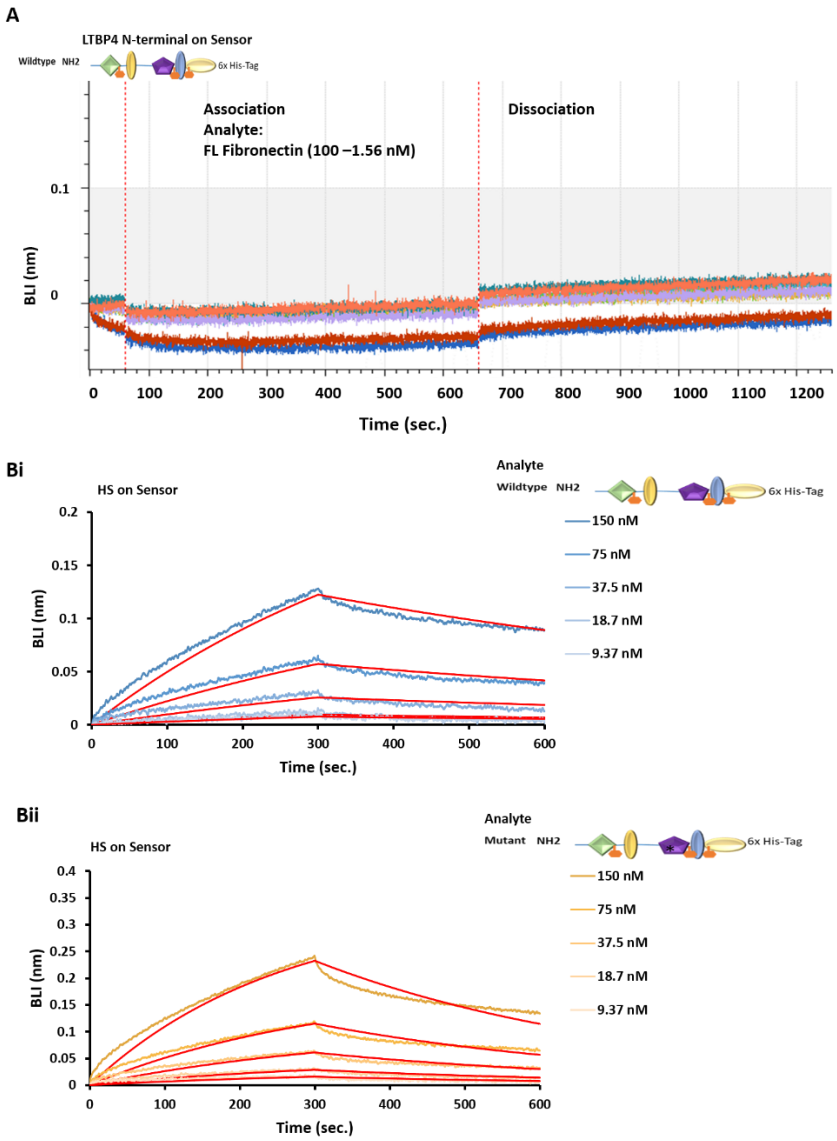

Figure 4-6: Analysis of LTBP4 N-terminal region interaction with fibronectin and heparan sulphate Using Biolayer Interferometry (BLI). (A) OctetRED system sensorgram showing no binding response detected between immobilized wildtype LTBP4 N-terminal and a range of concentrations (100 – 1.56 nM) of fibronectin. (B) OctetRED sensorgrams showing both (Bi) Wildtype and (Bii) Mutant N-termini at a range of concentrations (150 – 9.37 nM) bind to immobilised heparin. The binding affinity K_D was 52.6 nM for the wildtype and 53.4 nM for the mutant, determined by fitting to a 1:1 Langmuir binding model (red fits). All experiments were performed in duplicates and representative results are shown.

Discussion:

Despite the primary role LTBP4 plays in elastogenesis, the molecular mechanism by which it regulates elastic fibre assembly is poorly understood. Therefore, analysing the structure of LTBP4 and investigating the conformational and functional consequences of ARCL1C mutation are necessary to understand the role of LTBP4 in elastic fibre assembly.

Our study provides novel structural information on the LTBP4 N-terminal region. SEC-MALS and SV-AUC data show that the LTBP4 N-terminal region is monomeric in solution, but SV-AUC also showed that this region tends to form higher ordered species. This is in-line with our previous study on LTBP1 where the LTBP1 N-terminal region is also a monomer in solution but readily multimerises in low calcium concentrations (Troilo et al., 2016). The mutant LTBP4 N-terminal region is also monomeric in solution, but had an increased propensity to form higher-ordered species, indicating the production of a less stable protein. The determined molecular masses for both wildtype and mutant proteins obtained from SEC-MALS were slightly larger than expected from sequence, consistent with the presence of N-linked sugars. Full-length LTBP4S contains six potential N-linked glycosylation sites (Saharinen et al., 1998, Bultmann-Mellin et al., 2015), which is important for folding, conformation and function of proteins (Dalziel et al., 2014). SV-AUC analysis, suggested a moderate elongation in the conformation of the wildtype LTBP4 N-terminal region. However, the incorporation of a mutation in the hybrid domain induced a more compact conformation compared with the wildtype. This finding is consistent with a previous study on substitutions occurring in the hybrid domain of fibrillin-1 that resulted in the production of more compact proteins compared with the wildtype (Mellody et al., 2006). These findings, indicate the importance of the hybrid domain in both LTBP4 and fibrillin-1. Consistent with the SV-AUC analysis, SAXS data also showed that the N-terminal region has an elongated inflexible conformation. This is consistent with our recent study on the N-terminal region of the LTBP4 homologue, LTBP1, which also adopts an elongated and inflexible conformation (Troilo et al., 2016). Our CD data shows that there is no change in the secondary structure caused by the cysteine substitution in the hybrid domain of the LTBP4 N-terminal region.

Our BLI binding studies showed wildtype LTBP4 N-terminal region bound to fibulin-4 with a K_D of 1294 nM. This interaction has previously been analysed using SPR with binding affinity of 15.4 nM (Bultmann-Mellin et al., 2015). Another recent study demonstrated that fibulin-4

multimers but not monomers that bind efficiently to LTBP4 and that the central domains of fibulin-4 showed the strongest binding affinity to LTBP4 (Kumra et al., 2019). The different binding techniques, LTBP4S N-terminal region constructs, and protein solutions (monodisperse in our study), used in this study and the published data might explain the differences in the determined K_D. Nonetheless, the mutated LTBP4 bound to fibulin-4 with higher affinity (K_D = 177.3 nM) compared to the wildtype. LTBP4 interaction with fibulin-4 is vital for fibulin-4-elastin complex linear deposition onto microfibril scaffolds (Bultmann-Mellin et al., 2015). We attempted to investigate LTBP4 interaction with fibulin-5, but we were unable to detect binding response, this also could be explained by using fibulin-5 monomers and not multimers. Both LTBP4 long and short isoforms bind to fibulin-4, but with different binding affinities (Bultmann-Mellin et al., 2016, Bultmann-Mellin et al., 2015). It has been demonstrated that the short isoform of LTBP4 favors binding to fibulin-5 than fibulin-4 to regulate elastic fibre assembly (Bultmann-Mellin et al., 2015, Bultmann-Mellin et al., 2016, Kumra et al., 2019). However, future binding studies using fibulin-4 and fibulin-5 multimers might be useful to explain the inconsistent binding affinities obtained from our binding studies with those of the previously published data (Bultmann-Mellin et al., 2015). Comparative binding studies between LTBP4 wildtype and mutant interaction with fibulin-4 and fibulin-5 multimers are also required to understand the outcome of LTBP4 mutation.

LTBP4 has been demonstrated to interact with fibronectin via the N-terminal region (Kantola et al., 2008). We used BLI binding studies to investigate whether LTBP4 directly interacts with fibronectin but could not detect an interaction. This is inconsistent with a previous study that used solid phase binding methods to show binding between LTBP4 and plasma fibronectin, whereas we used purified cellular fibronectin which could account for the difference (Kantola et al., 2008). Another possible reason for this inconsistency is that, the previous study (Kantola et al., 2008) used LTBP4 N-terminal construct that has an intact hinge region, while our LTBP4 construct lacked this region. It has been this region mediated LTBP1 interaction with fibronectin (Fontana et al., 2005). Immunolocalisation studies have demonstrated that LTBP4 colocalises initially with fibronectin but then it deposits into the matrix in a fibronectin independent manner and localises with fibrillin-1 (Kantola et al., 2008), indicating that fibronectin might be required for the initial matrix deposition of LTBP4 but not in matured tissue. Our finding is consistent with a previous study that demonstrated that LTBP1 interacts

indirectly with fibronectin and through a direct interaction with HS (Chen et al., 2007). Using heparin affinity chromatography, the LTBP4 N-terminal region has been demonstrated to directly interact with heparin, this also suggested that LTBP4 might interact with heparan sulphate (Kantola et al., 2008). Our real time binding studies confirmed a direct interaction between LTBP4 and heparan Sulphate. Moreover, the mutated LTBP4 N-terminal region had no impact on the binding affinity to HS. It has been suggested that the direct interaction of LTBP4 with heparin/heparan sulphate is important for its matrix deposition (Kantola et al., 2008). Future work using binding studies are required to investigate whether the hinge region and HS are required for LTBP4 and fibronectin interaction. Moreover, *in vitro* and *in vivo* studies are required to investigate the importance of HS in LTBP4 ECM deposition.

In summary, the data presented here show for the first time the solution structure of the wildtype LTBP4S N-terminal region and show the structural and functional consequences of the ARCL1C point mutation. Our data indicate that this region is monomeric and adopts an elongated structure. Our binding data show that LTBP4 strongly and directly interacts with HS.

References

BAX, D. V., MAHALINGAM, Y., CAIN, S., MELLODY, K., FREEMAN, L., YOUNGER, K., SHUTTLEWORTH, C. A., HUMPHRIES, M. J., COUCHMAN, J. R. & KIELTY, C. M. 2007. Cell adhesion to fibrillin-1: identification of an Arg-Gly-Asp-dependent synergy region and a heparin-binding site that regulates focal adhesion formation. J Cell Sci, 120, 1383-92.

BULTMANN-MELLIN, I., CONRADI, A., MAUL, A. C., DINGER, K., WEMPE, F., WOHL, A. P., IMHOF, T., WUNDERLICH, F. T., BUNCK, A. C., NAKAMURA, T., KOLI, K., BLOCH, W., GHANEM, A., HEINZ, A., VON MELCHNER, H., SENGLE, G. & STERNER-KOCK, A. 2015. Modeling autosomal recessive cutis laxa type 1C in mice reveals distinct functions for Ltbp-4 isoforms. Dis Model Mech, 8, 403-15.

BULTMANN-MELLIN, I., DINGER, K., DEBUSCHEWITZ, C., LOEWE, K. M. A., MELCHER, Y., PLUM, M. T. W., APPEL, S., RAPPL, G., WILLENBORG, S., SCHAUSS, A. C., JUNGST, C., KRUGER, M., DRESSLER, S., NAKAMURA, T., WEMPE, F., ALEJANDRE ALCAZAR, M. A. & STERNER-KOCK, A. 2017. Role of LTBP4 in alveolarization, angiogenesis, and fibrosis in lungs. Am J Physiol Lung Cell Mol Physiol, 313, L687-L698.

BULTMANN-MELLIN, I., ESSERS, J., VAN HEIJINGEN, P. M., VON MELCHNER, H., SENGLE, G. & STERNER-KOCK, A. 2016. Function of Ltbp-4L and fibulin-4 in survival and elastogenesis in mice. Dis Model Mech, 9, 1367-1374.

CALLEWAERT, B., SU, C. T., VAN DAMME, T., VLUMMENS, P., MALFAIT, F., VANAKKER, O., SCHULZ, B., MAC NEAL, M., DAVIS, E. C., LEE, J. G., SALHI, A., UNGER, S., HEIMDAL, K., DE ALMEIDA, S., KORNAK, U., GASPAR, H., BRESSON, J. L., PRESCOTT, K., GOSENDI, M. E., MANSOUR, S., PIERARD, G. E., MADAN-KHETARPAL, S., SCIURBA, F. C., SYMOENS, S., COUCKE, P. J., VAN MALDERGEM, L., URBAN, Z. & DE PAEPE, A. 2013. Comprehensive clinical and molecular analysis of 12 families with type 1 recessive cutis laxa. Hum Mutat, 34, 111-21.

CHEN, Q., SIVAKUMAR, P., BARLEY, C., PETERS, D. M., GOMES, R. R., FARACH-CARSON, M. C. & DALLAS, S. L. 2007. Potential role for heparan sulfate proteoglycans in regulation of transforming growth factor-beta (TGF-beta) by modulating assembly of latent TGF-beta-binding protein-1. J Biol Chem, 282, 26418-30.

CHENG, A., CAIN, S. A., TIAN, P., BALDWIN, A. K., UPPANAN, P., KIELTY, C. M. & KIMBER, S. J. 2018. Recombinant Extracellular Matrix Protein Fragments Support Human Embryonic Stem Cell Chondrogenesis. Tissue Eng Part A, 24, 968-978.

CHOUDHURY, R., MCGOVERN, A., RIDLEY, C., CAIN, S. A., BALDWIN, A., WANG, M. C., GUO, C., MIRONOV, A., JR., DRYMOUSSI, Z., TRUMP, D., SHUTTLEWORTH, A., BALDOCK, C. & KIELTY, C. M. 2009. Differential regulation of elastic fiber formation by fibulin-4 and -5. J Biol Chem, 284, 24553-67.

DABOVIC, B., CHEN, Y., CHOI, J., VASSALLO, M., DIETZ, H. C., RAMIREZ, F., VON MELCHNER, H., DAVIS, E. C. & RIFKIN, D. B. 2009. Dual functions for LTBP in lung development: LTBP-4 independently modulates elastogenesis and TGF-beta activity. J Cell Physiol, 219, 14-22.

DABOVIC, B., ROBERTSON, I. B., ZILBERBERG, L., VASSALLO, M., DAVIS, E. C. & RIFKIN, D. B. 2015. Function of latent TGFbeta binding protein 4 and fibulin 5 in elastogenesis and lung development. J Cell Physiol, 230, 226-36.

DALZIEL, M., CRISPIN, M., SCANLAN, C. N., ZITZMANN, N. & DWEK, R. A. 2014. Emerging principles for the therapeutic exploitation of glycosylation. Science, 343, 1235681.

FRANKE, D. & SVERGUN, D. I. 2009. DAMMIF, a program for rapid ab-initio shape determination in small-angle scattering. J Appl Crystallogr, 42, 342-346.

GILTAY, R., KOSTKA, G. & TIMPL, R. 1997. Sequence and expression of a novel member (LTBP-4) of the family of latent transforming growth factor-beta binding proteins. FEBS Lett, 411, 164-8.

ISOGAI, Z., ONO, R. N., USHIRO, S., KEENE, D. R., CHEN, Y., MAZZIERI, R., CHARBONNEAU, N. L., REINHARDT, D. P., RIFKIN, D. B. & SAKAI, L. Y. 2003. Latent transforming growth factor beta-binding protein 1 interacts with fibrillin and is a microfibril-associated protein. J Biol Chem, 278, 2750-7.

JENSEN, S. A., IQBAL, S., LOWE, E. D., REDFIELD, C. & HANDFORD, P. A. 2009. Structure and interdomain interactions of a hybrid domain: a disulphide-rich module of the fibrillin/LTBP superfamily of matrix proteins. Structure, 17, 759-68.

KANTOLA, A. K., KESKI-OJA, J. & KOLI, K. 2008. Fibronectin and heparin binding domains of latent TGF-beta binding protein (LTBP)-4 mediate matrix targeting and cell adhesion. Exp Cell Res, 314, 2488-500.

KANTOLA, A. K., RYYNANEN, M. J., LHOTA, F., KESKI-OJA, J. & KOLI, K. 2010. Independent regulation of short and long forms of latent TGF-beta binding protein (LTBP)-4 in cultured fibroblasts and human tissues. J Cell Physiol, 223, 727-36.

KOLI, K., HYYTIAINEN, M., RYYNANEN, M. J. & KESKI-OJA, J. 2005. Sequential deposition of latent TGF-beta binding proteins (LTBPs) during formation of the extracellular matrix in human lung fibroblasts. Exp Cell Res, 310, 370-82.

KUMRA, H., NELEA, V., HAKAMI, H., PAGLIUZZA, A., DJOKIC, J., XU, J., YANAGISAWA, H. & REINHARDT, D. P. 2019. Fibulin-4 exerts a dual role in LTBP-4L–mediated matrix assembly and function. 116, 20428-20437.

LACK, J., O'LEARY, J. M., KNOTT, V., YUAN, X., RIFKIN, D. B., HANDFORD, P. A. & DOWNING, A. K. 2003. Solution structure of the third TB domain from LTBP1 provides insight into assembly of the large latent complex that sequesters latent TGF-beta. J Mol Biol, 334, 281-91.

LIU, J. & PEDERSEN, L. C. 2007. Anticoagulant heparan sulfate: structural specificity and biosynthesis. Appl Microbiol Biotechnol, 74, 263-72.

MELLODY, K. T., FREEMAN, L. J., BALDOCK, C., JOWITT, T. A., SIEGLER, V., RAYNAL, B. D., CAIN, S. A., WESS, T. J., SHUTTLEWORTH, C. A. & KIELTY, C. M. 2006. Marfan syndrome-causing mutations in fibrillin-1 result in gross morphological alterations and highlight the structural importance of the second hybrid domain. J Biol Chem, 281, 31854-62.

NODA, K., DABOVIC, B., TAKAGI, K., INOUE, T., HORIGUCHI, M., HIRAI, M., FUJIKAWA, Y., AKAMA, T. O., KUSUMOTO, K., ZILBERBERG, L., SAKAI, L. Y., KOLI, K., NAITOH, M., VON MELCHNER, H., SUZUKI, S., RIFKIN, D. B. & NAKAMURA, T. 2013. Latent TGF-beta binding protein 4 promotes elastic fiber assembly by interacting with fibulin-5. Proc Natl Acad Sci U S A, 110, 2852-7.

OKLU, R. & HESKETH, R. 2000. The latent transforming growth factor beta binding protein (LTBP) family. Biochem J, 352 Pt 3, 601-10.

ONO, R. N., SENGLE, G., CHARBONNEAU, N. L., CARLBERG, V., BACHINGER, H. P., SASAKI, T., LEE-ARTEAGA, S., ZILBERBERG, L., RIFKIN, D. B., RAMIREZ, F., CHU, M. L. & SAKAI, L. Y. 2009. Latent transforming growth factor beta-binding proteins and fibulins compete for fibrillin-1 and exhibit exquisite specificities in binding sites. J Biol Chem, 284, 16872-81.

RIFKIN, D. B. 2005. Latent transforming growth factor-beta (TGF-beta) binding proteins: orchestrators of TGF-beta availability. J Biol Chem, 280, 7409-12.

RITELLI, M., CAMMARATA-SCALISI, F., CINQUINA, V. & COLOMBI, M. 2019. Clinical and molecular characterization of an 18-month-old infant with autosomal recessive cutis laxa type 1C due to a novel LTBP4 pathogenic variant, and literature review. Mol Genet Genomic Med, 7, e00735.

ROBERTSON, I., JENSEN, S. & HANDFORD, P. 2011. TB domain proteins: evolutionary insights into the multifaceted roles of fibrillins and LTBPs. Biochem J, 433, 263-76.

ROBERTSON, I. B. & RIFKIN, D. B. 2016. Regulation of the Bioavailability of TGF-beta and TGF-beta-Related Proteins. Cold Spring Harb Perspect Biol, 8.

SAHARINEN, J., HYYTIAINEN, M., TAIPALE, J. & KESKI-OJA, J. 1999. Latent transforming growth factor-beta binding proteins (LTBPs)--structural extracellular matrix proteins for targeting TGF-beta action. Cytokine Growth Factor Rev, 10, 99-117.

SAHARINEN, J. & KESKI-OJA, J. 2000. Specific sequence motif of 8-Cys repeats of TGF-beta binding proteins, LTBPs, creates a hydrophobic interaction surface for binding of small latent TGF-beta. Mol Biol Cell, 11, 2691-704.

SAHARINEN, J., TAIPALE, J., MONNI, O. & KESKI-OJA, J. 1998. Identification and characterization of a new latent transforming growth factor-beta-binding protein, LTBP-4. J Biol Chem, 273, 18459-69.

SCHUCK, P. 2000. Size-distribution analysis of macromolecules by sedimentation velocity ultracentrifugation and lamm equation modeling. Biophys J, 78, 1606-19.

STERNER-KOCK, A., THOREY, I. S., KOLI, K., WEMPE, F., OTTE, J., BANGSOW, T., KUHLMEIER, K., KIRCHNER, T., JIN, S., KESKI-OJA, J. & VON MELCHNER, H. 2002. Disruption of the gene encoding the latent transforming growth factor-beta binding protein 4 (LTBP-4) causes abnormal lung development, cardiomyopathy, and colorectal cancer. Genes Dev, 16, 2264-73.

SVERGUN, V. V. V. A. D. I. 2003. Uniqueness of ab-initio shape determination in small-angle scattering. J. Appl. Cryst., 36, 860-864.

TODOROVIC, V. & RIFKIN, D. B. 2012. LTBPs, more than just an escort service. J Cell Biochem, 113, 410-8.

TROILO, H., STEER, R., COLLINS, R. F., KIELTY, C. M. & BALDOCK, C. 2016. Independent multimerization of Latent TGFβ Binding Protein-1 stabilized by cross-linking and enhanced by heparan sulfate. Scientific Reports, 6, 34347.

URBAN, Z., HUCTHAGOWDER, V., SCHURMANN, N., TODOROVIC, V., ZILBERBERG, L., CHOI, J., SENS, C., BROWN, C. W., CLARK, R. D., HOLLAND, K. E., MARBLE, M., SAKAI, L. Y., DABOVIC, B., RIFKIN, D. B. & DAVIS, E. C. 2009. Mutations in LTBP4 cause a syndrome of impaired pulmonary, gastrointestinal, genitourinary, musculoskeletal, and dermal development. Am J Hum Genet, 85, 593-605.

VEHVILAINEN, P., HYYTIAINEN, M. & KESKI-OJA, J. 2003. Latent transforming growth factor-beta-binding protein 2 is an adhesion protein for melanoma cells. J Biol Chem, 278, 24705-13.

WIERZBICKA-PATYNOWSKI, I. & SCHWARZBAUER, J. E. 2003. The ins and outs of fibronectin matrix assembly. J Cell Sci, 116, 3269-76.

Supplementary

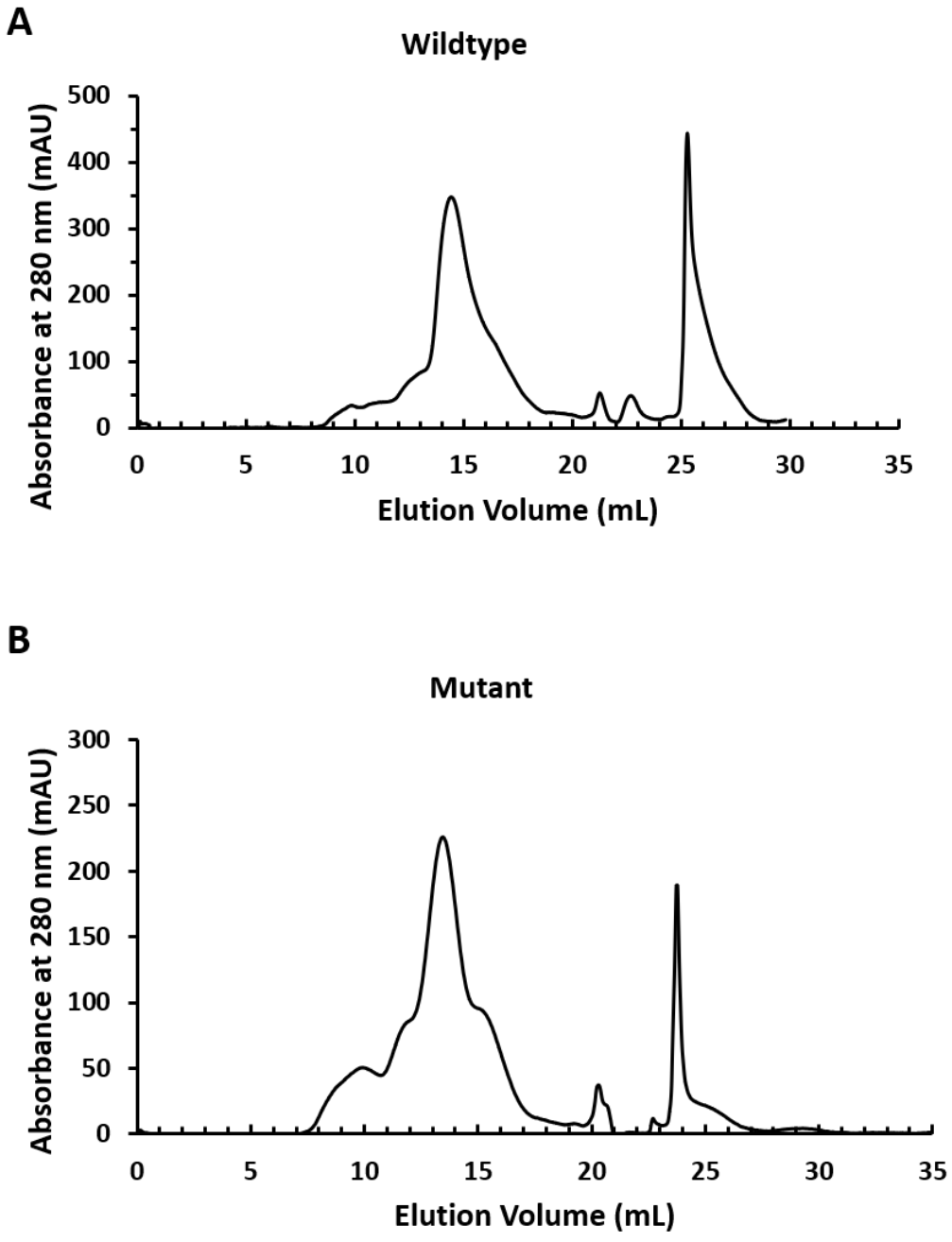

Figure 1: Purification of LTBP4 N-terminal region constructs. Size exclusion chromatograms of the **(A)** wildtype LTBP4 N-terminal region, **(B)** Mutant LTBP4 N-terminal region displaying similar elution volumes of the monomer species for each construct. Purified proteins were in buffer containing 10 mM Tris and 150 mM NaCl at pH 7.8 and eluted at a flow rate of 0.5 ml/min.

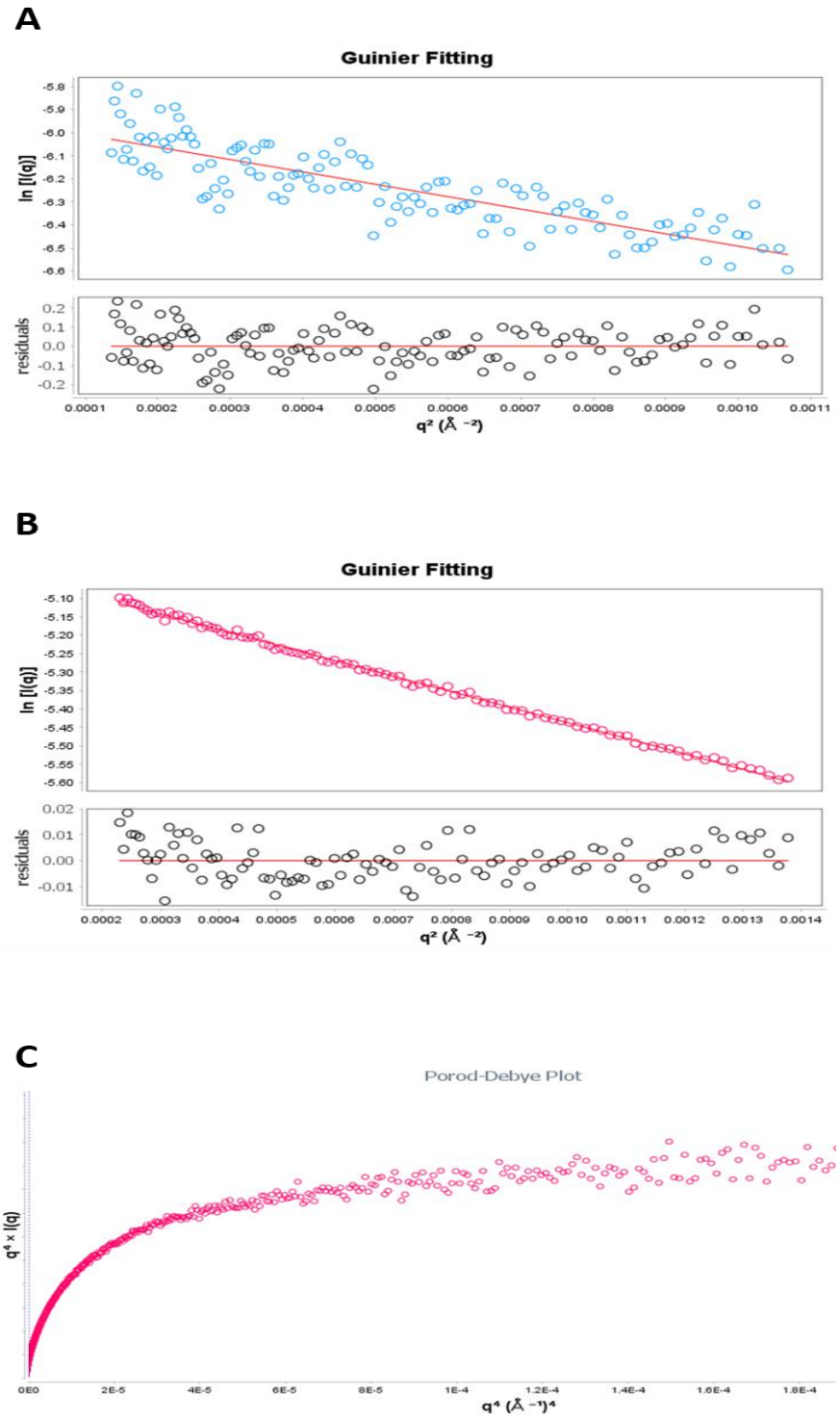

Figure 2: SAXS analysis of wildtype and mutated LTBP4 N-terminal region constructs. Guinier plot of the low q region for the **(A)** wildtype LTBP4 N-terminal region and **(B)** Mutant LTBP4 N-terminal region showing linearity. **(C)** Porod-Debye plot for the mutated LTBP4 N-terminal region showing plateau at high q value, indicating inflexible structure for this region.

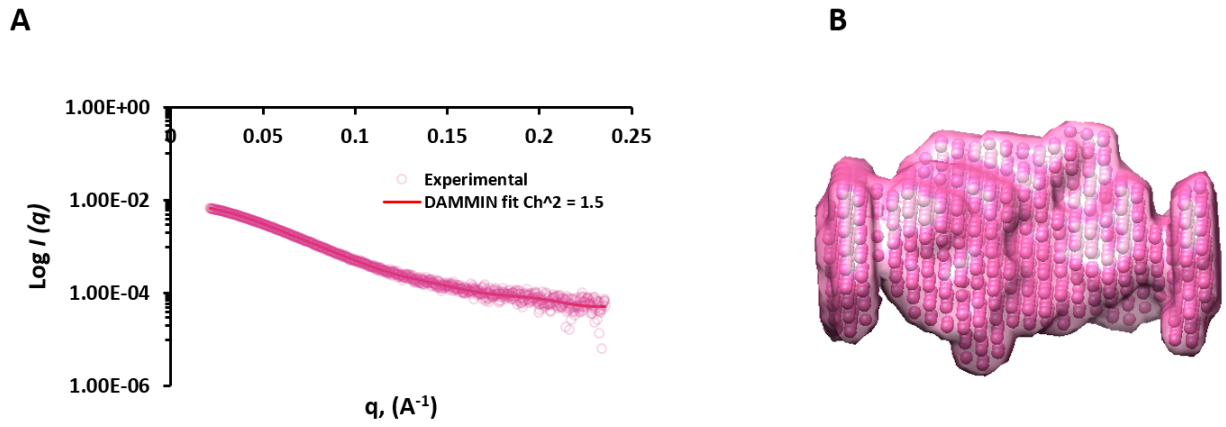

Figure 3: *ab initio* modeling of mutated LTBP4 N-terminal region construct. (A) The experimental 1D scattering intensity I plotted as a function of q for the mutated LTBP4 N-terminal region. **(B)** *ab initio* bead model of one of the ten generated DAMMIN modles with best fit to the experimental data and discrepancy factor χ^2 of (1.5) for the mutated LTBP4 N-terminal region showing extended conformation for this region.

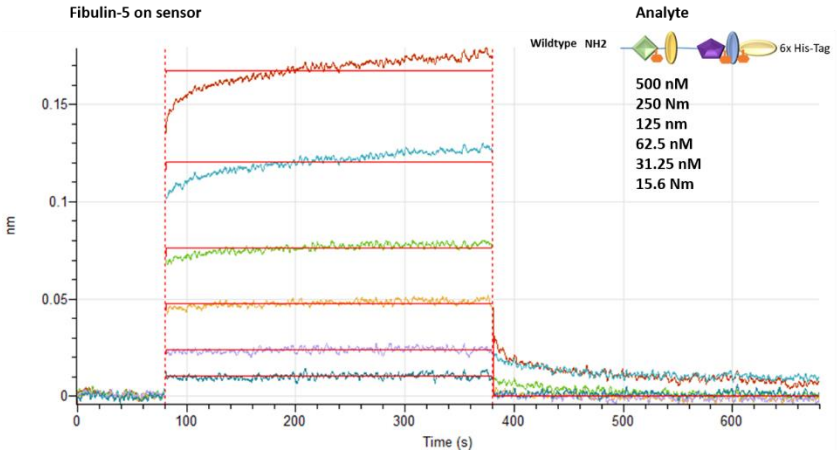

Figure 4: LTBP4 interaction with Fibulin-5. OctetRED96 biolayer interferometry sensorgram showing no binding response between immobilised fibulin-5 and a range of concentrations (500 – 15.6 nM) of wildtype LTBP4 N-terminal region.

5. Chapter 5

Functional similarities and interaction between Latent TGFβ binding protein 4 and Latent TGFβ binding protein 1

Functional similarities and interaction between Latent TGFβ binding protein 4 and Latent TGFβ binding protein 1

Yasmene F. Alanazi, Thomson J. and Clair Baldock

Wellcome Trust Centre for Cell Matrix Research, Division of Cell Matrix Biology and Regenerative Medicine, School of Biological Science, Faculty of Biology, Medicine and Health, Manchester Academic Health Science Centre, University of Manchester, UK

Abstract

Latent TGFβ binding proteins are essential for regulating TGFβ biology. Among all LTBPs, LTBP1 and LTBP4 show the highest similarity. LTBP1 is required for TGFβ activation and cross-linking via the matrix transglutaminase-2 (TG2). LTBP4 possesses a TGFβ-independent role in elastogenesis. However, no previous study has tested whether LTBPs interact with each other. Here we show that LTBP4 does not cross-link via TG2. LTBP4 also does not cross-link to fibrillin-1 via TG2. We identify LTBP1 as new interaction partner for LTBP4. LTBP4 directly interacts with LTBP1 via its N-terminal region. We also show that mutated LTBP4 N-terminal region slightly interfere with the LTBP1 interaction. We demonstrate that the N-terminal but not the C-terminal region of LTBP4 directly interacts with LTBP1 C-terminal region. This data might suggest a new matrix role for LTBP4 and LTBP1. Moreover, we show that LTBP4 weakly interacts with the small latent complex (SLC) and that the formation of the large latent complex (LLC) does not effect the interaction of LTBP1 with fibrillin-1.

Introduction

The latent TGFβ binding proteins (LTBP1-4) are large extracellular glycoproteins that belong to the fibrillin/LTBP family (Kanzaki et al., 1990, Moren et al., 1994, Yin et al., 1995, Saharinen et al., 1998), that share typical tandem repeats of the disulphide-rich epidermal growth factor-like domains (EGF) and TGFβ binding protein-like domains (TB) (Saharinen et al., 1999, Oklu and Hesketh, 2000, Robertson et al., 2011). LTBPs possess an important extracellular matrix function. TGFβ binding LTBPs (LTBP1, 3 and 4) have a role in regulating the biology of the pluripotent growth factor, TGFβ. They are required for folding and secretion of the small latent complex and for targeting it to the extracellular matrix for activation (Rifkin, 2005). The

TGFβ is secreted as an inactive small latent complex (SLC), which includes the C-terminal region of TGFβ homodimer non-covalently bound to the N-terminal region latency associated propeptide dimer (LAP) (Gentry et al., 1988, Gray and Mason, 1990). The SLC prevents TGFβ from binding to its receptor and TGFβ remains inactive due to the strong binding affinity between it and its propeptide LAP (Annes et al., 2003). LTBP1 was the first LTBP identified as a part of the large latent complex (Miyazono et al., 1988). All TGFβ binding LTBPs, except LTBP2, are implicated in mediating TGFβ dissociation from its LAP by different several mechanisms involving proteases and integrins (Saharinen and Keski-Oja, 2000, Annes et al., 2004, Robertson and Rifkin, 2016). The covalent association between LTBPs and the SLC involves cysteine residues within the second TB domain of LTBPs and cysteine 33 residues in the LAP dimer (Lack et al., 2003), that is stabilised by specific surrounding amino acids (Saharinen and Keski-Oja, 2000, Chen et al., 2005, Walton et al., 2010). LTBP2 cannot bind TGFβ-LAP due to the absence of a specific TGFβ binding motif (Saharinen and Keski-Oja, 2000), but it has crucial role in matrix. LTBP2 play an essential role in the formation of microfibrils in the ciliary zonules and in cell adhesion (Vehvilainen et al., 2003), that are a TGFβ-independent functions. TGFβ binding LTBPs also have a TGFβ-independent role in cell adhesion (Kantola et al., 2008), cell surface receptor stabilisation (Su et al., 2015), and elastogenesis (Dabovic et al., 2015). LTBPs play an essential structural role in microfibril and elastic fibre assembly via their interaction with several other extracellular matrix proteins such as fibrillin, fibronectin, and fibulins (Thomson et al., 2019). Previous studies demonstrated that the LTBPs are initially incorporated into the ECM by interaction with fibronectin through their N-termini (Chen et al., 2007, Fontana et al., 2005, Hyytiainen and Keski-Oja, 2003). While LTBPs interaction with fibrillin-1 has been demonstrated to be important for their ECM deposition and LLC sequestration (Isogai et al., 2003, Zilberberg et al., 2012). All LTBPs except LTBP3, directly interact with the N-terminal region of fibrillin-1 via their C-termini (Isogai et al., 2003, Ono et al., 2009, Massam-Wu et al., 2010). However, LTBPs might also cooperate with or compensate for each other (Koli et al., 2008, Fujikawa et al., 2017). Among the LTBP family, LTBP1 and LTBP4 exist in two major isoforms in mammalian cells, long and short forms that are produced by alternative splicing (Koski et al., 1999, Kantola et al., 2010). LTBP1 is capable of binding to all TGFβ isoforms (TGFβ1-3) with high affinity, whereas LTBP4 can bind TGFβ1 only and with weak binding affinity (Saharinen and Keski-Oja, 2000). LTBP1 is primarily involved in the regulation of TGFβ activation by integrins (Fontana et al., 2005, Annes et al., 2003), whereas

LTBP4 is primarily involved in elastogenesis (Noda et al., 2013). A previous *in vitro* study demonstrated that neutralising LTBP1 blocked the activation of latent TGFβ in both endothelial and smooth muscle cell cultures and inhibited embryonic stem cell differentiation (Gualandris et al., 2000). LTBP1L$^{-/-}$ mice showed severely disrupted great vessels and cardia valve that are accompanied with decreased TGFβ activity (Todorovic et al., 2007, Todorovic et al., 2005). Similar phenotype was observed in LTBP1 null mice (Horiguchi et al., 2015). Interestingly, no human pathology has been linked to LTBP1 mutations. LTBP4 deficient mice and humans displayed the same pathology of defective elastogenesis in multiple organs including the lung (Sterner-Kock et al., 2002, Urban et al., 2009). However, LTBP4 shows the highest similarity percentage (52%) in its sequence with LTBP1 (Saharinen et al., 1998). Both LTBP1 and LTBP4 C-termini bind equally to the N-terminal region of fibrillin-1, suggesting that LTBP4 might compensate LTBP1 in some tissues where LTBP1 is not expressed (Isogai et al., 2003). We previously showed that the LTBP1 has the capacity to assemble into elongated filamentous structure in an N- to N- or N- to C-terminal region manner (Troilo et al., 2016). LTBP1 also can be cross-linked to fibrillin-1 by TG2 (Steer, 2014). These together led us to hypothesise that LTBP4 might interact/cross-link in the same manner and/or interact with LTBP1. A previous study has using immunoprecipitation assays, investigated the possibility of a non-covalent interaction between the SLC and LTBPs, demonstrated that LTBP1 interacts non-covalently with SLC (Saharinen and Keski-Oja, 2000). However, to our knowledge there is no study demonstrating a non-covalent interaction for LTBP4 to SLC. Here we show that LTBP4 both N- and C- termini do not interact nor cross link with each other and cannot be cross-linked to fibrillin-1. LTBP4 directly interacts with full length LTBP1. We also show that ARCL1C point mutation has impact on this interaction. Moreover, we show that the N-terminal region but not the C-terminal region of LTBP4 directly interacts with LTBP1 C-terminal region. Finally, we show that LTBP4 non-covalently interacts with SLC, but this interaction was very weak.

Materials and methods

Expression and purification

Human wildtype and mutant LTBP4 N-terminal region fragments (residues 29-394) and wildtype LTBP4 C-terminal region fragment (residues 1114-1557) were expressed in Human Embryonic Kidney (293)-EBNA cells using a modified mammalian expression vector pCEP4

(Invitrogen), pCEP-Pu/AC7 that contains a C-terminal region six-histidine residue tag (6x His-tag). The recombinant human wildtype and mutant LTBP4 N- and C-terminal region constructs were the purified using nickel affinity column (GE Healthcare) followed by size-exclusion chromatography on an AKTA purifier FPLC using a Superdex 200 10/300GL column (GE Healthcare). 10 mM HEPES and 150 mM NaCl at pH 7.8 buffer was used to equilibrate the column at a flow rate of 0.5 mL/min. Full length and C-terminal regionLTBP1 were expressed and purified as previously described (Troilo et al., 2016).The LTBP1CT-TGFβ-LAP and SLC were provided by (Rana Dajani, University of Manchester). The proteins were analysed by SDS-PAGE and Western blotting using anti-His antibodies. BCA protein assay (Thermo Fisher Scientific) was used to determine proteins concentration.

Biolayer Interferometry (BLI)

BLI binding studies were performed using an OctetRED96 system (ForteBio) with Streptavidin (SA) biosensors. The SA biosensors were first hydrated with buffer containing 10 mM HEPES, 150 NaCl, pH7.4 buffer supplemented with 0.005% (v/v) Tween-20 for 10 minutes then were loaded with the biotinylated ligands at constant concentration. The loaded biosensors were then incubated with the analyte diluted at a range of concentrations in the same buffer used for hydration. 10 mM glycine at pH 2.5 buffer was used to regenerate the biosensors. The binding kinetics was analysed using Octet software version 7 (ForteBio). Steady state analysis was used. Baseline subtraction was performed with reference biosensors, that are dipped into buffer without analyte. The goodness of binding data fitting was assessed by X^2 and R^2 values. All binding experiments were performed in solid-black 96 well plates at 25^{o}C with an agitation speed of 1000 rpm and repeated at least twice.

Cross-linking

Cross-linking assay was performed using guinea pig liver-derived commercial transglutaminase-2 (TG2) (Sigma-Aldrich). TG2 was incubated with LTBP4 and LTBP1 and or fibrillin-1 (PF3 (Rock et al., 2004)) fragments in a ratio of 0.1:1 for 2 hours at 30 °C in 10 mM HEPES, 150 mM NaCl pH 7.4 buffer containing 1 mM CaCl2. Equal molar ratios of cross-linking LTBP4 and LTBP1 were used. Cross-linked proteins were then analysed by SDS-PAGE and immunoblotting using anti-His antibodies.

Results

LTBP4 Cannot be Cross-linked by TG2 nor Directly Interact

We have previously demonstrated that the LTBP4 close homolog, LTBP1, has the capacity to self-oligomerise under calcium dependency and its oligomerisation is stabilised by transglutaminase-2 (TG2) (Troilo et al., 2016).Here we investigate whether LTBP4 possesses the same capacity, using the cross-linker TG2 in the same conditions as previously described (Troilo et al., 2016); however, neither LTBP4 N- or C-termini formed larger species (Figure 5.1C). We also performed BLI to test whether LTBP4 N- and C-termini can interact with immobilised wildtype LTBP4 N-terminal region independent of TG2. However, no direct interaction was observed for either LTBP4 termini to the wildtype LTBP4 N-terminal region (Supplementary Figure 1 A & B).

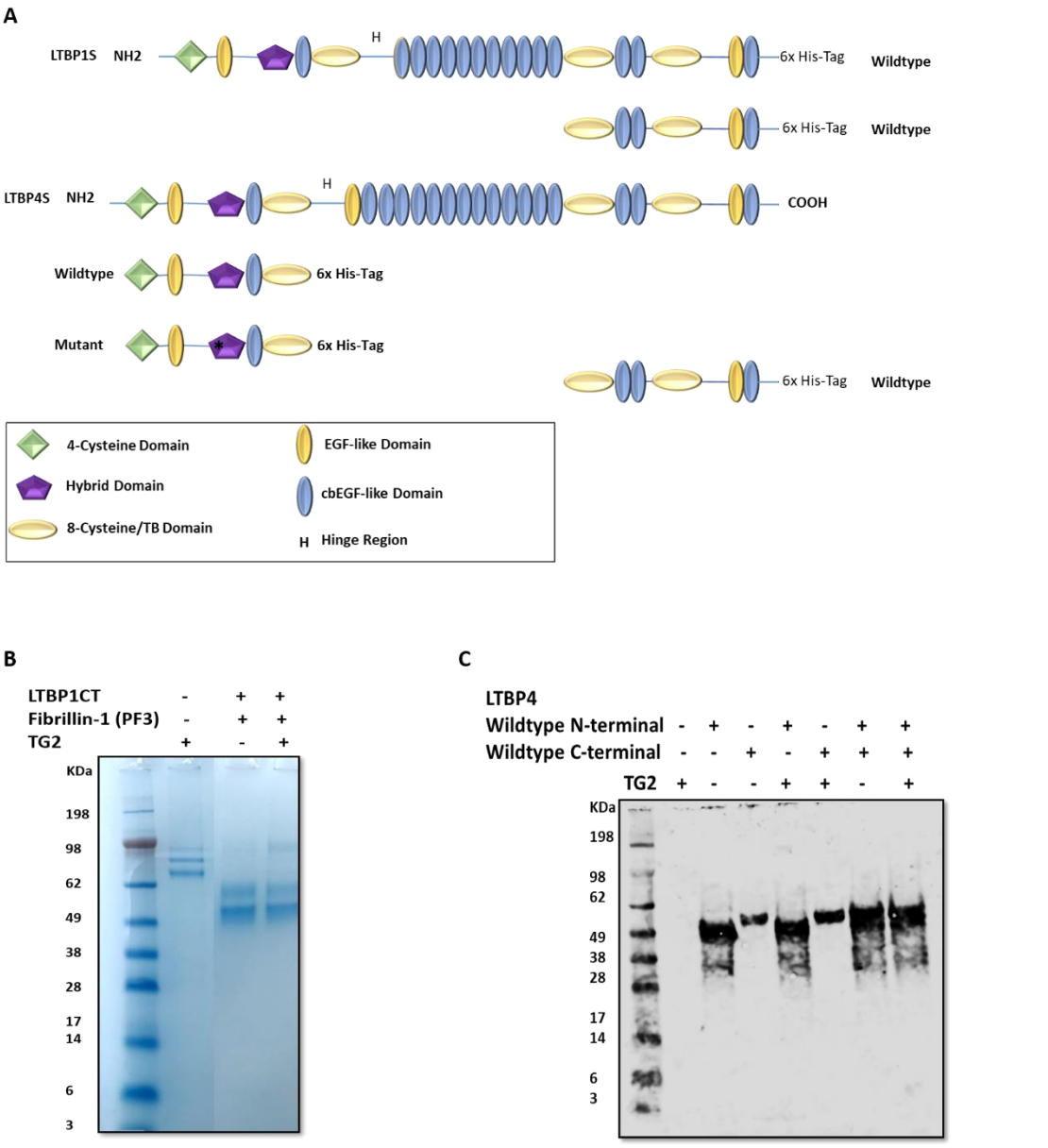

Figure 5-1: LTBP4 and LTBP1 constructs. Schematic representation of the domain organisation of the full length LTBP4S and the 6xHis tagged LTBP1 and LTBP4 constructs used in this study. (B) Non-reducing SDS-PAGE showing LTBP1 C-terminal cross-linking with fibrillin-1 (PF3) via TG2 as a positive control. (C) Western blot showing no cross-linking of wildtype LTBP4 via TG2 was observed. Wildtype LTBP4 N- and C-termini do not cross-link to themselves nor to each other to form larger species in presence of TG2.

LTBP4 Monomer cannot be Cross-linked to Fibrillin-1 (PF3 fragment) by Transglutaminase-2 (TG2)

LTBP4, associates with the ECM by cross-linking with an unknown matrix protein. It colocalises with the integral microfibril component, fibrillin-1 (Isogai et al., 2003). LTBP4 C-terminal region has been demonstrated to directly interact with the fibrillin-1 N-terminal region (Isogai et al., 2003, Ono et al., 2009). The importance of this direct interaction has been demonstrated to be essential for LTBP4 matrix deposition (Isogai et al., 2003, Zilberberg et al., 2012). Therefore, we tested whether the LTBP4 C-terminal region cross-links with the N-terminal region of fibrillin-1 by TG2 using a shortened fragment of fibrillin-1 (PF3) described previously in (Rock et al., 2004). As it has been previously shown that the LTBP1 C-terminal region can cross-link with fibrillin-1 PF3 fragment (Steer, 2014). However, no higher molecular weight complexes were present, indicating that the LTBP4 C-terminal region did not cross-link with the fibrillin-1 N-terminal region (Figure 5-2). It was noted that fibrillin-1 PF3 fragment can form higher ordered spices without the presence of TG2 (Figure 5-2).

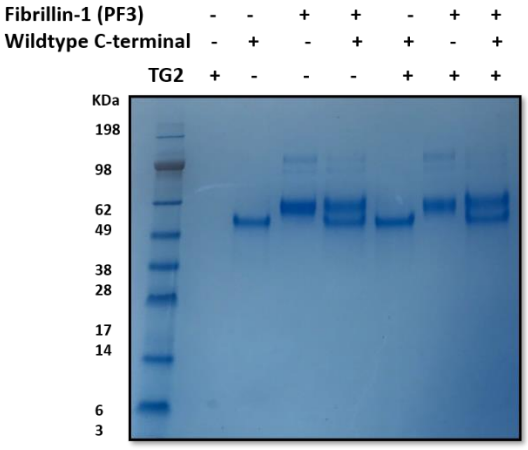

Figure 5-2: Investigating LTBP4 cross-linking by transglutaminase-2 (TG2). Non-reduced SDS-PAGE showing no cross-linking between the wildtype LTBP4 C-terminal region and fibrillin-1 (PF3 fragment).

LTBP4 N-terminal region directly interacts with full-length LTBP1

Previous binding studies were performed to investigate whether LTBPs interact with fibrillin-1 due to the high similarity in their structure and colocalisation in many tissues (Isogai et al., 2003, Ono et al., 2009). Among all LTBPs, LTBP1 and LTBP4 show the highest sequence similarity (52 %)(Saharinen et al., 1998). Both LTBP1 and LTBP4 are highly expressed in heart and lung (Robertson et al., 2015). However, no previous study has tested whether LTBPs interact with each other. Here we performed BLI to investigate whether LTBP4 interacts with

LTBP1. Our BLI sensorgrams showed that both the wildtype and mutant LTBP4 N-terminal region directly interacted with immobilized full-length LTBP1 (Figure 5-3). The calculated averaged binding affinity for the wildtype LTBP4 N-terminal region was 189.6 nM. While the ARCL1C point mutation reduced the binding affinity to 319.4 nM, indicating that the cysteine substitution in the hybrid domain of LTBP4 did slightly affect this interaction. The mutant also showed bi-phasic association/dissociation steps compared to the wildtype (Figure 5-3Bi).

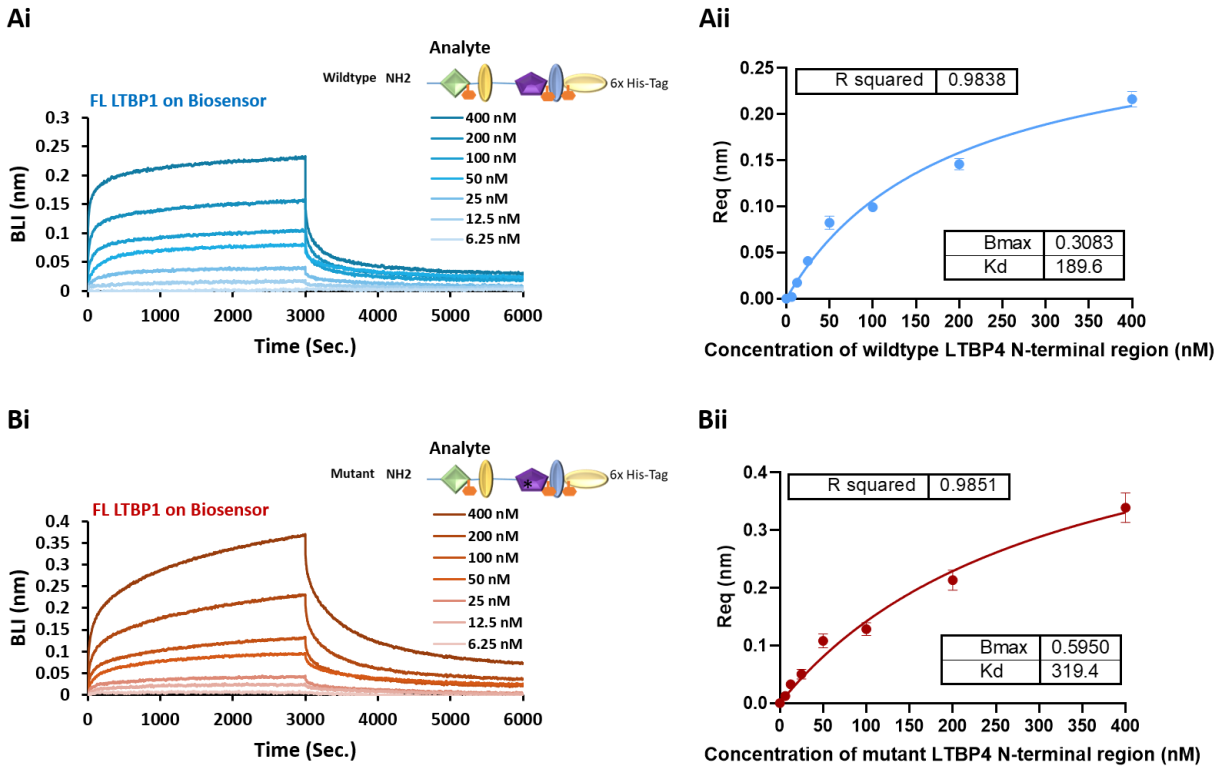

Figure 5-3: Analysis of the LTBP4 N-terminal region interaction with full-length LTBP1 using Biolayer Interferometry (BLI). OctetRED system sensorgram showing binding response detected between immobilized wildtype full-length LTBP1 and a range of concentrations (400 – 6.25 nM) of (Ai) wildtype LTBP4 N-terminal region and (Bi) mutant LTBP4 N-terminal region. The binding affinity K_D was determined by steady state fitting (Aii and Bii). All experiments were performed in duplicates and averaged Kd are presented. Error bars represent standard error of the mean.

LTBP4 N-terminal region-specific interaction with LTBP1 C-terminal region

Further binding studies using BLI were conducted to determine the LTBP1 LTBP4 binding site. A shortened construct of LTBP1 including the C-terminal region domains TB2, cbEGF13, cbEGF14, TB3, EGF2, and cbEGF15 (Troilo et al., 2016) and the LTBP4 N- and C-terminal regions were used (Figure 5-1A). The LTBP1 C-terminal region was immobilised on streptavidin biosensors at a range of concentrations (200 – 0 nM) and constant concentration

at 50 nM of LTBP4 N- and C-termini were used as analytes. There was no binding detected between the C-termini of LTBP1 and LTBP4 (Supplementary Figure 2A). In contrast, the N-terminal region of LTBP4 interacted with the immobilised LTBP1 C-terminal region, indicating that there is a direct and specific interaction between these two regions (Supplementary Figure 2B). Kinetic analysis of this interaction was performed (Figure 5-4). The calculated averaged binding affinity for wildtype LTBP4 N-terminal region was 511 nM (Figure 5Aii), weaker than the binding affinity to the full-length LTBP1, indicating that there might be another binding site for LTBP4 in the full length LTBP1 (Figure 5-4Aii). We also tested whether the mutation in the LTBP4 N-terminal region effected on this specific interaction. However, a similar binding affinity was calculated 493.6 nM (Figure 5-4Bii), indicating that the ARCL1C substitution did not impact on the interaction with the LTBP1 C-terminal region.

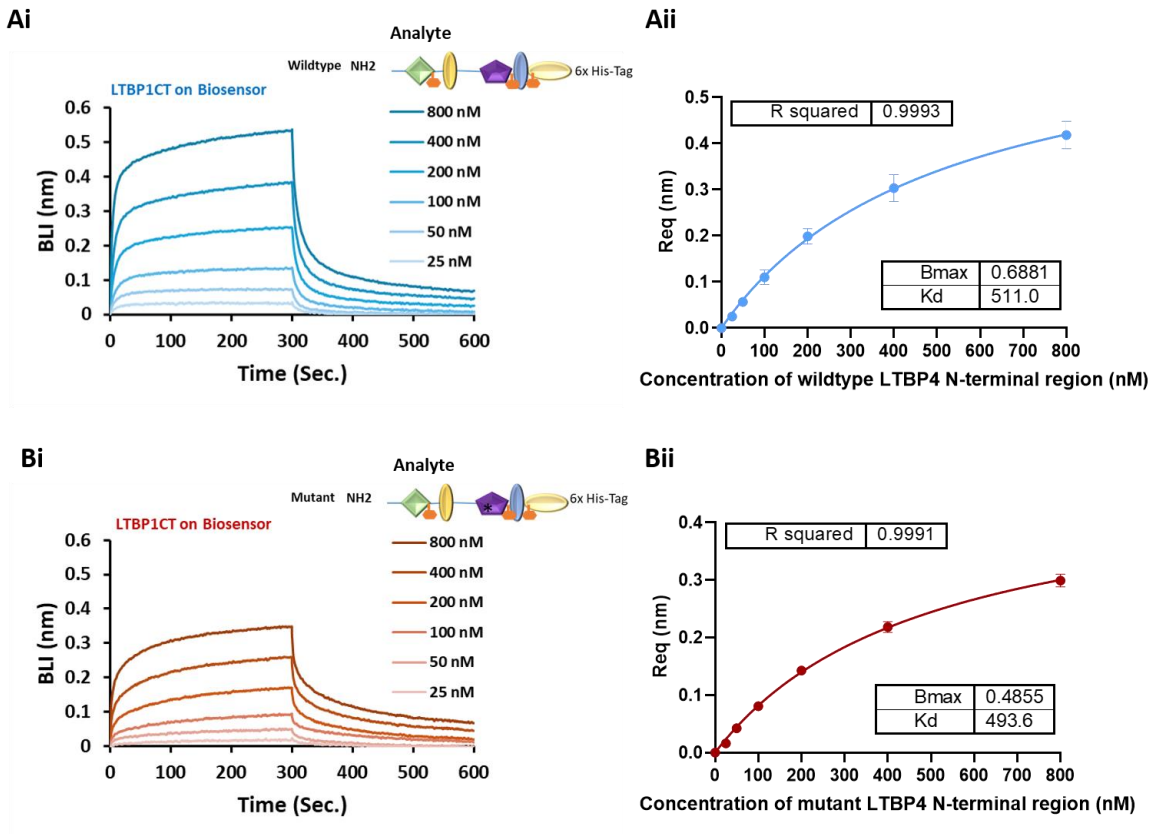

Figure 5-4: Analysis of the LTBP4 N-terminal region interaction with the LTBP1 C-terminal region using Biolayer Interferometry (BLI). OctetRED system sensorgram showing binding response detected between immobilised wildtype LTBP1 C-terminal region and different concentrations (800 – 25 nM) of (Ai) wildtype LTBP4 N-terminal region and (Bi) mutant LTBP4 N-terminal region. The binding affinity K_D was determined by steady state fitting (Aii and Bii). All experiments were performed in duplicates and averaged Kd are presented. Error bars represent standard error of the mean.

LTBP4 non-covalent Interaction with TGFβ1-LAP Complex

LTBP4 as other TGFβ binding LTBPs (LTBP1 and LTBP3), directly binds the TGFβ-LAP by disulphide bonding mediated by the 2nd TB domain of LTBP4 and cysteine 33 in TGFβ-LAP. A previous *in vitro* study demonstrated that LTBP4, in contrast to other TGFβ binding LTBPs that strongly bind to all TGFβ isoforms (TGFβ1-3), showed inefficient binding to the TGFβ1 isoform only (Saharinen and Keski-Oja, 2000). LTBP1 has been shown to non-covalently interact with SLC (Saharinen and Keski-Oja, 2000). To our knowledge no other *in vitro* binding studies have tested whether LTBP4 directly interacts with TGFβ1-LAP complex. Therefore, we used BLI to investigate the kinetics of LTBP4 and the SLC interaction. The sensorgrams showed a binding response between the immobilised LTBP4 C-terminal region and a range of concentrations of the TGFβ1-LAP complex (Figure 5-5). The calculated binding affinity between the LTBP4 C-terminal region and TGFβ1-LAP was 2540 nM, indicating a weak interaction between LTBP4 and TGFβ1-LAP complex.

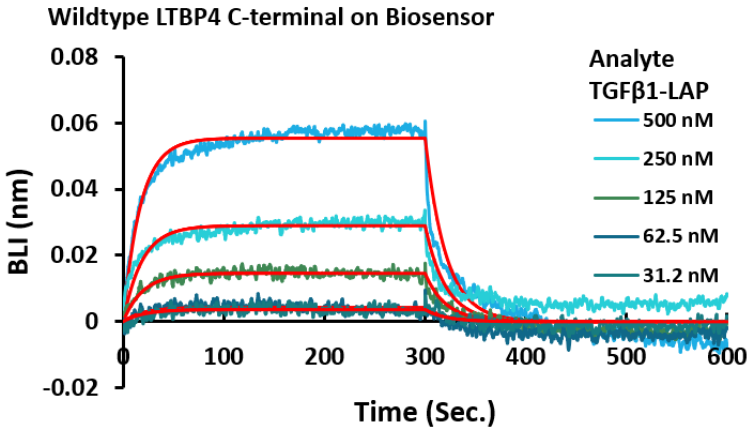

Figure 5-5: Analysis of the LTBP4 C-terminal region interaction with TGFβ-LAP complex using Biolayer Interferometry (BLI).OctetRED system sensorgram showing the binding response detected between immobilised LTBP4 C-terminal region and a range of concentrations (500 – 31.2 nM) of TGFβ1-LAP complex. The binding affinity K_D was determined by fitting to a 1:1 Langmuir binding model (red curves). Experiments were performed in duplicates and representative results are shown.

LTBP1CT-TGFβ-LAP complex interaction with fibrillin-1

LTBPs bind to the fibrillin-1 N-terminal region via their C-terminal region (Isogai et al., 2003, Ono et al., 2009). LTBPs also covalently bind TGFβ-LAP complex via their C-termini involving the 2nd TB domain. Here we tested whether the formation of the large latent complex changed the binding affinity between LTBP and the fibrillin-1 N-terminal region. Binding studies using OctetRED96 BLI were performed. Since LTBP4 inefficiently binds TGFβ1-LAP complex, we decided to use LTBP1 that strongly and efficiently formed a latent complex with the TGFβ-LAP complex (Saharinen and Keski-Oja, 2000). Although, there is difference in the binding epitopes required for fibrillin-1 interaction between LTBP1 and LTBP4 (Ono et al., 2009), we were wondering whether the formation of the LLC affect on fibrillin-1 interaction. Our sensorgrams showed tight binding (K_D = 4.7 nM) between immobilised LTBP1CT-TGFβ-LAP complex and concentrations of fibrillin-1 N-terminal region (PF3 fragment) (Figure 5-6). We also performed SPR to determine the binding affinity of LTBP1 C-terminal region without the TGFβ-LAP complex interaction with fibrillin-1 (PF3 fragment) (Supplementary Figure 3). The calculated binding affinity was 17.6 nM, indicating that TGFβ-LAP complex disulphide bonding with LTBP1 does not affect the fibrillin-1 interaction.

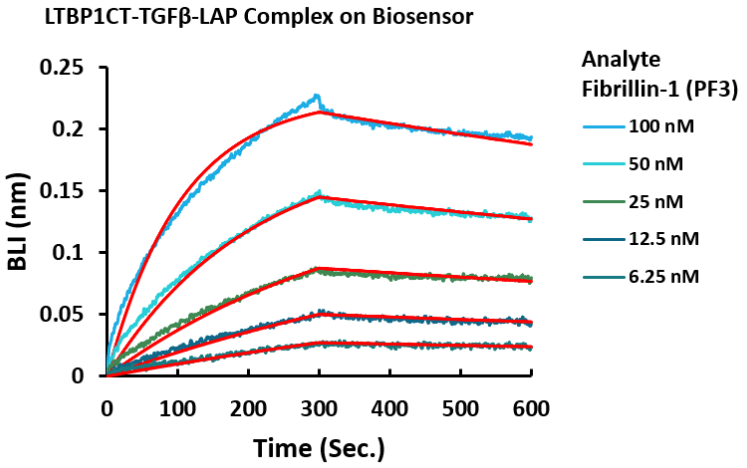

Figure 5-6: Analysis of LTBP1CT-TGF-LAP complex interaction with fibrillin-1 N-terminal region using Biolayer Interferometry (BLI).OctetRED system sensorgram showing binding response detected between immobilised LTBP1CT-TGFβ-LAP complex and a range of concentrations (100- 6.25 nM) of fibrillin-1 N-terminal region (PF3 fragment). The binding affinity K_D was determined by fitting to a 1:1 Langmuir binding model (red curves). Experiments were performed in duplicates and representative results are shown.

Discussion

LTBPs are key players in several different matrix functions, including regulation of TGFβ bioavailability (Saharinen and Keski-Oja, 2000), microfibril organisation (Fujikawa et al., 2017), elastogenesis and cell adhesion (Kantola et al., 2008, Dabovic et al., 2015). All LTBPs share similar domain structure, but LTBP1 and LTBP4 are highly structurally related among other LTBPs (Saharinen et al., 1998). LTBP1 possesses an important TGF-dependent role, it is primarily involved in TGFβ storage and activation by integrins (Fontana et al., 2005), while LTBP4 is a promoter for elastogenesis (Noda et al., 2013). An early study has demonstrated that LTBP1 is a substrate for matrix transglutaminase-2 and it cross-links via its N-terminal region as it contains the transglutaminase reactive site (Nunes et al., 1997), that is essential for TGFβ activation (Kojima et al., 1993). LTBP1 has also been demonstrated to covalently bind fibronectin (Zilberberg et al., 2012). We previously showed that LTBP1 is cross-linked by TG2 in an N- to N- and N- to C-terminal region manner. LTBP1 was also able to self-assemble into higher ordered species independent of TG2 (Troilo et al., 2016). In the present study we show that LTBP4 is incapable of interacting nor cross-linking in an N- to N- or N- to C-terminal region manner via TG2, indicating that LTBP4 might not be a substrate for TG2 or might require other proteins to mediate its cross-linking and self-assembly. LTBP4 has been demonstrated to cross-link to the ECM, but it is still not known to which ECM protein is LTBP4 cross-linked. It was also suggested that LTBP4 might covalently binds fibrillin-1 (Zilberberg et al., 2012). LTBP4 colocalises with fibrillin-1 and interacts with the fibrillin-1 N-terminus via its C-terminal region (Isogai et al., 2003, Ono et al., 2009). LTBP4 also requires fibrillin-1 for its matrix deposition (Zilberberg et al., 2012). And the C-termini of both LTBP1 and LTBP4 bind with the same affinity to the N-terminus of fibrillin-1 (Isogai et al., 2003). It has been shown that the LTBP1 C-terminal region can cross-link to the fibrillin-1 N-terminal region via TG2 (Steer, 2014). Therefore, we hypothesised that LTBP4 can also be cross-linked to fibrillin-1 via TG2. Here we show that the LTBP4 C-terminal region cannot cross-link with fibrillin-1 N-terminal region, confirming that LTBP4 C-terminal region might not be a substrate for TG2 and or that it doesn't cross-link with fibrillin-1 but with another matrix protein, for example LTBP4 deposition requires fibronectin (Kantola et al., 2008). Future cross-linking assays are required to investigate whether LTBP4 can be cross-linked to fibronectin.

Our BLI binding result show that LTBP4 directly interacts with its full-length homolog, LTBP1 via its N-terminal. This suggests that LTBP1 and LTBP4 might cooperate in a unique matrix

function. Indeed, previous studies have reported a cooperative and compensatory role for other LTBPs. It has been demonstrated that both LTBP1 and LTBP3 cooperate in human mesenchymal stem cell differentiation to osteoblasts, where LTBP3 regulates TGFβ activation during early phases whereas LTBP1 regulates TGFβ activity in matured cells (Koli et al., 2008). A more recent study has showed that LTBP4 can compensate for LTBP2 in regulating the formation of microfibrils in the ciliary zonules in LTBP2 null mice (Fujikawa et al., 2017).

Our binding data show that the N-terminal region but not the C-terminal region of LTBP4 interacts with the C-terminal region of LTBP1, indicating the specificity of this interaction. The binding affinity between the N-terminal of LTBP4 and full-length LTBP1 was stronger than binding to the C-terminal region of LTBP1, indicating that there might be another binding site in LTBP1. The ARCL1C mutation in the LTBP4 N-terminal region, where a highly conserved cysteine residue within the hybrid domain is substituted, resulted in decreased binding affinity to full-length LTBP1, suggesting the involvement of this domain in the interaction with LTBP1. However, since the mutated LTBP4 N-terminal region did not reduce binding with the C-terminal region of LTBP1, the hybrid domain probably is not essential for binding to LTBP1 C-terminal region. The importance of this interaction is not yet known as there are no studies investigating whether the other LTBPs interact with each other. Therefore, future studies are required to investigate the significance of LTBP4 and LTBP1 interaction and whether this interaction is involved in elastic fibre assembly or TGF-β activation using *in vitro* cell-based studies.

Previous study showed that LTBP1 can interact non-covalently with TGFβ-LAP (Saharinen and Keski-Oja, 2000). We show that the LTBP4 C-terminal region can also interact TGFβ-LAP complex but with very weak binding affinity. This might be due to the requirement of the intracellular disulphide bond between LTBP4 and TGFβ1-LAP for this interaction. Since we know from an earlier study that LTBP4 inefficiently binds TGFβ1-LAP (Saharinen and Keski-Oja, 2000), we attempted to investigate whether LTBP1 covalent binding with the TGFβ-LAP complex effected the fibrillin-1 interaction. Our binding data showed that the formation of a covalent complex with TGFβ-LAP does not impact on the LTBP1-fibrillin-1 interaction.

In summary, we provide novel functional information for LTBP4. We also identify LTBP1 as a new matrix partner for LTBP4. This interaction might contribute to further understanding of the role of LTBPs in the matrix.

References

Kanzaki, T., et al., TGF-beta 1 binding protein: a component of the large latent complex of TGF-beta 1 with multiple repeat sequences. Cell, 1990. 61(6): p. 1051-61.

Moren, A., et al., Identification and characterization of LTBP-2, a novel latent transforming growth factor-beta-binding protein. J Biol Chem, 1994. 269(51): p. 32469-78.

Yin, W., et al., Isolation of a novel latent transforming growth factor-beta binding protein gene (LTBP-3). J Biol Chem, 1995. 270(17): p. 10147-60.

Saharinen, J., et al., Identification and characterization of a new latent transforming growth factor-beta-binding protein, LTBP-4. J Biol Chem, 1998. 273(29): p. 18459-69.

Saharinen, J., et al., Latent transforming growth factor-beta binding proteins (LTBPs)--structural extracellular matrix proteins for targeting TGF-beta action. Cytokine Growth Factor Rev, 1999. 10(2): p. 99-117.

Oklu, R. and R. Hesketh, The latent transforming growth factor beta binding protein (LTBP) family. Biochem J, 2000. 352 Pt 3: p. 601-10.

Robertson, I., S. Jensen, and P. Handford, TB domain proteins: evolutionary insights into the multifaceted roles of fibrillins and LTBPs. Biochem J, 2011. 433(2): p. 263-76.

Rifkin, D.B., Latent transforming growth factor-beta (TGF-beta) binding proteins: orchestrators of TGF-beta availability. J Biol Chem, 2005. 280(9): p. 7409-12.

Gentry, L.E., et al., Molecular events in the processing of recombinant type 1 pre-pro-transforming growth factor beta to the mature polypeptide. Mol Cell Biol, 1988. 8(10): p. 4162-8.

Gray, A.M. and A.J. Mason, Requirement for activin A and transforming growth factor--beta 1 pro-regions in homodimer assembly. Science, 1990. 247(4948): p. 1328-30.

Annes, J.P., J.S. Munger, and D.B. Rifkin, Making sense of latent TGFbeta activation. J Cell Sci, 2003. 116(Pt 2): p. 217-24.

Miyazono, K., et al., Latent high molecular weight complex of transforming growth factor beta 1. Purification from human platelets and structural characterization. J Biol Chem, 1988. 263(13): p. 6407-15.

Saharinen, J. and J. Keski-Oja, Specific sequence motif of 8-Cys repeats of TGF-beta binding proteins, LTBPs, creates a hydrophobic interaction surface for binding of small latent TGF-beta. Mol Biol Cell, 2000. 11(8): p. 2691-704.

Annes, J.P., et al., Integrin alphaVbeta6-mediated activation of latent TGF-beta requires the latent TGF-beta binding protein-1. J Cell Biol, 2004. 165(5): p. 723-34.

Robertson, I.B. and D.B. Rifkin, Regulation of the Bioavailability of TGF-beta and TGF-beta-Related Proteins. Cold Spring Harb Perspect Biol, 2016. 8(6).

Lack, J., et al., Solution structure of the third TB domain from LTBP1 provides insight into assembly of the large latent complex that sequesters latent TGF-beta. J Mol Biol, 2003. 334(2): p. 281-91.

Chen, Y., et al., Amino acid requirements for formation of the TGF-beta-latent TGF-beta binding protein complexes. J Mol Biol, 2005. 345(1): p. 175-86.

Walton, K.L., et al., Two distinct regions of latency-associated peptide coordinate stability of the latent transforming growth factor-beta1 complex. J Biol Chem, 2010. 285(22): p. 17029-37.

Vehvilainen, P., M. Hyytiainen, and J. Keski-Oja, Latent transforming growth factor-beta-binding protein 2 is an adhesion protein for melanoma cells. J Biol Chem, 2003. 278(27): p. 24705-13.

Kantola, A.K., J. Keski-Oja, and K. Koli, Fibronectin and heparin binding domains of latent TGF-beta binding protein (LTBP)-4 mediate matrix targeting and cell adhesion. Exp Cell Res, 2008. 314(13): p. 2488-500.

Su, C.T., et al., Latent transforming growth factor binding protein 4 regulates transforming growth factor beta receptor stability. Hum Mol Genet, 2015. 24(14): p. 4024-36.

Dabovic, B., et al., Function of latent TGFbeta binding protein 4 and fibulin 5 in elastogenesis and lung development. J Cell Physiol, 2015. 230(1): p. 226-36.

Thomson, J., et al., Fibrillin microfibrils and elastic fibre proteins: Functional interactions and extracellular regulation of growth factors. Semin Cell Dev Biol, 2019. 89: p. 109-117.

Chen, Q., et al., Potential role for heparan sulfate proteoglycans in regulation of transforming growth factor-beta (TGF-beta) by modulating assembly of latent TGF-beta-binding protein-1. J Biol Chem, 2007. 282(36): p. 26418-30.

Fontana, L., et al., Fibronectin is required for integrin alphavbeta6-mediated activation of latent TGF-beta complexes containing LTBP-1. FASEB J, 2005. 19(13): p. 1798-808.

Hyytiainen, M. and J. Keski-Oja, Latent TGF-beta binding protein LTBP-2 decreases fibroblast adhesion to fibronectin. J Cell Biol, 2003. 163(6): p. 1363-74.

Isogai, Z., et al., Latent transforming growth factor beta-binding protein 1 interacts with fibrillin and is a microfibril-associated protein. J Biol Chem, 2003. 278(4): p. 2750-7.

Ono, R.N., et al., Latent transforming growth factor beta-binding proteins and fibulins compete for fibrillin-1 and exhibit exquisite specificities in binding sites. J Biol Chem, 2009. 284(25): p. 16872-81.

Massam-Wu, T., et al., Assembly of fibrillin microfibrils governs extracellular deposition of latent TGF beta. J Cell Sci, 2010. 123(Pt 17): p. 3006-18.

Koli, K., M.J. Ryynanen, and J. Keski-Oja, Latent TGF-beta binding proteins (LTBPs)-1 and -3 coordinate proliferation and osteogenic differentiation of human mesenchymal stem cells. Bone, 2008. 43(4): p. 679-88.

Fujikawa, Y., et al., Latent TGF-beta binding protein 2 and 4 have essential overlapping functions in microfibril development. Sci Rep, 2017. 7: p. 43714.

Koski, C., J. Saharinen, and J. Keski-Oja, Independent promoters regulate the expression of two amino terminally distinct forms of latent transforming growth factor-beta binding protein-1 (LTBP-1) in a cell type-specific manner. J Biol Chem, 1999. 274(46): p. 32619-30.

Kantola, A.K., et al., Independent regulation of short and long forms of latent TGF-beta binding protein (LTBP)-4 in cultured fibroblasts and human tissues. J Cell Physiol, 2010. 223(3): p. 727-36.

Miyazono, K., et al., A role of the latent TGF-beta 1-binding protein in the assembly and secretion of TGF-beta 1. EMBO J, 1991. 10(5): p. 1091-101.

Gualandris, A., et al., The latent transforming growth factor-beta-binding protein-1 promotes in vitro differentiation of embryonic stem cells into endothelium. Mol Biol Cell, 2000. 11(12): p. 4295-308.

Todorovic, V., et al., Long form of latent TGF-beta binding protein 1 (Ltbp1L) is essential for cardiac outflow tract septation and remodeling. Development, 2007. 134(20): p. 3723-32.

Todorovic, V., et al., Long form of latent TGF-beta binding protein 1 (Ltbp1L) regulates cardiac valve development. Dev Dyn, 2011. 240(1): p. 176-87.

Horiguchi, M., et al., Abrogation of both short and long forms of latent transforming growth factor-beta binding protein-1 causes defective cardiovascular development and is perinatally lethal. Matrix Biol, 2015. 43: p. 61-70.

Sterner-Kock, A., et al., Disruption of the gene encoding the latent transforming growth factor-beta binding protein 4 (LTBP-4) causes abnormal lung development, cardiomyopathy, and colorectal cancer. Genes Dev, 2002. 16(17): p. 2264-73.

Urban, Z., et al., Mutations in LTBP4 cause a syndrome of impaired pulmonary, gastrointestinal, genitourinary, musculoskeletal, and dermal development. Am J Hum Genet, 2009. 85(5): p. 593-605.

Troilo, H., et al., Independent multimerization of Latent TGFβ Binding Protein-1 stabilized by cross-linking and enhanced by heparan sulfate. Scientific Reports, 2016. 6: p. 34347.

Rock, M.J., et al., Molecular basis of elastic fiber formation. Critical interactions and a tropoelastin-fibrillin-1 cross-link. J Biol Chem, 2004. 279(22): p. 23748-58.

Steer, R., Investigations of the extracellular deposition of latent TGF-beta binding protein-1 (LTBP-1) (PhD thesis). Retrieved from 2014.

Robertson, I.B., et al., Latent TGF-beta-binding proteins. Matrix Biol, 2015. 47: p. 44-53.

Noda, K., et al., Latent TGF-beta binding protein 4 promotes elastic fiber assembly by interacting with fibulin-5. Proc Natl Acad Sci U S A, 2013. 110(8): p. 2852-7.

Nunes, I., et al., Latent transforming growth factor-beta binding protein domains involved in activation and transglutaminase-dependent cross-linking of latent transforming growth factor-beta. J Cell Biol, 1997. 136(5): p. 1151-63.

Kojima, S., K. Nara, and D.B. Rifkin, Requirement for transglutaminase in the activation of latent transforming growth factor-beta in bovine endothelial cells. J Cell Biol, 1993. 121(2): p. 439-48.

Supplementary

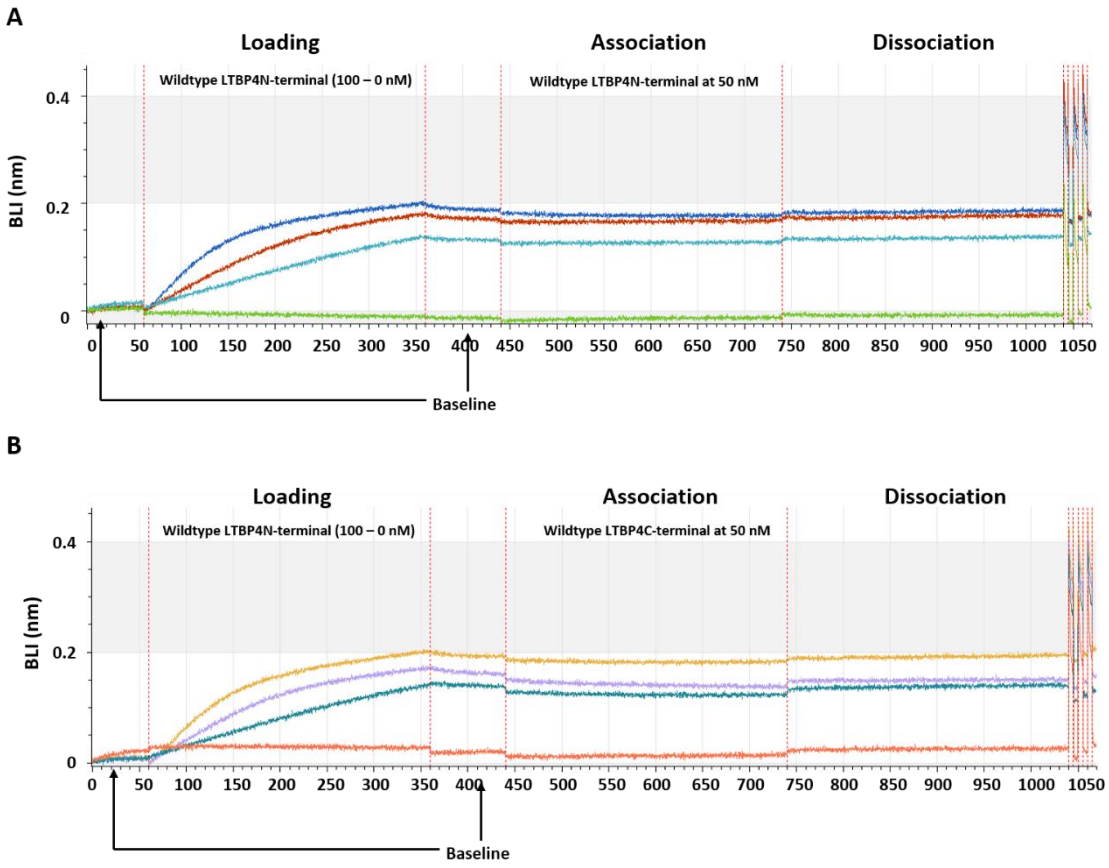

Figure 1: OctetRED96 system sensorgrams showing no binding response detected between concentrations (100 – 0 nM) immobilised wildtype LTBP4 N-terminal region and constant concentration at 50 Nm of **(A)** wildtype LTBP4 N-terminal region and **(B)** wildtype LTBP4 C-terminal.

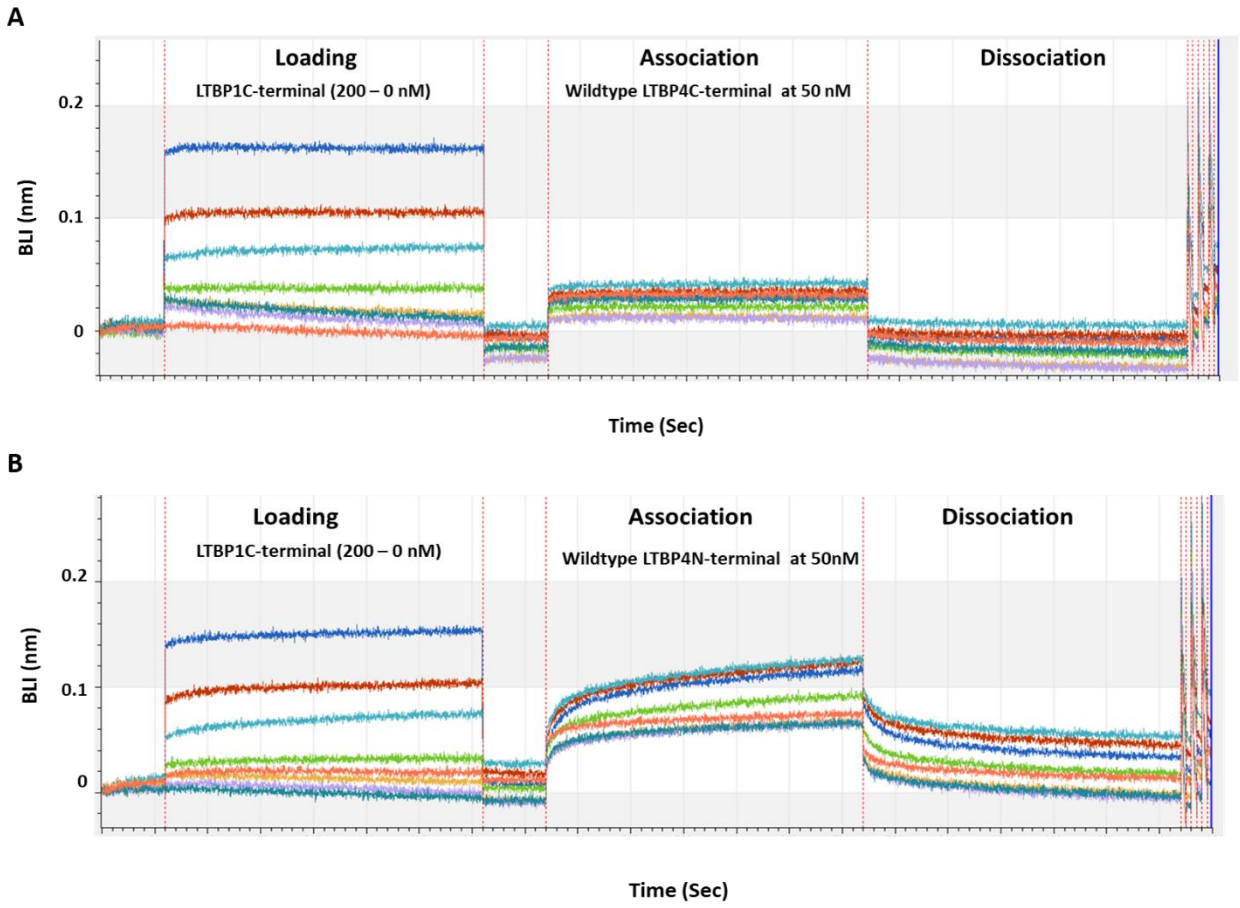

Figure 2: (A) OctetRED96 system sensorgrams showing no binding response detected between (200 – 0 nM) immobilized wildtype LTBP1 C-terminal region and a constant concentration at 50 nM of wildtype LTBP4 C-terminal. **(B)** OctetRED96 system sensorgrams showing direct binding detected (200 – 0 nM) immobilised wildtype LTBP1 C-terminal region and a constant concentration at 50 nM of wildtype LTBP4 N-terminal.

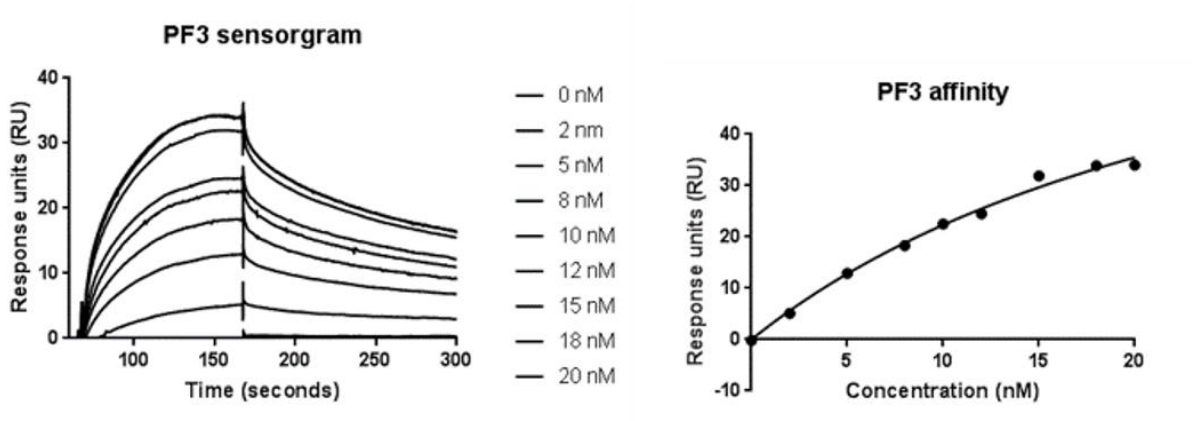

Figure 3: Surface plasmon resonance (SPR) analysis of the fibrillin-1 PF3 construct binding to LTBP1 C-terminal region. LTBP1 was immobilised on the sensor chip (GLC) using amine-coupling and purified fibrillin-1 (PF3) was injected as analyte at different concentrations (0 – 20 nM) over the immobilised LTBP1 (left panel). The binding affinity (K_D = 17. 6 nM) was determined by steady state with equilibrium response plotted against fibrillin-1 concentration (right panel).

6. Chapter 6

General Discussion

6. General Discussion

6.1. Summary

LTBP4 is an important promoter for elastogenesis and its genetic mutations are linked to the severe human disease, ARCL1C, among other LTBPs deficiency syndromes. ARCL1C is characterised by high mortality due to severely disrupted elastogenesis that affect many several organs, including the lung (Urban et al., 2009). LTBP4 possesses two independent matrix functions, a structural and TGFβ-independent role in elastic fibre assembly and a functional and TGFβ-dependent role in TGFβ ECM bioavailability (Noda et al., 2013, Saharinen and Keski-Oja, 2000). The elastic fibre assembly is a multistep process that requires several microfibril-associating molecules (Thomson et al., 2019), including LTBP4, the focus of this thesis. The mechanism by which LTBP4 is regulating elastogenesis is poorly understood and how LTBP4 mutations disrupt elastic fibre assembly in ARCL1C is not clear.

The work presented in this thesis contributes to better understanding of the role of LTBP4 in elastogenesis and the impact of ARCL1C point mutations on LTBP4 structure and function. First, we demonstrated novel structural information for the LTBP4 C-terminal region and confirmed the predicted impact of the missense mutation, C1186R, found in the 2nd TB domain of LTBP4 (Callewaert et al., 2013). Consistent with previous studies that demonstrated that substitutions of the conserved cysteines in TB and hybrid domains of the LTBPs/fibrillin family interfere with their conformation and function (Lack et al., 2003, Jensen et al., 2009), our data showed that ARCL1C causing point mutation, C1186R in the C-terminal region had a slight impact on LTBP4 structure and interaction with fibrillin-1. We also identified tropoelastin as a novel matrix protein partner for LTBP4. Following on from this work, we also investigated the structure of the N-terminal region of LTBP4 and whether an ARCL1C point mutation within the hybrid domain effects LTBP4 structure and function. Our data provided preliminary structural information for the N-terminal region of LTBP4 and suggested that the ARCL1C point mutation within the hybrid domain did not have a gross impact on the structure nor on LTBP4 interaction with heparan sulphate. Interestingly, this mutation increased binding to fibulin-4. Finally, we showed that LTBP4 cannot be cross-linked to itself nor to fibrillin-1 by TG2. We also identified LTBP1 as a novel N-terminal matrix partner

for LTBP4. These data contribution to a better understanding of the role of LTBP4 in regulating elastic fibre assembly and have been presented in Figure 6-1.

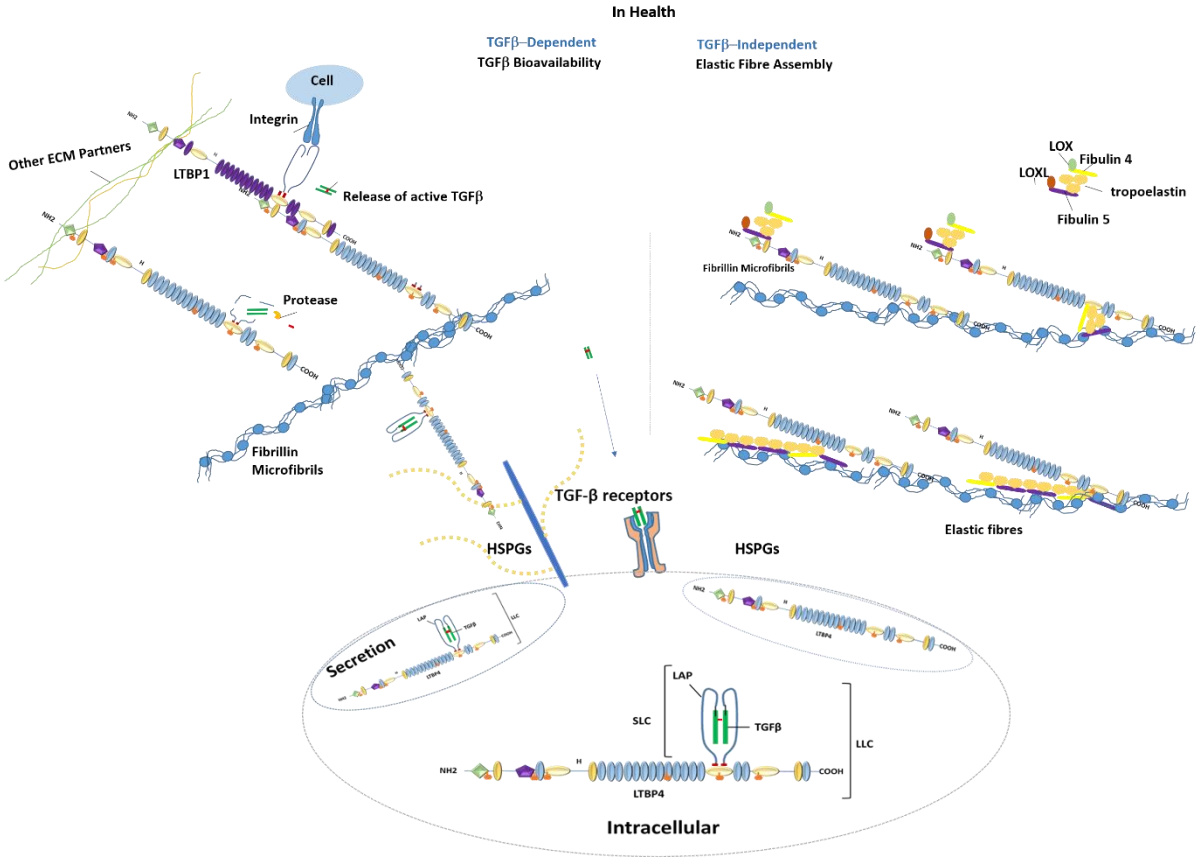

Figure 6-1: LTBP4 matrix functions. In health, LTBP4 is secreted as a part of the LLC and may be integrated into the ECM via its N-terminal region through interaction with heparan sulphate proteoglycans (HSPGs) and through interaction with fibrillin-1 via its C-terminal region, thus targeting the TGFβ latent complex for ECM sequestration (Kantola et al., 2008, Zilberberg et al., 2012). TGFβ then can be activated by several activation mechanisms such as activation by proteases that might degrade LAP and or LTBP4 and activation by heparanase (Horiguchi et al., 2012). LTBP4 can also be secreted free from TGFβ-LAP complex and promotes elastogenesis by regulating linear deposition of elastin-fibulin-4 and elastin-fibulin-5 complexes onto microfibril scaffolds through direct interaction with fibulin-4 and fibulin-5 via its N-terminal region (Noda et al., 2013, Bultmann-Mellin et al., 2015). In the first paper draft of this thesis, we showed that the ARCL1C point mutation, C1186R, changed the secondary structure and slightly altered fibrillin-1 interaction; this might lead to impaired matrix deposition of LTBP4 and consequently latent TGFβ ECM sequestration resulting in an increased activation of TGFβ as observed in ARCL1C patients and LTBP4$^{-/-}$ mice (Urban et al., 2009). We also identified tropoelastin as a new C-terminal partner for LTBP4 and the ARCL1C point mutations C1186R and C1286S interfere with tropoelastin interaction, suggesting a new role for LTBP4 in directly

regulating elastin deposition onto microfibrils. Interference with this interaction might contribute to the formation of large elastin deposits and patchy elastic fibres observed in ARCL1C patients. It should be noted that the elastin deposits were larger and patchier than that observed in fibulin-5 mutants (Noda et al., 2013, Callewaert et al., 2013). In the second paper draft, we demonstrated that LTBP4 directly interacts with heparan sulphate. This interaction might me important for LTBP4 matrix deposition. Moreover, we showed that this mutation increased binding with fibulin-4, this might lead to the formation of elastin-fibulin-5 complex aggregates. As it has been previously demonstrated that LTBP4S and LTBPL preferentially bind fibulin-5 and fibulin-4, respectively (Bultmann-Mellin et al., 2015, Bultmann-Mellin et al., 2016). In the third paper draft, we identified LTBP1 as a new N-terminal region partner for LTBP4, suggesting a new role for LTBP4 and LTBP1 in matrix. LTBP1 and LTBP4 might cooperate in TGFβ activation and elastic fibre formation.

6.2. General discussion

The literature on LTBP4 mutations focused on the molecular and clinical features of ARCL1C patients due to the considerable clinical overlap between ARCL1C and other ARCL diseases (Urban et al., 2009, Ritelli et al., 2019, Callewaert et al., 2013). This rare disease is caused by frameshift, nonsense and splice variant mutations in LTBP4 that lead to premature termination and severe reduction of LTBP4 mRNA expression (Urban et al., 2009, Ritelli et al., 2019). Three missense mutations in LTBP4, the focus of this thesis, have been also reported to cause ARCL1C (Urban et al., 2009, Callewaert et al., 2013, Su et al., 2015). These mutations affect highly conserved cysteine residues within the hybrid [1], the 16th cbEGF (Su et al., 2015) , and the TB2 domains, respectively (Callewaert et al., 2013). No *in vitro* studies have investigated the impact of these missense mutations on LTBP4 biology.

LTBP4 has dual independent matrix functions; promoting elastogenesis and regulating TGFβ bioavailability. Although some of the mechanisms are known for LTBP4 in regulating elastic fibre formation, its role in elastic fibre assembly and disruption in ARCL1C is still poorly understood. Previous studies have demonstrated that LTBP4 elastogenic role is driven by direct interaction with fibulin-4 and fibulin-5 that directly binds tropoelastin and LTBP4 acts as a carrier for elastin-fibulin4/fibulin-5 complex facilitating its linear deposition onto microfibrils (Noda et al., 2013, Dabovic et al., 2015, Bultmann-Mellin et al., 2015, Bultmann-Mellin et al., 2016). It also has been demonstrated that LTBP4 function in elastic fibre formation is a TGFβ-independent (Noda et al., 2013). LTBP4 as other LTBPs except LTBP2,

regulate ECM TGFβ bioavailability by facilitating TGFβ folding, secretion, and sequestration by direct interaction with fibrillin-1. In contrast to LTBP1 and LTBP3 that efficiently bind to all TGFβ isoforms, LTBP4 binds less efficiently to TGFβ-LAP and it binds to TGFβ1-LAP only, suggesting that LTBP4 may not play a central role in TGFβ bioavailability. Moreover, it has been shown that LTBP4 is majorly secreted as TGFβ-LAP-free form (Saharinen and Keski-Oja, 2000). However, reduces LTBP4 expression in ARCL1C patents and LTBP4$^{-/-}$ mice show impaired TGFβ signaling (Urban et al., 2009, Su et al., 2015). Although, LTBP4 is important for elastic fibre assembly, its structure is not yet defined and the outcome of its point mutations is not clear.

In the first study of this thesis, we determined the nanostructure of LTBP4 C-terminal monomer using SAXS and as expected we demonstrated that this region has an elongated and flexible conformation due to the presence of the unstructured protease sensitive linkers on either side of TB3 domain (Robertson et al., 2014). This is in line with our previous study on LTBP1 where the C-terminal region adopts an elongated and flexible nanostructure (Troilo et al., 2016) and with a study that demonstrated a highly dynamic and an elongated model for four C-terminal domains cbEGF14,TB3,EGF3,and cbEGF15 of LTBP1, using nuclear magnetic resonance (NMR) (Robertson et al., 2014). It has been suggested that the flexibility of this region might be essential for LTBP interactions with fibrillin-1 and latent TGFβ (Robertson et al., 2014). We also determined the secondary structure of the LTBP4 C-terminal region using CD and showed that it is composed of low α-helix content and higher contents of β-sheet and unordered structure. These, data are consistent with previous structural studies where the TB and cbEGF domains of fibrillin-1 have similar composition (Rao et al., 1995, Downing et al., 1996). Additionally, our structural data indicated differences between the wildtype LTBP4 C-terminal region and ARCL1C mutants, suggesting the importance of the highly conserved cysteines within the TB2 and cbEGF16 domains in stabilising LTBP4 structure. The C1286S substitution produced a protein with more compact nanostructure, while the C1186R produced a protein with more elongated structure compared with the wildtype. C1186R, but not C1286S, also showed significant secondary structure transition with lower β-sheet and higher unordered structure contents compared with the wildtype.

The demonstrated structural differences caused by the ARCL1C cysteine substitutions raised the hypothesis that these mutations might also interfere with LTBP4 matrix molecular

interactions. Previous studies using solid phase and SPR binding experiments demonstrated that the LTBP4 C-terminal region interacts with the N-terminal region of fibrillin-1 (Isogai et al., 2003, Ono et al., 2009). The data in chapter 3 confirm that both wildtype and mutants interact with fibrillin-1. However, the C1186R but not C1286S, slightly reduced fibrillin-1 binding affinity, indicating that cysteine substitution within the cbEGF16 domain of LTBP4 had minimal impact on fibrillin-1 binding, while cysteine substitution within the TB2 domain slightly alters the affinity of this binding. It is possible that the secondary structure transition caused by this mutation could perturb the interaction with fibrillin-1. Alternatively, the data could suggest that the TB2 domain contributes to fibrillin-1 binding. Fibrillin-1 is implicated in the matrix deposition of LTBP4, as fibrillin-$1^{-/-}$ dermal fibroblasts lacked fibrillin-1 and LTBP4 matrix deposition even after matrix maturation, while LTBP4 was deposited in a fibrillar pattern with fibrillin-1 in wildtype cells (Ono et al., 2009, Zilberberg et al., 2012). It has also been demonstrated that disruption of LTBP4 interaction with fibrillin-1 by mutation in fibrillin-1 N-terminal region, causes reduced matrix deposition of LTBP4 (Ono et al., 2009, Zilberberg et al., 2012). Therefore, we hypothesised that ARCL1C mutations might disturb this important interaction leading to less LTBP4 matrix deposition thus contributing to the disease. Future *in vivo* and *in vitro* cell-based work should be performed to confirm this hypothesis.

Previous, *in vivo* and *in vitro* studies have demonstrated that LTBP4 promotes elastogenesis in a TGFβ-independent manner (Noda et al., 2013, Dabovic et al., 2015, Dabovic et al., 2009, Kumra et al., 2019). Noda et.al observed no linear deposition of elastin or fibulin-5 onto microfibril scaffolds in LTBP4 knockdown human dermal fibroblasts (HDFs) (Noda et al., 2013). This was rescued by the addition of recombinant LTBP4S but not fibulin-5, indicating that LTBP4 is required for the linear deposition of both elastin and fibulin-5. The addition of more (at higher concentrations) recombinant LTBP4S enhanced more elastic fibre assembly compared with the wildtype cells and elastin has been observed to fully colocalise with LTBP4. Moreover, the addition of recombinant LTBP4S increased the amount of matured elastin. It has been observed that both elastin and the added recombinant LTBP4S colocalise with fibrilin-1, suggesting that LTBP4 regulates tropoelastin deposition on microfibrils (Noda et al., 2013). This led us to speculate that LTBP4 might directly interact with tropoelastin. Our BLI binding assays demonstrated that the LTBP4 C-terminal region but not the N-terminal region specifically and directly interacts with tropoelastin. This finding contrasts with a previous

study that showed indirect binding between LTBP4 and tropoelastin using solid phase binding assays (Noda et al., 2013). One possible explanation for this contradiction is the usage of full-length proteins in the previous study (Noda et al., 2013), as it has been recently demonstrated that full-length LTBP4L adopts a compact structure that converts to an extended conformation after binding with fibulin-4 multimers (Kumra et al., 2019), thus the tropoelastin binding site in full-length LTBP4S could be masked prior to interaction with fibulin-4 (Noda et al., 2013). However, the tropoelastin binding site could also be more accessible in our shortened LTBP4 construct. Noda et al. also demonstrated that the LTBP4 indirect interaction with tropoelastin is mediated by interaction with fibulin-5 (Noda et al., 2013). Potentially, in a similar mechanism to fibulin-4, fibulin-5 could also induce a conformational change in LTBP4S that might expose a tropoelastin binding site which would be interesting to test in the future. It would be relevant to use cell cultures and investigate whether LTBP4 directly regulates deposition of elastin onto microfibril scaffolds and how LTBP4 mutants would effect elastogenesis. The ARCL1C mutants also bound to tropoelastin but both C1186R and C1286S mutations interfered with tropoelastin binding. This data identifies tropoelastin as a novel matrix partner for LTBP4 and led us to hypothesise that elastogenesis might require both the indirect and direct interaction between LTBP4 and tropoelastin. Future work is required to test this hypothesis and investigate whether LTBP4 directly deposit elastin onto microfibrils using in vitro cell-based studies. It has been observed in previous studies that there are ultrastructural anomalies of elastic fibres in patients with fibulin-5 and LTBP4 mutations, where patients displayed abnormal globular elastin deposits that were poorly integrated into the microfibrils in their skin. While LTBP4 mutants displayed larger elastin deposits and patchier elastic fibres than those observed in fibulin-5 mutants (Callewaert et al., 2013). This is in line with the more recent immunolocalisation studies of both proteins in knockdown cells (Noda et al., 2013).

From our data we observed that the ARCL1C point mutation C1186R showed more impact on both the structure and interaction of LTBP4 than the C1286S mutation. However, why this difference is not clear but it could be attributed to either the position of the substituted cysteine residue or the substitution type. The C1186R mutation within the TB2 domain affects the C7 residue that disulphide bonds with the C4 residue to stabilise the intramolecular folding of the domain. It has been demonstrated that the area between C6 and C7 within the

TB2 domain is an important hydrophobic area that is responsible for TGFβ-LAP complex binding (Saharinen and Keski-Oja, 2000). Therefore, we hypothesised that substitution of C7 in TB2 might disturb the hydrophobic area leading to the production of less functional protein. Indeed, it has been previously shown that fibroblasts from ARCL1C patients displayed higher levels of active TGFβ compared to the wildtype but normal levels of TGFβ1 mRNA were observed, suggesting that LTBP4 mutations impaired the ECM sequestration of the latent TGFβ (Urban et al., 2009, Callewaert et al., 2013, Su et al., 2015). In agreement with findings with ARCL1C patients, LTBP4$^{-/-}$ mice showed increased pSmad2 in their lungs (Dabovic et al., 2009). It is important to elucidate whether ARCL1C-causing point mutations could alter TGFβ signaling, thus future work using TGFβ reporter cells could investigate the impact of ARCL1C mutants on TGFβ activation and signaling. The C1186S mutation within the cbEGF16 domain affects the C5 that disulphide bond with the C6. It has been demonstrated that the disulphide bridges in the cbEGF domains of fibrillin-1 stabilise the antiparallel β-sheet that enhance calcium binding (Downing et al., 1996, Schrijver et al., 1999). Another reason for the milder effect of cysteine to serine substitution relative to the more dramatic change caused by cysteine to arginine substitution could be the comparable size of cysteine and serine, while arginine side chain is much larger than cysteine and charged positively.

In the second paper draft of this thesis, using AUC we demonstrated that the LTBP4 N-terminal monomer has an elongated conformation. We also determined the secondary structure of this region using CD and showed that it is composed of low α-helix and higher content of β-sheet and unordered structure as expected due to the presence of TB and cbEGF domains (Rao et al., 1995, Downing et al., 1996). No difference in the secondary structure content were observed between the LTBP4 wildtype and mutant N-terminal, indicating that the ARCL1C point mutation within the hybrid domain did not cause a secondary structure alteration. From our AUC data, this point mutation caused the production of a more compact protein than the wildtype (Mellody et al., 2006). This finding is in line with a previous study on fibrillin-1 which demonstrated that substitution of a conserved cysteine residue within the hybrid domain led to the production of more compact protein compared with the wildtype. While our SAXS data showed that the mutant had an elongated and inflexible conformation, we were unable to determine the nanostructure of the wildtype LTBP4 N-terminal due to the propensity of this region to aggregate when concentrating it. Interestingly, based on our

findings, we observed that the mutant LTBP4 N-terminal region appeared to stabilize this region and showed less aggregation during concentration compared to the wildtype LTBP4 N-terminal region. Determining the nanostructure of the wildtype LTBP4 N-terminal could be one of the future studies.

In vivo and *in vitro* studies have demonstrated that LTBP4 supports elastic fibre formation by direct interaction with fibulin-4 (Bultmann-Mellin et al., 2015, Bultmann-Mellin et al., 2016, Kumra et al., 2019). This interaction, in common with the LTBP4 interaction with fibulin-5, involves the four-cysteine domain in the N-terminal region of LTBP4 (Noda et al., 2013, Bultmann-Mellin et al., 2015). Since the N-terminal region of LTBP4 is functionally important in promoting elastogenesis, we hypothesised that ARCL1C missense mutation in this region could interfere with binding fibulin-4. Using BLI binding assays, it has been demonstrated in this thesis that the ARCL1C cysteine substitution within the hybrid domain of the short LTBP4 isoform caused increased binding affinity to fibulin-4 compared with the wildtype, indicating that this mutation does impact on interaction with fibulin-4. As it has been previously demonstrated that both LTBP4 isoforms interact with fibulin-4, but the long and not the short isoform of LTBP4 favors binding with fibulin-4 (Bultmann-Mellin et al., 2016). We attempted to test the impact of this mutation on the interaction with fibulin-5 but we were unable to detect binding response between LTBP4S N-terminal region and fibulin-5. One possible explanation is that LTBP4S might bind more efficiently with fibulin-5 multimers but not monomers. As it has been demonstrated recently that LTBP4L strongly binds fibulin-4 multimers but not to lower molecular species (Kumra et al., 2019). Future binding work could thus test this hypothesis and study the interactions with multimers of fibulin-4 and fibulin-5.

The LTBP4 N-terminal region is important in its initial matrix deposition. An *in vitro* study has demonstrated that the initial deposition of LTBP4 is mediated by fibronectin (Kantola et al., 2008). Using solid-phase binding assays, LTBP4S has previously been shown to directly interact with fibronectin via its N-terminal region. Therefore, we hypothesised that the ARCL1C point mutation within the hybrid domain might interfere with this interaction leading to impaired matrix deposition of LTBP4. However, in this thesis, our binding studies contrast with the previous study (Kantola et al., 2008). As we show that the N-terminal region of LTBP4 did not bind to fibronectin. One possible explanation for the contrasting findings could be attributed to the different fibronectin used, as the previous study used a plasma fibronectin,

while in this thesis we used purified cellular fibronectin. Moreover, the fibronectin in the previous study contained the hinge region, while ours did not, so this could also explain the contradicted result. Indeed, It has been demonstrated that the hinge region is important for mediating the interaction between LTBP1 and fibronectin (Fontana et al., 2005). Future binding studies using LTBP4 construct containing this region would be useful to investigate whether the hinge region is important for LTBP4 interaction with fibronectin. Another explanation which could account for the difference, is that LTBP4 might indirectly bind fibronectin as it has been demonstrated that LTBP1 indirectly binds fibronectin via its N-terminal region and through interaction with heparan sulfate (Chen et al., 2007). Indeed, a previous study has shown that the LTBP4 N-terminal region binds heparin, and this binding has been suggested to be important for LTBP4 matrix deposition (Kantola et al., 2008). In this thesis we showed that the LTBP4 N-terminal region directly binds heparan sulphate. We also demonstrated that the ARCL1C mutation within the hybrid domain did not change the binding affinity with heparan sulfate. However, the significance of this interaction on LTBP4 matrix deposition needs to be investigated further. Further binding studies are also required to investigated whether heparan sulphate mediates the LTBP4 interaction with fibronectin.

An early study has demonstrated that LTBP1 possess a TG2 reactive site in its N-terminal region and that LTBP1 matrix incorporation is TG2 dependent (Nunes et al., 1997). We previously showed that LTBP1 can self-oligomerise in an N- to N- and N- to C-terminal manner and these assemblies are stabilised by TG2 (Troilo et al., 2016). It has also been shown by Ruth Steer (PhD thesis) (Steer, 2014), that LTBP1 and fibrillin-1 do cross-link mediated by TG2. To date it is still not known to with ECM protein is LTBP4 covalently linked and whether TG2 is implicated in its matrix association. It has been shown that LTBP4 requires fibrillin-1 for its matrix incorporation (Zilberberg et al., 2012). These data led us to speculate that LTBP4 might possess the same dependence on TG2 and or can be cross-linked to fibrillin-1. However, in the third paper draft of this thesis, we showed that LTBP4 does not self-associate nor is it cross-linked in an N- to N- or N- to C-terminal manner by TG2, indicating that LTBP4 might not be a substrate for TG2 or might require other proteins to mediate its cross-linking and self-assembly. We also show that the same region in LTBP4 does not cross-link with fibrillin-1, confirming that the LTBP4 C-terminal region does not appear to be a substrate for TG2.

In this thesis, we identified LTBP1 as a novel matrix partner for LTBP4. Using BLI binding, we observed that LTBP4 directly interacts with the full-length LTBP1 via its N-terminal. We also showed that the LTBP4 N-terminal but not the C-terminal interacts with the C-terminal of LTBP1, suggesting a head-to-tail interaction. Moreover, we observed that LTBP4 N-terminal binds stronger to the full-length than the C-terminal region of LTBP1, suggesting that there might be another binding site for LTBP4 in full length LTBP1. The significance of this interaction is not known yet and further studies are required for elucidation. However, we also showed that the ARCL1C point mutation within the hybrid domain, slightly interfered with the interaction of full-length LTBP1 but not the C-terminal region of LTBP1. These findings led us to suggest that LTBP1 and LTBP4 might cooperate in a unique matrix function. As previous studies have demonstrated cooperative and compensatory roles for other LTBPs (Koli et al., 2008, Fujikawa et al., 2017).

All LTBPs except LTBP3, directly bind the N-terminal of fibrillin-1 via their C-terminal (Isogai et al., 2003, Ono et al., 2009). LTBPs also covalently bind TGFβ-Latent complex via their C-terminal, therefore, tested whether the covalent interaction with TGFβ-LAP could interfere with LTBPs interaction with fibrillin-1. As a LTBP4-TGFβ-LAP complex was not available, we showed that the covalent binding between LTBP1 and TGFβ1-LAP did not interfere with the interaction with fibrillin-1.

6.3. Future Directions

It was demonstrated here that the LTBP4 C-terminal region missense mutation, C1286R, slightly interferes interaction with fibrillin-1, investigating whether this mutation impairs LTBP4 matrix deposition and colocalization with fibrillin-1 could be a future interest. This aim could be achieved by using fibroblast cells the overexpress the mutant LTBP4 and use immunolocalisation studies using anti-LTBP4 and anti-fibrillin-1 antibodies. BLI binding studies here identified tropoelastin as new matrix partner for LTBP4 and that the missense mutations C1186S and C1286R reduced the affinity of this binding, investigating the significance of this interaction and the effect of these mutations on elastic fibre formation and whether LTBP4 itself can deposit elastin on to microfibrils, is of future interest. This could be achieved using *in vivo* and *in vitro* studies using fibulin-5$^{-/-}$/fibulin-4$^{-/-}$ fibroblasts and using recombinant LTBP4 protein. The determined binding affinity of the interaction between

LTBP4 and fibulin-4 was weak and inconsistent with the previous studies (Bultmann-Mellin et al., 2015, Kumra et al., 2019). Moreover, we could not show any binding between LTBP4 and fibulin-5. It has been demonstrated that the fibulins multimers but not monomers nor dimers, that bind LTBP4, while fibulins monomers were used in our binding studies. So future binding studies using multimers could explain this discrepancy. Our binding studies on LTBP4 and fibronectin interaction did not show binding, which contradicts a previous study that showed a direct interaction using solid-phase binding (Kantola et al., 2008). The previous study used LTBP4 construct that contains the hinge region but our LTBP4 does not. It has been demonstrated that LTBP1 requires the hinge region to interact with fibronectin (Fontana et al., 2005). Future work is required to investigate whether the hinge region is required for the direct interaction between LTBP4 and fibronectin. This can be achieved by binding studies using LTBP4 construct that contain the hinge region. We also showed here that LTBP4 directly interacts with heparan sulphate. It has been suggested that heparin is important for LTBP4 matrix deposition (Kantola et al., 2008). Future work is required to test the significance of the LTBP4 and heparan sulphate interaction on LTBP4 matrix deposition using fibroblasts that overexpress LTBP4 and heparanase treatments. Additionally, data here identify a new molecular interaction for LTBP4 with LTBP1. The significance of this interaction is not known. Therefore, future work is essential to elucidate the importance of this interaction and whether this interaction is important for elastic fibre formation or for the TGFβ bioavailability and activation. This can be achieved by *in vitro* studies and cell-based TGFβ activity assays. It is also worth investigating whether LTBP4 mutants effect on TGFβ activity.

References

ALI, M., MCKIBBIN, M., BOOTH, A., PARRY, D. A., JAIN, P., RIAZUDDIN, S. A., HEJTMANCIK, J. F., KHAN, S. N., FIRASAT, S., SHIRES, M., GILMOUR, D. F., TOWNS, K., MURPHY, A. L., AZMANOV, D., TOURNEV, I., CHERNINKOVA, S., JAFRI, H., RAASHID, Y., TOOMES, C., CRAIG, J., MACKEY, D. A., KALAYDJIEVA, L., RIAZUDDIN, S. & INGLEHEARN, C. F. 2009. Null mutations in LTBP2 cause primary congenital glaucoma. *Am J Hum Genet,* 84**,** 664-71.

ANNES, J. P., CHEN, Y., MUNGER, J. S. & RIFKIN, D. B. 2004. Integrin alphaVbeta6-mediated activation of latent TGF-beta requires the latent TGF-beta binding protein-1. *J Cell Biol,* 165**,** 723-34.

ANNES, J. P., MUNGER, J. S. & RIFKIN, D. B. 2003. Making sense of latent TGFbeta activation. *J Cell Sci,* 116**,** 217-24.

ARGRAVES, W. S., GREENE, L. M., COOLEY, M. A. & GALLAGHER, W. M. 2003. Fibulins: physiological and disease perspectives. *EMBO Rep,* 4**,** 1127-31.

BAX, D. V., MAHALINGAM, Y., CAIN, S., MELLODY, K., FREEMAN, L., YOUNGER, K., SHUTTLEWORTH, C. A., HUMPHRIES, M. J., COUCHMAN, J. R. & KIELTY, C. M. 2007. Cell adhesion to fibrillin-1: identification of an Arg-Gly-Asp-dependent synergy region and a heparin-binding site that regulates focal adhesion formation. *J Cell Sci,* 120**,** 1383-92.

BEIRNE, J., TRUCHAN, H. & RAO, L. 2011. Development and qualification of a size exclusion chromatography coupled with multiangle light scattering method for molecular weight determination of unfractionated heparin. *Anal Bioanal Chem,* 399**,** 717-25.

BERK, D. R., BENTLEY, D. D., BAYLISS, S. J., LIND, A. & URBAN, Z. 2012. Cutis laxa: a review. *J Am Acad Dermatol,* 66**,** 842 e1-17.

BICKNELL, L. S., PITT, J., AFTIMOS, S., RAMADAS, R., MAW, M. A. & ROBERTSON, S. P. 2008. A missense mutation in ALDH18A1, encoding Delta1-pyrroline-5-carboxylate synthase (P5CS), causes an autosomal recessive neurocutaneous syndrome. *Eur J Hum Genet,* 16**,** 1176-86.

BULTMANN-MELLIN, I., CONRADI, A., MAUL, A. C., DINGER, K., WEMPE, F., WOHL, A. P., IMHOF, T., WUNDERLICH, F. T., BUNCK, A. C., NAKAMURA, T., KOLI, K., BLOCH, W., GHANEM, A., HEINZ, A., VON MELCHNER, H., SENGLE, G. & STERNER-KOCK, A. 2015. Modeling autosomal recessive cutis laxa type 1C in mice reveals distinct functions for Ltbp-4 isoforms. *Dis Model Mech,* 8**,** 403-15.

BULTMANN-MELLIN, I., DINGER, K., DEBUSCHEWITZ, C., LOEWE, K. M. A., MELCHER, Y., PLUM, M. T. W., APPEL, S., RAPPL, G., WILLENBORG, S., SCHAUSS, A. C., JUNGST, C., KRUGER, M., DRESSLER, S., NAKAMURA, T., WEMPE, F., ALEJANDRE ALCAZAR, M. A. & STERNER-KOCK, A. 2017. Role of LTBP4 in alveolarization, angiogenesis, and fibrosis in lungs. *Am J Physiol Lung Cell Mol Physiol,* 313**,** L687-L698.

BULTMANN-MELLIN, I., ESSERS, J., VAN HEIJINGEN, P. M., VON MELCHNER, H., SENGLE, G. & STERNER-KOCK, A. 2016. Function of Ltbp-4L and fibulin-4 in survival and elastogenesis in mice. *Dis Model Mech,* 9**,** 1367-1374.

CALLEWAERT, B., SU, C. T., VAN DAMME, T., VLUMMENS, P., MALFAIT, F., VANAKKER, O., SCHULZ, B., MAC NEAL, M., DAVIS, E. C., LEE, J. G., SALHI, A., UNGER, S., HEIMDAL, K., DE ALMEIDA, S., KORNAK, U., GASPAR, H., BRESSON, J. L., PRESCOTT, K., GOSENDI, M. E., MANSOUR, S., PIERARD, G. E., MADAN-KHETARPAL, S., SCIURBA, F. C., SYMOENS, S., COUCKE, P. J., VAN MALDERGEM, L., URBAN, Z. & DE PAEPE, A. 2013. Comprehensive clinical and molecular analysis of 12 families with type 1 recessive cutis laxa. *Hum Mutat,* 34**,** 111-21.

CHARBONNEAU, N. L., ONO, R. N., CORSON, G. M., KEENE, D. R. & SAKAI, L. Y. 2004. Fine tuning of growth factor signals depends on fibrillin microfibril networks. 72**,** 37-50.

CHEN, Q., SIVAKUMAR, P., BARLEY, C., PETERS, D. M., GOMES, R. R., FARACH-CARSON, M. C. & DALLAS, S. L. 2007. Potential role for heparan sulfate proteoglycans in regulation of transforming growth factor-beta (TGF-beta) by modulating assembly of latent TGF-beta-binding protein-1. *J Biol Chem,* 282**,** 26418-30.

CHEN, Y., ALI, T., TODOROVIC, V., O'LEARY J, M., KRISTINA DOWNING, A. & RIFKIN, D. B. 2005. Amino acid requirements for formation of the TGF-beta-latent TGF-beta binding protein complexes. *J Mol Biol,* 345**,** 175-86.

CHENG, A., CAIN, S. A., TIAN, P., BALDWIN, A. K., UPPANAN, P., KIELTY, C. M. & KIMBER, S. J. 2018. Recombinant Extracellular Matrix Protein Fragments Support Human Embryonic Stem Cell Chondrogenesis. *Tissue Eng Part A,* 24**,** 968-978.

CHOI, J., BERGDAHL, A., ZHENG, Q., STARCHER, B., YANAGISAWA, H. & DAVIS, E. C. 2009. Analysis of dermal elastic fibers in the absence of fibulin-5 reveals potential roles for fibulin-5 in elastic fiber assembly. *Matrix Biol,* 28**,** 211-20.

CHOUDHURY, R., MCGOVERN, A., RIDLEY, C., CAIN, S. A., BALDWIN, A., WANG, M. C., GUO, C., MIRONOV, A., JR., DRYMOUSSI, Z., TRUMP, D., SHUTTLEWORTH, A., BALDOCK, C. & KIELTY, C. M. 2009. Differential regulation of elastic fiber formation by fibulin-4 and -5. *J Biol Chem,* 284**,** 24553-67.

CLARKE, A. W., WISE, S. G., CAIN, S. A., KIELTY, C. M. & WEISS, A. S. 2005. Coacervation is promoted by molecular interactions between the PF2 segment of fibrillin-1 and the domain 4 region of tropoelastin. *Biochemistry,* 44**,** 10271-81.

COLAROSSI, C., CHEN, Y., OBATA, H., JURUKOVSKI, V., FONTANA, L., DABOVIC, B. & RIFKIN, D. B. 2005. Lung alveolar septation defects in Ltbp-3-null mice. *Am J Pathol,* 167**,** 419-28.

COMEGLIO, P., EVANS, A. L., BRICE, G., COOLING, R. J. & CHILD, A. H. 2002. Identification of FBN1 gene mutations in patients with ectopia lentis and marfanoid habitus. *Br J Ophthalmol,* 86**,** 1359-62.

CONCEPCION, J., WITTE, K., WARTCHOW, C., CHOO, S., YAO, D., PERSSON, H., WEI, J., LI, P., HEIDECKER, B., MA, W., VARMA, R., ZHAO, L. S., PERILLAT, D., CARRICATO, G., RECKNOR, M., DU, K., HO, H., ELLIS, T., GAMEZ, J., HOWES, M., PHI-WILSON, J., LOCKARD, S., ZUK, R. & TAN, H. 2009. Label-free detection of biomolecular interactions using BioLayer interferometry for kinetic characterization. *Comb Chem High Throughput Screen,* 12**,** 791-800.

CSISZAR, K. 2001. Lysyl oxidases: a novel multifunctional amine oxidase family. *Prog Nucleic Acid Res Mol Biol,* 70**,** 1-32.

DABOVIC, B., CHEN, Y., CHOI, J., VASSALLO, M., DIETZ, H. C., RAMIREZ, F., VON MELCHNER, H., DAVIS, E. C. & RIFKIN, D. B. 2009. Dual functions for LTBP in lung development: LTBP-4 independently modulates elastogenesis and TGF-beta activity. *J Cell Physiol,* 219**,** 14-22.

DABOVIC, B., CHEN, Y., COLAROSSI, C., ZAMBUTO, L., OBATA, H. & RIFKIN, D. B. 2002. Bone defects in latent TGF-beta binding protein (Ltbp)-3 null mice; a role for Ltbp in TGF-beta presentation. *J Endocrinol,* 175**,** 129-41.

DABOVIC, B., ROBERTSON, I. B., ZILBERBERG, L., VASSALLO, M., DAVIS, E. C. & RIFKIN, D. B. 2015. Function of latent TGFbeta binding protein 4 and fibulin 5 in elastogenesis and lung development. *J Cell Physiol,* 230**,** 226-36.

DALZIEL, M., CRISPIN, M., SCANLAN, C. N., ZITZMANN, N. & DWEK, R. A. 2014. Emerging principles for the therapeutic exploitation of glycosylation. *Science,* 343**,** 1235681.

DOWNING, A. K., KNOTT, V., WERNER, J. M., CARDY, C. M., CAMPBELL, I. D. & HANDFORD, P. A. 1996. Solution structure of a pair of calcium-binding epidermal growth factor-like domains: implications for the Marfan syndrome and other genetic disorders. *Cell,* 85**,** 597-605.

DRESCHER, D. G., RAMAKRISHNAN, N. A. & DRESCHER, M. J. 2009. Surface plasmon resonance (SPR) analysis of binding interactions of proteins in inner-ear sensory epithelia. *Methods Mol Biol,* 493**,** 323-43.

DREYFUSS, J. L., REGATIERI, C. V., JARROUGE, T. R., CAVALHEIRO, R. P., SAMPAIO, L. O. & NADER, H. B. 2009. Heparan sulfate proteoglycans: structure, protein interactions and cell signaling. *An Acad Bras Cienc,* 81**,** 409-29.

ESPINOSA-DE LA GARZA, C. E., MIRANDA-HERNANDEZ, M. P., ACOSTA-FLORES, L., PEREZ, N. O., FLORES-ORTIZ, L. F. & MEDINA-RIVERO, E. 2015. Analysis of therapeutic proteins and

peptides using multiangle light scattering coupled to ultra high performance liquid chromatography. *J Sep Sci,* 38**,** 1537-43.

FAZIO, M. J., OLSEN, D. R., KUIVANIEMI, H., CHU, M. L., DAVIDSON, J. M., ROSENBLOOM, J. & UITTO, J. 1988. Isolation and characterization of human elastin cDNAs, and age-associated variation in elastin gene expression in cultured skin fibroblasts. *Lab Invest,* 58**,** 270-7.

FONTANA, L., CHEN, Y., PRIJATELJ, P., SAKAI, T., FASSLER, R., SAKAI, L. Y. & RIFKIN, D. B. 2005. Fibronectin is required for integrin alphavbeta6-mediated activation of latent TGF-beta complexes containing LTBP-1. *FASEB J,* 19**,** 1798-808.

FRANKE, D. & SVERGUN, D. I. 2009. DAMMIF, a program for rapid ab-initio shape determination in small-angle scattering. *J Appl Crystallogr,* 42**,** 342-346.

FRANTZ, C., STEWART, K. M. & WEAVER, V. M. 2010. The extracellular matrix at a glance. *J Cell Sci,* 123**,** 4195-200.

FUJIKAWA, Y., YOSHIDA, H., INOUE, T., OHBAYASHI, T., NODA, K., VON MELCHNER, H., IWASAKA, T., SHIOJIMA, I., AKAMA, T. O. & NAKAMURA, T. 2017. Latent TGF-beta binding protein 2 and 4 have essential overlapping functions in microfibril development. *Sci Rep,* 7**,** 43714.

FUJITA, H. 1975. *Foundations of ultracentrifugal analysis,* New York, John Wiley.

GE, G. & GREENSPAN, D. S. 2006. BMP1 controls TGFbeta1 activation via cleavage of latent TGFbeta-binding protein. *J Cell Biol,* 175**,** 111-20.

GENTRY, L. E., LIOUBIN, M. N., PURCHIO, A. F. & MARQUARDT, H. 1988. Molecular events in the processing of recombinant type 1 pre-pro-transforming growth factor beta to the mature polypeptide. *Mol Cell Biol,* 8**,** 4162-8.

GILTAY, R., KOSTKA, G. & TIMPL, R. 1997. Sequence and expression of a novel member (LTBP-4) of the family of latent transforming growth factor-beta binding proteins. *FEBS Lett,* 411**,** 164-8.

GLEIZES, P. E., BEAVIS, R. C., MAZZIERI, R., SHEN, B. & RIFKIN, D. B. 1996. Identification and characterization of an eight-cysteine repeat of the latent transforming growth factor-beta binding protein-1 that mediates bonding to the latent transforming growth factor-beta1. *J Biol Chem,* 271**,** 29891-6.

GODWIN, A. R. F., SINGH, M., LOCKHART-CAIRNS, M. P., ALANAZI, Y. F., CAIN, S. A. & BALDOCK, C. 2019. The role of fibrillin and microfibril binding proteins in elastin and elastic fibre assembly. *Matrix Biol*.

GODWIN, A. R. F., STARBORG, T., SMITH, D. J., SHERRATT, M. J., ROSEMAN, A. M. & BALDOCK, C. 2018. Multiscale Imaging Reveals the Hierarchical Organization of Fibrillin Microfibrils. *J Mol Biol,* 430**,** 4142-4155.

GRAY, A. M. & MASON, A. J. 1990. Requirement for activin A and transforming growth factor--beta 1 pro-regions in homodimer assembly. *Science,* 247**,** 1328-30.

GREENFIELD, N. & FASMAN, G. D. 1969. Computed circular dichroism spectra for the evaluation of protein conformation. *Biochemistry,* 8**,** 4108-16.

GREENFIELD, N. J. 2006. Using circular dichroism spectra to estimate protein secondary structure. *Nat Protoc,* 1**,** 2876-90.

GUALANDRIS, A., ANNES, J. P., ARESE, M., NOGUERA, I., JURUKOVSKI, V. & RIFKIN, D. B. 2000. The latent transforming growth factor-beta-binding protein-1 promotes in vitro differentiation of embryonic stem cells into endothelium. *Mol Biol Cell,* 11**,** 4295-308.

GUERNSEY, D. L., JIANG, H., EVANS, S. C., FERGUSON, M., MATSUOKA, M., NIGHTINGALE, M., RIDEOUT, A. L., PROVOST, S., BEDARD, K., ORR, A., DUBE, M. P., LUDMAN, M. & SAMUELS, M. E. 2009. Mutation in pyrroline-5-carboxylate reductase 1 gene in families with cutis laxa type 2. *Am J Hum Genet,* 85**,** 120-9.

HANDFORD, P. A., DOWNING, A. K., REINHARDT, D. P. & SAKAI, L. Y. 2000. Fibrillin: from domain structure to supramolecular assembly. *Matrix Biol,* 19**,** 457-70.

HEYDEMANN, A., CECO, E., LIM, J. E., HADHAZY, M., RYDER, P., MORAN, J. L., BEIER, D. R., PALMER, A. A. & MCNALLY, E. M. 2009. Latent TGF-beta-binding protein 4 modifies muscular dystrophy in mice. *J Clin Invest,* 119**,** 3703-12.

HIELSCHER, A., ELLIS, K., QIU, C., PORTERFIELD, J. & GERECHT, S. 2016. Fibronectin Deposition Participates in Extracellular Matrix Assembly and Vascular Morphogenesis. *PLoS One,* 11**,** e0147600.

HINEK, A. 1995. The 67 kDa spliced variant of beta-galactosidase serves as a reusable protective chaperone for tropoelastin. *Ciba Found Symp,* 192**,** 185-91; discussion 191-6.

HIRAI, M., HORIGUCHI, M., OHBAYASHI, T., KITA, T., CHIEN, K. R. & NAKAMURA, T. 2007a. Latent TGF-beta-binding protein 2 binds to DANCE/fibulin-5 and regulates elastic fiber assembly. *EMBO J,* 26**,** 3283-95.

HIRAI, M., OHBAYASHI, T., HORIGUCHI, M., OKAWA, K., HAGIWARA, A., CHIEN, K. R., KITA, T. & NAKAMURA, T. 2007b. Fibulin-5/DANCE has an elastogenic organizer activity that is abrogated by proteolytic cleavage in vivo. *J Cell Biol,* 176**,** 1061-71.

HOLZWARTH, G. & DOTY, P. 1965. The Ultraviolet Circular Dichroism of Polypeptides. *J Am Chem Soc,* 87**,** 218-28.

HORIGUCHI, M., INOUE, T., OHBAYASHI, T., HIRAI, M., NODA, K., MARMORSTEIN, L. Y., YABE, D., TAKAGI, K., AKAMA, T. O., KITA, T., KIMURA, T. & NAKAMURA, T. 2009. Fibulin-4 conducts proper elastogenesis via interaction with cross-linking enzyme lysyl oxidase. *Proc Natl Acad Sci U S A,* 106**,** 19029-34.

HORIGUCHI, M., OTA, M. & RIFKIN, D. B. 2012. Matrix control of transforming growth factor-beta function. *J Biochem,* 152**,** 321-9.

HORIGUCHI, M., TODOROVIC, V., HADJIOLOVA, K., WEISKIRCHEN, R. & RIFKIN, D. B. 2015. Abrogation of both short and long forms of latent transforming growth factor-beta binding protein-1 causes defective cardiovascular development and is perinatally lethal. *Matrix Biol,* 43**,** 61-70.

HOWLETT, G. J., MINTON, A. P. & RIVAS, G. 2006. Analytical ultracentrifugation for the study of protein association and assembly. *Curr Opin Chem Biol,* 10**,** 430-6.

HUBMACHER, D., TIEDEMANN, K. & REINHARDT, D. P. 2006. Fibrillins: from biogenesis of microfibrils to signaling functions. *Curr Top Dev Biol,* 75**,** 93-123.

HUCTHAGOWDER, V., SAUSGRUBER, N., KIM, K. H., ANGLE, B., MARMORSTEIN, L. Y. & URBAN, Z. 2006. Fibulin-4: a novel gene for an autosomal recessive cutis laxa syndrome. *Am J Hum Genet,* 78**,** 1075-80.

HYYTIAINEN, M. & KESKI-OJA, J. 2003. Latent TGF-beta binding protein LTBP-2 decreases fibroblast adhesion to fibronectin. *J Cell Biol,* 163**,** 1363-74.

IAIN D. CAMPBELL, P. B. 1993. Epidermal growth factor-like modules. *Current Opinion in Structural Biology,* Volume 3, **,** 385-392.

ISOGAI, Z., ONO, R. N., USHIRO, S., KEENE, D. R., CHEN, Y., MAZZIERI, R., CHARBONNEAU, N. L., REINHARDT, D. P., RIFKIN, D. B. & SAKAI, L. Y. 2003. Latent transforming growth factor beta-binding protein 1 interacts with fibrillin and is a microfibril-associated protein. *J Biol Chem,* 278**,** 2750-7.

JENSEN, S. A., IQBAL, S., LOWE, E. D., REDFIELD, C. & HANDFORD, P. A. 2009. Structure and interdomain interactions of a hybrid domain: a disulphide-rich module of the fibrillin/LTBP superfamily of matrix proteins. *Structure,* 17**,** 759-68.

KAILASHIYA, J., MUKHERJEE, A. & DASH, D. 2017. Essentials of medical biochemistry: With clinical cases. 145**,** 576-577.

KANTOLA, A. K., KESKI-OJA, J. & KOLI, K. 2008. Fibronectin and heparin binding domains of latent TGF-beta binding protein (LTBP)-4 mediate matrix targeting and cell adhesion. *Exp Cell Res,* 314**,** 2488-500.

KANTOLA, A. K., RYYNANEN, M. J., LHOTA, F., KESKI-OJA, J. & KOLI, K. 2010. Independent regulation of short and long forms of latent TGF-beta binding protein (LTBP)-4 in cultured fibroblasts and human tissues. *J Cell Physiol,* 223**,** 727-36.

KANZAKI, T., OLOFSSON, A., MOREN, A., WERNSTEDT, C., HELLMAN, U., MIYAZONO, K., CLAESSON-WELSH, L. & HELDIN, C. H. 1990. TGF-beta 1 binding protein: a component of the large latent complex of TGF-beta 1 with multiple repeat sequences. *Cell,* 61**,** 1051-61.

KEENE, D. R., MADDOX, B. K., KUO, H. J., SAKAI, L. Y. & GLANVILLE, R. W. 1991. Extraction of extendable beaded structures and their identification as fibrillin-containing extracellular matrix microfibrils. *J Histochem Cytochem,* 39**,** 441-9.

KIELTY, C. M., SHERRATT, M. J., MARSON, A. & BALDOCK, C. 2005. Fibrillin microfibrils. *Adv Protein Chem,* 70**,** 405-36.

KIKHNEY, A. G. & SVERGUN, D. I. 2015. A practical guide to small angle X-ray scattering (SAXS) of flexible and intrinsically disordered proteins. *FEBS Lett,* 589**,** 2570-7.

KOBAYASHI, N., KOSTKA, G., GARBE, J. H., KEENE, D. R., BACHINGER, H. P., HANISCH, F. G., MARKOVA, D., TSUDA, T., TIMPL, R., CHU, M. L. & SASAKI, T. 2007. A comparative analysis of the fibulin protein family. Biochemical characterization, binding interactions, and tissue localization. *J Biol Chem,* 282**,** 11805-16.

KOLI, K., HYYTIAINEN, M., RYYNANEN, M. J. & KESKI-OJA, J. 2005. Sequential deposition of latent TGF-beta binding proteins (LTBPs) during formation of the extracellular matrix in human lung fibroblasts. *Exp Cell Res,* 310**,** 370-82.

KOLI, K., RYYNANEN, M. J. & KESKI-OJA, J. 2008. Latent TGF-beta binding proteins (LTBPs)-1 and -3 coordinate proliferation and osteogenic differentiation of human mesenchymal stem cells. *Bone,* 43**,** 679-88.

KORNAK, U., REYNDERS, E., DIMOPOULOU, A., VAN REEUWIJK, J., FISCHER, B., RAJAB, A., BUDDE, B., NURNBERG, P., FOULQUIER, F., GROUP, A. D.-T. S., LEFEBER, D., URBAN, Z., GRUENEWALD, S., ANNAERT, W., BRUNNER, H. G., VAN BOKHOVEN, H., WEVERS, R., MORAVA, E., MATTHIJS, G., VAN MALDERGEM, L. & MUNDLOS, S. 2008. Impaired glycosylation and cutis laxa caused by mutations in the vesicular H+-ATPase subunit ATP6V0A2. *Nat Genet,* 40**,** 32-4.

KOSKI, C., SAHARINEN, J. & KESKI-OJA, J. 1999. Independent promoters regulate the expression of two amino terminally distinct forms of latent transforming growth factor-beta binding protein-1 (LTBP-1) in a cell type-specific manner. *J Biol Chem,* 274**,** 32619-30.

KUMRA, H., NELEA, V., HAKAMI, H., PAGLIUZZA, A., DJOKIC, J., XU, J., YANAGISAWA, H. & REINHARDT, D. P. 2019. Fibulin-4 exerts a dual role in LTBP-4L–mediated matrix assembly and function. 116**,** 20428-20437.

LACK, J., O'LEARY, J. M., KNOTT, V., YUAN, X., RIFKIN, D. B., HANDFORD, P. A. & DOWNING, A. K. 2003. Solution structure of the third TB domain from LTBP1 provides insight into assembly of the large latent complex that sequesters latent TGF-beta. *J Mol Biol,* 334**,** 281-91.

LAUE, T. M. 1995. Sedimentation equilibrium as thermodynamic tool. *Methods Enzymol,* 259**,** 427-52.

LEAO-TELES, E., QUELHAS, D., VILARINHO, L. & JAEKEN, J. 2010. De Barsy syndrome and ATP6V0A2-CDG. *Eur J Hum Genet,* 18**,** 526; author reply 526.

LEWIS, K. G., BERCOVITCH, L., DILL, S. W. & ROBINSON-BOSTOM, L. 2004. Acquired disorders of elastic tissue: Part II. decreased elastic tissue. *J Am Acad Dermatol,* 51**,** 165-85; quiz 186-8.

LI, D. Y., BROOKE, B., DAVIS, E. C., MECHAM, R. P., SORENSEN, L. K., BOAK, B. B., EICHWALD, E. & KEATING, M. T. 1998. Elastin is an essential determinant of arterial morphogenesis. *Nature,* 393**,** 276-80.

LI, Y., TRAN, A. H., DANISHEFSKY, S. J. & TAN, Z. 2019. Chemical biology of glycoproteins: From chemical synthesis to biological impact. *Methods Enzymol,* 621**,** 213-229.

LI, Y. J., BI, L. J., ZHANG, X. E., ZHOU, Y. F., ZHANG, J. B., CHEN, Y. Y., LI, W. & ZHANG, Z. P. 2006. Reversible immobilization of proteins with streptavidin affinity tags on a surface plasmon resonance biosensor chip. *Anal Bioanal Chem,* 386**,** 1321-6.

LIU, J., ANDYA, J. D. & SHIRE, S. J. 2006. A critical review of analytical ultracentrifugation and field flow fractionation methods for measuring protein aggregation. *AAPS J,* 8**,** E580-9.

LIU, J. & PEDERSEN, L. C. 2007. Anticoagulant heparan sulfate: structural specificity and biosynthesis. *Appl Microbiol Biotechnol,* 74**,** 263-72.

LOEYS, B., VAN MALDERGEM, L., MORTIER, G., COUCKE, P., GERNIERS, S., NAEYAERT, J. M. & DE PAEPE, A. 2002. Homozygosity for a missense mutation in fibulin-5 (FBLN5) results in a severe form of cutis laxa. *Hum Mol Genet,* 11**,** 2113-8.

LUCERO, H. A. & KAGAN, H. M. 2006. Lysyl oxidase: an oxidative enzyme and effector of cell function. *Cell Mol Life Sci,* 63**,** 2304-16.

MASSAM-WU, T., CHIU, M., CHOUDHURY, R., CHAUDHRY, S. S., BALDWIN, A. K., MCGOVERN, A., BALDOCK, C., SHUTTLEWORTH, C. A. & KIELTY, C. M. 2010. Assembly of fibrillin microfibrils governs extracellular deposition of latent TGF beta. *J Cell Sci,* 123**,** 3006-18.

MCCARTY, M. J., DAVIDSON, J. M., CARDONE, J. S. & ANDERSON, L. L. 1996. Cutis laxa acquisita associated with multiple myeloma: a case report and review of the literature. *Cutis,* 57**,** 267-70.

MCLAUGHLIN, P. J., CHEN, Q., HORIGUCHI, M., STARCHER, B. C., STANTON, J. B., BROEKELMANN, T. J., MARMORSTEIN, A. D., MCKAY, B., MECHAM, R., NAKAMURA, T. & MARMORSTEIN, L. Y. 2006. Targeted Disruption of Fibulin-4 Abolishes Elastogenesis and Causes Perinatal Lethality in Mice. 26**,** 1700-1709.

MECHAM, R. P. 1991. Elastin synthesis and fiber assembly. *Ann N Y Acad Sci,* 624**,** 137-46.

MELLODY, K. T., FREEMAN, L. J., BALDOCK, C., JOWITT, T. A., SIEGLER, V., RAYNAL, B. D., CAIN, S. A., WESS, T. J., SHUTTLEWORTH, C. A. & KIELTY, C. M. 2006. Marfan syndrome-causing mutations in fibrillin-1 result in gross morphological alterations and highlight the structural importance of the second hybrid domain. *J Biol Chem,* 281**,** 31854-62.

MENEGHETTI, M. C., HUGHES, A. J., RUDD, T. R., NADER, H. B., POWELL, A. K., YATES, E. A. & LIMA, M. A. 2015. Heparan sulfate and heparin interactions with proteins. *J R Soc Interface,* 12**,** 0589.

MERTENS, H. D. & SVERGUN, D. I. 2010. Structural characterization of proteins and complexes using small-angle X-ray solution scattering. *J Struct Biol,* 172**,** 128-41.

MILEWICZ, D. M., PYERITZ, R. E., CRAWFORD, E. S. & BYERS, P. H. 1992. Marfan syndrome: defective synthesis, secretion, and extracellular matrix formation of fibrillin by cultured dermal fibroblasts. *J Clin Invest,* 89**,** 79-86.

MIYAZONO, K., HELLMAN, U., WERNSTEDT, C. & HELDIN, C. H. 1988. Latent high molecular weight complex of transforming growth factor beta 1. Purification from human platelets and structural characterization. *J Biol Chem,* 263**,** 6407-15.

MOHAMED, M., VOET, M., GARDEITCHIK, T. & MORAVA, E. 2014. Cutis Laxa. *Adv Exp Med Biol,* 802**,** 161-84.

MORAVA, E., GUILLARD, M., LEFEBER, D. J. & WEVERS, R. A. 2009. Autosomal recessive cutis laxa syndrome revisited. *Eur J Hum Genet,* 17**,** 1099-110.

MOREMEN, K. W., TIEMEYER, M. & NAIRN, A. V. 2012. Vertebrate protein glycosylation: diversity, synthesis and function. *Nat Rev Mol Cell Biol,* 13**,** 448-62.

MOREN, A., OLOFSSON, A., STENMAN, G., SAHLIN, P., KANZAKI, T., CLAESSON-WELSH, L., TEN DIJKE, P., MIYAZONO, K. & HELDIN, C. H. 1994. Identification and characterization of LTBP-2, a novel latent transforming growth factor-beta-binding protein. *J Biol Chem,* 269**,** 32469-78.

NAROOIE-NEJAD, M., PAYLAKHI, S. H., SHOJAEE, S., FAZLALI, Z., REZAEI KANAVI, M., NILFORUSHAN, N., YAZDANI, S., BABRZADEH, F., SURI, F., RONAGHI, M., ELAHI, E. & PAISAN-RUIZ, C. 2009. Loss of function mutations in the gene encoding latent transforming growth factor beta binding protein 2, LTBP2, cause primary congenital glaucoma. *Hum Mol Genet,* 18**,** 3969-77.

NGUYEN, H. H., PARK, J., KANG, S. & KIM, M. 2015. Surface plasmon resonance: a versatile technique for biosensor applications. *Sensors (Basel),* 15**,** 10481-510.

NODA, K., DABOVIC, B., TAKAGI, K., INOUE, T., HORIGUCHI, M., HIRAI, M., FUJIKAWA, Y., AKAMA, T. O., KUSUMOTO, K., ZILBERBERG, L., SAKAI, L. Y., KOLI, K., NAITOH, M., VON MELCHNER, H., SUZUKI, S., RIFKIN, D. B. & NAKAMURA, T. 2013. Latent TGF-beta binding protein 4 promotes elastic fiber assembly by interacting with fibulin-5. *Proc Natl Acad Sci U S A,* 110**,** 2852-7.

NOOR, A., WINDPASSINGER, C., VITCU, I., ORLIC, M., RAFIQ, M. A., KHALID, M., MALIK, M. N., AYUB, M., ALMAN, B. & VINCENT, J. B. 2009. Oligodontia is caused by mutation in LTBP3, the gene encoding latent TGF-beta binding protein 3. *Am J Hum Genet,* 84**,** 519-23.

NUNES, I., GLEIZES, P. E., METZ, C. N. & RIFKIN, D. B. 1997. Latent transforming growth factor-beta binding protein domains involved in activation and transglutaminase-dependent cross-linking of latent transforming growth factor-beta. *J Cell Biol,* 136**,** 1151-63.

OKLU, R. & HESKETH, R. 2000. The latent transforming growth factor beta binding protein (LTBP) family. *Biochem J,* 352 Pt 3**,** 601-10.

ONO, R. N., SENGLE, G., CHARBONNEAU, N. L., CARLBERG, V., BACHINGER, H. P., SASAKI, T., LEE-ARTEAGA, S., ZILBERBERG, L., RIFKIN, D. B., RAMIREZ, F., CHU, M. L. & SAKAI, L. Y. 2009. Latent transforming growth factor beta-binding proteins and fibulins compete for fibrillin-1 and exhibit exquisite specificities in binding sites. *J Biol Chem,* 284**,** 16872-81.

PAPKE, C. L. & YANAGISAWA, H. 2014. Fibulin-4 and fibulin-5 in elastogenesis and beyond: Insights from mouse and human studies. *Matrix Biol,* 37**,** 142-9.

PHILO, J. S. 1994. Measuring Sedimentation, Diffusion, and Molecular Weights of Small Molecules by Direct Fitting of Sedimentation Velocity Concentration Profiles. 156-170.

PHILO, J. S. 2000. Sedimentation equilibrium analysis of mixed associations using numerical constraints to impose mass or signal conservation. *Methods Enzymol,* 321**,** 100-20.

PONIATOWSKI, L. A., WOJDASIEWICZ, P., GASIK, R. & SZUKIEWICZ, D. 2015. Transforming growth factor Beta family: insight into the role of growth factors in regulation of fracture healing biology and potential clinical applications. *Mediators Inflamm,* 2015**,** 137823.

QIAN, R. Q. & GLANVILLE, R. W. 1997. Alignment of fibrillin molecules in elastic microfibrils is defined by transglutaminase-derived cross-links. *Biochemistry,* 36**,** 15841-7.

RAGHUNATH, M., PUTNAM, E. A., RITTY, T., HAMSTRA, D., PARK, E. S., TSCHODRICH-ROTTER, M., PETERS, R., REHEMTULLA, A. & MILEWICZ, D. M. 1999. Carboxy-terminal conversion of profibrillin to fibrillin at a basic site by PACE/furin-like activity required for incorporation in the matrix. *J Cell Sci,* 112 (Pt 7)**,** 1093-100.

RAO, Z., HANDFORD, P., MAYHEW, M., KNOTT, V., BROWNLEE, G. G. & STUART, D. 1995. The structure of a Ca(2+)-binding epidermal growth factor-like domain: its role in protein-protein interactions. *Cell,* 82**,** 131-41.

REINHARDT, D. P., ONO, R. N. & SAKAI, L. Y. 1997. Calcium stabilizes fibrillin-1 against proteolytic degradation. *J Biol Chem,* 272**,** 1231-6.

REVERSADE, B., ESCANDE-BEILLARD, N., DIMOPOULOU, A., FISCHER, B., CHNG, S. C., LI, Y., SHBOUL, M., THAM, P. Y., KAYSERILI, H., AL-GAZALI, L., SHAHWAN, M., BRANCATI, F., LEE, H., O'CONNOR, B. D., SCHMIDT-VON KEGLER, M., MERRIMAN, B., NELSON, S. F., MASRI, A., ALKAZALEH, F., GUERRA, D., FERRARI, P., NANDA, A., RAJAB, A., MARKIE, D., GRAY, M., NELSON, J., GRIX, A., SOMMER, A., SAVARIRAYAN, R., JANECKE, A. R., STEICHEN, E., SILLENCE, D., HAUSSER, I., BUDDE, B., NURNBERG, G., NURNBERG, P., SEEMANN, P., KUNKEL, D., ZAMBRUNO, G., DALLAPICCOLA, B., SCHUELKE, M., ROBERTSON, S., HAMAMY, H., WOLLNIK, B., VAN MALDERGEM, L., MUNDLOS, S. & KORNAK, U. 2009. Mutations in PYCR1 cause cutis laxa with progeroid features. *Nat Genet,* 41**,** 1016-21.

RIFKIN, D. B. 2005. Latent transforming growth factor-beta (TGF-beta) binding proteins: orchestrators of TGF-beta availability. *J Biol Chem,* 280**,** 7409-12.

RIFKIN, D. B., RIFKIN, W. J. & ZILBERBERG, L. 2018. LTBPs in biology and medicine: LTBP diseases. *Matrix Biol,* 71-72**,** 90-99.

RITELLI, M., CAMMARATA-SCALISI, F., CINQUINA, V. & COLOMBI, M. 2019. Clinical and molecular characterization of an 18-month-old infant with autosomal recessive cutis laxa type 1C due to a novel LTBP4 pathogenic variant, and literature review. *Mol Genet Genomic Med,* 7**,** e00735.

ROBERTS, A. B., HEINE, U. I., FLANDERS, K. C. & SPORN, M. B. 1990. Transforming growth factor-beta. Major role in regulation of extracellular matrix. *Ann N Y Acad Sci,* 580**,** 225-32.

ROBERTSON, I., JENSEN, S. & HANDFORD, P. 2011. TB domain proteins: evolutionary insights into the multifaceted roles of fibrillins and LTBPs. *Biochem J,* 433**,** 263-76.

ROBERTSON, I. B., HANDFORD, P. A. & REDFIELD, C. 2014. NMR spectroscopic and bioinformatic analyses of the LTBP1 C-terminus reveal a highly dynamic domain organisation. *PLoS One,* 9**,** e87125.

ROBERTSON, I. B., HORIGUCHI, M., ZILBERBERG, L., DABOVIC, B., HADJIOLOVA, K. & RIFKIN, D. B. 2015. Latent TGF-beta-binding proteins. *Matrix Biol,* 47**,** 44-53.

ROBERTSON, I. B. & RIFKIN, D. B. 2016. Regulation of the Bioavailability of TGF-beta and TGF-beta-Related Proteins. *Cold Spring Harb Perspect Biol,* 8.

ROCK, M. J., CAIN, S. A., FREEMAN, L. J., MORGAN, A., MELLODY, K., MARSON, A., SHUTTLEWORTH, C. A., WEISS, A. S. & KIELTY, C. M. 2004. Molecular basis of elastic fiber formation. Critical interactions and a tropoelastin-fibrillin-1 cross-link. *J Biol Chem,* 279**,** 23748-58.

ROMERE, C., DUERRSCHMID, C., BOURNAT, J., CONSTABLE, P., JAIN, M., XIA, F., SAHA, P. K., DEL SOLAR, M., ZHU, B., YORK, B., SARKAR, P., RENDON, D. A., GABER, M. W., LEMAIRE, S. A., COSELLI, J. S., MILEWICZ, D. M., SUTTON, V. R., BUTTE, N. F., MOORE, D. D. & CHOPRA, A. R. 2016. Asprosin, a Fasting-Induced Glucogenic Protein Hormone. *Cell,* 165**,** 566-79.

ROSS, R., FIALKOW, R. J. & ALTMAN, L. K. 1977. The morphogenesis of elastic fibers. *Adv Exp Med Biol,* 79**,** 7-17.

ROZARIO, T. & DESIMONE, D. W. 2010. The extracellular matrix in development and morphogenesis: a dynamic view. *Dev Biol,* 341**,** 126-40.

SAHARINEN, J., HYYTIAINEN, M., TAIPALE, J. & KESKI-OJA, J. 1999. Latent transforming growth factor-beta binding proteins (LTBPs)--structural extracellular matrix proteins for targeting TGF-beta action. *Cytokine Growth Factor Rev,* 10**,** 99-117.

SAHARINEN, J. & KESKI-OJA, J. 2000. Specific sequence motif of 8-Cys repeats of TGF-beta binding proteins, LTBPs, creates a hydrophobic interaction surface for binding of small latent TGF-beta. *Mol Biol Cell,* 11**,** 2691-704.

SAHARINEN, J., TAIPALE, J. & KESKI-OJA, J. 1996. Association of the small latent transforming growth factor-beta with an eight cysteine repeat of its binding protein LTBP-1. *EMBO J,* 15**,** 245-53.

SAHARINEN, J., TAIPALE, J., MONNI, O. & KESKI-OJA, J. 1998. Identification and characterization of a new latent transforming growth factor-beta-binding protein, LTBP-4. *J Biol Chem,* 273**,** 18459-69.

SANDERS, M., MCPARTLIN, D., MORAN, K., GUO, Y., EECKHOUT, M., O'KENNEDY, R., DE SAEGER, S. & MARAGOS, C. 2016. Comparison of Enzyme-Linked Immunosorbent Assay, Surface Plasmon Resonance and Biolayer Interferometry for Screening of Deoxynivalenol in Wheat and Wheat Dust. *Toxins (Basel),* 8**,** 103.

SCHAEFER, L. & SCHAEFER, R. M. 2010. Proteoglycans: from structural compounds to signaling molecules. *Cell Tissue Res,* 339**,** 237-46.

SCHRIJVER, I., LIU, W., BRENN, T., FURTHMAYR, H. & FRANCKE, U. 1999. Cysteine substitutions in epidermal growth factor-like domains of fibrillin-1: distinct effects on biochemical and clinical phenotypes. *Am J Hum Genet,* 65**,** 1007-20.

SCHUCK, P. 2000. Size-distribution analysis of macromolecules by sedimentation velocity ultracentrifugation and lamm equation modeling. *Biophys J,* 78**,** 1606-19.

SHIBAHARA, K., OTA, M., HORIGUCHI, M., YOSHINAGA, K., MELAMED, J. & RIFKIN, D. B. 2013. Production of gastrointestinal tumors in mice by modulating latent TGF-beta1 activation. *Cancer Res,* 73**,** 459-68.

SIEGEL, R. C., PINNELL, S. R. & MARTIN, G. R. 1970. Cross-linking of collagen and elastin. Properties of lysyl oxidase. *Biochemistry,* 9**,** 4486-92.

SIMON DAVIS, D. A. & PARISH, C. R. 2013. Heparan sulfate: a ubiquitous glycosaminoglycan with multiple roles in immunity. *Front Immunol,* 4**,** 470.

SMALLRIDGE, R. S., WHITEMAN, P., WERNER, J. M., CAMPBELL, I. D., HANDFORD, P. A. & DOWNING, A. K. 2003. Solution structure and dynamics of a calcium binding epidermal growth factor-like domain pair from the neonatal region of human fibrillin-1. *J Biol Chem,* 278**,** 12199-206.

SMITH, M. L., GOURDON, D., LITTLE, W. C., KUBOW, K. E., EGUILUZ, R. A., LUNA-MORRIS, S. & VOGEL, V. 2007. Force-induced unfolding of fibronectin in the extracellular matrix of living cells. *PLoS Biol,* 5**,** e268.

SOUTO, D. E. P., VOLPE, J., GONÇALVES, C. D. C., RAMOS, C. H. I. & KUBOTA, L. T. 2019. A brief review on the strategy of developing SPR-based biosensors for application to the diagnosis of neglected tropical diseases. *TAL Talanta,* 205**,** 2019-12.

SREERAMA, N. & WOODY, R. W. 2000. Estimation of protein secondary structure from circular dichroism spectra: comparison of CONTIN, SELCON, and CDSSTR methods with an expanded reference set. *Anal Biochem,* 287**,** 252-60.

STEER, R. 2014. *Investigations of the extracellular deposition of latent TGF-beta binding protein-1 (LTBP-1)* (PhD Thesis). Retrieved from

STERNER-KOCK, A., THOREY, I. S., KOLI, K., WEMPE, F., OTTE, J., BANGSOW, T., KUHLMEIER, K., KIRCHNER, T., JIN, S., KESKI-OJA, J. & VON MELCHNER, H. 2002. Disruption of the gene encoding the latent transforming growth factor-beta binding protein 4 (LTBP-4) causes abnormal lung development, cardiomyopathy, and colorectal cancer. *Genes Dev,* 16**,** 2264-73.

SU, C. T., HUANG, J. W., CHIANG, C. K., LAWRENCE, E. C., LEVINE, K. L., DABOVIC, B., JUNG, C., DAVIS, E. C., MADAN-KHETARPAL, S. & URBAN, Z. 2015. Latent transforming growth factor beta-binding proteins and fibulins compete for fibrillin-1 and exhibit exquisite specificities in binding sites. *Hum Mol Genet,* 24**,** 4024-36.

SUN, T., REID, F., LIU, Y., CAO, Y., ESTEP, P., NAUMAN, C. & XU, Y. 2013. High throughput detection of antibody self-interaction by bio-layer interferometry. *MAbs,* 5**,** 838-41.

SVERGUN, D. I. 1999. Restoring low resolution structure of biological macromolecules from solution scattering using simulated annealing. *Biophys J,* 76**,** 2879-86.

SVERGUN, D. I., PETOUKHOV, M. V. & KOCH, M. H. 2001. Determination of domain structure of proteins from X-ray solution scattering. *Biophys J,* 80**,** 2946-53.

SVERGUN, V. V. V. A. D. I. 2003. Uniqueness of ab-initio shape determination in small-angle scattering. *J. Appl. Cryst.,* 36**,** 860-864.

THOMSON, J., SINGH, M., ECKERSLEY, A., CAIN, S. A., SHERRATT, M. J. & BALDOCK, C. 2019. Fibrillin microfibrils and elastic fibre proteins: Functional interactions and extracellular regulation of growth factors. *Semin Cell Dev Biol,* 89**,** 109-117.

TIMMER, D. E. M. L., BROEKHUIJSEN, V. A. N. H. D. M., OLDHOFF, J. M., DB, D. E. G., SIGURDSSON, V. & PASMANS, S. G. 2009. Acquired cutis laxa in childhood Sweet's syndrome. *Pediatr Dermatol,* 26**,** 358-60.

TODOROVIC, V., FRENDEWEY, D., GUTSTEIN, D. E., CHEN, Y., FREYER, L., FINNEGAN, E., LIU, F., MURPHY, A., VALENZUELA, D., YANCOPOULOS, G. & RIFKIN, D. B. 2007. Long form of latent TGF-beta binding protein 1 (Ltbp1L) is essential for cardiac outflow tract septation and remodeling. *Development,* 134**,** 3723-32.

TODOROVIC, V., JURUKOVSKI, V., CHEN, Y., FONTANA, L., DABOVIC, B. & RIFKIN, D. B. 2005. Latent TGF-beta binding proteins. *Int J Biochem Cell Biol,* 37**,** 38-41.

TODOROVIC, V. & RIFKIN, D. B. 2012. LTBPs, more than just an escort service. *J Cell Biochem,* 113**,** 410-8.

TROILO, H., STEER, R., COLLINS, R. F., KIELTY, C. M. & BALDOCK, C. 2016. Independent multimerization of Latent TGFβ Binding Protein-1 stabilized by cross-linking and enhanced by heparan sulfate. *Scientific Reports,* 6**,** 34347.

TROILO, H., ZUK, A. V., TUNNICLIFFE, R. B., WOHL, A. P., BERRY, R., COLLINS, R. F., JOWITT, T. A., SENGLE, G. & BALDOCK, C. 2014. Nanoscale structure of the BMP antagonist chordin supports cooperative BMP binding. *Proc Natl Acad Sci U S A,* 111**,** 13063-8.

TUUKKANEN, A. T., SPILOTROS, A. & SVERGUN, D. I. 2017. Progress in small-angle scattering from biological solutions at high-brilliance synchrotrons. *IUCrJ,* 4**,** 518-528.

UITTO, J., CHRISTIANO, A. M., KÄHÄRI, V.-M., BASHIR, M. M. & ROSENBLOOM, J. 1991. Molecular biology and pathology of human elastin. *Biochemical Society Transactions,* 19**,** 824-829.

UITTO, J., LI, Q. & URBAN, Z. 2013. The complexity of elastic fibre biogenesis in the skin--a perspective to the clinical heterogeneity of cutis laxa. *Exp Dermatol,* 22**,** 88-92.

URBAN, Z., HUCTHAGOWDER, V., SCHURMANN, N., TODOROVIC, V., ZILBERBERG, L., CHOI, J., SENS, C., BROWN, C. W., CLARK, R. D., HOLLAND, K. E., MARBLE, M., SAKAI, L. Y., DABOVIC, B., RIFKIN, D. B. & DAVIS, E. C. 2009. Mutations in LTBP4 cause a syndrome of impaired pulmonary, gastrointestinal, genitourinary, musculoskeletal, and dermal development. *Am J Hum Genet,* 85**,** 593-605.

UVERSKY, V. N. & DUNKER, A. K. 2010. Understanding protein non-folding. *Biochim Biophys Acta,* 1804**,** 1231-64.

VAN DAMME, T., GARDEITCHIK, T., MOHAMED, M., GUERRERO-CASTILLO, S., FREISINGER, P., GUILLEMYN, B., KARIMINEJAD, A., DALLOYAUX, D., VAN KRAAIJ, S., LEFEBER, D. J., SYX, D., STEYAERT, W., DE RYCKE, R., HOISCHEN, A., KAMSTEEG, E. J., WONG, S. Y., VAN SCHERPENZEEL, M., JAMALI, P., BRANDT, U., NIJTMANS, L., KORENKE, G. C., CHUNG, B. H. Y., MAK, C. C. Y., HAUSSER, I., KORNAK, U., FISCHER-ZIRNSAK, B., STROM, T. M., MEITINGER, T., ALANAY, Y., UTINE, G. E., LEUNG, P. K. C., GHADERI-SOHI, S., COUCKE, P., SYMOENS, S., DE PAEPE, A., THIEL, C., HAACK, T. B., MALFAIT, F., MORAVA, E., CALLEWAERT, B. & WEVERS, R. A. 2017. Mutations in ATP6V1E1 or ATP6V1A Cause Autosomal-Recessive Cutis Laxa. *Am J Hum Genet,* 100**,** 216-227.

VEHVILAINEN, P., HYYTIAINEN, M. & KESKI-OJA, J. 2003. Latent transforming growth factor-beta-binding protein 2 is an adhesion protein for melanoma cells. *J Biol Chem,* 278**,** 24705-13.

VENYAMINOV, S., BAIKALOV, I. A., SHEN, Z. M., WU, C. S. & YANG, J. T. 1993. Circular dichroic analysis of denatured proteins: inclusion of denatured proteins in the reference set. *Anal Biochem,* 214**,** 17-24.

WAGENSEIL, J. E. & MECHAM, R. P. 2007. New insights into elastic fiber assembly. *Birth Defects Res C Embryo Today,* 81**,** 229-40.

WALTON, K. L., MAKANJI, Y., CHEN, J., WILCE, M. C., CHAN, K. L., ROBERTSON, D. M. & HARRISON, C. A. 2010. Two distinct regions of latency-associated peptide coordinate stability of the latent transforming growth factor-beta1 complex. *J Biol Chem,* 285**,** 17029-37.

WANG, D. S. & FAN, S. K. 2016. Microfluidic Surface Plasmon Resonance Sensors: From Principles to Point-of-Care Applications. *Sensors (Basel),* 16.

WEISS, A. & ATTISANO, L. 2013. The TGFbeta superfamily signaling pathway. *Wiley Interdiscip Rev Dev Biol,* 2**,** 47-63.

WIERZBICKA-PATYNOWSKI, I. & SCHWARZBAUER, J. E. 2003. The ins and outs of fibronectin matrix assembly. *J Cell Sci,* 116**,** 3269-76.

WILLIAMS, J. W., VAN HOLDE, K. E., BALDWIN, R. L. & FUJITA, H. 1958. The Theory Of Sedimentation Analysis. *Chem. Rev. Chemical Reviews,* 58**,** 715-744.

YIN, W., SMILEY, E., GERMILLER, J., MECHAM, R. P., FLORER, J. B., WENSTRUP, R. J. & BONADIO, J. 1995. Isolation of a novel latent transforming growth factor-beta binding protein gene (LTBP-3). *J Biol Chem,* 270**,** 10147-60.

YOSHINAGA, K., OBATA, H., JURUKOVSKI, V., MAZZIERI, R., CHEN, Y., ZILBERBERG, L., HUSO, D., MELAMED, J., PRIJATELJ, P., TODOROVIC, V., DABOVIC, B. & RIFKIN, D. B. 2008. Perturbation of transforming growth factor (TGF)-beta1 association with latent TGF-beta binding protein yields inflammation and tumors. *Proc Natl Acad Sci U S A,* 105**,** 18758-63.

YUAN, X., DOWNING, A. K., KNOTT, V. & HANDFORD, P. A. 1997. Solution structure of the transforming growth factor beta-binding protein-like module, a domain associated with matrix fibrils. *EMBO J,* 16**,** 6659-66.

ZILBERBERG, L., TODOROVIC, V., DABOVIC, B., HORIGUCHI, M., COUROUSSE, T., SAKAI, L. Y. & RIFKIN, D. B. 2012. Specificity of latent TGF-beta binding protein (LTBP) incorporation into matrix: role of fibrillins and fibronectin. *J Cell Physiol,* 227**,** 3828-36.

7. Appendix 1

The role of fibrillin and microfibril binding proteins in elastin and elastic fibre assembly

Appendix 1: The role of fibrillin and microfibril binding proteins in elastin and elastic fibre assembly

Status: Published

Authors: Alan R.F. Godwin, Mukti Singh, Michael P. Lockhart-Cairns, Yasmene F. Alanazi, Stuart A. Cain and Clair Baldock

Affiliations:

Wellcome Centre for Cell-Matrix Research, Division of Cell-Matrix Biology and Regenerative Medicine, School of Biological Sciences, Faculty of Biology, Medicine and Health, University of Manchester, Manchester Academic Health Science Centre, Manchester M13 9PT, UK

Contribution: These authors contributed equally.

I contributed to an invited review and wrote part of sections (LTBPs in elastic fibre assembly) and (Fibulin-4 and Fibulin-5 in elastogenesis).

ARTICLE IN PRESS

Review

MATBIO-1574; No. of pages: 14; 4C:

The role of fibrillin and microfibril binding proteins in elastin and elastic fibre assembly

Alan R.F. Godwin, Mukti Singh, Michael P. Lockhart-Cairns, Yasmene F. Alanazi, Stuart A. Cain and Clair Baldock

Wellcome Centre for Cell-Matrix Research, Division of Cell-Matrix Biology and Regenerative Medicine, School of Biological Sciences, Faculty of Biology, Medicine and Health, University of Manchester, Manchester Academic Health Science Centre, Manchester M13 9PT, UK

Correspondence to Stuart A. Cain and Clair Baldock: *stuart.a.cain@manchester.ac.uk.*
https://doi.org/10.1016/j.matbio.2019.06.006

Abstract

Fibrillin is a large evolutionarily ancient extracellular glycoprotein that assembles to form beaded microfibrils which are essential components of most extracellular matrices. Fibrillin microfibrils have specific biomechanical properties to endow animal tissues with limited elasticity, a fundamental feature of the durable function of large blood vessels, skin and lungs. They also form a template for elastin deposition and provide a platform for microfibril-elastin binding proteins to interact in elastic fibre assembly. In addition to their structural role, fibrillin microfibrils mediate cell signalling via integrin and syndecan receptors, and microfibrils sequester transforming growth factor (TGF)β family growth factors within the matrix to provide a tissue store which is critical for homeostasis and remodelling.

Introduction

Elastic fibres are essential components of all mammalian elastic tissues such as blood vessels, lung, joints and skin. The main components of elastic fibres are elastin and fibrillin, however an array of other matrix proteins are required for their correct assembly and function [1,2]. Elastic fibre proteins are critically important in the development and homeostasis of elastic tissues both in terms of their key roles in linking cells and matrix macromolecules [3] and in the extracellular regulation of TGFβ family member growth factors [4]. Fibrillin assembles to form beaded microfibrils [5] and the formation of elastic fibres requires a fibrillin microfibril scaffold for the correct deposition of elastin. Fibrillin also interacts with other elastic fibre proteins including the fibulins and latent TGFβ binding proteins to support elastic fibre assembly and function. In this review, we will describe our understanding of the function of fibrillin and fibrillin microfibrils, focusing on its structure, assembly and interaction with other elastic fibre proteins as well as their functional role in elastogenesis.

Fibrillin microfibrils

Fibrillin domain structure

The fibrillin superfamily family is composed of three fibrillin isoforms, fibrillin1–3, each encoded by a separate gene [6–9], and the related extracellular matrix (ECM) proteins the latent transforming growth factor (TGF)β binding proteins (LTBPs)1–4 (Fig. 1). The domain structure of the fibrillin superfamily consists primarily of arrays of epidermal growth factor-like (EGF) domains interspersed with TGFβ-binding like (TB) domains and hybrid domains [6]. The three fibrillin isoforms are highly homologous to each other with differences including a proline rich

Please cite this article as: A. R.F. Godwin, M. Singh, M. P. Lockhart-Cairns, et al., The role of fibrillin and microfibril binding proteins in elastin and elastic fibre assembly, Matrix Biology, https://doi.org/10.1016/j.matbio.2019.06.006

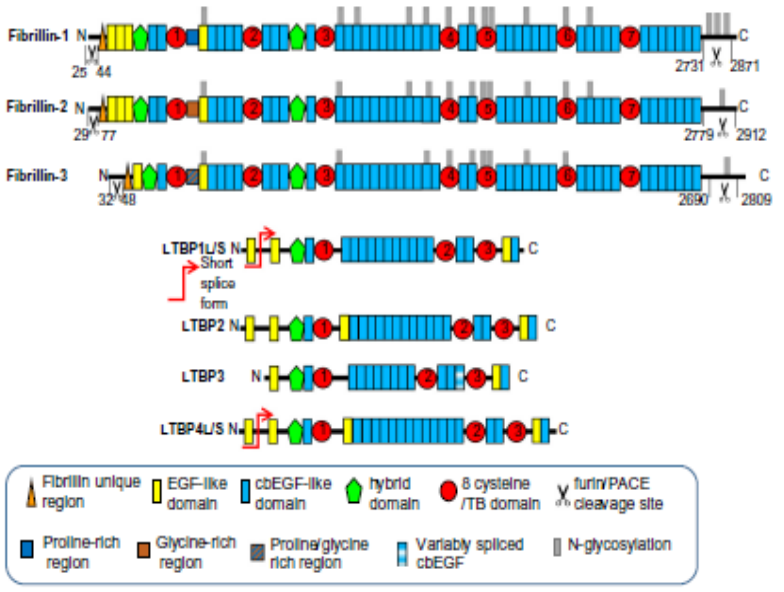

Fig. 1. Cartoon representation of the domain structures of the fibrillin superfamily members including fibrillins1–3 and LTBPs1–4.

region in fibrillin-1 which in fibrillin-2 is glycine rich and in fibrillin-3 is proline and glycine rich. Of the 47 EGF domains in fibrillin, 43 are calcium binding (cb) [6]. There are seven TB domains (also referred to as 8 cysteine domains) which are unique to the fibrillin superfamily. They have a globular structure [10,11] and domain TB4 contains an RGD motif which is involved in binding to $\alpha_5\beta_1$ $\alpha_v\beta_3$ and $\alpha_v\beta_6$ integrins and essential for the interaction between fibrillin-1 and the cell surface [12–15]. Hybrid domains have structural similarity to both EGF and TB domains [6,16,17] and there are two hybrid domains in fibrillin. The fibrillins have unique N- and C-termini which are both proteolytically processed by furin, essential for the assembly of fibrillin into microfibrils [18–20]. The processed C-terminal peptide, also known as asprosin, has been shown to be involved in glucose release from the liver [21]. The fibrillins undergo several other post translation modifications, fibrillin-1 has 14 predicted glycosylation sites and there are 12 sites in fibrillin-2 and 10 sites in fibrillin-3. Fibrillin-1 can also be phosphorylated at serine 2702 by FAM20C [22] but the function of phosphorylation has not yet been investigated.

Supramolecular organisation into microfibrils

Fibrillin microfibrils are beaded filaments with ~56 nm periodicity mainly composed of fibrillin molecules [23]. The microfibrils are polar polymers which linearly assemble through interaction between the N- and C-termini of adjacent fibrillin molecules [24]. Lateral association also occurs and is driven by homotypic interaction between the termini to form microfibrils [25–27]. Scanning transmission electron microscopy (STEM) mass mapping has shown that microfibrils have a mass of ~2500 kDa per repeat [28] which is consistent with 8 fibrillin molecules in cross section which is supported by 3D reconstructions [29] and 2D images of microfibrils viewed in cross section [30,31]. After linear and lateral assembly, microfibrils are then further stabilised by the formation of transglutaminase cross links between their N- and C-termini [32].

Fibrillin microfibrils are flexible and have a hollow cylindrical appearance when visualised in three dimensions by electron microscopy with single particle image analysis, this is consistent with tube-like structures observed using quick freeze deep etch electron microscopy [29,33]. The microfibril can be described by three distinct regions based on their banding pattern, these have been termed the bead, arms and interbead regions [34,35] (Fig. 2). The

Please cite this article as: A. R.F. Godwin, M. Singh, M. P. Lockhart-Cairns, et al., The role of fibrillin and microfibril binding proteins in elastin and elastic fibre assembly, Matrix Biology, https://doi.org/10.1016/j.matbio.2019.06.006

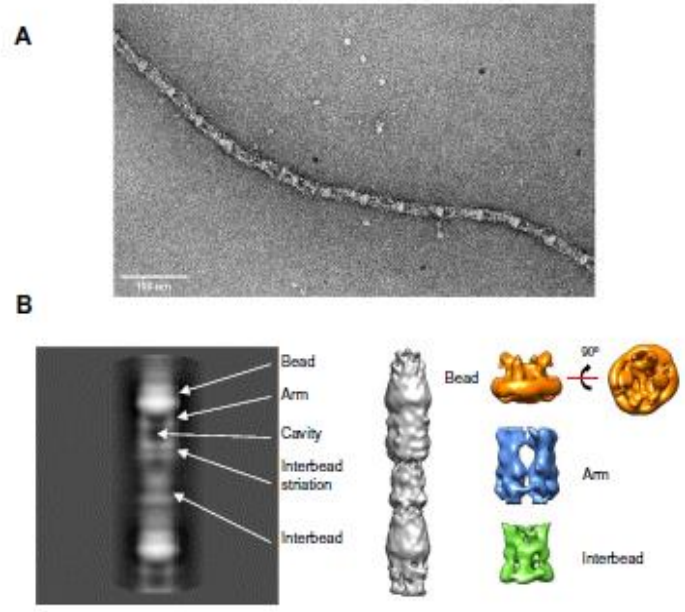

Fig. 2. (A) Negative stain transmission electron microscopy (TEM) image of a microfibril extracted from bovine ciliary zonule tissue. Scale bar = 100 nm. (B) The left panel shows an aligned single particle average of a fibrillin microfibril repeat. Box size = 102 × 102 nm. In grey is a 3D reconstruction of a fibrillin microfibril. Separate reconstructions of the bead, arm and interbead regions of the microfibril are shown.

microfibril bead region has a dense interwoven core surrounded by a ring structure which forms four arms which combine into the denser interbead region [29]. The bead region contains the N- and C-termini of the fibrillin molecules [24,153]. The microfibril is pseudo-symmetrical, supporting models that describe eight fibrillin molecules in cross-section [29,31]. Extracted microfibrils have a 56 nm repeating periodicity [34], similar to the 50–60 nm periodicity measured in tissues and can reversibly extend to ~80 nm [36,37]. Microfibril diameter is typically ~20 nm and does not vary from tissue to tissue [35] suggesting that this is carefully controlled during assembly, either limited by the packing of fibrillin molecules or by microfibril associated binding proteins.

How fibrillin molecules are organised into mature microfibrils however is still unclear. Extracted and recombinant fibrillin molecules have a length of ~148 nm [5,25] which does not reconcile readily with the periodicity of 56 nm seen for mature microfibrils. Therefore, several models of molecular organisation have been proposed which fall into two categories: the molecular folding model where a single molecule spans one 56 nm repeat [38,154] and staggered models where the fibrillin molecules are staggered by a half or a third and span two or three repeats [11,39]. Both packing models can explain antibody localisation of fibrillin regions within the microfibril, therefore higher resolution imaging or further labelling is required to provide resolution of the microfibril structure.

Microfibril assembly

Role of Heparan Sulphate in microfibril assembly

Although the precise mechanism of microfibril assembly is not fully understood, there is considerable evidence supporting the molecular and cellular interactions involved. Microfibril assembly consists of multimerization of the fibrillin molecules, deposition into the ECM, then recruitment of other microfibrillar components such as elastin and MAGP-1. It has been demonstrated that fibrillin monomers can multimerize by interactions between

Please cite this article as: A. R.F. Godwin, M. Singh, M. P. Lockhart-Cairns, et al., The role of fibrillin and microfibril binding proteins in elastin and elastic fibre assembly, Matrix Biology, https://doi.org/10.1016/j.matbio.2019.06.006

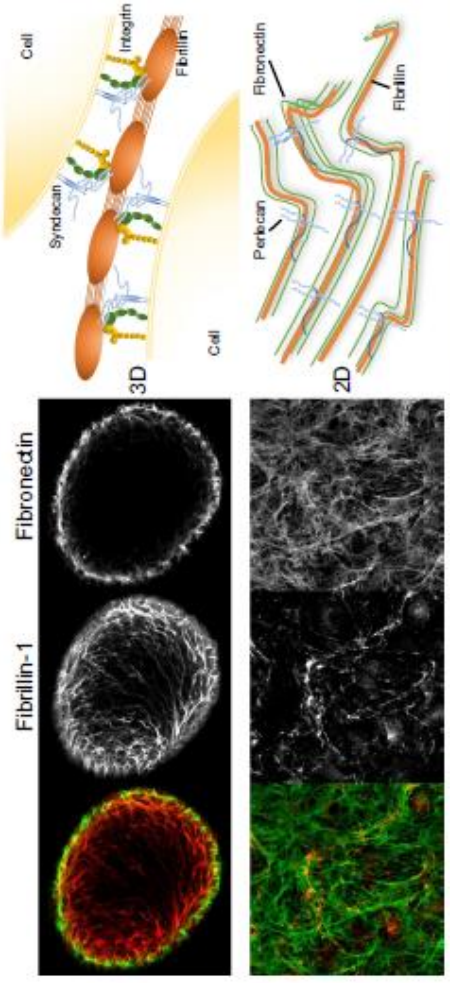

Fig. 3. Fibrillin deposition in 3D and 2D cell cultures. Human dermal fibroblasts were cultured in either non-adherent U bottom wells (top) or on glass coverslips (bottom) for 6 days. Fibrillin deposition (red) is seen throughout the whole spheroid, while fibronectin (green) is primarily on the outer cell layers. In comparison, fibrillin is entirely colocalised with fibronectin in cells in 2D culture. Also shown, in the right handside panel, are schematic diagrams illustrating fibrillin interactions with cell surface receptors, such as integrins and HS containing proteoglycans such as surface bound syndecans and ECM bound perlecan, in 3D (top) and 2D cultures (bottom). (For interpretation of the references to colour in this figure legend, the reader is referred to the web version of this article.)

Please cite this article as: A. R.F. Godwin, M. Singh, M. P. Lockhart-Cairns, et al., The role of fibrillin and microfibril binding proteins in elastin and elastic fibre assembly, Matrix Biology, https://doi.org/10.1016/j.matbio.2019.06.006

the N- and C-termini, as well as N – N and C – C interactions [25,26,40,41], also the interaction strength is increased between multimers of N- and C-terminal fragments [27]. Fibrillin expression and secretion alone is not sufficient to support microfibril formation, as demonstrated with fibrillin expressing HEK293 cells which have to be co-cultured with fibroblasts for matrix fibrillin microfibril deposition [42]. Other ECM molecules or specific cellular interactions are also required.

A key driver of microfibril assembly is interaction with Heparan Sulphate (HS). Heparan sulphate proteoglycans have a key role in the elastic fibre interactome [43], and HS has a strong interaction with fibrillin-1 at several sites [44–46]. HS has the ability to promote multimerization of fibrillin molecules prior to furin cleavage of newly secreted fibrillin [44,47] and fibrillin multimers also bind HS more strongly [48]. At higher concentrations, addition of heparin/HS is known to inhibit microfibril deposition [45,46,49]. HS is available through post-translational modifications on both membrane bound receptors, such as syndecans and glypicans, and non-membrane bound ECM molecules such as perlecan and agrin, where the interaction with perlecan and fibrillin-1 is via both HS and non-HS perlecan domains [50].

Requirement for fibronectin for microfibril assembly

Interactions with HS containing syndecans in conjunction with integrin binding of the RGD containing TB4 domain of fibrillin both influence fibrillin assembly. The fibrillin-1 RGD region primarily interacts with integrin α5β1 on fibroblasts but interactions with integrin αvβ3 were seen on other cell types [12], and it has been found that only fibrillin-1 fragments containing the RGD sequence support cell adhesion, for a variety different cell types including mesenchymal stem cells, chondrocyte progenitors and induced pluripotent stem cells [51,52]. However, unlike fibronectin, fibrillin does not need integrin mediated cell adhesion to assemble if fibronectin is also present [42]. Fibrillin microfibrils precede the evolution of the RGD site by 500 million years [53], indicating that the RGD site is not needed for microfibril assembly in invertebrates. The RGD site, integrins and fibronectin are only seen in vertebrate biology, and mutations affecting the TB4 domain of fibrillin result in altered microfibril deposition causing stiff skin syndrome [54], which can be recapitulated in mice by mutating the RGD site to RGE [55], suggesting for vertebrate microfibril deposition other more complex factors are needed via integrin mediated cell signalling. Indeed, it has also been found that interactions with the RGD site of fibrillin-1 by fibroblasts, control the expression of over one hundred microRNAs, some of which regulate TGFβ signalling (including miR-503) and focal adhesion formation (including miR-612 and miR-3185) [56]. Ancestral Fibrillin also preceded elastin which first appeared in gnathostomes (jawed vertebrates), so fibrillin did not evolve to assemble elastin. However the evolution of elastin which also led to the appearance of closed circulatory systems [57,58], also coincided with the divergence of ancestral fibrillin to fibrillin-1 and fibrillin 2/3 [53], although this period of duplication also known as 2R resulted in a large number of genetic changes.

In mesenchymal cells such as fibroblasts, fibrillin is deposited on the fibronectin network, and knock-down of fibronectin results in perturbation of fibrillin deposition in 2D cell cultures [59,60]. However In 3D mesenchymal cell cultures, fibronectin is located almost entirely in the outer cell layers, whilst fibrillin both colocalises with fibronectin on the outer cell layers but is also abundantly deposited in the tightly cell packed inner volume [61]. This suggests that fibrillin deposition can switch between fibronectin directed or cell surface interaction directed depending on the extracellular environment (Fig. 3).

Close cellular contact is also seen in epithelial cells sheets, where fibronectin is not required but does enhance deposition. In retinal pigmented epithelial cells, syndecan 4 as well as integrins α5β1 or α8β1 are required for microfibril deposition, and fibronectin is not needed but does enhance deposition [62]. The same study showed inhibition of cadherin junctions also disrupted microfibril deposition in retinal pigmented epithelial cells, and was independent of fibronectin deposition, indicating that the close cell-cell contact is needed for this mode of fibrillin deposition. It has been proposed that HS-rich cell junctions promote microfibril assembly, where fibronectin is not available [63].

Role of ADAMTS and ADAMTSL proteins in microfibril assembly

Members of the A Disintegrin And Metalloprotease with Thrombospondin type-1 repeats (ADAMTS) and ADAMTS-Like (ADAMTSL) family have been implicated in fibrillin microfibril assembly which influences elastic fibre formation. ADAMTS10 co-localises with microfibrils and enhances their deposition in vitro [64]. It is required for focal adhesion formation via interactions with both heparan sulphate and fibronectin [65]. Contrary to this, ADAMTS6 depletes HS reducing the number of focal adhesion complexes, required for fibrillin-1 microfibril deposition [65]. Therefore, the modulatory effects of both ADAMTS6 and -10 on focal adhesions play a vital role in microfibril deposition and subsequent elastic fibre assembly. Mouse models with disruption to ADAMTS10 show an accumulation of fibrillin-2 microfibrils in various tissues suggesting fibrillin-2

Please cite this article as: A. R.F. Godwin, M. Singh, M. P. Lockhart-Cairns, et al., The role of fibrillin and microfibril binding proteins in elastin and elastic fibre assembly, Matrix Biology, https://doi.org/10.1016/j.matbio.2019.06.006

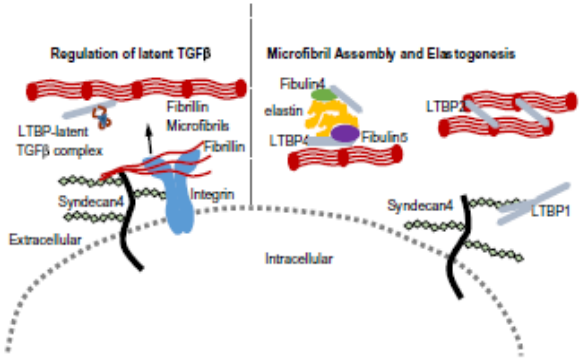

Fig. 4. Schematic diagram illustrating the dual roles of the LTBP family in TGFβ regulation and matrix assembly. Shown on the left, LTBP1, -3 and -4 form a large latent TGFβ complex which binds fibrillin to sequester TGFβ in the matrix. In TGFβ-independent mechanisms, shown on the right, LTBP1 can multimerize which is enhanced by HS (potentially on syndecans) and stabilised by TG2 cross-linking, LTBP2 stabilises fibrillin bundles and LTBP4 binds fibulin-4 and -5 to aid in deposition of elastin aggregates on fibrillin microfibrils in elastogenesis.

could be a substrate of ADAMTS10 [66,67]. ADAMTS17 co-localises with fibrillin-1, -2 and fibronectin fibres, binds to the N- and C-termini of fibrillin-2 but does not cleave either fibrillin-1 or -2 [68].

ADAMTS-Like proteins do not have catalytic activity but their interactions and localisation with fibrillin microfibrils support a regulatory role in microfibril formation and deposition. ADAMTSL2 binds to fibrillin-1 and the N-terminal binding site encompasses a fibrillin-1 mutation which results in Weill Marchesani Syndrome (WMS) [69]. ADAMTSL2 also binds to fibrillin-2 and deletion of ADAMTSL2 results in an accumulation of fibrillin-2 microfibrils [70]. ADAMTSL4 forms an independent fibrillar network which co-localises with fibrillin-1 microfibrils and enhances microfibril biogenesis [71,72]. Although interaction studies have demonstrated binding of ADAMTSL5 to fibrillin-1 and fibrillin-2, as well as its co-localisation with microfibrils, there is no evidence of ADAMTSL5 having a direct role in microfibril assembly [73]. On the other hand, ADAMTSL6α and -β variants promote fibrillin-1 microfibril biogenesis and localise with fibrillin-1 microfibrils in elastic and non-elastic tissues [74].

Tissue assembly of fibrillin microfibrils

In tissues, fibrillin microfibrils are organised into larger tissue specific structures which are important for the mechanical properties of that tissue. In the reticular dermis of skin, fibrillin-1 is formed into thick horizontally arranged elastic fibres which are connected to the dermal-epidermal junction through perpendicularly arranged bundles of microfibrils called elaunin and oxytalan fibres [75]. In normal skin, fibrillin-2 is only detected at the dermal-epidermal-junction and in vessel walls but has increased expression in wound healing [76]. In the lung, elastic fibres form branched networks which surround the alveoli allowing for elastic recoil during breathing and in the medial layer of the aorta, elastic fibres form sheets which surround layers of smooth muscle cells. In the ciliary zonule of the eye, microfibrils are found in the absence of elastin, here they bundle together to form ciliary zonule fibres. These fibres then form larger bundles which span between the ciliary body and the lens and deform the lens during accommodation. The large bundles of ciliary zonule fibres are held together by perpendicularly arranged ciliary zonule fibres which wrap around their circumference [29,77]. Microfibrils in the ciliary zonule are connected via bridging complexes [29,33], two candidates proteins for this role are ADAMTSL4 [78] and LTBP2 [79] which when absent result in ciliary zonule disruption.

Role of fibrillin in elastogenesis

Developmental expression of fibrillin and tropoelastin

In elastic tissues, elastic fibre assembly commences during early gestation with the expression and deposition of fibrillin microfibrils. In humans, fibrillin-1, -2 and -3 are expressed during development [80]; however, fibrillin-1 expression is the most abundant and dominates from late morphogenesis

Please cite this article as: A. R.F. Godwin, M. Singh, M. P. Lockhart-Cairns, et al., The role of fibrillin and microfibril binding proteins in elastin and elastic fibre assembly, Matrix Biology, https://doi.org/10.1016/j.matbio.2019.06.006

to adult life [81]. Moreover, proteomic data show that fibrillin isoform expression is both species and tissue dependent [82,83]. Fibrillin-3 is predominantly expressed in developing tissues, but the fibrillin-3 gene is disrupted in mice, so may be less important in mammals [8]. In developing elastic and non-elastic tissues, fibrillin-1 and -2 co-express and co-assemble in the matrix [84] and the requirement for both fibrillin-1 and fibrillin-2 isoforms has been demonstrated by a double knockout mouse model with early embryonic lethality [85]. Fibrillin microfibril deposition in developing elastic tissues precedes the expression of the elastin precursor, tropoelastin. Tropoelastin is highly expressed during embryogenesis, in comparison to the low levels detected in adult tissues [86–88].

The role of fibrillin in elastic fibre assembly

The assembly of elastic fibres in the ECM is a highly organised and multifaceted process requiring the expression and contribution of several ECM proteins.

The amorphous core of insoluble elastic fibres is comprised of cross-linked tropoelastin, glycosaminoglycans such as HS [89] and proteoglycans such a biglycan [90] deposited on a scaffold of co-assembled fibrillin-1 and -2 microfibrils [3]. Tropoelastin secretion is aided by elastin binding protein, an inactive splice variant of β-galactosidase [91], where C-terminal interactions with cell surface heparan and chondroitin sulphates mediate the coacervation of tropoelastin into larger dense globules [92,93]. Interactions between the hydrophobic regions of individual monomers results in the alignment of lysine residues that are enzymatically cross-linked by lysyl oxidase (LOX) and LOX-like 1 (LOXL1) to form larger aggregates [94–96]. Recently, we have shown that LOXL2 interacts with tropoelastin and LOXL2 catalyses the deamination of tropoelastin resulting in cross-linked tropoelastin peptides. The elastin-like material generated by LOXL2 was resistant to trypsin proteolysis and displayed mechanical properties similar to mature elastin. As LOXL2 co-distributes with elastin in the vascular wall this suggests that LOXL2 could participate in elastogenesis in vivo [97].

Once cross-linked, tropoelastin aggregates interact with co-assembled fibrillin-1 and -2 microfibrils near the cell surface via defined interactive domains. Tropoelastin interacts with microfibril associated glycoprotein-1 (MAGP1) [98,99] and MAGP1 interacts with the N-terminal region of fibrillin-1, suggesting tethering of tropoelastin to microfibrils [98,100]. A similar role for microfibrillar-associated protein 4 (MFAP4) is likely as it also binds to fibrillin and tropoelastin and promotes tropoelastin assembly [101]. Tropoelastin also directly interacts with the N-terminal region of fibrillin-1 via the TB2 domain and a covalent cross-link between tropoelastin and fibrillin is formed by transglutaminase-2 (TG2) [100,102]. The cross-link between the fibrillin TB2 domain and tropoelastin was mapped to residues Q669 in fibrillin and K38 in domain 4 of tropoelastin and addition of this region of fibrillin enhanced the coacervation of tropoelastin [103]. There is also a second high affinity binding site in the central region of fibrillin-1 encompassing the TB3 domain [102]. The initial deposition of tropoelastin aggregates onto fibrillin microfibrils is believed to be the primary step required for further coacervation and an augmentation of tropoelastin globule recruitment to form larger elastic fibres [103]. Once deposited on to fibrillin microfibrils, the tropoelastin aggregates coalesce to form stable, insoluble elastic fibres.

Microfibril binding proteins that facilitate elastogenesis

LTBPs in elastic fibre assembly

The LTBPs are extracellular glycoproteins in the fibrillin superfamily with similar modular domain structure [104–107]. There are four LTBPs with LTBP1, -3 and -4 having important roles in the processing and secretion of TGFβ [108]. LTBP2 does not interact with TGFβ [109], but has a role in stabilising fibrillin microfibril bundles in the eye [79]. Indeed, dual functionalities have been proposed for members of the LTBP family, in either secretion of TGFβ or microfibril assembly and elastogenesis [110] (Fig. 4). LTBP1 has both long and short isoforms generated by alternate splicing at the N-terminus [111,112], as does LTBP4 [107,113]. Both LTBP2 and -4 have been implicated in the formation of elastic fibres in elastogenesis and LTBP2 and -4 have some commonalities in their functional roles, as LTBP4 can compensate for LTBP2 in some tissues [114]. However, even though LTBP3 and -4 are both expressed in the lung, they can only partially compensate for each other in lung development suggesting that the LTBP family have only some over-lapping functions [115].

Fibrillin is required for the deposition of LTBP2, -3 and -4 [116] but LTBP1 can be assembled in the absence of fibrillin [116]. In contrast, LTBP1 requires fibronectin for its deposition [116,117] and interacts with fibronectin [118]. Binding of LTBP1 to fibulin-4 may act as an additional mediator for fibrillin microfibril association [49,119]. The C-terminal region of LTBP1, -2 and -4 binds to fibrillin [120,121] but an equivalent region of LTBP3 does not interact with fibrillin [120] despite fibrillin being required for its deposition. LTBP1, -2 and -4 bind HS [122–124], suggesting they may interaction with HS proteoglycans (HSPGs) such as syndecans.

Please cite this article as: A. R.F. Godwin, M. Singh, M. P. Lockhart-Cairns, et al., The role of fibrillin and microfibril binding proteins in elastin and elastic fibre assembly, Matrix Biology, https://doi.org/10.1016/j.matbio.2019.06.006

LTBP1 is a substrate for transglutaminase type II (TG2) and can be cross-linked into the matrix to enhance latency of the latent TGFβ complex [125,126]. Our recent study showed that both the N- and C-terminus of LTBP1 are substrates for TG2 and intermolecular N – N and N – C cross-links can form [122]. Oligomerisation of LTBP1 can occur in the absence of other proteins and is calcium dependent. LTBP1 multimerization is promoted by HS and stabilised by TG2 crosslinking suggesting a mechanism whereby LTBP1 filaments could support the bridging of fibrillin microfibrils to the matrix.

LTBP2 colocalises with elastic fibres and the deposition of LTBP2 into the matrix is dependent on the presence of a preformed fibrillin-1 network as fibrillin-1 knockdown disrupts LTBP2 deposition [127,128]. LTBP2 has been suggested to regulate elastic fibre formation in a fibrillin-independent manner via fibulin-5, and can compete for the fibulin-5 tropoelastin interaction potentially displacing elastin assemblies in elastogenesis [129,130]. LTBP3 is expressed in heart, skeletal muscle, prostate and ovaries [131] with interactions with fibrillin-1 important for matrix incorporation [116], although colocalisation of LTBP3 has been shown with fibronectin [118]. Secretion of LTBP3 requires co-expression with TGFβ and is dependent on binding to LAP [131,132].

Several studies have investigated the elastogenic role of LTBP4 where a dual functionality for LTBP4 has been proposed as a regulator of either elastic fibre assembly or TGFβ levels in lung [110,133]. LTBP4 is important in elastic fibre assembly with LTBP4 mutations resulting in Urban-Rifkin-Davis Syndrome (URDS) also known as autosomal recessive cutis laxa type 1C [134] which is replicated in knockout mouse models [135,136]. A lack of LTBP4 results in abnormal distribution and formation of elastic fibres [134,136]. Fibroblasts from URDS patients show increased TGFβ activity [134], consistent with data from *LTBP4*$^{-/-}$ mice [135,137]. However, reducing the level of TGFβ does not normalize elastogenesis indicating that LTBP4 has a dual functionality in regulating both elastogenesis and TGFβ signalling and the role of LTBP4 in elastogenesis is TGFβ independent [110].

Fibulin-4 and fibulin-5 in elastogenesis

Several elastic-fibre associated proteins are involved in the different stages of elastogenesis, from the micro-assembly of tropoelastin coacervates to the macro-assembly of elastic fibres. The fibulins are a multifunctional family of ECM glycoproteins comprising both long (fibulin-1, -2, -6) and short fibulins (fibulin-3, -4, -5, -7) [138]. Fibulin-1, -2, -3, -4, and -5 bind tropoelastin [139] and fibulin-2, -3, -4, and -5 are involved in elastic fibre formation. In particular, fibulin-4 and fibulin-5 (also known as developing arteries and neural crest EGF-like (DANCE)) play an important role in elastogenesis. Fibulin-4 and fibulin-5 null mice lack well-developed elastic fibres, demonstrating the importance of both glycoproteins in elastic fibre formation [140–142]. Functional studies have shown that fibulin-4 binds LOX with high affinity, which further results in a stronger interaction with tropoelastin, suggesting a role for fibulin-4 in the recruitment of LOX and the coacervation of tropoelastin [143,144]. Fibulin-5 has a strong interaction with tropoelastin and interacts with LOX, LOXL1, LOXL2 and LOXL4 to induce elastic fibre assembly and cross-linking [96,143,145]. Additionally, both fibulin-4 and -5 bind to the N-terminal region of fibrillin-1, suggesting a role in chaperoning tropoelastin aggregates to fibrillin microfibrils and facilitating the formation of cross-linked elastic fibres [139,143].

LTBP4 colocalises to and interacts with fibulin-5 via the four-cysteine domain at its N-terminus which binds to the C-terminal region of fibulin-5 [133]. LTBP4-fibulin interactions are important for elastogenesis as LTBP4 knockdown disrupts fibulin-5 and tropoelastin deposition which can be rescued by addition of LTBP4 [133]. These findings indicate that LTBP4 is essential for proper deposition of fibulin-5-elastin complexes onto fibrillin microfibril scaffolds. LTBP4 also interacts with fibulin-4 and fibulin-4 deposition is disrupted in LTBP4$^{-/-}$ mice but normal in LTBP4S$^{-/-}$ mice that express the LTBP4L isoform [136,146]. This raised the question whether the different LTBP4 isoforms differentially bind fibulin-4. Indeed mice expressing only the LTBP4L isoform with reduced expression of fibulin-4 die during the early postnatal period [146]. In contrast LTBP4S$^{-/-}$;fibulin-4$^{R/R}$ mice survive to adulthood [135,147], indicating that LTBP4L interacts with fibulin-4 and this interaction is essential for survival [146]. Together these findings imply that the elastogenic role of LTBP4 is both fibulin-4 and fibulin-5 dependent and that fibulin-5 cannot compensate for fibulin-4. Moreover, LTBP4S favours binding to fibulin-5 [133], whereas LTBP4L favours binding to fibulin-4 [136]. Overall, both LTBP4 isoforms are required for deposition of both fibulin-5-elastin and fibulin-4-elastin complexes onto fibrillin microfibrils.

The Emilins in elastic fibre formation

Emilin (Elastin Microfibril Interface-Located ProteIN)-1 and -2 are found at sites where elastin and fibrillin microfibrils are in close proximity [148]. The Emilins are deposited on and co-regulated with fibrillin-1 [149] and they are required for elastic fibre formation. They have a regulatory role in cell adhesion, migration and wound healing, and have been implicated in blood vascular morphology, tumour cell invasiveness and dermal proliferation

Please cite this article as: A. R.F. Godwin, M. Singh, M. P. Lockhart-Cairns, et al., The role of fibrillin and microfibril binding proteins in elastin and elastic fibre assembly, Matrix Biology, https://doi.org/10.1016/j.matbio.2019.06.006

[149–151]. Fibulin-4 has been identified as an Emilin-1 binding partner with Emilin-1 knockdown preventing fibulin-4 deposition, suggesting a requirement for Emilin-1 in fibulin-4 incorporation in the matrix [152].

Final considerations

Fibrillin is large, modular, extracellular matrix glycoprotein that assembles into beaded microfibrils which have roles in elastic fibre assembly, elastic tissue function and extracellular signalling events. In most tissues, fibrillin microfibrils associate with elastin to form elastic fibres and hence make key contributions to the elastic function of these tissues acting as a stiff reinforcer of elastin-containing tissues. Fibrillin microfibrils also provide limited elasticity in tissues devoid of elastin. They also provide a multifunctional platform for the interaction of many matrix molecules required for elastic fibre assembly and function and provide a connection to the cell surface. Fibrillin is needed for the correct assembly of many microfibril associated proteins, including members of the LTBP family, and mediate interactions between fibulin-4 or fibulin-5 and LTBPs or LOX/L enzymes facilitating their functions. Indeed fibrillin microfibril and elastic fibre biology is highly complex which provides a challenge to the research community to unravel the multiple molecular and cellular interactions that underpin elastogenesis. However, understanding these events provides a future opportunity to inform future regenerative medicine strategies and intervene in disease processes.

Acknowledgements

The Wellcome Trust Centre for Cell-Matrix Research is supported by funding from the Wellcome Trust (088785/Z/09/Z). C•B gratefully acknowledges BBSRC funding (Ref: BB/N015398/1, BB/R008221/1 and BB/S015779/1).

Received 3 April 2019;
Received in revised form 16 June 2019;
Accepted 17 June 2019
Available online xxxx

References

[1] J. Thomson, M. Singh, A. Eckersley, S.A. Cain, M.J. Sherratt, C. Baldock, Fibrillin microfibrils and elastic fibre proteins: functional interactions and extracellular regulation of growth factors, Semin. Cell Dev. Biol. 89 (2019) 109–117.
[2] R.P. Mecham, Elastin in lung development and disease pathogenesis, Matrix Biol. 73 (2018) 6–20.
[3] J.E. Wagenseil, R.P. Mecham, New insights into elastic fiber assembly, Birth Defects Res C Embryo Today 81 (4) (2007) 229–240.
[4] G. Sengle, L.Y. Sakai, The fibrillin microfibril scaffold: a niche for growth factors and mechanosensation? Matrix Biol. 47 (2015) 3–12.
[5] L.Y. Sakai, D.R. Keene, R.W. Glanville, H.P. Bachinger, Purification and partial characterization of fibrillin, a cysteine-rich structural component of connective tissue microfibrils, J. Biol. Chem. 266 (22) (1991) 14763–14770.
[6] L. Pereira, M. D'Alessio, F. Ramirez, J.R. Lynch, B. Sykes, T. Pangilinan, J. Bonadio, Genomic organization of the sequence coding for fibrillin, the defective gene product in Marfan syndrome, Hum. Mol. Genet. 2 (7) (1993) 961–968.
[7] H. Zhang, S.D. Apfelroth, W. Hu, E.C. Davis, C. Sanguineti, J. Bonadio, R.P. Mecham, F. Ramirez, Structure and expression of fibrillin-2, a novel microfibrillar component preferentially located in elastic matrices, J. Cell Biol. 124 (5) (1994) 855–863.
[8] G.M. Corson, N.L. Charbonneau, D.R. Keene, L.Y. Sakai, Differential expression of fibrillin-3 adds to microfibril variety in human and avian, but not rodent, connective tissues, Genomics 83 (3) (2004) 461–472.
[9] C.L. Maslen, G.M. Corson, B.K. Maddox, R.W. Glanville, L. Y. Sakai, Partial sequence of a candidate gene for the Marfan syndrome, Nature 352 (6333) (1991) 334–337.
[10] X. Yuan, A.K. Downing, V. Knott, P.A. Handford, Solution structure of the transforming growth factor beta-binding protein-like module, a domain associated with matrix fibrils, EMBO J. 16 (22) (1997) 6659–6666.
[11] S.S. Lee, V. Knott, J. Jovanovic, K. Harlos, J.M. Grimes, L. Choulier, H.J. Mardon, D.I. Stuart, P.A. Handford, Structure of the integrin binding fragment from fibrillin-1 gives new insights into microfibril organization, Structure (London, England: 1993) 12 (4) (2004) 717–729.
[12] D.V. Bax, S.E. Bernard, A. Lomas, A. Morgan, J. Humphries, C.A. Shuttleworth, M.J. Humphries, C.M. Kielty, Cell adhesion to fibrillin-1 molecules and microfibrils is mediated by alpha 5 beta 1 and alpha v beta 3 integrins, J. Biol. Chem. 278 (36) (2003) 34605–34616.
[13] J. Jovanovic, J. Takagi, L. Choulier, N.G. Abrescia, D.I. Stuart, P.A. van der Merwe, H.J. Mardon, P.A. Handford, AlphaVbeta6 is a novel receptor for human fibrillin-1. Comparative studies of molecular determinants underlying integrin-rgd affinity and specificity, J. Biol. Chem. 282 (9) (2007) 6743–6751.
[14] H. Sakamoto, T. Broekelmann, D.A. Cheresh, F. Ramirez, J. Rosenbloom, R.P. Mecham, Cell-type specific recognition of RGD- and non-RGD-containing cell binding domains in fibrillin-1, J. Biol. Chem. 271 (9) (1996) 4916–4922.
[15] M. Pfaff, D.P. Reinhardt, L.Y. Sakai, R. Timpl, Cell adhesion and integrin binding to recombinant human fibrillin-1, FEBS Lett. 384 (3) (1996) 247–250.
[16] S.A. Jensen, S. Iqbal, E.D. Lowe, C. Redfield, P.A. Handford, Structure and interdomain interactions of a hybrid domain: a disulphide-rich module of the fibrillin/LTBP

Please cite this article as: A. R.F. Godwin, M. Singh, M. P. Lockhart-Cairns, et al., The role of fibrillin and microfibril binding proteins in elastin and elastic fibre assembly, Matrix Biology, https://doi.org/10.1016/j.matbio.2019.06.006

superfamily of matrix proteins, Structure (London, England: 1993) 17 (5) (2009) 759–768.
[17] G.M. Corson, S.C. Chalberg, H.C. Dietz, N.L. Charbonneau, L.Y. Sakai, Fibrillin binds calcium and is coded by cDNAs that reveal a multidomain structure and alternatively spliced exons at the 5′ end, Genomics 17 (2) (1993) 476–484.
[18] D.D. Wallis, E.A. Putnam, J.S. Cretoiu, S.G. Carmical, S.N. Cao, G. Thomas, D.M. Milewicz, Profibrillin-1 maturation by human dermal fibroblasts: proteolytic processing and molecular chaperones, J. Cell. Biochem. 90 (3) (2003) 641–652.
[19] S.A. Jensen, G. Aspinall, P.A. Handford, C-terminal propeptide is required for fibrillin-1 secretion and blocks premature assembly through linkage to domains cbEGF41-43, Proc. Natl. Acad. Sci. U. S. A. 111 (28) (2014) 10155–10160.
[20] L. Lonnqvist, D. Reinhardt, L. Sakai, L. Peltonen, Evidence for furin-type activity-mediated C-terminal processing of profibrillin-1 and interference in the processing by certain mutations, Hum. Mol. Genet. 7 (13) (1998) 2039–2044.
[21] C. Romero, C. Duerschmid, J. Bournat, P. Constable, M. Jain, F. Xia, P.K. Saha, M. Del Solar, B. Zhu, B. York, P. Sarkar, D.A. Rendon, M.W. Gaber, S.A. LeMaire, J.S. Coselli, D.M. Milewicz, V.R. Sutton, N.F. Butte, D.D. Moore, A.R. Chopra, Asprosin, a fasting-induced glucogenic protein hormone, Cell 165 (3) (2016) 566–579.
[22] V.S. Tagliabracci, S.E. Wiley, X. Guo, L.N. Kinch, E. Durrant, J. Wen, J. Xiao, J. Cui, K.B. Nguyen, J.L. Engel, J.J. Coon, N. Grishin, L.A. Pinna, D.J. Pagliarini, J.E. Dixon, A single kinase generates the majority of the secreted phosphoproteome, Cell 161 (7) (2015) 1619–1632.
[23] D.R. Keene, B.K. Maddox, H.J. Kuo, L.Y. Sakai, R.W. Glanville, Extraction of extendable beaded structures and their identification as fibrillin-containing extracellular matrix microfibrils, J. Histochem. Cytochem. 39 (4) (1991) 441–449.
[24] D.P. Reinhardt, D.R. Keene, G.M. Corson, E. Poschl, H.P. Bachinger, J.E. Gambee, L.Y. Sakai, Fibrillin-1: organization in microfibrils and structural properties, J. Mol. Biol. 258 (1) (1996) 104–116.
[25] G. Lin, K. Tiedemann, T. Vollbrandt, H. Peters, B. Batge, J. Brinckmann, D.P. Reinhardt, Homo- and heterotypic fibrillin-1 and -2 interactions constitute the basis for the assembly of microfibrils, J. Biol. Chem. 277 (52) (2002) 50795–50804.
[26] A. Marson, M.J. Rock, S.A. Cain, L.J. Freeman, A. Morgan, K. Mellody, C.A. Shuttleworth, C. Baldock, C.M. Kielty, Homotypic fibrillin-1 interactions in microfibril assembly, J. Biol. Chem. 280 (6) (2005) 5013–5021.
[27] D. Hubmacher, E.I. El-Hallous, V. Nelea, M.T. Kaartinen, E. R. Lee, D.P. Reinhardt, Biogenesis of extracellular microfibrils: multimerization of the fibrillin-1 C terminus into bead-like structures enables self-assembly, Proc. Natl. Acad. Sci. U. S. A. 105 (18) (2008) 6548–6553.
[28] M.J. Sherratt, D.F. Holmes, C.A. Shuttleworth, C.M. Kielty, Scanning transmission electron microscopy mass analysis of fibrillin-containing microfibrils from foetal elastic tissues, Int. J. Biochem. Cell Biol. 29 (8–9) (1997) 1063–1070.
[29] A.R.F. Godwin, T. Starborg, D.J. Smith, M.J. Sherratt, A.M. Roseman, C. Baldock, Multiscale imaging reveals the hierarchical organization of fibrillin microfibrils, J. Mol. Biol. 430 (21) (2018) 4142–4155.
[30] E.G. Cleary, M.A. Gibson, Elastin-associated microfibrils and microfibrillar proteins, International review of connective tissue research 10 (1983) 97–209.
[31] M.C. Wang, Y. Lu, C. Baldock, Fibrillin microfibrils: a key role for the interbead region in elasticity, J. Mol. Biol. 388 (1) (2009) 168–179.
[32] R.Q. Qian, R.W. Glanville, Alignment of fibrillin molecules in elastic microfibrils is defined by transglutaminase-derived cross-links, Biochemistry 36 (50) (1997) 15841–15847.
[33] E.C. Davis, R.A. Roth, J.E. Heuser, R.P. Mecham, Ultrastructural properties of ciliary zonule microfibrils, J. Struct. Biol. 139 (2) (2002) 65–75.
[34] M.J. Sherratt, T.J. Wess, C. Baldock, J. Ashworth, P.P. Purslow, C.A. Shuttleworth, C.M. Kielty, Fibrillin-rich microfibrils of the extracellular matrix: ultrastructure and assembly, Micron (Oxford, England: 1993) 32 (2) (2001) 185–200.
[35] Y. Lu, M.J. Sherratt, M.C. Wang, C. Baldock, Tissue specific differences in fibrillin microfibrils analysed using single particle image analysis, J. Struct. Biol. 155 (2) (2006) 285–293.
[36] M.J. Sherratt, C. Baldock, J.L. Haston, D.F. Holmes, C.J. Jones, C.A. Shuttleworth, T.J. Wess, C.M. Kielty, Fibrillin microfibrils are stiff reinforcing fibres in compliant tissues, J. Mol. Biol. 332 (1) (2003) 183–193.
[37] T.J. Wess, P.P. Purslow, C.M. Kielty, X-ray diffraction studies of fibrillin-rich microfibrils: effects of tissue extension on axial and lateral packing, J. Struct. Biol. 122 (1–2) (1998) 123–127.
[38] C. Baldock, V. Siegler, D.V. Bax, S.A. Cain, K.T. Mellody, A. Marson, J.L. Haston, R. Berry, M.C. Wang, J.G. Grossmann, M. Roessle, C.M. Kielty, T.J. Wess, Nanostructure of fibrillin-1 reveals compact conformation of EGF arrays and mechanism for extensibility, Proc. Natl. Acad. Sci. U. S. A. 103 (32) (2006) 11922–11927.
[39] C.L. Kuo, Z. Isogai, D.R. Keene, N. Hazeki, R.N. Ono, G. Sengle, H.P. Bachinger, L.Y. Sakai, Effects of fibrillin-1 degradation on microfibril ultrastructure, J. Biol. Chem. 282 (6) (2007) 4007–4020.
[40] J.L. Ashworth, V. Kelly, M.J. Rock, C.A. Shuttleworth, C.M. Kielty, Regulation of fibrillin carboxy-terminal furin processing by N-glycosylation, and association of amino- and carboxy-terminal sequences, J. Cell Sci. 112 (Pt 22) (1999) 4163–4171.
[41] T.M. Trask, T.M. Ritty, T. Broekelmann, C. Tisdale, R.P. Mecham, N-terminal domains of fibrillin 1 and fibrillin 2 direct the formation of homodimers: a possible first step in microfibril assembly, Biochem. J. 340 (Pt 3) (1999) 693–701.
[42] D. Hubmacher, E. Bergeron, C. Fagotto-Kaufmann, L.Y. Sakai, D.P. Reinhardt, Early fibrillin-1 assembly monitored through a modifiable recombinant cell approach, Biomacromolecules 15 (4) (2014) 1456–1468.
[43] S.A. Cain, A. McGovern, E. Small, L.J. Ward, C. Baldock, A. Shuttleworth, C.M. Kielty, Defining elastic fiber interactions by molecular fishing: an affinity purification and mass spectrometry approach, Mol. Cell. Proteomics 8 (12) (2009) 2715–2732.
[44] S.A. Cain, A.K. Baldwin, Y. Mahalingam, B. Raynal, T.A. Jowitt, C.A. Shuttleworth, J.R. Couchman, C.M. Kielty, Heparan sulfate regulates fibrillin-1 N- and C-terminal interactions, J. Biol. Chem. 283 (40) (2008) 27017–27027.
[45] T.M. Ritty, T.J. Broekelmann, C.C. Werneck, R.P. Mecham, Fibrillin-1 and -2 contain heparin-binding sites important for

Please cite this article as: A. R.F. Godwin, M. Singh, M. P. Lockhart-Cairns, et al., The role of fibrillin and microfibril binding proteins in elastin and elastic fibre assembly, Matrix Biology, https://doi.org/10.1016/j.matbio.2019.06.006

matrix deposition and that support cell attachment, Biochem. J. 375 (Pt 2) (2003) 425–432.
[46] K. Tiedemann, B. Batge, P.K. Muller, D.P. Reinhardt, Interactions of fibrillin-1 with heparin/heparan sulfate, implications for microfibrillar assembly, J. Biol. Chem. 276 (38) (2001) 36035–36042.
[47] D.A. Yadin, I.B. Robertson, J. McNaught-Davis, P. Evans, D. Stoddart, P.A. Handford, S.A. Jensen, C. Redfield, Structure of the fibrillin-1 N-terminal domains suggests that heparan sulfate regulates the early stages of microfibril assembly, Structure (London, England: 1993) 21 (10) (2013) 1743–1756.
[48] L. Sabatier, J. Djokic, D. Hubmacher, D. Dzafik, V. Nelea, D. P. Reinhardt, Heparin/heparan sulfate controls fibrillin-1, -2 and -3 self-interactions in microfibril assembly, FEBS Lett. 588 (2014) 2890–2897.
[49] T. Massam-Wu, M. Chiu, R. Choudhury, S.S. Chaudhry, A. K. Baldwin, A. McGovern, C. Baldock, C.A. Shuttleworth, C. M. Kielty, Assembly of fibrillin microfibrils governs extracellular deposition of latent TGF[beta], J. Cell Sci. 123 (Pt 17) (2010) 3006–3018.
[50] K. Tiedemann, T. Sasaki, E. Gustafsson, W. Göhring, B. Batge, H. Notbohm, R. Timpl, T. Wedel, U. Schlötzer-Schrehardt, D.P. Reinhardt, Microfibrils at basement membrane zones interact with perlecan via fibrillin-1, J. Biol. Chem. 280 (12) (2005) 11404–11412.
[51] A. Cheng, S.A. Cain, P. Tian, A.K. Baldwin, P. Upparan, C. M. Kielty, S.J. Kimber, Recombinant extracellular matrix protein fragments support human embryonic stem cell chondrogenesis, Tissue Eng. Part A 24 (11–12) (2018) 968–978.
[52] A. Leha, N. Moens, R. Meleckyte, O.J. Culley, M.K. Gervasio, M. Kerz, A. Reimer, S.A. Cain, I. Streeter, A. Folarin, O. Stegle, C.M. Kielty, C. HipSci, R. Durbin, F.M. Watt, D. Danovi, A high-content platform to characterise human induced pluripotent stem cell lines, Methods 96 (2016) 85–96.
[53] A. Piha-Gossack, W. Sossin, D.P. Reinhardt, The evolution of extracellular fibrillins and their functional domains, PLoS One 7 (3) (2012), e33560.
[54] B.L. Loeys, E.E. Gerber, D. Riegert-Johnson, S. Iqbal, P. Whiteman, V. McConnell, C.R. Chillakuri, D. Macaya, P.J. Coucke, A. De Paepe, D.P. Judge, F. Wigley, E.C. Davis, H. J. Mardon, P. Handford, D.R. Keene, L.Y. Sakai, H.C. Dietz, Mutations in fibrillin-1 cause congenital scleroderma: stiff skin syndrome, Sci Transl Med 2 (23) (2010) (23ra20).
[55] E.E. Gerber, E.M. Gallo, S.C. Fontana, E.C. Davis, F.M. Wigley, D.L. Huso, H.C. Dietz, Integrin-modulating therapy prevents fibrosis and autoimmunity in mouse models of scleroderma, Nature 503 (7474) (2013) 126–130.
[56] K.A. Zeyer, R.-M. Zhang, H. Kumra, A. Hassan, D.P. Reinhardt, The fibrillin-1 RGD integrin binding site regulates gene expression and cell function through microRNAs, J. Mol. Biol. 431 (2) (2019) 401–421.
[57] M.I.S. Chung, M. Ming, R.J. Stahl, E. Chan, J. Parkinson, F. W. Keeley, Sequences and domain structures of mammalian, avian, amphibian and teleost tropoelastins: clues to the evolutionary history of elastins, Matrix Biol. 25 (8) (2006) 492–504.
[58] G. Faury, Function-structure relationship of elastic arteries in evolution: from microfibrils to elastin and elastic fibres, Pathol. Biol. (Paris) 49 (4) (2001) 310–325.
[59] L. Sabatier, D. Chen, C. Fagotto-Kaufmann, D. Hubmacher, M.D. McKee, D.S. Annis, D.F. Mosher, D.P. Reinhardt, Fibrillin assembly requires fibronectin, Mol. Biol. Cell 20 (3) (2009) 846–858.
[60] R. Kinsey, M.R. Williamson, S. Chaudhry, K.T. Mellody, A. McGovern, S. Takahashi, C.A. Shuttleworth, C.M. Kielty, Fibrillin-1 microfibril deposition is dependent on fibronectin assembly, J. Cell Sci. 121 (Pt 16) (2008) 2696–2704.
[61] E. Redondo-Castro, C.J. Cunningham, J. Miller, S.A. Cain, S.M. Allan, E. Pinteaux, Generation of human mesenchymal stem cell 3D spheroids using low-binding plates, Bio Protoc 8 (16) (2018), e2968.
[62] A.K. Baldwin, S.A. Cain, R. Lennon, A. Godwin, C.L. Merry, C.M. Kielty, Epithelial-mesenchymal status influences how cells deposit fibrillin microfibrils, J. Cell Sci. 127 (Pt 1) (2014) 158–171.
[63] C.M. Kielty, Fell-Muir Lecture: fibrillin microfibrils: structural tensometers of elastic tissues? Int. J. Exp. Pathol. 98 (4) (2017) 172–190.
[64] W.E. Kutz, L.W. Wang, H.L. Bader, A.K. Majors, K. Iwata, E. I. Traboulsi, L.Y. Sakai, D.R. Keene, S.S. Apte, ADAMTS10 protein interacts with fibrillin-1 and promotes its deposition in extracellular matrix of cultured fibroblasts, J. Biol. Chem. 286 (19) (2011) 17156–17167.
[65] S.A. Cain, E.J. Mularczyk, M. Singh, T. Massam-Wu, C.M. Kielty, ADAMTS-10 and -6 differentially regulate cell-cell junctions and focal adhesions, Sci. Rep. 6 (2016) 35956.
[66] E.J. Mularczyk, M. Singh, A.R.F. Godwin, F. Galli, N. Humphreys, A.D. Adamson, A. Mironov, S.A. Cain, G. Sengle, R.P. Boot-Handford, G. Cossu, C.M. Kielty, C. Baldock, ADAMTS10-mediated tissue disruption in Weill-Marchesani syndrome, Hum. Mol. Genet. 27 (21) (2018) 3675–3687.
[67] L.W. Wang, W.E. Kutz, T.J. Mead, L.C. Beene, S. Singh, M. W. Jenkins, D.P. Reinhardt, S.S. Apte, Adamts10 inactivation in mice leads to persistence of ocular microfibrils subsequent to reduced fibrillin-2 cleavage, Matrix Biol. 77 (2019) 117–128.
[68] D. Hubmacher, M. Schneider, S.J. Berardinelli, H. Takeuchi, B. Willard, D.P. Reinhardt, R.S. Halthwanger, S. S. Apte, Unusual life cycle and impact on microfibril assembly of ADAMTS17, a secreted metalloprotease mutated in genetic eye disease, Sci. Rep. 7 (2017) 41871.
[69] G. Sengle, K. Tsutsui, D.R. Keene, S.F. Tufa, E.J. Carlson, N.L. Charbonneau, R.N. Ono, T. Sasaki, M.K. Wirtz, J.R. Samples, L.I. Fessler, J.H. Fessler, K. Sekiguchi, S.J. Hayflick, L.Y. Sakai, Microenvironmental regulation by fibrillin-1, PLoS Genet. 8 (1) (2012), e1002425.
[70] D. Hubmacher, L.W. Wang, R.P. Mecham, D.P. Reinhardt, S.S. Apte, Adamts12 deletion results in bronchial fibrillin microfibril accumulation and bronchial epithelial dysplasia – a novel mouse model providing insights into geleophysic dysplasia, Dis. Model. Mech. 8 (5) (2015) 487–499.
[71] L.A. Gabriel, L.W. Wang, H. Bader, J.C. Ho, A.K. Majors, J. G. Hollyfield, E.I. Traboulsi, S.S. Apte, ADAMTSL4, a secreted glycoprotein widely distributed in the eye, binds fibrillin-1 microfibrils and accelerates microfibril biogenesis, Invest. Ophthalmol. Vis. Sci. 53 (1) (2012) 461–469.
[72] A. Chandra, M. Jones, P. Cottrill, K. Eastlake, G.A. Limb, D. G. Charteris, Gene expression and protein distribution of ADAMTSL-4 in human iris, choroid and retina, Br. J. Ophthalmol. 97 (9) (2013) 1208–1212.
[73] H.L. Bader, L.W. Wang, J.C. Ho, T. Tran, P. Holden, J. Fitzgerald, R.P. Atit, D.P. Reinhardt, S.S. Apte, A disintegrin-like and metalloprotease domain containing

Please cite this article as: A. R.F. Godwin, M. Singh, M. P. Lockhart-Cairns, et al., The role of fibrillin and microfibril binding proteins in elastin and elastic fibre assembly, Matrix Biology, https://doi.org/10.1016/j.matbio.2019.06.006

thrombospondin type 1 motif-like 5 (ADAMTSL5) is a novel fibrillin-1-, fibrillin-2-, and heparin-binding member of the ADAMTS superfamily containing a netrin-like module, Matrix Biol. 31 (7) (2012) 398–411.
[74] K. Tsutsui, R. Manabe, T. Yamada, I. Nakano, Y. Oguri, D. R. Keene, G. Sengle, L.Y. Sakai, K. Sekiguchi, ADAMTSL-6 is a novel extracellular matrix protein that binds to fibrillin-1 and promotes fibrillin-1 fibril formation, J. Biol. Chem. 285 (7) (2010) 4870–4882.
[75] I.M. Braverman, E. Fonferko, Studies in cutaneous aging: I. The elastic fiber network, J. Investig. Dermatol. 78 (5) (1982) 434–443.
[76] J. Brinckmann, N. Hunzelmann, B. Kahle, J. Rohwedel, J. Kramer, M.A. Gibson, D. Hubmacher, D.P. Reinhardt, Enhanced fibrillin-2 expression is a general feature of wound healing and sclerosis: potential alteration of cell attachment and storage of TGF-beta, Lab. Investig. 90 (5) (2010) 739–752.
[77] M. Hiraoka, K. Inoue, C. Ohtaka-Maruyama, S. Ohsako, N. Kojima, H. Senoo, M. Takada, Intracapsular organization of ciliary zonules in monkey eyes, Anat. Rec. 293 (10) (2010) 1797–1804.
[78] G.B. Collin, D. Hubmacher, J.R. Charette, W.L. Hicks, L. Stone, M. Yu, J.K. Naggert, M.P. Krebs, N.S. Peachey, S.S. Apte, P.M. Nishina, Disruption of murine Adamtsl4 results in zonular fiber detachment from the lens and in retinal pigment epithelium dedifferentiation, Hum. Mol. Genet. 24 (24) (2015) 6958–6974.
[79] T. Inoue, T. Ohbayashi, Y. Fujikawa, H. Yoshida, T.O. Akama, K. Noda, M. Horiguchi, K. Kameyama, Y. Hata, K. Takahashi, K. Kusumoto, T. Nakamura, Latent TGF-beta binding protein-2 is essential for the development of ciliary zonule microfibrils, Hum. Mol. Genet. 23 (21) (2014) 5672–5682.
[80] H. Zhang, W. Hu, F. Ramirez, Developmental expression of fibrillin genes suggests heterogeneity of extracellular microfibrils, J. Cell Biol. 129 (1995) 1165–1176.
[81] L. Sabatier, N. Miosge, D. Hubmacher, G. Lin, E.C. Davis, D.P. Reinhardt, Fibrillin-3 expression in human development, Matrix Biol. 30 (1) (2011) 43–52.
[82] S.A. Cain, A. Morgan, M.J. Sherratt, S.G. Ball, C.A. Shuttleworth, C.M. Kielty, Proteomic analysis of fibrillin-rich microfibrils, Proteomics 6 (1) (2006) 111–122.
[83] A. De Maria, P.A. Wilmarth, L.L. David, S. Bassnett, Proteomic analysis of the bovine and human ciliary zonule, Invest. Ophthalmol. Vis. Sci. 58 (1) (2017) 573–585.
[84] N.L. Charbonneau, B.J. Dzamba, R.N. Ono, D.R. Keene, G. M. Corson, D.P. Reinhardt, L.Y. Sakai, Fibrillins can co-assemble in fibrils, but fibrillin fibril composition displays cell-specific differences, J. Biol. Chem. 278 (4) (2003) 2740–2749.
[85] L. Carta, L. Pereira, E. Arteaga-Solis, S.Y. Lee-Arteaga, B. Lenart, B. Starcher, C.A. Merkel, M. Sukoyan, A. Kerkis, N. Hazeki, D.R. Keene, L.Y. Sakai, F. Ramirez, Fibrillins 1 and 2 perform partially overlapping functions during aortic development, J. Biol. Chem. 281 (12) (2006) 8016–8023.
[86] M.L. Duque Lasio, B.A. Kozel, Elastin-driven genetic diseases, Matrix Biol. 71-72 (2018) 144–160.
[87] M.J. Fazio, M.G. Mattei, E. Passage, M.L. Chu, D. Black, E. Solomon, J.M. Davidson, J. Uitto, Human elastin gene: new evidence for localization to the long arm of chromosome 7, Am. J. Hum. Genet. 48 (4) (1991) 696–703.
[88] M.H. Swee, W. Parks, R. Pierce, Developmental regulation of elastin production: Expression of tropoelastin pre-mRNA persists after down-regulation of steady-state mRNA levels, J. Biol. Chem. 270 (1995) 14899–14906.
[89] D. Gheduzzi, D. Guerra, B. Bochicchio, A. Pepe, A.M. Tamburro, D. Quaglino, S. Mithieux, A.S. Weiss, I. Pasquali Ronchetti, Heparan sulphate interacts with tropoelastin, with some tropoelastin peptides and is present in human dermis elastic fibers, Matrix Biol. 24 (1) (2005) 15–25.
[90] B. Reinboth, E. Hanssen, E.G. Cleary, M.A. Gibson, Molecular interactions of biglycan and decorin with elastic fiber components: biglycan forms a ternary complex with tropoelastin and microfibril-associated glycoprotein 1, J. Biol. Chem. 277 (6) (2002) 3950–3957.
[91] A. Hinek, M. Rabinovitch, 67-kD elastin-binding protein is a protective "companion" of extracellular insoluble elastin and intracellular tropoelastin, J. Cell Biol. 126 (2) (1994) 563–574.
[92] T.J. Broekelmann, B.A. Kozel, H. Ishibashi, C.C. Werneck, F.W. Keeley, L. Zhang, R.P. Mecham, Tropoelastin interacts with cell-surface glycosaminoglycans via its COOH-terminal domain, J. Biol. Chem. 280 (49) (2005) 40939–40947.
[93] B.A. Kozel, B.J. Rongish, A. Czirok, J. Zach, C.D. Little, E.C. Davis, R.H. Knutsen, J.E. Wagenseil, M.A. Levy, R.P. Mecham, Elastic fiber formation: a dynamic view of extracellular matrix assembly using timer reporters, J. Cell. Physiol. 207 (1) (2006) 87–96.
[94] L.B. Dyksterhuis, C. Baldock, D. Lammie, T.J. Wess, A.S. Weiss, Domains 17–27 of tropoelastin contain key regions of contact for coacervation and contain an unusual turn-containing crosslinking domain, Matrix Biol. 26 (2) (2007) 125–135.
[95] R.C. Siegel, S.R. Pinnell, G.R. Martin, Cross-linking of collagen and elastin. Properties of lysyl oxidase, Biochemistry 9 (23) (1970) 4486–4492.
[96] X. Liu, Y. Zhao, J. Gao, B. Pawlyk, B. Starcher, J.A. Spencer, H. Yanagisawa, J. Zuo, T. Li, Elastic fiber homeostasis requires lysyl oxidase-like 1 protein, Nat. Genet. 36 (2) (2004) 178–182.
[97] C.E.H. Schmelzer, A. Heinz, H. Troilo, M.P. Lockhart-Cairns, T.A. Jowitt, M.F. Marchand, L. Bidault, M. Bignon, T. Hedtke, A. Barret, J.C. McConnell, M.J. Sherratt, S. Germain, D.J.S. Hulmes, C. Baldock, L. Muller, Lysyl oxidase-like 2 (LOXL2)-mediated cross-linking of tropoelastin, FASEB J. 33 (2019) 5468–5481.
[98] S.A. Jensen, D.P. Reinhardt, M.A. Gibson, A.S. Weiss, Protein interaction studies of MAGP-1 with tropoelastin and fibrillin-1, J. Biol. Chem. 276 (43) (2001) 39661–39666.
[99] C.S. Craft, T.J. Broekelmann, R.P. Mecham, Microfibril-associated glycoproteins MAGP-1 and MAGP-2 in disease, Matrix Biol. 71-72 (2018) 100–111.
[100] T.M. Trask, B.C. Trask, T.M. Ritty, W.R. Abrams, J. Rosenbloom, R.P. Mecham, Interaction of tropoelastin with the amino-terminal domains of fibrillin-1 and fibrillin-2 suggests a role for the fibrillins in elastic fiber assembly, J. Biol. Chem. 275 (32) (2000) 24400–24406.
[101] B. Pilecki, A.T. Holm, A. Schlosser, J.B. Moeller, A.P. Wohl, A.V. Zuk, S.E. Heumuller, R. Wallis, S.K. Moestrup, G. Sengle, U. Holmskov, G.L. Sorensen, Characterization of microfibrillar-associated protein 4 (MFAP4) as a tropoelastin- and fibrillin-binding protein involved in elastic fiber formation, J. Biol. Chem. 291 (3) (2016) 1103–1114.
[102] M.J. Rock, S.A. Cain, L.J. Freeman, A. Morgan, K. Mellody, A. Marson, C.A. Shuttleworth, A.S. Weiss, C.M. Kielty, Molecular basis of elastic fiber formation. Critical

Please cite this article as: A. R.F. Godwin, M. Singh, M. P. Lockhart-Cairns, et al., The role of fibrillin and microfibril binding proteins in elastin and elastic fibre assembly, Matrix Biology, https://doi.org/10.1016/j.matbio.2019.06.006

interactions and a tropoelastin-fibrillin-1 cross-link, J Biol Chem 279 (22) (2004) 23748–23758.
[103] A.W. Clarke, S.G. Wise, S.A. Cain, C.M. Kielty, A.S. Weiss, Coacervation is promoted by molecular interactions between the PF2 segment of fibrillin-1 and the domain 4 region of tropoelastin, Biochemistry 44 (30) (2005) 10271–10281.
[104] T. Kanzaki, A. Olofsson, A. Moren, C. Wernstedt, U. Hellman, K. Miyazono, L. Claesson-Welsh, C.H. Heldin, TGF-beta 1 binding protein: a component of the large latent complex of TGF-beta 1 with multiple repeat sequences, Cell 61 (6) (1990) 1051–1061.
[105] A. Moren, A. Olofsson, G. Stenman, P. Sahlin, T. Kanzaki, L. Claesson-Welsh, P. ten Dijke, K. Miyazono, C.H. Heldin, Identification and characterization of LTBP-2, a novel latent transforming growth factor-beta-binding protein, J. Biol. Chem. 269 (51) (1994) 32469–32478.
[106] W. Yin, E. Smiley, J. Germiller, R.P. Mecham, J.B. Florer, R. J. Wenstrup, J. Bonadio, Isolation of a novel latent transforming growth factor-beta binding protein gene (LTBP-3), J. Biol. Chem. 270 (17) (1995) 10147–10160.
[107] R. Giltay, G. Kostka, R. Timpl, Sequence and expression of a novel member (LTBP-4) of the family of latent transforming growth factor-beta binding proteins, FEBS Lett. 411 (2–3) (1997) 164–168.
[108] K. Miyazono, A. Olofsson, P. Colosetti, C.H. Heldin, A role of the latent TGF-beta 1-binding protein in the assembly and secretion of TGF-beta 1, EMBO J. 10 (5) (1991) 1091–1101.
[109] J. Saharinen, J. Keski-Oja, Specific sequence motif of 8-Cys repeats of TGF-beta binding proteins, LTBPs, creates a hydrophobic interaction surface for binding of small latent TGF-beta, Mol. Biol. Cell 11 (8) (2000) 2691–2704.
[110] B. Dabovic, Y. Chen, J. Choi, M. Vassallo, H.C. Dietz, F. Ramirez, H. von Melchner, E.C. Davis, D.B. Rifkin, Dual functions for LTBP in lung development: LTBP-4 independently modulates elastogenesis and TGF-beta activity, J. Cell. Physiol. 219 (1) (2009) 14–22.
[111] A. Olofsson, H. Ichijo, A. Moren, P. ten Dijke, K. Miyazono, C.H. Heldin, Efficient association of an amino-terminally extended form of human latent transforming growth factor-beta binding protein with the extracellular matrix, J. Biol. Chem. 270 (52) (1995) 31294–31297.
[112] K. Miyazono, U. Hellman, C. Wernstedt, C.H. Heldin, Latent high molecular weight complex of transforming growth factor beta 1. Purification from human platelets and structural characterization, J. Biol. Chem. 263 (13) (1988) 6407–6415.
[113] J. Saharinen, J. Taipale, O. Monni, J. Keski-Oja, Identification and characterization of a new latent transforming growth factor-beta-binding protein, LTBP-4, J. Biol. Chem. 273 (29) (1998) 18459–18469.
[114] Y. Fujikawa, H. Yoshida, T. Inoue, T. Ohbayashi, K. Noda, H. von Melchner, T. Iwasaka, I. Shiojima, T.O. Akama, T. Nakamura, Latent TGF-beta binding protein 2 and 4 have essential overlapping functions in microfibril development, Sci. Rep. 7 (2017) 43714.
[115] B. Dabovic, Y. Chen, J. Choi, E.C. Davis, L.Y. Sakai, V. Todorovic, M. Vassallo, L. Zilberberg, A. Singh, D.B. Rifkin, Control of lung development by latent TGF-beta binding proteins, J. Cell. Physiol. 226 (6) (2011) 1499–1509.
[116] L. Zilberberg, V. Todorovic, B. Dabovic, M. Horiguchi, T. Courousse, L.Y. Sakai, D.B. Rifkin, Specificity of latent TGF-beta binding protein (LTBP) incorporation into matrix: role of fibrillins and fibronectin, J. Cell. Physiol. 227 (12) (2012) 3828–3836.
[117] S.L. Dallas, P. Sivakumar, C.J. Jones, Q. Chen, D.M. Peters, D.F. Mosher, M.J. Humphries, C.M. Kielty, Fibronectin regulates latent transforming growth factor-beta (TGF beta) by controlling matrix assembly of latent TGF beta-binding protein-1, J. Biol. Chem. 280 (19) (2005) 18871–18880.
[118] L. Fontana, Y. Chen, P. Prijatelj, T. Sakai, R. Fassler, L.Y. Sakai, D.B. Rifkin, Fibronectin is required for integrin alphavbeta6-mediated activation of latent TGF-beta complexes containing LTBP-1, FASEB J. 19 (13) (2005) 1798–1808.
[119] R.N. Ono, G. Sengle, N.L. Charbonneau, V. Carlberg, H.P. Bachinger, T. Sasaki, S. Lee-Arteaga, L. Zilberberg, D.B. Rifkin, F. Ramirez, M.L. Chu, L.Y. Sakai, Latent transforming growth factor beta-binding proteins and fibulins compete for fibrillin-1 and exhibit exquisite specificities in binding sites, J. Biol. Chem. 284 (25) (2009) 16872–16881.
[120] Z. Isogai, R.N. Ono, S. Ushiro, D.R. Keene, Y. Chen, R. Mazzieri, N.L. Charbonneau, D.P. Reinhardt, D.B. Rifkin, L. Y. Sakai, Latent transforming growth factor beta-binding protein 1 interacts with fibrillin and is a microfibril-associated protein, J. Biol. Chem. 278 (4) (2003) 2750–2757.
[121] R. Hirani, E. Hanssen, M.A. Gibson, LTBP-2 specifically interacts with the amino-terminal region of fibrillin-1 and competes with LTBP-1 for binding to this microfibrillar protein, Matrix Biol. 26 (4) (2007) 213–223.
[122] H. Troilo, R. Steer, R.F. Collins, C.M. Kielty, C. Baldock, Independent multimerization of Latent TGFbeta Binding Protein-1 stabilized by cross-linking and enhanced by heparan sulfate, Sci. Rep. 6 (2016) 34347.
[123] M.K. Parsi, J.R. Adams, J. Whitelock, M.A. Gibson, LTBP-2 has multiple heparin/heparan sulfate binding sites, Matrix Biol. 29 (5) (2010) 393–401.
[124] A.K. Kantola, J. Keski-Oja, K. Koli, Fibronectin and heparin binding domains of latent TGF-beta binding protein (LTBP)-4 mediate matrix targeting and cell adhesion, Exp. Cell Res. 314 (13) (2008) 2488–2500.
[125] I. Nunes, P.E. Gleizes, C.N. Metz, D.B. Rifkin, Latent transforming growth factor-beta binding protein domains involved in activation and transglutaminase-dependent cross-linking of latent transforming growth factor-beta, J. Cell Biol. 136 (5) (1997) 1151–1163.
[126] E. Verderio, C. Gaudry, S. Gross, C. Smith, S. Downes, M. Griffin, Regulation of cell surface tissue transglutaminase: effects on matrix storage of latent transforming growth factor-beta binding protein-1, J. Histochem. Cytochem. 47 (11) (1999) 1417–1432.
[127] M.A. Gibson, G. Hatzinikolas, E.C. Davis, E. Baker, G.R. Sutherland, R.P. Mecham, Bovine latent transforming growth factor beta 1-binding protein 2: molecular cloning, identification of tissue isoforms, and immunolocalization to elastin-associated microfibrils, Mol. Cell. Biol. 15 (12) (1995) 6932–6942.
[128] P. Vehviläinen, M. Hyytiäinen, J. Keski-Oja, Matrix association of latent TGF-beta binding protein-2 (LTBP-2) is dependent on fibrillin-1, J. Cell. Physiol. 221 (3) (2009) 586–593.
[129] M. Hirai, M. Horiguchi, T. Ohbayashi, T. Kita, K.R. Chien, T. Nakamura, Latent TGF-beta-binding protein 2 binds to DANCE/fibulin-5 and regulates elastic fiber assembly, EMBO J. 26 (14) (2007) 3283–3295.

Please cite this article as: A. R.F. Godwin, M. Singh, M. P. Lockhart-Cairns, et al., The role of fibrillin and microfibril binding proteins in elastin and elastic fibre assembly, Matrix Biology, https://doi.org/10.1016/j.matbio.2019.06.006

[130] M.A. Sideek, C. Menz, M.K. Parsi, M.A. Gibson, LTBP-2 competes with tropoelastin for binding to fibulin-5 and heparin, and is a negative modulator of elastinogenesis, Matrix Biol. 34 (2014) 114–123.
[131] C. Penttinen, J. Saharinen, K. Weikkolainen, M. Hyytiäinen, J. Keski-Oja, Secretion of human latent TGF-beta-binding protein-3 (LTBP-3) is dependent on co-expression of TGF-beta, J. Cell Sci. 115 (Pt 17) (2002) 3457–3468.
[132] Y. Chen, B. Dabovic, J.P. Annes, D.B. Rifkin, Latent TGF-beta binding protein-3 (LTBP-3) requires binding to TGF-beta for secretion, FEBS Lett. 517 (1–3) (2002) 277–280.
[133] K. Noda, B. Dabovic, K. Takagi, T. Inoue, M. Horiguchi, M. Hirai, Y. Fujikawa, T.O. Akama, K. Kusumoto, L. Zilberberg, L.Y. Sakai, K. Koli, M. Naitoh, H. von Melchner, S. Suzuki, D.B. Rifkin, T. Nakamura, Latent TGF-beta binding protein 4 promotes elastic fiber assembly by interacting with fibulin-5, Proc. Natl. Acad. Sci. U. S. A. 110 (8) (2013) 2852–2857.
[134] Z. Urban, V. Hucthagowder, N. Schurmann, V. Todorovic, L. Zilberberg, J. Choi, C. Sens, C.W. Brown, R.D. Clark, K.E. Holland, M. Marble, L.Y. Sakai, B. Dabovic, D.B. Rifkin, E.C. Davis, Mutations in LTBP4 cause a syndrome of impaired pulmonary, gastrointestinal, genitourinary, musculoskeletal, and dermal development, Am. J. Hum. Genet. 85 (5) (2009) 593–605.
[135] A. Sterner-Kock, I.S. Thorey, K. Koli, F. Wempe, J. Otte, T. Bangsow, K. Kuhlmeier, T. Kirchner, S. Jin, J. Keski-Oja, H. von Melchner, Disruption of the gene encoding the latent transforming growth factor-beta binding protein 4 (LTBP-4) causes abnormal lung development, cardiomyopathy, and colorectal cancer, Genes Dev. 16 (17) (2002) 2264–2273.
[136] I. Bultmann-Mellin, A. Conradi, A.C. Maul, K. Dinger, F. Wempe, A.P. Wohl, T. Imhof, F.T. Wunderlich, A.C. Bunck, T. Nakamura, K. Koli, W. Bloch, A. Ghanem, A. Heinz, H. von Melchner, G. Sengle, A. Sterner-Kock, Modeling autosomal recessive cutis laxa type 1C in mice reveals distinct functions for Ltbp-4 isoforms, Dis. Model. Mech. 8 (4) (2015) 403–415.
[137] I. Bultmann-Mellin, K. Dinger, C. Debuschewitz, K.M.A. Loewe, Y. Melcher, M.T.W. Plum, S. Appel, G. Rappl, S. Willenborg, A.C. Schauss, C. Jungst, M. Kruger, S. Dressler, T. Nakamura, F. Wempe, M.A. Alejandre Alcazar, A. Sterner-Kock, Role of LTBP4 in alveolarization, angiogenesis, and fibrosis in lungs, Am. J. Phys. Lung Cell. Mol. Phys. 313 (4) (2017) L687–L698.
[138] C.L. Papke, H. Yanagisawa, Fibulin-4 and fibulin-5 in elastogenesis and beyond: insights from mouse and human studies, Matrix Biol. 37 (2014) 142–149.
[139] E. El-Hallous, T. Sasaki, D. Hubmacher, M. Getie, K. Tiedemann, J. Brinckmann, B. Batge, E.C. Davis, D.P. Reinhardt, Fibrillin-1 interactions with fibulins depend on the first hybrid domain and provide an adaptor function to tropoelastin, J. Biol. Chem. 282 (12) (2007) 8935–8946.
[140] T. Nakamura, P.R. Lozano, Y. Ikeda, Y. Iwanaga, A. Hinek, S. Minamisawa, C.F. Cheng, K. Kobuke, N. Dalton, Y. Takada, K. Tashiro, J. Ross Jr., T. Honjo, K.R. Chien, Fibulin-5/DANCE is essential for elastogenesis in vivo, Nature 415 (6868) (2002) 171–175.
[141] H. Yanagisawa, E.C. Davis, B.C. Starcher, T. Ouchi, M. Yanagisawa, J.A. Richardson, E.N. Olson, Fibulin-5 is an elastin-binding protein essential for elastic fibre development in vivo, Nature 415 (6868) (2002) 168–171.
[142] P.J. McLaughlin, Q. Chen, M. Horiguchi, B.C. Starcher, J.B. Stanton, T.J. Broekelmann, A.D. Marmorstein, B. McKay, R. Mecham, T. Nakamura, L.Y. Marmorstein, Targeted disruption of fibulin-4 abolishes elastogenesis and causes perinatal lethality in mice, Mol. Cell. Biol. 26 (5) (2006) 1700–1709.
[143] R. Choudhury, A. McGovern, C. Ridley, S.A. Cain, A. Baldwin, M.C. Wang, C. Guo, A. Mironov Jr., Z. Drymoussi, D. Trump, A. Shuttleworth, C. Baldock, C.M. Kielty, Differential regulation of elastic fiber formation by fibulin-4 and -5, J. Biol. Chem. 284 (36) (2009) 24553–24567.
[144] M. Horiguchi, T. Inoue, T. Ohbayashi, M. Hirai, K. Noda, L.Y. Marmorstein, D. Yabe, K. Takagi, T.O. Akama, T. Kita, T. Kimura, T. Nakamura, Fibulin-4 conducts proper elastogenesis via interaction with cross-linking enzyme lysyl oxidase, Proc. Natl. Acad. Sci. 106 (45) (2009) 19029.
[145] M. Hirai, T. Ohbayashi, M. Horiguchi, K. Okawa, A. Hagiwara, K.R. Chien, T. Kita, T. Nakamura, Fibulin-5/DANCE has an elastogenic organizer activity that is abrogated by proteolytic cleavage in vivo, J. Cell Biol. 176 (7) (2007) 1061–1071.
[146] I. Bultmann-Mellin, J. Essers, P.M. van Heijingen, H. von Melchner, G. Sengle, A. Sterner-Kock, Function of Ltbp-4L and fibulin-4 in survival and elastogenesis in mice, Dis. Model. Mech. 9 (11) (2016) 1367–1374.
[147] N.W. Ramnath, K.M. van de Luijtgaarden, I. van der Pluijm, M. van Nimwegen, P.M. van Heijningen, S.M. Swagemakers, B.S. van Thiel, R.Y. Ridwan, N. van Vliet, M. Vermeij, L.J. Hawinkels, A. de Munck, O. Dzyubachyk, E. Meijering, P. van der Spek, R. Rottier, H. Yanagisawa, R. W. Hendriks, R. Kanaar, E.V. Rouwet, A. Kleinjan, J. Essers, Extracellular matrix defects in aneurysmal Fibulin-4 mice predispose to lung emphysema, PLoS One 9 (9) (2014), e106054.
[148] A. Colombatti, P. Spessotto, R. Doliana, M. Mongiat, G.M. Bressan, G. Esposito, The EMILIN/multimerin family, Frontiers in Immunology 2, 2012.
[149] A. Schiavinato, D.R. Keene, A.P. Wohl, D. Corallo, A. Colombatti, R. Wagener, M. Paulsson, P. Bonaldo, G. Sengle, Targeting of EMILIN-1 and EMILIN-2 to fibrillin microfibrils facilitates their incorporation into the extracellular matrix, J. Investig. Dermatol. 136 (6) (2016) 1150–1160.
[150] C. Danussi, A. Petrucco, B. Wassermann, E. Pivetta, T.M.E. Modica, L.D. Belluz, A. Colombatti, P. Spessotto, EMILIN1-alpha 4/alpha 9 integrin interaction inhibits dermal fibroblast and keratinocyte proliferation, J. Cell Biol. 195 (1) (2011) 131–145.
[151] M. Rabajdova, P. Urban, I. Spakova, L. Saksun, R. Dudic, A. Ostro, M. Caprnda, P. Kruzliak, M. Adamek, M. Marekova, The crucial role of emilin 1 gene expression during progression of tumor growth, J. Cancer Res. Clin. Oncol. 142 (11) (2016) 2397–2402.
[152] A. Schiavinato, D.R. Keene, T. Imhof, R. Doliana, T. Sasaki, G. Sengle, Fibulin-4 deposition requires EMILIN-1 in the extracellular matrix of osteoblasts, Scientific Reports 7, 2017.
[153] C. Baldock, A.J. Koster, U. Ziese, M.J. Rock, M.J. Sherratt, K.E. Kadler, C.A. Shuttleworth, C.M. Kielty, The supramolecular organization of fibrillin-rich microfibrils, J. Cell Biol. 152 (2001) 1045–1056 (d PMID: 11238459).
[154] Y. Lu, D.F. Holmes, C. Baldock, Evidence for the intramolecular pleating model of fibrillin microfibril organisation from single particle image analysis, J. Mol. Biol. 349 (2005) 73–85 (PMID: 15876369).

Please cite this article as: A. R.F. Godwin, M. Singh, M. P. Lockhart-Cairns, et al., The role of fibrillin and microfibril binding proteins in elastin and elastic fibre assembly, Matrix Biology, https://doi.org/10.1016/j.matbio.2019.06.006

8. Appendix 2

Supplementary Data and Methods

Appendix 2: Supplementary

8.1. Protein sequence and domains of LTBP4 constructs used in this thesis

8.1.1. Protein sequence of LTBP4S N-terminal region construct

Example: EGF1

Example: Hybrid

Example: cbEGF1

Example: TB1

```
  10         20         30         40         50         60
AAPLAGERLR VRFTPVVCGL RCVHGPTGSR CTPTCAPRNA TSVDSGAPGG AAPGGPGFRA

         70         80         90        100        110        120
FLCPLICHNG GVCVKPDRCL CPPDFAGKFC QLHSSGARPP APAVPGLTRS VYTMPLANHR

        130        140        150        160        170        180
DDEHGVASMV SVHVEHPQEA SVVVHQVERV SGPWEEADAE AVARAEAAAR AEAAAPYTVL

        190        200        210        220        230        240
AQSAPREDGY SDASGFGYCF RELRGGECAS PLPGLRTQEV CCRGAGLAWG VHDCQLCSER

        250        260        270        280        290        300
LGNSERVSAP DGPCPTGFER VNGSCEDVDE CATGGRCQHG ECANTRGGYT CVCPDGFLLD

        310        320        330        340        350        360
SSRSSCISQH VISEAKGPCF RVLRDGGCSL PILRNITKQI CCCSRVGKAW GRGCQLCPPF

        370        380
GSEGPREICP ALVPRGSHHH HHHLEAGKX
```

Figure 8-1: Protein sequence of truncated LTBP4S N-terminal region construct. The domains are highlighted as above and the ARCL1C-causing point mutation in the hybrid domain is highlighted by red. The construct was tagged with 6X-His in its C-terminal region end.

8.1.2. protein sequence of LTBP4 C-terminal region construct

Example: TB2 & TB3

Example: cbEGF15, cbEGF16, cbEGF17

Example: Proline-rich

Example: EGF3

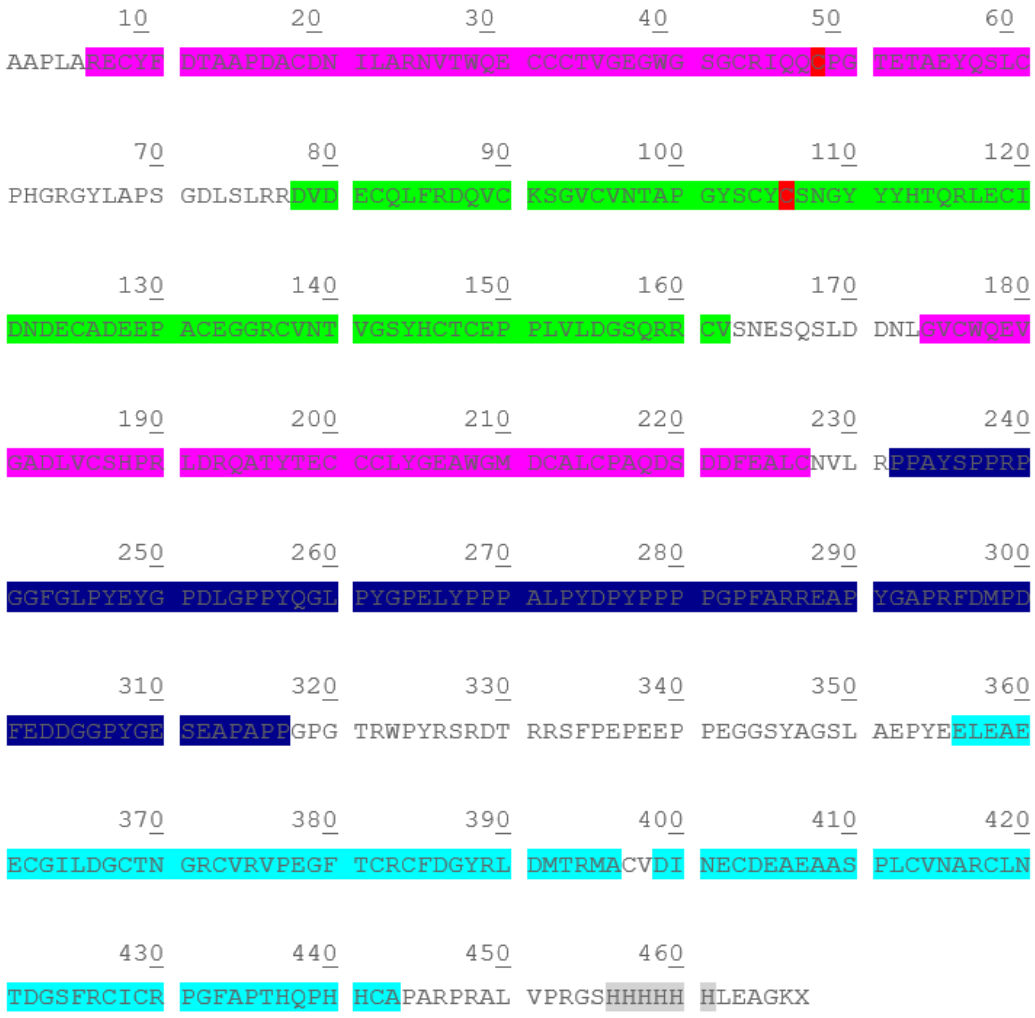

Figure 8-2: Protein sequence of truncated LTBP4 C-terminal region construct. The domains are highlighted as above and the ARCL1C-causing point mutations within the TB2 and cbEGF16 are highlighted by red. The constructs were tagged with 6X-His in its C-terminal region end.

8.2. Expression and purification of Fibulin-4, Fibulin-5 and Fibronectin

Human embryonic kidney (HEK) 293 cells that stably express the Epstein-Barr virus nuclear antigen-1 (EBNA) were available in the lab prior to the start of this project (Troilo et al., 2014). HEK293-EBNA were previously transfected with fibulin-4, fibulin-5 and fibronectin (Choudhury et al., 2009, Cheng et al., 2018). Previously stored transfected HEK-293 EBNA cells were thawed at 37 ^{O}C and then resuspended in 9 mL of growth media (Dulbecco's modified Eagle's medium DMEM (Sigma-Aldrich) supplemented with 1% glutamine, 1% penicillin/streptomycin, and 10% fetal bovine serum). Cells were then seeded in T75 flask and grown at 37°C and 5% CO2 until 95-100% confluency. Cell number was increased by transferring them to larger culture flasks T225 followed by hyper flasks. For protein expression, a 1:1 serum free culture mixture of Dulbecco's Modified Eagle's Medium and Ham's F-12 was used to wash the cells and subsequently added media was collected and replenished every 2-3 days, which was stored in -20°C. The expression media were collected for 3-4 weeks, until cells started to detach from culturing flask surface.

The collected serum-free media, containing the secreted His-tagged proteins was filtered using 0.65 µm filter (Whatman). Before protein purification, a 5 mL nickel affinity column (GE Healthcare) was equilibrated at 4°C with 20 ml of binding buffer, containing 10 mM Tris, 500 mM NaCl and 10 mM imidazole pH 7.8 at a flow rate of 1ml/min. Then 1.5 - 2L of media containing the recombinant protein was loaded, washed with 10 mL of binding buffer and then eluted using a buffer containing 10 mM Tris, 500 mM NaCl and 500 mM imidazole pH 7.8. The most concentrated eluates were further purified and proteins were separated by size-exclusion chromatography on an AKTA purifier FPLC using a Superdex 200 of Superose 6 10/300GL column (GE Healthcare) and a buffer containing 10mM Tris or 10 mM HEPES and 150mM NaCl pH7.8 at a flow rate of 0.5 mL/min. The purity and identity of the His-tagged proteins in eluted fractions was verified using SDS-PAGE. All buffers were filtered using 0.2 µm filters before use.

8.2.1. Purification of Fibulin-4

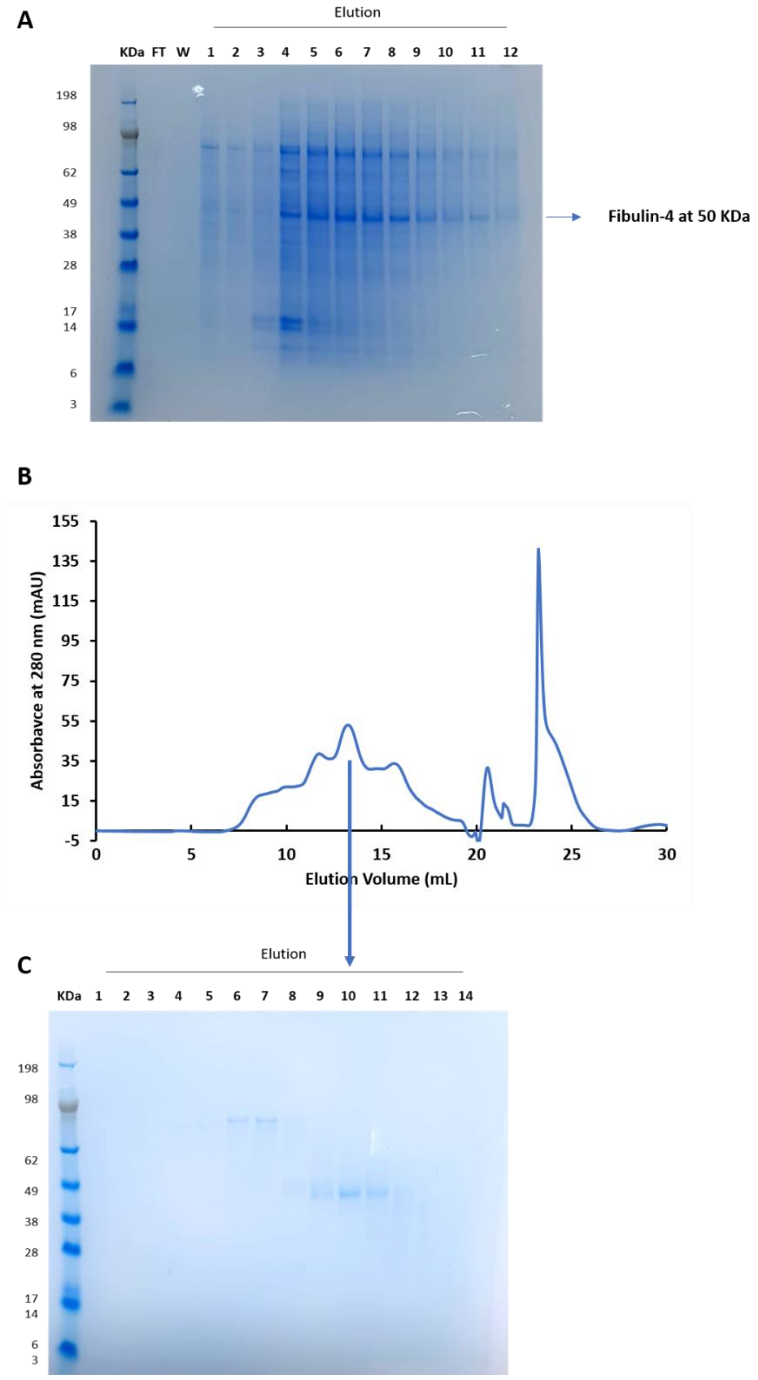

Figure 8-3: Purification of Fibulin-4. (A) Non-reducing SDS-PAGE analysis of 6xHis-tagged Ni-affinity chromatography proteins after elution. (B) Size exclusion chromatograms of fibulin-4. Purified proteins were in buffer containing 10 mM HEPES and 150 mM NaCl at pH 7.8 and eluted at a flow rate of 0.5 ml/min. (C) Non-reducing SDS-PAGE analysis of SEC fractions. The arrow showing fraction corresponding to the monomer species observed in SEC trace. FT, follow-through and W, wash.

8.2.2. Purification of Fibulin-5

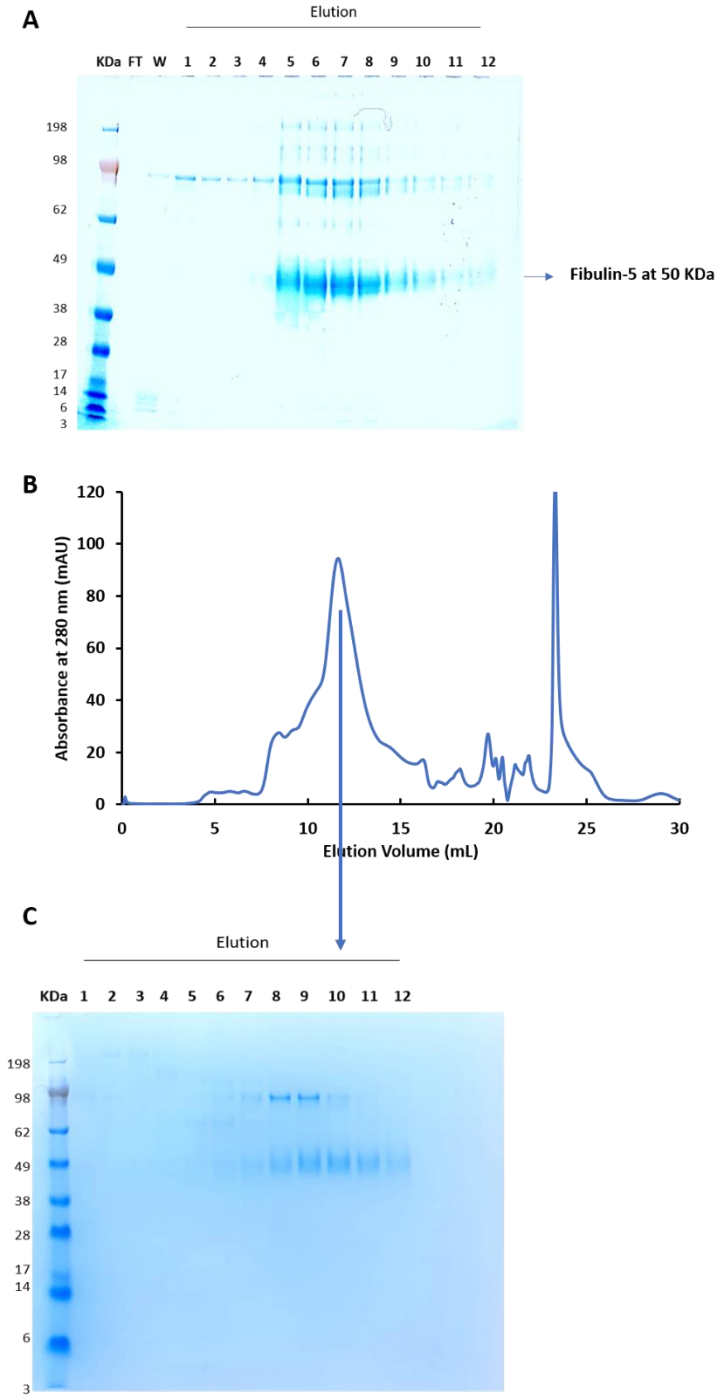

Figure 8-4: Purification of Fibulin-5. (A) Non-reducing SDS-PAGE analysis of 6xHis-tagged Ni-affinity chromatography proteins after elution. (B) Size exclusion chromatograms of fibulin-4. Purified proteins were in buffer containing 10 mM HEPES and 150 mM NaCl at pH 7.8 and eluted at a flow rate of 0.5 ml/min. (C) Non-reducing SDS-PAGE analysis of SEC fractions. The arrow showing fraction corresponding to the monomer species observed in SEC trace. FT, follow-through and W, wash.

8.2.3. Purification of Fibronectin

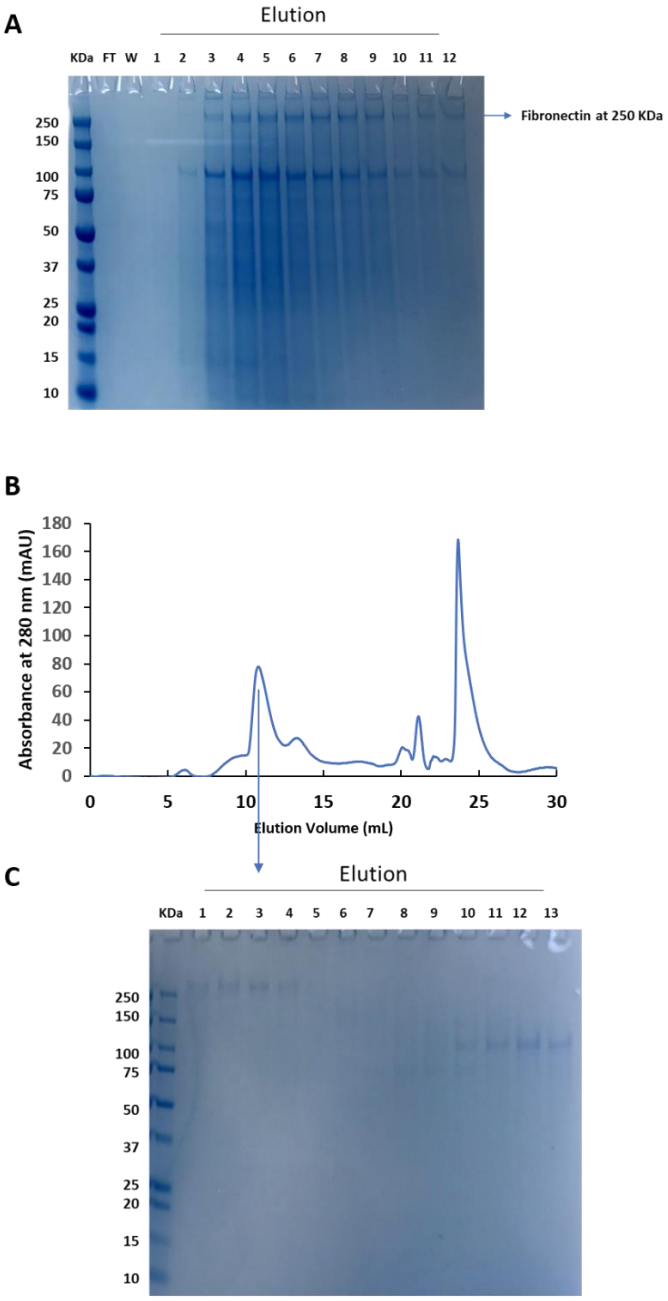

Figure 8-5: Purification of Fibronectin. (A) Non-reducing SDS-PAGE analysis of 6xHis-tagged Ni-affinity chromatography proteins after elution. (B) Size exclusion chromatogram of full-length fibronectin. Purified proteins were in buffer containing 10 mM HEPES and 150 mM NaCl at pH 7.8 and eluted at a flow rate of 0.5 ml/min. (C) Non-reducing SDS-PAGE analysis of SEC fractions. The arrow showing fraction corresponding to the monomer species observed in SEC trace. FT, follow-through and W, wash.

8.3. Investigating LTBP4 C-terminal region cross-linking with Tropoelastin by TG2

In this thesis we identified tropoelastin as a new matrix partner for LTBP4 and showed that the C-terminal but not the N-terminal region strongly bound to full-length tropoelastin. Previous studies have demonstrated that tropoelastin strongly binds fibrillin-1 and both proteins form cross-linked complex in the presence of TG2 (Clarke et al., 2005, Rock et al., 2004). Altogether, these findings led us to investigate whether LTBP4 C-terminal region could cross-link with tropoelastin by TG2.

One µg of purified LTBP4 C-terminal region and full-length tropoelastin were incubated separately or together with 0.1 µg of the guinea pig liver-derived commercial transglutaminase-2 (TG2) (Sigma-Aldrich) for 2 hours at 30 °C in 10 mM HEPES, 150 mM NaCl pH 7.4 buffer containing 1 mM CaCL2. The cross-linked proteins were then analysed by non-reducing SDS-PAGE (Figure 8-6).

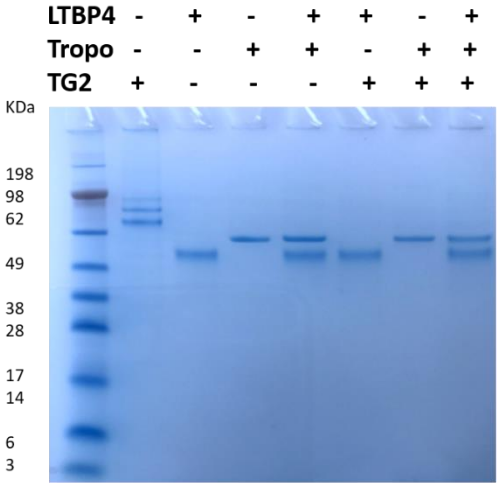

Figure 8-6: Investigating LTBP4 C-terminal region cross-linking with tropoelastin by TG2. Non-reducing SDS-PAGE showing no higher molecular weight species were formed in the pretense of the cross-linker TG2.

8.4. Investigating LTBP4 N-terminal region cross-linking with Fibulin-5 by TG2

LTBP4 as other LTBPs family members, is incorporated into the ECM via its N-terminal region (Todorovic and Rifkin, 2012). LTBP4 is known to promote elastic fibre assembly through its direct binding to fibulin-5 via its N-terminal region (Noda et al., 2013). These data led us to investigate whether LTBP4 N-terminal region is capable to cross-link with fibulin-5. Cross-linking assay was performed as described in section 7.6. LTBP1 C-terminal region has been previously shown to cross-link with fibrillin-1 (PF3 fragment), therefore we used it as positive control (Figure 8-7).

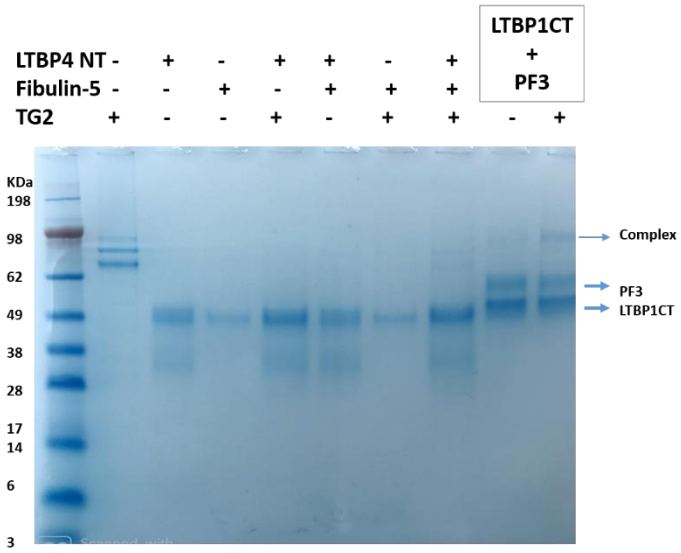

Figure 8-7: Investigating LTBP4 N-terminal region cross-linking with fibulin-5 by TG2. Non-reducing SDS-PAGE showing no higher molecular weight species were formed in the pretense of the cross-linker TG2. While there are higher molecular spices when cross-linking LTBP1 C-terminal region to fibrillin-1 N-terminal region (PF3 fragment), confirming that the cross-linker is active.

8.5. Generation of LTBP4L N-terminal region constructs

Since mammalian cells express two major isoforms of LTBP4, the long, LTBP4L and the short, LTBP4S, that are produced by alternative promoters (Kantola et al., 2010), we attempted to also characterise the long isoform of LTBP4 and compare its structural and functional properties with the obtained information in this thesis on the short isoform. Therefore, we purchased the Gene Synthesised sequence (ThermoFisher Scientific) for the wildtype LTBPL N-terminal region and for an ARCL1C mutant that contain the 5' Nhel restriction site, 6xHis-

tag, stop codon, C-terminal thrombin cleavage site, a stop codon, and 3' Xhol restriction site (Figures 8-8 and 8-9). The codon sequence was optimized using the manufactures software. The synthetic gene constructs were received as lyophilised DNA in a plasmid DNA, pMA-T (Figure 8-10).

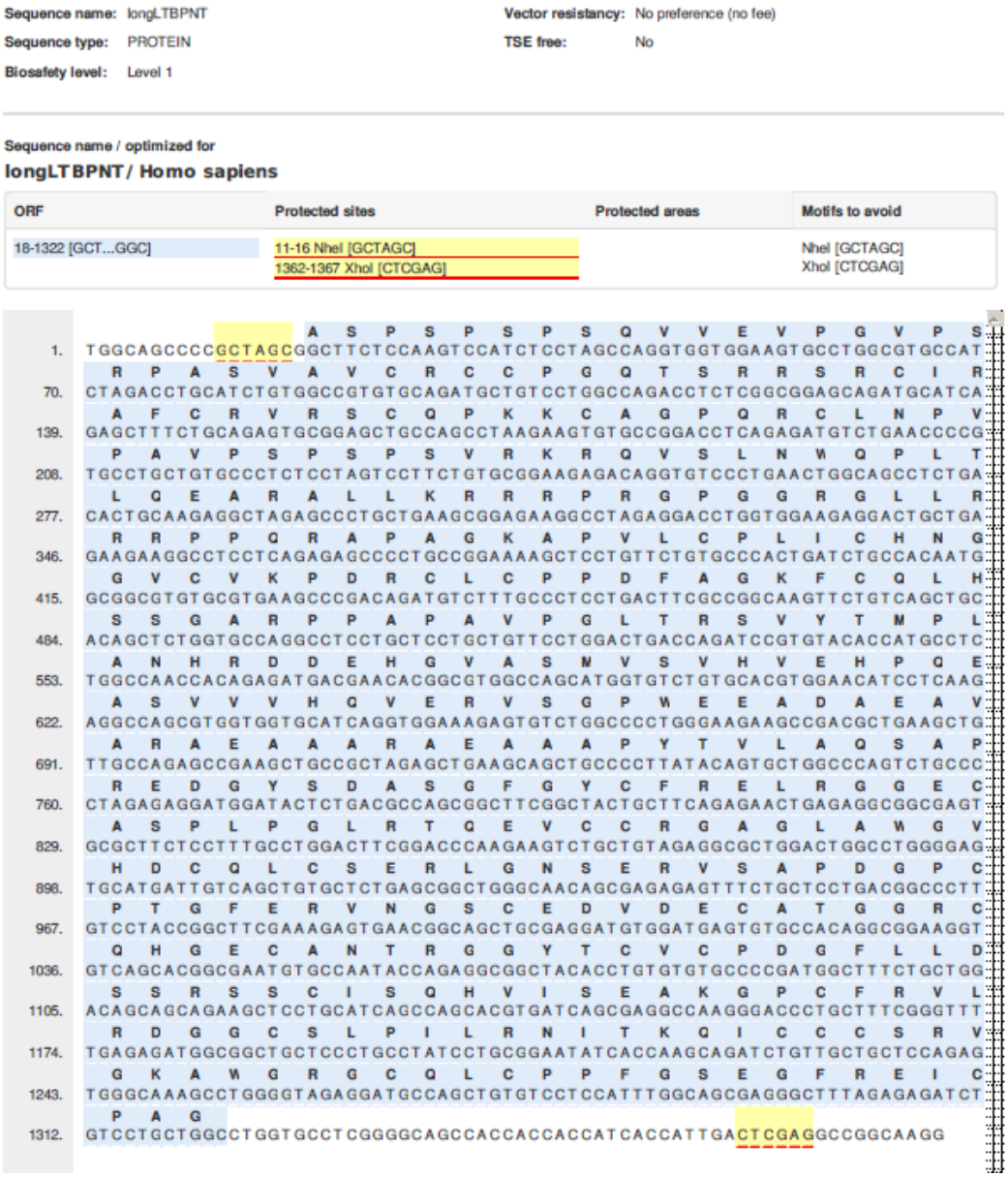

Figure 8-8: DNA and protein sequence of truncated wildtype LTBP4L N-terminal region construct. The construct was tagged with 6X-His in its C-terminal region end.

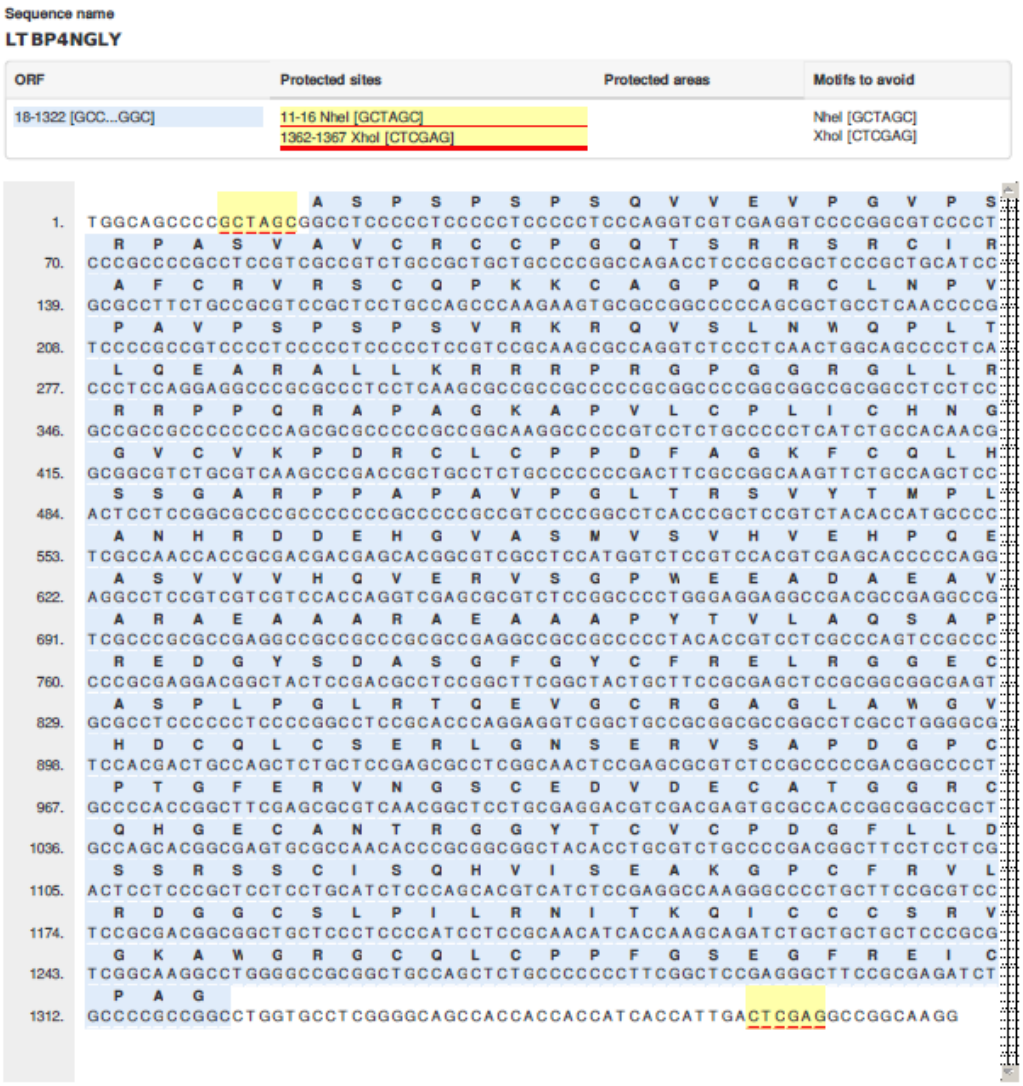

Figure 8-9: DNA and protein sequence of mutated LTBP4L N-terminal region construct. The construct was tagged with 6X-His in its C-terminal region end.

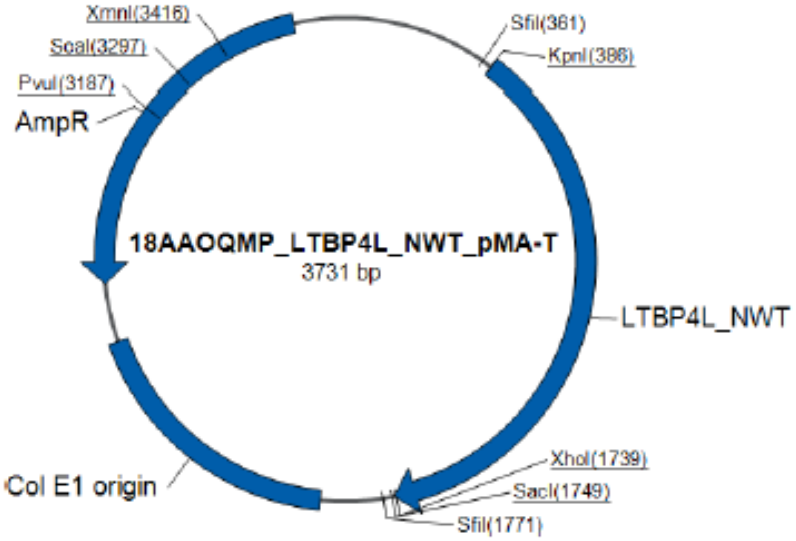

Figure 8-10: Plasmid map of pMA-T

8.5.1. Double Digestion of Vector Sequence

The LTBP4L synthetic genes were double digested from the Pmap-T vector using NheI-HF and XhoI restriction enzymes according to the manufactures protocol (New England Biolabs) then were ligated to the mammalian vector pCEP-Pu/Ac7. Briefly, between 5-10 units of enzyme was used per µg of DNA. The digestion reactions were performed in 1x CutSmart buffer (50 mM Potassium Acetate, 20 mM Tris-acetate, 10 mM Magnesium Acetate, 100 µg/mL BSA, PH 7.9) at 50 µl reaction and 60 minutes incubation time at 37°C.

8.5.2. Agarose gel Electrophoresis

DNA was separated by electrophoresis using 1% (w/v) agarose gels. Briefly, gels were prepared by the addition of 1% (w/v) agarose (Bioline) to 100 mL of TAE buffer (2 M Tris, 1 M acetic acid and 0.5 mM EDTA, PH 8.0) that was dissolved by heating in a microwave. The solution was then cooled and 0.005% (v/v) of SafeView nucleic acid stain was added (NBE Biologicals Ltd.). DNA samples were loaded and electrophoresis was performed at 120V for 40 minutes and DNA was visualised using visible spectrum blue light.

8.5.3. DNA Purification from Agarose Gel

DNA was purified from agarose gel using QIAqucik Gel Extraction Kit according to the manufactures protocol (Qiagen). Briefly, DNA bands were excised from agarose gel, weighted, and transferred to a microfuge tube. QG buffer (3-fold greater than the weighted gel) was added to the tube and incubated for 10 minutes at 50^{o}C. After dissolution of the gel, 1 volume of isopropanol was added and the sample was then passed through a QIAquick spin column (Qiagen) by centrifugation at 10000 *g*. Immobilised DNA was washed by 750 µL of PE buffer (Qiagen) then eluted from the column by 20 µL of DNAse-free sterile water.

8.5.4. Ligation of Insert

DNA ligation was performed using the Quick Ligation Kit according to the manufactures protocol (New England Biolabs). Briefly, about 50 ng of pCEP-Pu/Ac7 was mixed with 37 ng of insert and 1 µL of quick ligase was added. The reaction was carried out in 2x Quick ligase reaction buffer at a total volume of 20 µL incubated at room temperature for 5 minutes. The mix was then chilled on ice and transformed in competent cells.

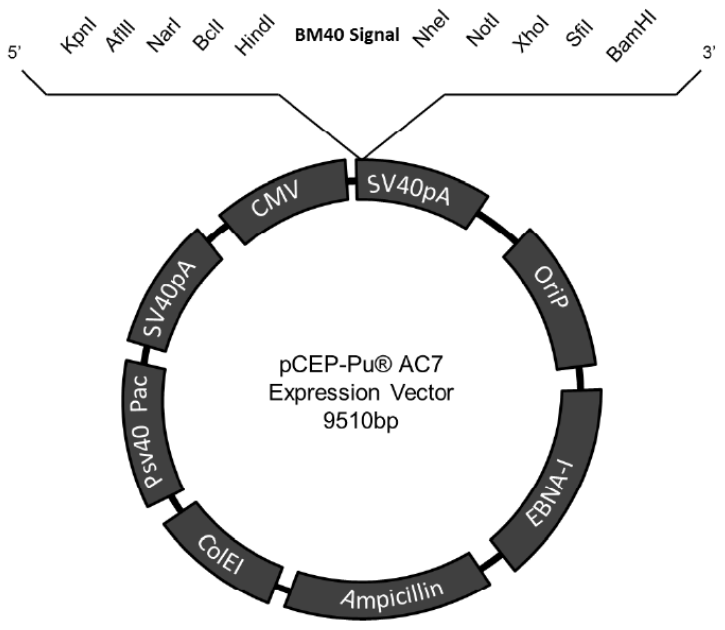

Figure 8-11: Plasmid map of pCEP-PuAC7.

8.5.5. NEB 10-beta competent E. coli Transformation of LTBP4L constructs and Isolation of Positive colonies from LB Agar Plates

Two µL of each wildtype LTBP4 and mutant constructed vector was transformed into 20 µL of 10-Beta Competent E. coli cells, incubated on ice for 30 minutes then heat-shocked at 42°C for 45 seconds. Cells were immediately placed back on ice for 2 minutes. 500 µL of warmed Super Optimal broth (SOC) media (Thermo Fisher Scientific) were added to the transformations and grown in 37°C shaking incubator for an hour. The mixture was centrifuged at 200 x *g* for a minute and 250 µL of the SOC media was discarded. The cells were re-suspended with the remaining 250 µL of SOC media. 75µL of the transformed cells were then plated onto solidified LB agar plates containing ampicillin (100 µg/mL). finally, the plates were incubated at 37°C overnight to allow for selection.

8.5.6. Inoculation and Growth of Bacterial Culture

Using sterile inoculating loop, a single colony from the ampicillin containing LB agar plate was picked and transferred into 50 mL centrifuge tube (Corning) containing 15mL Luria broth (LB) media supplemented with ampicillin (100 µg/ml). The LB bacterial culture was then grown overnight in a 37°C shaking incubator to grow up sufficient numbers of bacteria necessary to isolate plasmid DNA.

8.5.7. Miniprep Purification of LTBP4L Expression Vectors

Minipreps were performed on the overnight cell cultures to isolate the expression vectors using QIAprep Spin Miniprep Kit according to the manufacture's protocol (Qiagen). Briefly, a 15 mL of the overnight cell culture was pelleted by centrifugation at 10000 *g.* The pelleted cells were then re-suspended in a 250 µL of re-suspension buffer P1 (with added RNase) and then transferred to a 1.5 mL microcentrifuge tube. 250 µL of lysis buffer P2 was added, mixed thoroughly and allowed for the lysis reaction to proceed for 5 minutes. 350 µL of the neutralizing buffer N3 was added and immediately mixed gently. The precipitant was pelleted by centrifugation at 10000 x *g* for 10 minutes. The supernatant was transferred into the QIAprep spin column and centrifuged for 60 seconds. The bound DNA was washed with 750 µL of the washing buffer PE and centrifuged for 60 seconds followed by an additional step of 1-minute centrifugation to remove the excess material. The purified DNA was eluted from the

spin column by 50 µL of sterile water that was incubated for 1 minute before centrifugation for 1 minute. The purified DNA was quantified using nanodrop instrument. The DNA was stored at -20 °C.

8.5.8. DNA Sequencing of Expression Vectors

DNA sequencing reaction was prepared in total reaction volume of 10 µL including 5 µM of forward sequencing primer and 500 ng of plasmid DNA. For sequencing LTBP4L, THE forward sequencing primer (5'-TTCTTCACCCGACATCTC-3') was used. While sequencing of the mammalian pCEP-Pu/Ac7 construct, the pCEP forward sequencing primer (5'-AGAGCTCGTTTAGTGAACCG-3') was used. DNA sequencing samples were sent to GATC Biotech (Cologne, Germany) using the LIGHTrun service for sequencing.

8.6. Stable Episomal Vector Transfection of HEK293-EBNA

Mammalian expression vector pCEP-Pu/AC7 containing the His-tagged LTBP4L constructs were transfected into 70-80 % confluent HEK-293 EBNA cell culture using Lipofectamine 3000 reagent according to the manufacture's protocol (Invitrogen). Briefly, LTBP4 construct was mixed with diluted P3000 reagent with 125 µL of serum free Opti-MEM media (DMEM4 mixed in a 1:1 ratio with F12-HAMS supplemented with 5% (v/v) of Penicillin/Streptomycin mixture). Lipofectamine 3000 reagent was also diluted with serum free media. The diluted mixtures were then combined and incubated at room temperature for 5 minutes. The mixture was then added to the semiconfluent cell culture and incubated overnight at 37°C and 5% CO2. The cells then were passaged using media supplemented with 2 µg/mL of puromycin (Gibco) to select the transfected cells. Cell selection last for a period of 2-3 weeks. LTBP4L protein was expressed as previously described in section 8.2.

8.7. LTBP4L SDS-PAGE and Immunoblotting

SDS-PAGE was carried out using NuPAGE 4-12% gradient Bis-Tris pre-cast polyacrylamide gels (Invitrogen) and NuPAGE 1X MES or MOPS SDS running buffer (Life technologies). Protein samples were diluted in loading buffer with and/or without reducing agent, boiled at 100°C for 4-5min, then loaded into the pre-cast gels. Electrophoretically separated proteins were transferred to nitrocellulose membranes using a semi-dry blotting system (Bio-Rad). The proteins were transferred and blotted from the gel to the membrane using NuPAGE 1X transfer buffer (Life technologies). The blots were blocked with 5% skimmed milk in 1xTris-Buffered Saline, 0.1% Tween20 (TBS-Tween) composed of 20mM Tris and 150 mM NaCl pH 7.6 for an hour at room temperature. Immunodetection was performed using mouse anti-His-tag primary antibody (1:2000) (Bio-Rad) overnight at 4°C. Membranes were then washed 5 times at 5-minute intervals in TBS. Then a conjugated donkey anti-Mouse secondary antibody (IRDye 800 CW) was used at (1: 1000) (LI-COR Biosiences) and visualised using (ODYSSEY CLx) infrared imaging system (LI-COR Biosciences). The LTBP4L proteins were detected at larger molecular weight than expected (Figure 8.12), maybe due to the presence of N-linked glycosylation.

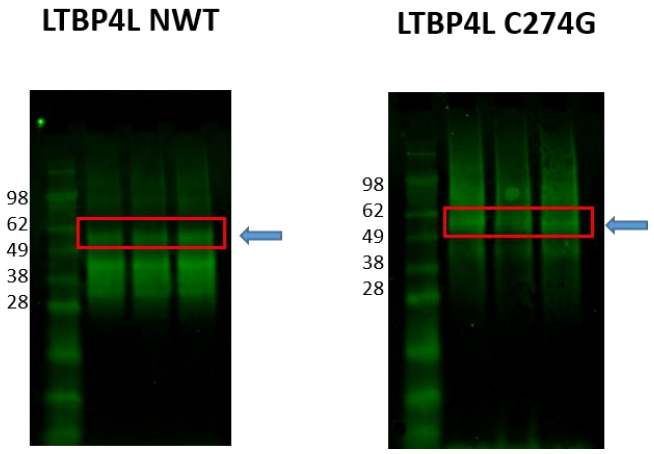

Figure 8-12: Immunoblotting of LTBP4L N-terminal constructs. Western blot showing the wildtype LTBP4L N-terminal region (left panel) and mutant (right panel) at slightly larger molecular weight than expected (46 KDa) from sequence.

8.8. LTBP4L Recombinant Protein Purification

The recombinant LTBPL was purified as previously described in section 8.3. The protein yield was very low, therefore we were unable to characterise the proteins (Figure 8.13).

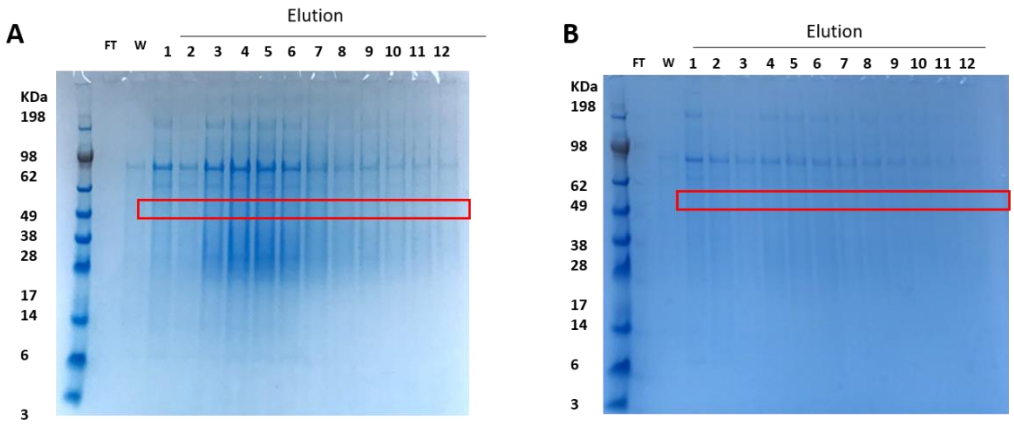

Figure 8-13: SDS-PAGE analysis of LTBP4L constructs. Non-reduced commassie blue stained SDS-PAGE gel were unable to detect purified LTBP4L N-terminal region constructs. (A) NWT and (B) mutant. Red box indicated expected size of proteins. Red box indicated expected size of proteins.